QUANTIFYING WATER USE AND WATER PRODUCTIVITY OF HIGH-PERFORMING PEAR ORCHARDS IN THE WINTER RAINFALL AREAS OF SOUTH AFRICA

Report to the

Water Research Commission & Hortgro

by

[1]S DZIKITI, [1]JC PIENAAR, [1,2]A SIDZUMO,[1,3]SJE MIDGLEY, [1]E CROUCH, [1]P DANGARE, [4]JM VISSER, [1]JK NGULUBE, [5]N GIULIANI

[1]*Department of Horticultural Science, Stellenbosch University*

[2] *Fruitways Pty Ltd*

[3] *Western Cape Department of Agriculture*

[4]*Department of Soil Science, Stellenbosch University*

[5] *Faculty of Agricultural, Environmental and Food Sciences, Free University of Bozen-Bolzano, Bolzano, Italy*

WRC report no. 3269/1/26

ISBN 978-0-6392-0810-7

July 2026

Obtainable from
Water Research Commission
Private Bag X03
Gezina, 0031
Download from www.wrc.org.za

The publication of this report emanates from a project entitled: *Quantifying water use and water productivity of high performing pear orchards in the winter rainfall areas of South Africa* (Project No. *WRC 2022/2023 - 00986*)

DISCLAIMER
This report has been reviewed by the Water Research Commission (WRC) and approved for publication. Approval does not signify that the contents necessarily reflect the views and policies of the WRC, nor does it mention the trade names or commercial products that constitute endorsement or recommendation for use.

ACKNOWLEDGEMENTS

We acknowledge the Water Research Commission and the South African Apple and Pear Producers' Association, which are represented by Hortgro, for initiating and funding this project. We sincerely thank the following entities for granting us permission to work in their productive orchards: the Buchuland Farm in Ceres, the Romansrivier Farm in Wolseley, the Graymead Farm (Fruitways Pty Ltd) in Vyeboom and the Elgin Farm in Elgin. Special thanks go to the following individuals for their help with the logistics during our experiments: Henk Rossouw and Phil Dicey of the Buchuland Farm, Ruan Zeeman of the Romansrivier Farm, Douw Vermeulen and Schalk Keyser of the Graymead Farm, as well as Dirk Meyer of Elgin Orchards and George Petro (Piet) of Buchuland for assistance with the irrigation trial. We also thank Mr Christo van der Westhuizen for his support in securing study sites in the Wolseley and Ceres areas, and Fruitways Pty, for securing the sites in EGVV.

Lastly, we gratefully acknowledge the guidance and advice from the following members of the project reference group:

Dr L Nhamo	:	Water Research Commission (Chairman)
Prof NS Mpandeli	:	Water Research Commission
Dr SN Hlophe-Ginindza	:	Water Research Commission
Ms M Kapari	:	Water Research Commission
Prof WJ Steyn	:	Hortgro
Dr S Hadebe	:	University of Limpopo
Dr JE Hoffman	:	Independent Consultant
Mr L Reynolds	:	Fruitful Crop Advice
Mr D Brink	:	Fruitmax Agri
Mr S Schoeman	:	Soetkalmoes Consulting
Ms K van der Westhuizen	:	Muddy Boots Pty Ltd
Dr NJ Taylor	:	University of Pretoria

EXECUTIVE SUMMARY

1.0 MOTIVATION

South Africa is a relatively small producer of pears (*Pyrus communis* L.), with a global production share of roughly 3% (Theron et al., 2008). In 2016, the country was ranked as the sixth-largest exporter of pears, being second only to Argentina in the southern hemisphere (DAFF, 2017). The biggest producers are China, Italy, the United States, Argentina and Turkey, which occupy the top five positions. Locally, pear production accounts for about 16% of the total deciduous fruit produced on 12 850 ha in the country, according to the Hortgro Tree Census of 2024. The sector generates close to R 4.0 billion (or 15.5%) of the total gross value for the deciduous fruit industry annually; therefore, it is an important contributor to the GDP (DAFF, 2017). Close to 50% of the fruit is exported, thereby earning foreign exchange for the country, creating jobs and forming linkages with support institutions. The remaining fruit is consumed locally as fresh fruit, which is either processed into juice, canned or dried. According to DAFF (2017), direct employment in the pear industry in 2015 was estimated to be 12 850 people, who supported about 51 398 dependents.

All pears that are produced commercially in the country are grown under irrigation (Volschenk et al., 2014; Dzikiti et al., 2024). The availability of adequate water is therefore critical for the sustainability and growth of the industry. However, no accurate quantitative information currently exists on the water requirements of this crop under local conditions. This paucity of data may cause inaccurate irrigation scheduling and water allocation decisions, which may lead to the inefficient use of the limited water resources. Little is also known about the drivers of water use and how this is affected by factors such as canopy cover, crop load, cultivar, soils, climate, irrigation system, etc. International studies report the water use and crop coefficients for pear orchards, mostly in Europe, Australia and Asia (Kang et al., 2002; Girona et al., 2011; Requena et al., 2011; Zhao et al., 2012; Goodwin et al., 2015; Zhang et al., 2018). This project therefore sought to close these important information gaps by conducting detailed field experiments and crop modelling that were aimed at quantifying the maximum unstressed water use of two pear cultivars, namely the ‘Packham’s Triumph’ and ‘Forelle’, in

different production regions in the Western Cape. These two cultivars are the dominant pear cultivars in South Africa, and they account for 32 and 30% of the land planted to pears in 2024 (Hortgro, 2024). The study also intended to quantify how water use relates to the yield quality and quantity of pears produced in the different growing regions.

2. AIMS AND OBJECTIVES

General aim

To quantify the water use and yield dynamics of the high-performing 'Forelle' and 'Packham's Triumph' pear cultivars in different production regions in the Western Cape Province.

Specific objectives

These were:

- to quantify the daily and seasonal water use patterns of 'Forelle' and 'Packham's Triumph' pear cultivars in different growing regions;
- to establish the drivers of the fruit yield and quality variations among different cultivars in different growing regions;
- to derive the biophysical and economic water productivity of pear orchards; and
- to develop a model to provide information on evapotranspiration in pear orchards, to provide insights on water use partitioning and to facilitate the scaling up of the study results to other pear-growing regions.

3. METHODOLOGY

Data were collected in four commercial pear orchards in the Western Cape Province of South Africa over two to three growing seasons per orchard. The study focused on the widely-planted 'Packham's Triumph' and 'Forelle' cultivars. 'Packham's Triumph' is a mid-season cultivar that is harvested in late January to early February in South Africa. It produces large green fruit with sweet and juicy flesh. 'Forelle', on the other hand, is a late season cultivar that tends

to produce small fruits, with a sweet, juicy flesh, and it has a distinctive red blush. This has a slightly longer growing season, as it is harvested in late February to early March in South Africa.

The first 'Forelle' orchard was a mature full-bearing block (33° 22' 42.90" S; 19° 21' 29.24" E, 512 m asl) at the Buchuland farm, which is about four kilometres to the east of the town of Ceres. The orchard was 22 years old, planted in 1994 on the BP1 rootstock when the project started in 2022. The orchard size was about 6.5 ha, and it was planted with a north-south row orientation. The tree density was 1 481 trees per ha, and the trees were irrigated with a micro-sprinkler system that delivered ~ 32 L/h (Table 1). This orchard was established on a clay soil with the highest concentration of clay found in the 300 to 500 mm layer. The climate of Ceres is classified according to the Köppen-Geiger climate classification as Csb, with a warm summer Mediterranean climate. The average temperatures range between 28° and 30°C. Winters are colder, with minimum temperatures averaging 2° to 4°C and with occasional snowfall on higher ground. Data were collected in this orchard over three growing seasons, from September 2022 to May 2025.

The second orchard was a 'Packham's Triumph' orchard at the Romansrivier Farm near the town of Wolseley (33° 27' 37.51" S; 19° 11' 40.44" E. 258 m asl). The orchard was planted in 2009; it flanks the banks of the Breede River on the western side of the river channel, and it has a north-south row orientation. The rootstock was the BP1 rootstock and orchard size was ~2.75 ha. The tree spacing was 4 m x 1.5 m, which gives a planting density of 1 667 trees per hectare (Table 1). Irrigation was via a micro-sprinkler system with one 32 L/h micro-sprinkler per tree. The soil type was a uniform fine sandy loam soil, with a low percentage of stone throughout the profile. The climate of Wolseley is classified according to the Köppen classification and is Csa, which is characterised by warm dry summers and cool wet winters. The summer temperatures in Wolseley are high, like those in Ceres, but the winters are warmer, averaging between 9° to 10°C. Data were collected in this orchard over two growing seasons, from September 2022 to May 2024.

The third orchard was a full-bearing, high-performing 'Packham's Triumph' orchard (-34° 1' 44,39" S; 19° 8' 10.98" E; 318 m asl) at the Graymead Farm near the town of Vyeboom. The orchard was planted in 2012 on 2.63 ha. The tree spacing was 4 m x 1.5 m, which gives a tree density of 1 667 trees per ha. Irrigation was via a 32 L/h micro-sprinkler system, with one sprinkler per tree. The soils were clayey loam soils with a high water-holding capacity. The yield

in this orchard was generally high, exceeding 120 t/ha in some years. The climate of Vyeboom is also of the Mediterranean-type (Köppen classification: Csb), which is characterised by warm, dry summers and cool, wet winters. The area receives higher rainfall than the other two sites, due to the orographic effects of the surrounding mountains. Data were collected in this orchard over two growing seasons, from September 2023 to May 2025.

The fourth orchard was planted to the ‘‘Forelle’’ cultivar in the Elgin (-34° 10' 48.48" 19° 1' 30.25"; 319 m asl). The ‘Forelle’ trees were grafted on the BP2 rootstock and pollinated by the ‘Early Bon Chretien’ cultivar. The trees were planted in 2003, with a spacing of 4.5 m x 1.5 m (~ 1 481 plants per ha). The total orchard area was ~ 4.2 ha, with a north-south row orientation. Irrigation was via a 32 L/h micro-sprinkler system. The climate of Elgin is also of the Mediterranean-type (Köppen Csb), which is characterised by mild, wet winters and warm, dry summers. The climate of the area is influenced by the higher altitude (250-500 m asl), with the surrounding mountains and proximity to the Atlantic Ocean producing cooler temperatures and frequent cloud cover. Data were collected from September 2023 to May 2025.

Table 1. Details of the four orchards with different microclimatic conditions in the Western Cape Province, South Africa

Site	Cultivar	Rootstock	Planting density (trees/ha)	Tree height (m)	Planting date	Orchard size (ha)	Irrigation
Ceres	‘Forelle’	BP1	1481	4.5	1994	6.50	Micro-sprinkler
Wolseley	‘P. Triumph’	BP1	1667	4.5	2009	2.75	Micro-sprinkler
Vyeboom	‘P Triumph’	BP1	1667	4.0	2012	2.63	Micro-sprinkler
Elgin	‘Forelle’	BP2	1481	4.5	2003	4.20	Micro-sprinkler

Climate data were collected by using automatic weather stations that were installed within 500 m of each of the four study orchards. The stations measured the basic hourly weather variables, namely, the solar irradiance, the wind speed and direction, the maximum and minimum air temperature, the maximum and minimum relative humidity, and the rainfall. The weather stations were installed over extensive short grass surfaces, as recommended by the FAO 56 (Allen et al., 1998). The volumetric soil water content in the root zone of the trees was measured hourly at 30, 60 and 90 cm depths at one location in each orchard, by using time domain reflectometer probes (Model CS616 - Campbell Scientific, USA). Irrigation was measured hourly by using electronic water flow meters that were installed on the irrigation lines and connected to dataloggers. The tree growth was monitored by measuring the canopy

dimensions (base area and height) and the Leaf Area Index (LAI - m^2 of one-sided leaf area per m^2 of ground area). The fruit growth, leaf gas exchange (transpiration, photosynthesis and stomatal conductance) and the tree water status (midday stem water potential) were also measured at selected intervals. The crop yield and quality were also determined for each orchard at the end of the season. The tree transpiration was measured by using the Heat Ratio Method (HRM) of monitoring the sap flow (Burgess et al., 2001) on three trees of different sizes in each orchard. The results were scaled to orchard-level transpiration in equivalent water depth units. The actual orchard evapotranspiration (ET) was measured using an open-path eddy covariance system (Model: IRGASON, Campbell Scientific, UT, USA). Because only one eddy covariance system was available, we rotated the tower among the orchards over short measurement periods. Therefore, it was not possible to obtain the ET measurements in each orchard for a full season. Gap filling for the missing ET data was done by using the dual source ET model, which is a modified version of the Shuttleworth-Wallace model (Shuttleworth & Wallace, 1985), as reported in Dzikiti et al. (2018) for apple orchards. This model simulates the orchard ET as the algebraic sum of the transpiration from the trees (T) and the orchard floor evaporation flux (E_s). Unlike the original Shuttleworth and Wallace ET model, the modified version uses a variable stomatal conductance that is estimated according to Jarvis et al. (1976). In this study, the model was reformulated for pears.

Climate change is a large concern in the key fruit-growing regions across the country (Jack et al., 2022). In this study, we used the validated dual source ET model to simulate the likely future trends in the water requirements of pear orchards under climate change. The unique contributions of the ET model used in the present study are: 1) that the model accounts for physiological stress on the trees under future warmer and drier conditions, thereby providing more realistic insights on future water requirements for pear orchards than what is currently available; and 2) the model distinguishes the respective trajectories of orchard floor evaporation and tree transpiration. This provides insights into opportunities for improving orchard water management as the climate changes, through the detailed simulation of the ET partitioning between the tree transpiration and orchard floor evaporation components.

4. RESULTS AND DISCUSSION

The measured climate data at each of the four sites were representative of the long-term climatic conditions for each area. For instance, the monthly maximum temperatures were highest in Elgin, reaching 40.0°C in February 2025, compared to 38.9°C in Ceres, which is most likely due to the higher altitude in Ceres. However, Ceres recorded the lowest average minimum temperature of – 3.2°C, compared to Elgin's – 0.92°C. There was no significant difference in the vapour pressure deficit of the air, with peak monthly values hovering around 1.36 and 1.42 kPa for Ceres and Elgin, respectively. The rainfall for Ceres during the growing season (September to April) was 334.5, 225.6 and 244.6 mm during the 2022-2025 growing seasons. The seasonal total reference evapotranspiration (ET_o) in Ceres was more than five times higher than the rainfall, namely, 1 132.6, 1 200.2 and 1 158.7 mm for the 2022-2023, 2023-2024 and 2024-2025 seasons, respectively. The Elgin area, on the other hand, received similar amounts of growing season rainfall, namely, 245. 2 and 231.6 mm during the 2023-2025 seasons, but with a much higher annual total rainfall (>1 050 mm) than in Ceres (~ 850 mm). The total reference evapotranspiration in Elgin was slightly lower than in Ceres, namely, 1 169.3 and 1 037.3 mm for the 2023-2025 seasons. The orchards were generally well-irrigated throughout the growing season, with the soil water content being kept close to the field capacity. Table 2 summarises the annual climatic data for all the four study sites.

Although cultivar differences in the water use rates are possible, the daily total transpiration of the pear trees in this study was strongly influenced by the canopy size. The 'Forelle' trees in Ceres and Elgin, which had the largest canopy sizes, with maximum LAI values of 3.8 and 3.5, respectively, also had the highest peak transpiration rates of 39.9 and 37.1 L/tree/d. These transpiration rates amounted to 5.9 and 5.5 mm/d. The maximum daily transpiration at Wolseley was 30.6 L/tree/d (5.1 mm/d) and 27.0 L/tree/d (4.5 mm/d) at Vyeboom, with lower peak LAI values of 3.2 and 2.8 for the two sites, respectively. These water use values are consistent with the measurements by Goodwin et al. (2015) in Australia, who observed daily transpiration values between 20 and 40 litres for individual full-bearing pear trees. However, the Australian orchards had a lower tree density (~ 1 111 trees per ha) and the trees may have had a slightly larger canopy size. The seasonal total transpiration was 750.3 mm for Ceres, when averaged over three growing seasons from 2022 to 2025, and 700.6 mm for Elgin, when averaged over two seasons (2023-2025). The 'Packham's Triumph' orchards in

Wolseley and Vyeboom had the lowest seasonal transpiration of 576.1 and 497.8 mm, respectively, with these being the averages for two growing seasons, as summarised in Table 2.

The daily total transpiration rate was strongly linear in relation to the daily total solar radiation, which explained the variation of up to 82% in the observed transpiration. The vapour pressure deficit, on the other hand, had a non-linear relationship with the transpiration, with a VPD threshold of between 1.0 and 1.5 kPa. The transpiration declined beyond this threshold, which suggests a strong stomatal limitation to transpiration at high VPD levels. Because the reference ET is calculated by using both the radiation and VPD, it is therefore not surprising that a non-linear relationship also existed between the ET_o and tree transpiration, due to the influence of the VPD. The average yields over two to three seasons were 56 t/ha for the 'Packham's Triumph' in Wolseley, 65 t/ha for the 'Forelle' in Ceres, 75 t/ha for the 'Packham's Triumph' in Vyeboom, and 50 t/ha for the 'Forelle' in Elgin. The biophysical water productivity (WPb), which is calculated as the ratio of the yield per unit volume of water transpired by the trees, was therefore 9.72 kg/m^3 for the 'Packham's Triumph' at Wolseley, 8.67 kg/m^3 for the 'Forelle' in Ceres, 15.07 kg/m^3 for the 'Packham's Triumph' in Vyeboom, and 7.14 kg/m^3 for the 'Forelle' in Elgin. The economic water productivity (WPe) was R43.9/m^3 for the 'Packham's Triumph' in Wolseley, R75 /m^3 for 'Forelle' in Ceres, R 74.4/m^3 for the 'Packham's Triumph' in Vyeboom. The farm income data were not available for the 'Forelle' in Elgin. These data suggest two important drivers for the economic water productivity. A higher income per cubic meter of water consumed can be achieved either through planting the blushed 'Forelle' cultivar, which fetches a higher price per kg, or through higher yields, as in the case of 'Packham's Triumph' in Vyeboom.

The whole orchard ET, which was measured with the eddy covariance system, varied between 0.4 and 7.7 mm/d among three of the four orchards. The dual source ET model was applied to all four pear orchards. The model explained between 47 and 83% of the variations in transpiration, with the lowest accuracy (R^2 ~ 0.47) obtained at the Vyeboom orchard, due to the poor data quality because of persistent problems with the sensors. The Nash-Satcliffe Efficiency (NSE) was positive at all sites and ranged from 0.30 to 0.68, which indicated an acceptable model performance (Morias et al., 2007). The RMSE varied between ±0.75 mm/d for the Ceres orchard and ±0.93 mm/d for that of Elgin. The R^2 for the orchard ET ranged

between 0.40 and 0.91, with the highest accuracy obtained for the 'Packham's Triumph' orchard in Wolseley, which had the longest measurement record. The root mean square error was less than 1.0 mm/d, and it ranged between ±0.72 mm/d for the Wolseley site and ±0.95 mm/d for the Elgin site. The NSE ranged between 0.29 and 0.85, with the highest prediction accuracy being for the Wolseley orchard.

The modelled average seasonal total (September to April) ET for the 'Packham's Triumph' in Wolseley was 803 mm (8 030 m^3/ha), 916 mm (9 160 m^3/ha) for the 'Forelle' in Ceres, 851 mm (8 510 m^3/ha) for the 'Forelle' in Elgin and 741 mm (7 410 m^3/ha) for the 'Packham's Triumph' in Vyeboom. The peak basal crop coefficient (K_{cb}) ranged from 0.67 to 0.74 for the 'Packham's Triumph' in Wolseley, 0.68 to 0.78 for the 'Packham's Triumph' in Vyeboom, 0.68 to 0.84 for the 'Forelle' in Ceres, and 0.79 to 0.90 for the 'Forelle' in Elgin. The crop coefficients (Kc) at peak canopy cover were not significantly different in the four orchards, namely, 0.80 to 0.92 in Wolseley, 0.97 to 1.14 in Vyeboom, 0.90 to 1.09 in Ceres, and 0.83 to 1.08 in Elgin. These values are consistent with those recorded in the FAO 56 (Allen et al., 1998) and those derived in Spain by Girona et al. (2011) (Kc ~ 1.0). However, these values are almost double the mid-season Kc for a mature pear orchard (~ 0.50) observed by Conceição et al. (2008) in Portugal for a drip irrigated orchard, which suggests that there is need to derive local crop coefficients for drip-irrigated pear orchards.

Most Global Climate Models (GCM) predict warmer and drier conditions in the Western Cape and other fruit-growing areas in the Mediterranean region (Lotter & le Maitre, 2014; Jack et al., 2022). The projected trajectory of the transpiration-constraining factors, namely the solar irradiance and VPD stress factors, suggest that increases in the intensity of solar radiation is unlikely to constrain transpiration, while the VPD will have a significant influence on transpiration reduction under future warmer and drier conditions. The six GCM models suggest that the reference evapotranspiration in pear-growing areas in the Western Cape will increase by about 2.6% between the current period (2020-2030) and the mid-century (2045-2065). This estimate is much lower than the 11% predicted by Agundeji and Jordaan (2017) for between 1980-1990 and mid-century. Our study projected an increase of up to 6.6% for ETo between the current period and the end of the century (2090-2099). Assuming that the orchards will always be well-watered, and that all the stress will be due to climatic factors, the orchard ET is projected to increase by 3.5% between the current period and mid-century, while a cumulative

increase of 9.7% is projected between the current period and the end of the century. The orchard transpiration is projected to increase by a somewhat smaller margin, at 3.1%, between the current and mid-centuries, and 9.1% by the end of the century. The orchard floor evaporation is, however, projected to increase by a larger margin of 4.4% between the current and mid-century, and up to 10.9% by the end of the century. These data suggest that the physiological responses of the trees to the future harsher growing conditions will most likely limit the increase in transpiration, due to their response to the rising VPD. The orchard floor evaporation, on the other hand, will be the largest contributor to the increase in orchard water use.

Table 2. Summary of water use and yield variables of four pear orchards in different growing regions in the Western Cape Province

Region	Cultivar	Max LAI	ET_o (mm/season)			Transpiration (mm/season)			Evapotranspiration (mm/season)			Yield (t/ha)			T-WP (Physical) (kg/m^3)	T-WP (Economic) (R/m^3)
			2023	2024	2025	2023	2024	2025	2023	2024	2025	2023	2024	2025		
Ceres	'Forelle'	3.8	1133	1200	1159	721	772	-	923	892	884	66.7	52.5	62	8.05	97.3
Wolseley	P. Triumph	3.2	1104	1219	-	597	555	-	778	800	-	59.0	55.3	-	9.72	43.9
Vyeboom	P. Triumph	2.8	-	1092	1066	-	498	576	-	697	641	-	80	88	15.68	79.9
Elgin	'Forelle'	3.6	-	1169	1037	-	675	701	-	831	872	-	-	56.2	7.14	-

5. CONCLUSIONS

Measurements of the actual water use of high-performing pear orchards show that the seasonal total evapotranspiration under South African conditions varies greatly between the production regions and that they are influenced by the local climatic conditions and by canopy management. According to previous studies, the crop load has an influence on the orchard water use, but the size of the transpiring leaf area and local microclimate override the influence of the crop load. For a maximum yield, pear orchards in the Western Cape province of South Africa require between 8 000 and 9 200 m^3/ha/season, depending on the canopy size and production region. Assuming that there is effective rainfall of 250 mm during the growing season, the irrigation requirements of high-performing pear orchards range from 5 500 m^3/ha/season to 6 700 m^3/ha/season. Exceptionally high crop loads may not affect the sustainable production of pears, provided that the growers can manage the challenges, like alternate bearing and poor fruit quality, which often result from excessive crop loads.

Projections of future crop water requirements that do not account for climate-related stresses are likely to significantly overestimate the future crop water needs. Substantial water savings are possible in the future with substantial reductions in orchard floor evaporation, which seems to contribute the most to future increases in ET. Therefore, the adoption and implementation of irrigation practices, like drip irrigation, and orchard floor management practices, such as mulching, will most likely play a critical role in the sustainable management of irrigation in orchards.

6. NEW KNOWLEDGE AND INNOVATION

This study has contributed new knowledge in several ways. Even though pears in South Africa are grown entirely under irrigation, there was no accurate quantitative information on the maximum unstressed water use of pear orchards. This study has closed this important information gap by providing detailed water use and yield data for two widely planted pear cultivars in South Africa. The data were collected over multiple seasons per orchard, in order to account for alternate bearing. Secondly, the study has also shown that the water use of pear orchards is strongly influenced by the climatic conditions and canopy management practices. Water use is greater in warmer and drier production regions. Based on the water use

measurements from the 'Packham's Triumph' at Vyeboom, which had the smallest canopy size but the highest crop load, the canopy size seems to have a larger impact on the orchard's water use than the crop load. However, this orchard had the lowest seasonal water requirements. Thirdly, this study developed and tested a dual-source water use model for pear orchards. This model was used to predict the likely changes in orchard water requirements under climate change. The key innovations behind this modelling approach are, firstly, that it considers changes in the physiology of the trees under climate change. Secondly, the model also partitions the orchard evapotranspiration into the tree transpiration and orchard floor evapotranspiration components, and it predicts the changes to each. This study suggests that the projected changes in water use by pear orchards, in the near and far future, are likely to be lower than those published by other local and international studies, which neglect the possible effect of climate change on the tree physiology. This information can be used for climate change adaptation planning, especially when it is related to optimising orchard water management practices.

7. RECOMMENDATIONS

Future research could focus on the following:

- a repeat of the study on drip-irrigated pear orchards, as the current study focused on micro-sprinkler irrigated trees;
- a detailed quantitative investigation on the effects of the crop load on the water consumption of pear trees for manipulating the fruit numbers;
- a quantification of the cultivar differences in water use and water stress responses;
- repeating the deficit irrigation trials on pear orchards, with irrigation being withheld during specific phenological stages, in view of the conflicting accounts on the response of pear orchards to deficit irrigation, as reported by Blanco et al. (2025);
- developing a spatial dual-source ET model for pear orchards; and
- incorporating yield predictions in the climate change model.

8. EXTENT TO WHICH THE OBJECTIVES HAVE BEEN MET

The main obligations involved in the quantification of the water use of high-performing 'Forelle' and 'Packham's Triumph' pear orchards growing in different production regions in the

Western Cape, including the effects on the fruit yield and quality, have been comprehensively addressed. A dual-source water use model was developed and tested robustly across four orchards. Data were collected over multiple seasons to account for the effects of variations in the crop load and the climatic conditions between the years.

We have exceeded the contractual agreements by:

1) incorporating a detailed study on how fruit vascular flows vary between cultivars over the course of a growing season, under the local hot and dry conditions. Previous studies on this topic have been conducted in temperate climates, with milder growing conditions. This study, which formed part of a student's MSc project, provided insights into the drivers of fruit growth and the quality of the two pear cultivars by quantifying the flow of photosynthates in and out of the fruit;
2) including a component that assessed the performance of 'Forelle' pear trees when deficit irrigation is applied at different times of the day throughout the irrigation season. This component of the study is still ongoing, as part of a PhD student's project; and
3) because of the substantial running costs of (2), we were unable to spatialise the dual-source ET model, due to financial constraints. Instead, we extended the application of the model to include climate change simulations, which added substantial value to the original study objectives.

9. CAPACITY BUILDING

Three students have been involved in this study, for degree purposes:

1) Mr Anele Sidzumo – PhD Agriculture (Horticulture), Stellenbosch University;
2) Mr Johan Pienaar – MSc Agriculture (Horticulture), Stellenbosch University; and
3) Mr Kondwani Ngulube – MSc Agriculture (Horticulture), Stellenbosch University

10. PUBLICATIONS

One article has been published in a peer-reviewed journal (see Appendix A for details). Two other articles are under review by international peer-reviewed journals, while an additional two articles are at an advanced stage of preparation, also to be submitted to international peer-reviewed journals.

TABLE OF CONTENTS

ACKNOWLEDGEMENTS iii

EXECUTIVE SUMMARY iv

LIST OF SYMBOLS AND ABBREVIATIONS xxii

LIST OF FIGURES xxvi

LIST OF TABLES xxxv

CHAPTER ONE 1

INTRODUCTION 1

1.1 BACKGROUND 1

1.2 AIMS AND OBJECTIVES 3

1.3 JUSTIFICATION FOR SELECTED STUDY AREAS 3

CHAPTER TWO 6

KNOWLEDGE REVIEW 6

2.0 PEAR PRODUCTION IN SOUTH AFRICA 6

2.1 CLIMATE, SOILS AND GEOGRAPHICAL DISTRIBUTION OF PEAR-PRODUCING REGIONS 6

2.2 PEAR CULTIVARS, ROOTSTOCKS AND PRODUCTION TRENDS 8

2.3 FACTORS AFFECTING THE YIELD AND QUALITY OF PEARS 11

2.3.1 Cultivars and rootstocks 11

2.3.2 Soil water availability and water stress 12

2.4 QUANTIFYING ORCHARD WATER USE 16

2.4.1 Transpiration measurements 17

2.4.2 Determining whole orchard evapotranspiration 25

CHAPTER THREE 32

MODELLING WATER USE AND YIELD OF PEAR ORCHARDS 32

3.0 INTRODUCTION 32

3.1 DESCRIPTION OF THE PEAR ORCHARD WATER USE MODEL 33

3.2 MODELLING YIELD OF PEAR ORCHARDS 38

CHAPTER FOUR 40
'FORELLE' ORCHARD, CERES 40
4.0 INTRODUCTION 40
4.1 SITE DESCRIPTION 41
4.2 SOIL PROPERTIES AT BUCHULAND 43
4.3 TREE, FRUIT GROWTH AND SOIL MOISTURE MEASUREMENTS 44
4.4 QUANTIFYING ORCHARD TRANSPIRATION 47
4.5 TREE WATER STATUS AND LEAF GAS EXCHANGE MEASUREMENTS 50
4.6 YIELD FOR THE 'FORELLE' ORCHARD IN CERES 51
4.7 FRUIT QUALITY 52
4.8 WATER PRODUCTIVITY OF 'FORELLE' PEARS IN CERES 55
4.8.1 Physical water productivity 55
4.8.2 Economic water productivity 55
4.9 RESULTS AND DISCUSSION 56
4.9.1 Climatic conditions 56
4.9.2 Soil water content dynamics and leaf area index 58
4.9.3 Diurnal and seasonal dynamics in the tree water status and leaf gas exchange 61
4.9.5 Orchard evapotranspiration 71
4.9.6 Modelling water use and its partitioning in the 'Forelle' orchard 73
4.9.7 Fruit growth and quality for the 'Forelle' orchard in Ceres 76
4.9.8 Fruit quality 78
4.9.9 Water productivity for the 'Forelle' orchard in Ceres 79
4.10 CONCLUSIONS 81
CHAPTER FIVE 82
'PACKHAM'S TRIUMPH' ORCHARD, WOLSELEY 82
5.0 INTRODUCTION 82
5.1 STUDY SITE AND PLANT MATERIAL 83
5.2 SOILS AND CLIMATE DATA 84

5.3 WATER USE MEASUREMENTS 85
5.4 WATER USE MODELLING: IMPACT OF CLIMATE CHANGE ON ORCHARD WATER USE 87
5.5 YIELD AND FRUIT QUALITY 89
5.6 RESULTS AND DISCUSSION 89
5.6.1 Climatic conditions for 2022-24 in Wolseley 89
5.6.2 Tree water status and soil moisture dynamics 91
5.6.3 Canopy development and orchard transpiration 100
5.6.4 Orchard evapotranspiration 104
5.6.5 Water use modelling and crop coefficients 105
5.6.6 Climate change impacts on the water use of pear orchards 108
5.6.7 Fruit yield and quality 112
5.7 CONCLUSIONS 115
CHAPTER SIX 117
'PACKHAM'S TRIUMPH' ORCHARD, VYEBOOM 117
6.0 INTRODUCTION 117
6.1 DESCRIPTION OF THE STUDY SITE 118
6.2 SOIL TYPE 119
6.3 TRANSPIRATION, SOIL MOISTURE, GROWTH AND CLIMATIC MEASUREMENTS 119
6.4 WATER PRODUCTIVITY 121
6.4.1 Seasonal transpiration 121
6.4.2 Yield, pack out and gross income 121
6.4.3 Physical and economic water productivity 121
6.5 FRUIT YIELD AND QUALITY 121
6.5.1 Fruit yield 121
6.5.2 Fruit quality assessment 122
6.6 RESULTS AND DISCUSSION 123
6.6.1 Weather conditions 123
6.6.2 Canopy growth and development 125

6.6.3 Transpiration and soil water content dynamics *126*

6.6.4 Water use modelling and orchard water balance *128*

6.6.5 Modelling the yield of 'Forelle' and 'Packham's Triumph' orchards *132*

6.6.6 Fruit yield and quality *135*

6.7 CONCLUSIONS 137

CHAPTER SEVEN 139

'FORELLE' ORCHARD, ELGIN 139

7.0 INTRODUCTION 139

7.1 DESCRIPTION OF THE 'FORELLE' ORCHARD IN ELGIN 139

7.2 CHARACTERISING THE SOILS AT THE ELGIN ORCHARD 140

7.3 TRANSPIRATION, SOIL MOISTURE, GROWTH AND WEATHER MEASUREMENTS 141

7.4 FRUIT YIELD AND QUALITY FOR EGVV ORCHARDS 142

7.4.1 Fruit yield *142*

7.4.2 Fruit quality assessment *142*

7.5 RESULTS AND DISCUSSIONS 144

7.5.1 Microclimate and tree growth *144*

7.5.2 Transpiration dynamics *146*

7.5.3 Fruit yield and quality results *148*

7.5.4 Water productivity of 'Forelle' pears in Elgin *149*

7.6 CONCLUSIONS 151

CHAPTER EIGHT 152

CONCLUSIONS AND RECOMMENDATIONS 152

8.0 INTRODUCTION 152

8.1 SUMMARY OF THE GROWING CONDITIONS IN THE PRODUCTION REGIONS 153

8.2 SUMMARY ON ORCHARD WATER USE 154

8.3 WATER PRODUCTIVITY AS INFLUENCED BY CULTIVAR AND GROWING REGION 157

8.3.1 'Forelle' orchards *157*

8.3.2 'Packham's Triumph' orchards *158*

8.4 CHALLENGES WITH THE STUDY AND RECOMMENDATIONS FOR FUTURE WORK 159

REFERENCES 161

APPENDIX A 166

CAPACITY BUILDING, CONFERENCE PRESENTATIONS & 166

PEER- REVIEWED PUBLICATIONS 166

APPENDIX B 169

DOES DEFICIT IRRIGATION APPLIED LATE AFTERNOON IMPROVE THE PERFORMANCE OF PEAR TREES? 169

APPENDIX C 178

VASCULAR FLOW DYNAMICS AND THEIR RELATIONSHIP TO FRUIT GROWTH IN P. TRIUMPH AND 'FORELLE' PEAR CULTIVARS 178

LIST OF SYMBOLS AND ABBREVIATIONS

ROMAN SYMBOLS

A	net photosynthesis (μmol m^{-2} s^{-1})
A_s	available energy at the orchard surface (W m^{-2})
B	Bowen ratio (-)
C_p	specific heat capacity of air at constant pressure (J kg^{-1} K^{-1})
C_c	a dimensionless canopy resistance coefficient
C_s	a dimensionless soil surface resistance coefficient
D	vapour pressure deficit of the air at the reference height (kPa)
E	leaf level transpiration (mmol m^{-2} s^{-1})
E_s	soil evaporation (mm d^{-1})
ET	actual evapotranspiration (mm d^{-1})
ET_o	short grass reference evapotranspiration (mm d^{-1})
G	soil heat flux (W m^{-2})
g_{sT}	stomatal conductance (m s^{-1})
g_c	canopy conductance (m s^{-1})
g_{smax}	maximum stomatal conductance (m s^{-1})
H	sensible heat flux (W m^{-2})
k	extinction coefficient for radiation (-)
K_c	single crop coefficient (-)
K_{cb}	basal crop coefficient (-)
k_r	parameter for the solar radiation stress factor (-)
k_{RS}	adjustment constant for extraterrestrial radiation (-)
k_{vpd}	parameter for the vapour pressure deficit stress factor (-)
R_a	extraterrestrial radiation (MJ m^{-2})
r^a_a	aerodynamic resistance between canopy and reference level (s m^{-1})
$r_a{}^c$	boundary layer resistance of canopy (s m^{-1})
$r_a{}^s$	aerodynamic resistance between the soil and the canopy (s m^{-1})
r_b	leaf boundary layer resistance (s m^{-1})
RH_{max}	maximum relative humidity (%)

RH_{min}	minimum relative humidity (%)
r_s^c	canopy resistance (s m^{-1})
r_s^s	soil surface resistance (s m^{-1})
r_{ST}	stomatal resistance (s m^{-1})
r_{STmin}	minimum stomatal resistance (s m^{-1})
R_n	net radiation (W m^{-2})
R_{ns}	net radiation at soil surface (W m^{-2})
R_s	downward solar irradiance (W m^{-2})
T	orchard level transpiration (mm d^{-1})
T_a	air temperature (°C)
T_{avg}	average air temperature (°C)
T_c	maximum crop transpiration (mm $season^{-1}$)
T_{leaf}	leaf surface temperature (°C)
T_{min}	minimum air temperature (°C)
T_{max}	maximum air temperature (°C)
T_{opt}	optimum air temperature for the growth of pear trees (°C)
T_x	air temperature at reference height within the canopy (°C)
VPD	vapour pressure deficit of the air at screen height (kPa)
VPD_{leaf}	leaf to air vapour pressure deficit (kPa)
U	sap flux density (cm^3 cm^{-2} d^{-1})
Y_a	actual crop yield (t/ha)
Y_{max}	maximum crop yield (t/ha)

GREEK SYMBOLS

Δ	slope of the saturation vapour pressure-temperature curve (kPa K^{-1})
λ	latent heat of vaporisation (J kg^{-1})
α	surface albedo (-)
θ	volumetric soil water content (m^3 m^{-3})
ρ	density of air (kg m^{-3})
γ	psychrometric constant (kPa K^{-1})
δ	Stefan-Boltmann constant (W m^{-2} K^{-4})

ε_a	emissivity of the air (-)
ε_s	emissivity of the surface (-)

ABBREVIATIONS

ARC	Agricultural Research Council
AWS	Automatic Weather Station
DD	Drip Deficit
DCT	Drip Control Time of Day
DDT	Drip Deficit Time of Day
DC	Drip Control
DG	Daily Growth
DM	Dry Mass
EGVV	Elgin/Grabouw/Villiersdorp/Vyeboom
EWP	Economic Water Productivity
FAO56	Food and Agriculture Organisation, Paper No 56
FC	Volumetric water content at Field Capacity
HRM	Heat Ratio Method
IRGA	Infrared Gas Analyser
KBV	Koue Bokkeveld
LAI	Leaf Area Index
MC	Micro Control
MD	Micro Deficit
MDS	Maximum Daily Shrinkage (stem/fruit)
NSE	Nash-Satcliffe Efficiency
PAR	Photosynthetically Active Radiation
RESP	Respiration
RMSE	Root Mean Square
R^2	Coefficient of Determination
P_{eff}	Effective precipitation
PWP	Permanent Wilting Point
SAI	Sapwood Area Index

SR	Surface Renewal method
SW	Shuttleworth and Wallace
SWB	Soil Water Balance
WUEi	Leaf Water Use Efficiency
WUE	Orchard Water Use Efficiency (kg of fruit per m^3 of water)
WP	Water Productivity
WRC	Water Research Commission

LIST OF FIGURES

Figure 1.1 Map of the study area showing the four study sites in the Ceres, Wolseley, Vyeboom and Elgin areas of the Western Cape 4

Figure 2.1 (a) Area planted to the top three pear cultivars, and (b) percentage change in the area planted to each cultivar relative to 2016 (after Hortgro, 2021) 9

Figure 2.2 Trends in the utilisation of pear fruit in South Africa from 2012 to 2021 (after Hortgro, 2021)..... **Error! Bookmark not defined.**

Figure 2.3 The growth cycle of pome fruit (after Boland et al., 2002) 13

Figure 2.4 Pear shoot and fruit growth and the timing of RDI (after Goodwin et al., 2015) 15

Figure 2.5 Schematic representation of the heat balance sap flow gauge (Dynamax, Houston, TX, USA): (a) Vertical section through the stem heat balance sap flow gauge; (b) Energy balance components of the heat balance sap flow sensor ..18

Figure 2.6 Measurement of transpiration on young trees using Granier probes 21

Figure 2.7 Schematic diagram of the heat ratio method (HRM) of monitoring sap flow (after Rafael Oliveira) 24

Figure 2.8 Schematic representation of an eddy covariance micrometeorological method. 27

Figure 2.9 An ideal surface renewal analysis ramp model with ramp amplitude for stable (a>0) and unstable (a<0) conditions, ramp period Lr, quiescent period Lq – during which there is no change in air temperature (after Mengistu & Savage, 2010). τ = Lr + Lq is the total ramp period 28

Figure 2.10 Components of the soil water balance in the root zone of plants (after Allen et al., 1998).....30

Figure 3.1 Schematic diagram of the S-W model for evaporation from a sparse crop (Shuttleworth & Wallace, 1985) 35

Figure 4.1 Location of the study sites where data were collected in the Wolseley and Ceres production regions.....41

Figure 4.2 Location of the IrriCheck irrigation probes (blue cones) used for irrigation scheduling in the 'Forelle' orchard in Ceres. The area bounded in yellow is the 'Forelle' orchard 42

Figure 4.3 The ‘Forelle’ orchard in Ceres in early spring (September) and at full canopy cover in mid-December 44
Figure 4.4 Installation of soil moisture monitoring equipment in the ‘Forelle’ orchard in Ceres 45
Figure 4.5 Monitoring fruit growth with a DEX 70 dendrometer (Dynamax Houston, USA) and irrigation, using a water flow meter installed along an irrigation line....46
Figure 4.6 Automatic weather station at Buchuland in Ceres installed during the 2023-2024 season 46
Figure 4.7 (a) Drilling holes for inserting probes into the tree stem across the four cardinal directions using a drilling jig; (b) Tree boxes monitoring sap flow of mature ‘Forelle’ trees in Ceres 48
Figure 4.8 Open path eddy covariance system measuring orchard evapotranspiration in the ‘Forelle’ orchard in Ceres 49
Figure 4.9 (a) Measuring the midday stem water potential of the ‘Forelle’ trees using a pressure chamber; (b) Leaf gas exchange measurements (photosynthesis and transpiration) using the LI 6800 infrared gas analyser....51
Figure 4.10 Background colour chart 53
Figure 4.11 Starch conversion chart 54
Figure 4.12 Monthly average daily solar radiation, (b) maximum and minimum temperatures, (c) vapour pressure deficit of the air, and (d) monthly total rainfall and reference evapotranspiration over three growing seasons from September 2022 to June 2025. 57
Figure 4.13 Total soil water content (mm) fluctuations (0 – 900 mm depth), along with irrigation amounts and timing over the 2023/2024 season for a ‘Forelle’ pear orchard situated close to Ceres. 59
Figure 4.14 Total soil water content (mm) fluctuations (0 – 900 mm) depth), along with irrigation amounts and timing over the 2024/2025 season for a ‘Forelle’ pear orchard situated close to Ceres. 60
Figure 4.15 Leaf area index of the ‘Forelle’ orchard at Buchuland during the 2022-2025 growing seasons....61

Figure 4.16 Hourly changes in the relationship between the leaf, the trees' xylem and fruit water potential during the (a) early, (b) mid- and (c) late season for the 'Forelle' pears measured from sunrise to sunset on typical clear days 62
Figure 4.17 Relationship of stem and leaf water potential of the 'Forelle' trees with VPD on typically-clear days 63
Figure 4.18 Relationship of midday stem water potential with the volumetric soil water content at midday in the depth intervals of 0-30 cm, 30-60 cm, and 60-90 cm in the rootzone over the season of 'Forelle' trees 64
Figure 4.19 Timeseries of daily VPD of the air and stomatal conductance (a & b), leaf transpiration (c & d), and of daily solar radiation and net photosynthesis (e & f) of leaves of 'Forelle' trees. Each data point represents the mean (±SE) of eight leaves. Measurements were taken firstly from the eastern and then the western side of the canopy on 30/11/2023 (a, c & e) and on 19/12/2023 (b, d & f) 65
Figure 4.20 Seasonal changes in the leaf, xylem and fruit water potentials of the 'Forelle' orchard over the 2024-2025 season 67
Figure 4.21 Accumulation of water stress in the 'Forelle' orchard over the 2024-2025 growing season in Ceres 68
Figure 4.22 (a) Reference evapotranspiration, and (b) actual tree transpiration (in L/tree/day) from October 2022 to February 2024 69
Figure 4.23 Reference evapotranspiration and transpiration expressed in mm/day over three growing seasons 69
Figure 4.24 Transpiration response of the 'Forelle' orchard to the daily atmospheric evaporative demand over two growing seasons 70
Figure 4.25 Effect of intercepted radiation on tree water use from bud-break to full canopy cover 71
Figure 4.26 Energy balance closure for the 'Forelle' orchard 72
Figure 4.27 Comparison of the measured ET_o, actual evapotranspiration and orchard transpiration 72
Figure 4.28 Comparison of measured vs modelled (a) daily transpiration, and (b) orchard evapotranspiration. 74

Figure 4.29 Partitioning of daily evapotranspiration (ET) into the transpiration and orchard floor evaporation components over the 2022 to 2024 growing seasons 75
Figure 4.30 Cumulative transpiration, actual evapotranspiration, reference evapotranspiration and irrigation for the 'Forelle' orchard during the 2023-2024 season.....75
Figure 4.31 Crop coefficients for a mature 'Forelle' orchard in Ceres over the course of the 2023-2024 growing season.....76
Figure 4.32 Fruit growth trends in relation to irrigation received an individual 'Forelle' tree ... .77
Figure 5.1 'Packham's Triumph' orchard at the Romansrivier Farm in Wolseley, showing the late spring and summer images 83
Figure 5.2 Automatic weather station at the Romansrivier Farm, Wolseley.....86
Figure 5.3 Eddy covariance system measuring the whole orchard evapotranspiration in Wolseley 86
Figure 5.4 Comparison of the observed (black line) and the simulated daily solar radiation over two years from September 2022 to July 2024 for the Wolseley weather station. 88
Figure 5.5 Monthly climatic conditions in Wolseley from 01 September 2022 to 31 May 2024 including (a) the average daily solar radiation for the month, (b) air temperature, (c) vapour pressure deficit of the air, (d) rainfall and the reference evapotranspiration.....90
Figure 5.6 Diurnal trends in the leaf, fruit and stem water potential (a) and their relationship with the VPD (b) on a typical clear day on 06/12/2023.....92
Figure 5.7 Average midday stem water potential on three different dates over the 2023/2024 season. The thresholds of moderate water stress (-1.3 MPa) and severe water stress (-1.8 MPa) are indicated, respectively, by the purple and red dashed lines 93
Figure 5.8 Changes in the total soil water content in the root zone (0 – 900 mm) of the 'Packham's Triumph' orchard at Wolseley; (a) during the 2022 – 2023 season, and (b) 2023 – 2024 season.....94
Figure 5.9 Time-series of daily VPD of the air and stomatal conductance (a & b), leaf transpiration (c & d), and of daily solar radiation and net photosynthesis (e & f)

of leaves of ‘‘Packham’s Triumph’’ trees. Each data point represents the mean (±SE) of eight leaves. Measurements were taken from firstly the eastern- and then western side of the canopy on 06/12/2023 (a, c, e) and on 16/01/2024 (b, d, f). 97

Figure 5.10 Relationship between (a) the hourly leaf transpiration rate and VPD of the air, and (b) hourly stem sap flow mid-season on 06/12/2023 and before harvest on 16/01/2024 98

Figure 5.11 Effect of the product of VPD of the air with stomatal conductance on leaf transpiration rate, using hourly values from 06:00 to 17:00 on two dates of measurement i.e. 06/12/2023 and 16/01/2024. 98

Figure 5.12 Effect of leaf stomatal conductance on leaf net photosynthetic rate, using hourly values from 06:00 to 17:00 on two dates of measurement: 06/12/2023 & 16/01/2024. Three outlier data points (at 06:00, 07:00 and 08:00 on 06/12/2023) were excluded from the calculation of the linear trendline; these points are indicated in red 99

Figure 5.13 Effect of solar radiation on net photosynthesis using hourly values from 06:00 to 17:00 on two dates of measurement i.e. 06/12/2023 and 16/01/2024 99

Figure 5.14 Leaf area index of the ‘Packham’s Triumph’ orchard in Wolseley during the 2022-2023 and 2023-2024 seasons 100

Figure 5.15 Seasonal changes in (a) the individual tree transpiration (in litres per tree per day); and (b) tree transpiration expressed in equivalent water depth units ...101

Figure 5.16 Effect of different climate drivers: (a) solar radiation, (b) VPD and (c) reference evapotranspiration on transpiration by ‘Packham’s Triumph’ trees in Wolseley 103

Figure 5.17 Seasonal course of the tree transpiration in equivalent water depth units and the reference evapotranspiration over two growing seasons.....104

Figure 5.18 Effect of the atmospheric evaporative demand on the evapotranspiration of the ‘Packham’s Triumph’ orchard in Wolseley. The slope of the line depicts the average crop coefficient for the orchard 105

Figure 5.19 Comparison of the measured and modelled (a) transpiration and (b) evapotranspiration for the ‘Packham’s Triumph’ 106

Figure 5.20 Comparison of the measured and modelled actual evapotranspiration of the 'Packham's Triumph' orchard at Wolseley.....106
Figure 5.21 Modelled partitioning of evapotranspiration of the 'Packham's Triumph' orchard at Wolseley over two growing seasons from September 2022 to May 2024 107
Figure 5.22 Weekly crop coefficients for the 'Packham's Triumph' orchard at Wolseley during the 2023-2024 growing season.....108
Figure 5.23 Time series of the solar radiation and vapour pressure deficit stress factors for the period 01 January 1961 to 31 December 2099 for 'Packham's Triumph' trees 109
Figure 5.24 Time series prediction of changes in (a) the atmospheric evaporative demand represented by the reference evapotranspiration, (b) actual orchard evapotranspiration, (c) orchard transpiration, and (d) orchard floor evaporation for 'Packham's Triumph' pear orchards in Wolseley for the period 01 January 1961 to 31 December 2099 110
Figure 6.1 'Packham's Triumph' orchard (marked in red) at the Graymead Farm, Vyeboom 118
Figure 6.2 Average monthly climatic conditions at Vyeboom over two growing seasons including (a) the solar radiation, (b) maximum and minimum temperatures, (c) vapour pressure deficit of the air, (d) monthly total rainfall and the reference evapotranspiration 124
Figure 6.3 Leaf area index of the 'Packham's Triumph' orchard at Vyeboom for the 2023-2024 and 2024-2025 seasons 126
Figure 6.4 (a) The reference evapotranspiration, and (b) transpiration dynamics for the 'Packham's Triumph' trees at Vyeboom over two growing seasons. 127
Figure 6.5 Trends in the measured and modelled transpiration for the 'Packham's Triumph' trees at Vyeboom over two growing seasons.....129
Figure 6.6 The measured transpiration and modelled evapotranspiration trends for the 'Packham's Triumph' trees at Vyeboom over two growing seasons 130
Figure 6.7 Water balance of the 'Packham's Triumph' orchard in Vyeboom for the 2024-2025 growing season 131

Figure 6.8 Monthly total water use partitioned into the actual transpiration (green bar), reference evapotranspiration (red bars) and actual evapotranspiration (blue bars) for the full-bearing 'Packham's Triumph' orchard in Vyeboom over two growing seasons 131
Figure 6.9 Weekly changes in the crop coefficients for the 'Packham's Triumph' orchard at Vyeboom over the 2023-2024 growing season 132
Figure 6.10 Yield trends for the 'Packham's Triumph' orchard from planting (2012) until the 2024/25 growing season 134
Figure 6.11 Comparison of the actual and modelled yield of a 'Packham's Triumph' orchard at Vyeboom, from planting in 2013 until its full-bearing age at around 2020-2022 134
Figure 7.1 'Forelle' orchard (marked around in white) at the farm in Elgin 140
Figure 7.2 Daily changes in orchard microclimatic conditions at Elgin from January 2023 to March 2025 representing (a) the solar radiation, (b) maximum and minimum air temperatures, (c) vapour pressure deficit of the air. (d) reference evapotranspiration and rainfall.....145
Figure 7.3 Leaf area of 'Forelle' trees in Elgin over the 2023-2024 and 2024-2025 seasons 146
Figure 7.4 Seasonal changes in (a) the reference evapotranspiration and (b) transpiration of the 'Forelle' orchard at Elgin over the 2023-2024 growing season 147
Figure 7.5 Comparison of the measured and modelled transpiration of the 'Forelle' orchard in Elgin for the 2023-2024 and 2024-2025 seasons.....148
Figure 7.6 Measured and modelled weekly and seasonal single and basal crop coefficients for the 'Forelle' orchard in Elgin 148
Figure 8.1 Performance of the dual-source ET model in estimating the orchard evapotranspiration across three study sites, namely Ceres, Wolseley and Elgin 155
Figure B1. Illustration of the tree water uptake (stem flow – dotted line) and loss .....170 (transpiration or gas exchange in circles) over the course of typical day 170
Figure B2. Three days schematic representation of irrigation treatments applied to 'Forelle' pear orchards, detailing micro-sprinkler (MC, MD) and drip (DC, DD, DCT, DDT) system configurations, application volumes and timings 173

Figure B3. Illustration of the irrigation applied to the various treatments over a five-day period during the peak irrigation period from 15 to 19 December 2025 174
Figure B4. Cumulative irrigation per treatment during the 2025-2026 growing season ..175
Figure B5. Soil water content averaged in the 20 to 60 cm depth for the micro sprinkler, drip control and the drip deficit applied late afternoon (drip deficit time of day) 175
Figure B6. Mid-day stem water potential measurements taken in the various treatments over the 2025-2026 growing season 176
Figure C1. Hourly fruit size dynamics for a Forelle fruit (a) early and (b) late in the growing season. The shaded regions represent the day time, and clear regions the night time (after Dzikiti et al., 2024) 179
Figure C2. Maximum daily shrinkage profile for Forelle and P. Triumph fruit over the course of a full growing season (after Dzikiti et al ., 2024) 180
Figure C3. Correlation between the maximum daily (a) fruit shrinkage early (green dots) and swelling late (orange dots) in the season and (b) with branch diameter shrinkage for the same pear tree with the soil water content in the rootzone181
Figure C4. Correlation between the daily growth and soil water content for a Forelle pear fruit in the early (green dots) and late (orange dots) season 182
Figure C5. Custom-made dendrometer for measuring the fruit size, which was converted to fruit mass by using mass-volume relationships for the pear fruit 182
Figure C6. Schematic representation of the subtraction method of quantifying fruit vascular flows 183
Figure C7. Visual representation of the three treatment conditions of the subtraction method, a) intact, b) girdled and c) detached.....184
Figure C8. The diurnal patterns of relative growth rate (RGR) and specific phloem-, xylem- and transpiration flow rates (mg/g/min) for ‘Forelle’ fruit at a) 47 days after full bloom (DAFB), b) 92 DAFB, c) 120 DAFB, and d) 148 DAFB. The flow- and growth rates were calculated using approach I of the subtraction method ...186
Figure C9. Diurnal patterns of the Relative Growth Rate (RGR) and specific phloem-, xylem- and transpiration flow rates (mg/g/min) for ‘P. Triumph’ fruit at a) 31 Days After Full Bloom (DAFB), b) 76 DAFB, and c) 104 DAFB. The flow- and

growth rates were calculated by using Approach I of the subtraction method 187

Figure C10. Mean daily a) absolute growth rate (AGR), and whole fruit b) phloem-, c) xylem-, and d) transpiration flow rates (g/fruit/day) for 'Forelle' and 'P. Triumph' fruit at different stages in the 2023/2024 growing season. The flow- and growth rates were calculated using approach I of the subtraction method 188

Figure C11. Relative contribution of the average daily phloem and -xylem inflows to the daily mass inflow for 'Forelle' on a) whole fruit- b) specific basis, and for 'P Triumph' on a c) whole fruit- and d) specific basis. The relative contributions were calculated at different times in the 2023/2024 growing season using Approach I of the subtraction method.....189

LIST OF TABLES

Table 1. Details of the four orchards with different microclimatic conditions in the Western Cape Province, South Africa vii

Table 2. Summary of water use and yield variables of four pear orchards in different growing regions in the Western Cape Province xiii

Table 2.1 Area planted to pear trees in different parts of South Africa (Hortgro Tree Census, 2024) 7

Table 2.2 Richardson Chill Units (RCU) for various pears cultivars in Ceres (Ogundeji & Jordaan, 2017) 8

Table 2.3 Major pear cultivars and changes in the size of the planted area (in ha) between 2008 and 2013 (HortGro Tree Census, 2024) 8

Table 3.2 Derivation of the yield response factors (Ky) for 'Packham's Triumph' and 'Forelle' pear cultivars 39

Table 4.1 Properties of the 'Forelle' orchard in Ceres.....43

Table 4.2 Physical properties of the soils at Buchuland, Ceres.....43

Table 4. 4 Monthly climatic conditions averaged over three years between September 2022 and May 2025.....58

Table 4.5 Average yield, fruit number and trunk circumference per tree for 'Forelle' trees .77

Table 4.6 Averages of the quality parameters, per position – and overall, for the 'Forelle' pears 78

Table 4.7 Averages of the additional quality parameters, per position – and overall, measured on the 'Forelle' pears.....79

Table 4.8 Physical Water Productivity (WP), Water Use Efficiency (WUE), and Economic Water Productivity (EWP), based on seasonal transpiration for the 'Forelle' pear orchard in Ceres in 2022-2023, 2023-2024 and 2024-2025.....80

Table 4.9 Physical Water Productivity (WP), Water Use Efficiency (WUE), and Economic Water Productivity (EWP) based on seasonal evapotranspiration for the 'Forelle' pear orchard in Ceres in 2022-2023, 2023-2024 and 2024-2025.....81

Table 5.1 Properties of the 'Packham's Triumph' orchard in Wolseley 84

Table 5.2 Soil physical properties for the 'Packham's Triumph' orchard in Wolseley 84

Table 5.3 Two-year average summary of the monthly weather conditions in Wolseley from September 2022 to May 2024 91
Table 5.4 Projected future changes in orchard water use fluxes from the current (2020-2030), to mid (2050-2060) and end of century (2090-2099). A full growing season is defined as the period from 01 September to 30 April 111
Table 5.5 Average yield: fruit number and trunk circumference per tree for 'Packham's Triumph' trees 112
Table 5.6 Averages of the quality parameters, per position – and overall, for the 'Packham's Triumph' pears 113
Table 5.7 Physical Water Productivity (WP), Water Use Efficiency (WUE), and Economic Water Productivity (EWP) based on seasonal transpiration for the 'Packham's Triumph' pear orchard in Wolseley in 2022-2023 and 2023-2024 114
Table 5.8 Physical Water Productivity (WP), Water Use Efficiency (WUE), and Economic Water Productivity (EWP) based on seasonal evapotranspiration for the 'Packham's Triumph' pear orchard in Wolseley in 2022-2023 and 2023-2024. 115
Table 6.1 Physical characteristics of the soils at the 'Packham's Triumph' orchard in Vyeboom 119
Table 6.2 Installation details for the sap flow probes in the 'Packham's Triumph' orchard at Vyeboom 120
Table 6.3 Summary of monthly climatic conditions at Vyeboom from September 2023 to May 2025 125
Table 6.4 Deriving of the yield response factor (Ky) for the 'Forelle' and 'Packham's Triumph' pear cultivars under South African conditions 133
Table 6.5 Average yield and main stem circumference 135
Table 6.6 Fruit maturity and quality in for the 'Packham's Triumph' orchard in Vyeboom. 135
Table 6.7 Physical Water Productivity (WP), Water Use Efficiency (WUE), and Economic Water Productivity (EWP) based on seasonal transpiration for the 'Packham's Triumph' pear orchard in Vyeboom in 2023-2024 and 2024-2025 136
Table 6.8 Physical Water Productivity (WP), Water Use Efficiency (WUE), and Economic Water Productivity (EWP), based on seasonal evapotranspiration for the 'Packham's Triumph' pear orchard in Vyeboom in 2023-2024 and 2024-2025 137
Table 7.1 Physical characteristics of the soils at the 'Forelle' orchard in Elgin 141

Table 7.2 Installation details for the HRM sap flow sensors at Elgin 141
Table 7.3 Average yield and main stem circumference 149
Table 7.4 Fruit maturity and quality in EGVV.....149
Table 7.5 Physical Water Productivity, Water Use Efficiency, and Economic Water Productivity based on measured seasonal transpiration for the 'Forelle' pear orchard in Elgin in 2023-2024 and 2024-2025.....150
Table 7.6 Physical Water Productivity, Water Use Efficiency, and Economic Water Productivity based on measured seasonal evapotranspiration for the 'Forelle' pear orchard in Elgin in 2023-2024 and 2024-2025.....151
Table 8.1 Summary of the statistics comparing the measured and modelled water-use variables for the four pear orchards 156
Table B1. Summary of the seasonal total irrigation, yield and irrigation water productivity..... 177

CHAPTER ONE

INTRODUCTION

1.1 BACKGROUND

South Africa is a relatively-small producer of pears (*Pyrus communis* L.), with a global production share of roughly 3% (Theron et al., 2008). In 2016, the country was ranked as the sixth-largest exporter of pears, being second only to Argentina in the southern hemisphere (DAFF, 2017). The biggest producers are China, Italy, the United States, Argentina and Turkey, which occupy the top-five positions. According to the Hortgro Tree Census of 2024, local pear production covers an area of 12 850 ha and accounts for about 16% of the total deciduous fruit produced in the country. The sector generates close to R 4.0 billion (or 15.5%) of the total gross value for the deciduous fruit industry annually. Therefore, it is an important contributor to the GDP (DAFF, 2017). Close to 50% of the fruit is exported, thereby earning foreign exchange for the country, creating jobs and forming linkages with support institutions. The remaining fruit is consumed locally as fresh fruit, or it is processed into juice, canned or dried. In 2024, the direct employment in the pear industry was estimated to be about 12 850 people who, in turn, supported about 51 398 dependents (Hortgro, 2024).

All pears that are produced commercially in the country are grown under irrigation (Volschenk et al., 2014; Dzikiti et al., 2024; Hortgro, 2024). Therefore, the availability of adequate water is critical for the sustainability and growth of the industry. However, no accurate quantitative information currently exists on the water requirements of this crop under local conditions. This paucity of data may cause inaccurate irrigation scheduling and water allocation decisions, which may lead to the inefficient use of the limited water resources. Little is also known about the drivers of the water use of fruit trees, such as the canopy cover, crop load, cultivar, soils, climate, irrigation type, etc. There is also limited information on how the water use of pear orchards relates to the quality and quantity of the fruit. A few international studies have reported the water use and crop coefficients for pear orchards, mostly in Europe, Australia and Asia (e.g. Kang et al., 2002; Girona et al., 2011; Requena et al., 2011; Zhao et al.,

2012; Goodwin et al., 2015; Zhang et al., 2018). The present study therefore aimed to close these important information gaps.

The availability of adequate water for irrigation in the prime fruit-producing areas (Figure 1.1) is one of the major factors that is expected to limit pear production in the future. The water resources in the Cape Province, which generates over 90% of pears produced in South Africa, are coming under increasing pressure from the rapidly-growing population of the Cape Town Metro, as well as from the increasing competition with other water users, including industries, recreation, the environment, invasive alien plants, etc. (Volschenk et al., 2003; Dzikiti et al., 2013; Dzikiti et al., 2016; le Maitre et al., 2016). Recent climate change studies also show that parts of the Cape region will become drier over the next 30-40 years, with significantly lower rainfall amounts, shorter rainfall seasons and increased evaporative losses that are driven by higher temperatures (Midgley et al., 2016; Jack et al., 2022). An increase in evapotranspiration in the range 5-15% is projected throughout the region by 2050 (Jack et al., 2022). This will inevitably increase the net water consumption of fruit trees.

Another threat to the availability of water for irrigation is the increasing regulation of the water sector. For example, the Third National Water Resources Strategy for South Africa (NWRS 3, 2022) cites irrigated agriculture as one of the most inefficient sectors, with respect to water use. The NWRS3 estimates that between 30 and 45% of the water allocated for irrigation is wasted, either through leakages, poor irrigation scheduling or other non-beneficial uses. Such water loss levels are not sustainable in a water-scarce country like South Africa. Some completed studies (e.g. Volschenk et al., 2003; Dzikiti et al., 2018) point towards over-irrigation in the fruit sector, due to poor, or a lack of, information and tools for efficient irrigation scheduling. According to the Irrigation Strategy for South Africa, the expansion of irrigated agriculture is critical for future food security, job creation and for supporting livelihoods. However, with the available water resources having been almost fully allocated in most major catchments, water for future irrigation expansion can only be derived from existing allocations. This calls for more accurate information on crop water use, in order to improve irrigation scheduling and water allocation planning.

In order to establish the maximum unstressed water requirements of pear orchards under local conditions, a decision was made, in consultation with the fruit industry experts, to focus on the ‘Packham’s Triumph’ cultivar, which is the most widely-planted pear cultivar in

South Africa and which accounted for 32% of the planted area in 2024 (Hortgro, 2024). 'Packham's Triumph' is an early- to mid-season cultivar that is harvested in late January to early February in South Africa. The second cultivar is the blushed 'Forelle', which is a high-value, late-maturing cultivar. It was the second-most widely planted cultivar in South Africa in 2024, and it accounted for 30% of the total area under pears (Hortgro, 2024). The focus of the current study was on high-performing orchards that are well managed, in order to establish the maximum unstressed water required to produce optimal yields. Data were collected in commercial orchards in prime pear-growing regions in the Western Cape Province, with contrasting microclimates.

1.2 AIMS AND OBJECTIVES

General aim:

To quantify the water use and yield dynamics of high-performing 'Forelle' and 'Packham's Triumph' pear cultivars in different production regions in the Western Cape Province.

The specific objectives are:

- to quantify the daily and seasonal water use patterns of the 'Forelle' and 'Packham's Triumph' pear cultivars in different growing regions;
- to establish the drivers of the fruit yield and quality variations among different cultivars in different growing regions;
- to derive the biophysical and economic water productivity of pear orchards; and
- to develop a model for providing information on evapotranspiration in pear orchards, in order to provide insights into water use partitioning and to facilitate the scaling up of the study results to other pear-growing regions.

1.3 JUSTIFICATION FOR SELECTED STUDY AREAS

More than 90% of the pears produced in South Africa are grown in the Western Cape region in areas with varying microclimatic conditions. This study was therefore conducted in four regions, namely, Ceres, Wolseley, Vyeboom and Elgin, as shown in Figure 1.1. The climate of Ceres is classified as Csb, according to the Köppen-Geiger climate classification, with a

warm summer Mediterranean climate. The average maximum daily temperatures range between 28° and 30°C. Winters are colder, with minimum daily temperatures averaging between 2° to 4°C and with the occasional snowfall on the higher ground. Data were collected in this orchard over three growing seasons, from September 2022 to May 2025. The climate of Wolseley was Csa, as classified according to the Köppen-Geiger classification, which is characterised by warm, dry summers and cool, wet winters. Summer high temperatures in Wolseley are like those in Ceres, but the winters are warmer, averaging 9° to 10°C. Data were collected from this orchard over two growing seasons, from September 2022 to May 2024.

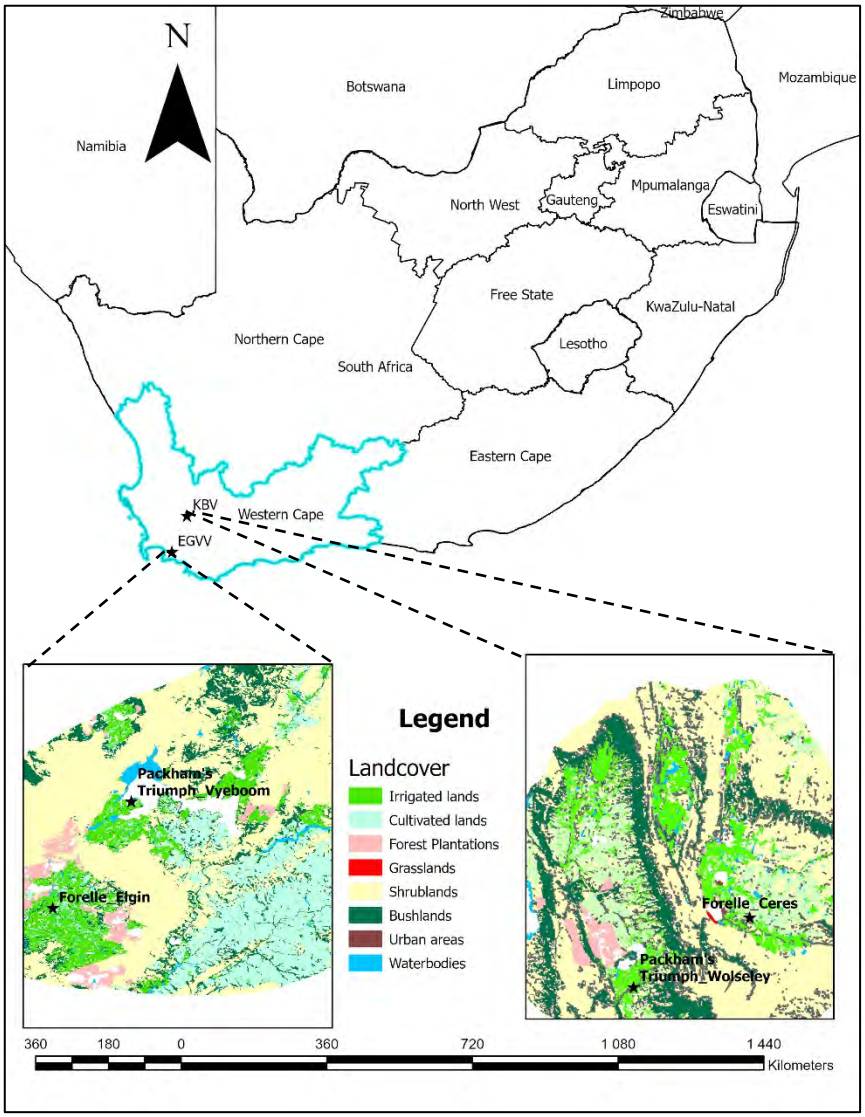


Figure 1.1 Map of the study area showing the four study sites in the Ceres, Wolseley, Vyeboom and Elgin areas of the Western Cape

The climate of Vyeboom is also of the Mediterranean-type, with a Köppen-Geiger classification of Csb, which is characterised by warm dry summers and cool wet winters. The maximum daily growing season temperatures in Vyeboom tend to be lower than those in Ceres and Wolseley. The area receives a higher rainfall than the other two sites, due to the orographic effects of the surrounding mountains. Data were collected from this orchard over two growing seasons, from September 2023 to May 2025. The climate of Elgin is also of the Mediterranean-type (Köppen-Geiger: Csb), which is characterised by mild, wet winters and warm, dry summers. The climate of the area is influenced by the higher altitude (250-500 m asl), the surrounding mountains and the proximity to the Atlantic Ocean, which produce cooler temperatures and frequent cloud cover. The area receives a much higher rainfall than the Ceres and Wolseley production regions. Data were collected from September 2023 to May 2025.

CHAPTER TWO

KNOWLEDGE REVIEW

2.0 PEAR PRODUCTION IN SOUTH AFRICA

2.1 CLIMATE, SOILS AND GEOGRAPHICAL DISTRIBUTION OF PEAR-PRODUCING REGIONS

The total area under pears in South Africa was estimated to be about 12 850 ha in 2024, as shown in Table 2.1 (Hortgro, 2024). Although the sector has seen little expansion in new plantings in recent years, the earnings have continued to grow, driven by a rising demand, mainly in the export markets (DAFF, 2017). More than 90% of the pears are produced in the Western Cape, mostly because of the suitable climate, which is characterised by cold winters and warm summers. The proximity to a harbour also plays a part, given that more than 50% of the pears are for export. The major production regions are in Ceres (37%), Groenland (13%), Langkloof East (13%), Wolseley/Tulbagh (11%), Villiersdorp/Vyeboom (10%), etc., as summarised in Table 2.1. There is about 1.0 ha of pears in the Mpumalanga Province, but none in the other regions.

Pear cultivation requires a climate that consists of warm days, cold nights and high radiation levels. These conditions are met, to various extents, in the key growing regions of South Africa. Sufficient chill units during the winter rest period, typically ~ 850-1200, are crucial for stimulating bud break. The exact number of chill units depends on the cultivar (Table 2.2) and various models exist for calculating the chill units (Lötze & Bergh, 2008). Besides the Koue Bokkeveld region, where winter chill units are theoretically sufficient, inadequate chill units are a significant problem in the warmer production areas of the country. Consequently, growers rely on rest-breaking agents, such as hydrogen cyanamide (Dormex) and winter oils, to promote the bursting of an adequate numbers of buds (Cook & Strydom, 2000).

Pear trees can grow in a wide range of soils, from sandy loam to clay loam. However, soils in most parts of the Western Cape are generally poor and lack uniformity (Cook & Strydom, 2000). Therefore, careful planning and management is critical for producing significant quantities of good quality yields. The preferred soil types for pear production are deep fertile

sandy and loam soils, with good drainage. In areas where waterlogging is a problem, most orchards are planted on ridges, to facilitate drainage. Pears grow best in neutral or slightly acidic soil, with the pH range not exceeding 7.5. Soils should be free from hard substrata and they should be well drained. Poor aeration, due to water logging, increases the incidence of crown rot (*Phytophtora cactorum*), while a pH that is too low/high will affect the availability of nutrients for the trees. Orchard management practices, e.g. tree spacing and vigour management, are adopted to maximise production, with an increasing tendency towards high-density plantings (du Plooy & van Huyssteen, 2000).

Table 2.1 Area planted to pear trees in different parts of South Africa (Hortgro Tree Census, 2024)

District	Number of Trees	Area (ha)
Ceres	6 690 394	4 734
Groenland	2 639 832	1 672
Langkloof East	2 139 525	1 621
Wolseley/Tulbagh	2 057 173	1 429
Villiersdorp/Vyeboom	1 838 351	1 228
Klein Karoo	1 150 073	984
Langkloof West	490 567	393
Piketberg	231 568	188
Worcester	205 401	142
Berg River	194 288	129
Somerset West	237 776	119
Boland	88 651	63
Olifants River	39 975	28
Eastern Cape	10 470	11
Mpumalanga	858	1
TOTAL	18 014 902	12 850

Table 2.2 Richardson Chill Units (RCU) for various pears cultivars in Ceres (Ogundeji & Jordaan, 2017)

Cultivar	RCU
'Forelle'	850
Williams Bon Chrestien	1200
'Packham's Triumph'	900
Abate Fetel	850

2.2 PEAR CULTIVARS, ROOTSTOCKS AND PRODUCTION TRENDS

More than 12 pear cultivars are grown in South Africa (Table 2.3). The main cultivars are 'Packham's Triumph', 'Forelle', Williams Bon Chretien and Abate Fetel (Hortgro, 2024). In 2024, 'Packham's Triumph' occupied the largest area, accounting for 33% of the total planted area, followed by 'Forelle' at 30%, 'Williams Bon Chretien' at 17% and 'Abate Fetel' at 5%. Year-on-year, there has been very little change in the planted area, with 2017 and 2018 seeing no change from 2016. There was a 3% increase in the planted area in 2019, compared to 2018, a 1% increase in 2020, compared to 2019, and a shrinkage of -1% in 2021, compared to the preceding year. There was no change in the planted area during the 2023 and 2024 seasons.

Table 2.3 Major pear cultivars and changes in the size of the planted area (in ha) between 2008 and 2013 (HortGro Tree Census, 2024)

Cultivar	2016	2017	2018	2019	2020	2021	2022	2023	2024
'Packham's Triumph'	4 064	4 072	4 158	4 275	4 354	4 232	4 292	4 237	4 126
'Forelle'	3 219	3 219	3 246	3 361	3 515	3 518	3 678	3 731	3 838
Williams Bon Chretien	2 515	2 451	2 361	2 329	2 275	2 200	2 110	2 074	1 978
Abate Fetel	800	776	729	744	720	700	715	694	685
Rosemarie	430	445	477	510	589	598	655	653	675
Cheeky	348	408	462	526	560	568	571	570	591
Celina	50	110	143	208	217	226	261	263	260
Flamingo	145	147	146	145	137	136	112	105	100
Doyenne Du Comice	158	149	139	130	111	110	93	81	87
Beurre Bosc	198	153	140	130	115	109	99	83	85
Clapp's Favourite	73	95	91	102	102	104	85	84	75
Golden Russet Bosc	111	99	92	88	96	91	85	79	73
Other	169	141	135	126	121	151	127	123	118
TOTAL	12 279	12 265	12 319	12 674	12 913	12 743	12 950	12 892	12 850

The changes in the area planted to the three main cultivars, i.e. 'Packham Triumph' (PT), 'Forelle' and 'William's Bon Chretien' over the period 2016 to 2021 are shown in Figure 2.1. Of these, 'Packham's Triumph' and 'Forelle' increased in area, while that under 'Williams Bon Chretien' showed a consistent decline. 'Forelle' showed the greatest increase of 9% between 2016 and 2020, which continued to 2024. Despite the initial increase in the area under 'Packham's Triumph', this has tended to decline in recent years. The area under 'William's Bon Chretien' has continued to decrease. The reasons for these changes are unclear. But these could be market related, because of the changing consumer preferences or the drive by growers towards cultivars with low chill requirements, given the increasing temperatures in the prime growing areas.

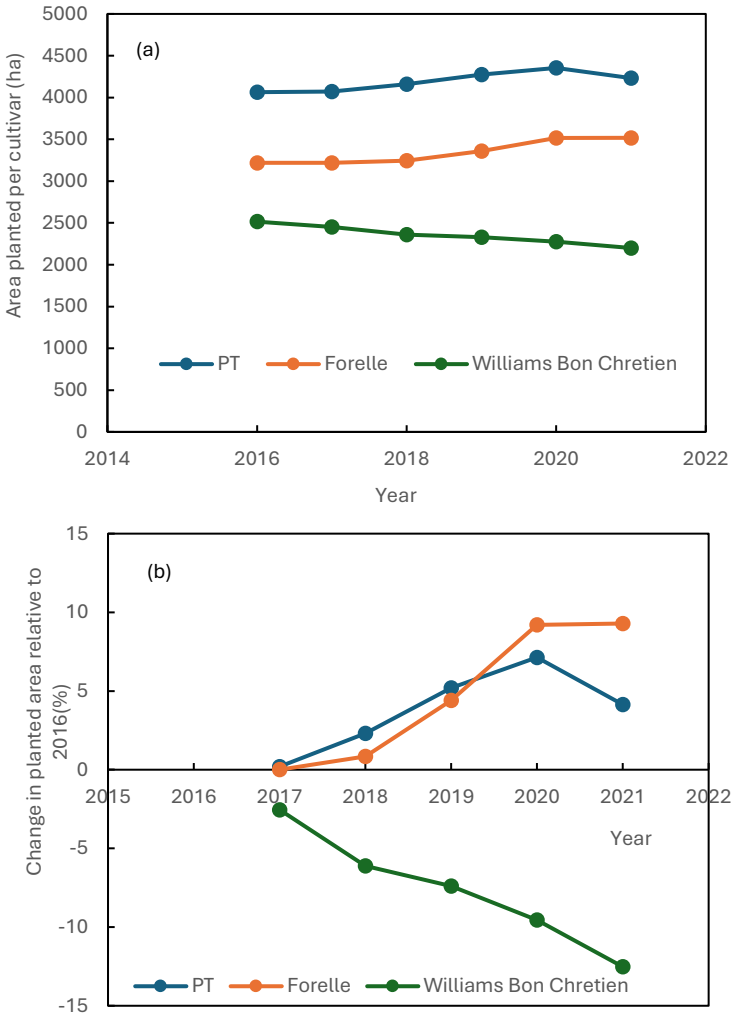


Figure 9.1 (a) Area planted to the top three pear cultivars, and (b) percentage change in the area planted to each cultivar relative to 2016 (after Hortgro, 2021)

Modern pear trees are comprised of two different genetic components i.e. a scion budded onto a rootstock. The scion is usually the cultivar of interest (see Table 2.3). European pears are grafted, either onto pear or quince rootstocks (Theron et al., 2008). Most pear rootstocks are too vigorous for intensive orchards, while quince rootstocks induce less vigour, but incompatibility may be a problem (North et al., 2015). Rootstocks play an integral role in influencing the tree vigour, growth habit, cropping, resistance to pests and diseases, as well as tolerance to unfavourable conditions in the growing environment. The rootstocks that are currently in use in South African pear orchards include pyrodwarf (PD), Old Home' × 'Farmingdale' (OHxF) 217, BU2/33, BP3, OHxF40 and BP1, as well as the dwarfing Quince C51 rootstocks, among others. The most-planted rootstocks are BP1 and BA29, with much smaller numbers of QC51 and OHxF (Ferrandi et al., 2002; Jacobs & Cook, 2002). Numerous studies have reported the performance of different pear rootstocks (du Plooy & van Huyssteen, 2000; Ferrandi et al., 2002; North et al., 2015).

Over the years, the production of pears has increased from about 362 161 tons in 2012 to 461 201 tons in 2021, which represents an increase of about 27%. On average, 50% of the pears are destined for the export market, 35% are processed, 12% are consumed by the local market and about 3% are dried (Hortgro, 2021). The trends in the utilisation of pears between 2012 and 2021 are shown in Figure 2.2.

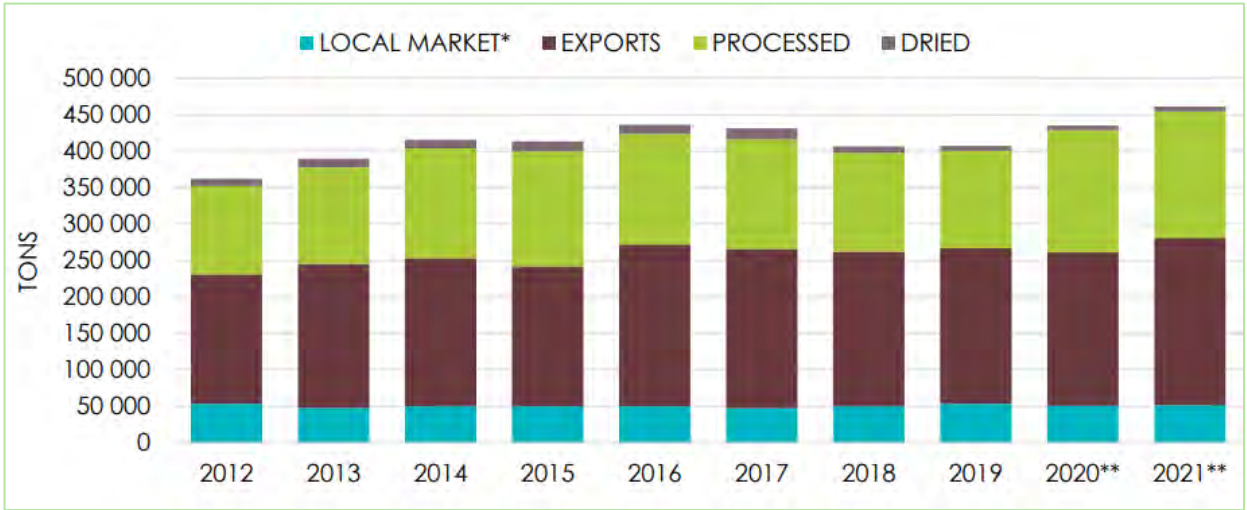


Figure 2.2 Trends in the utilisation of pear fruit in South Africa from 2012 to 2021 (after Hortgro, 2021)

The main markets for South African pears are in the European Union, as well as the UK, Asia and the Middle East.

2.3 FACTORS AFFECTING THE YIELD AND QUALITY OF PEARS

The intensification of fruit production in commercial orchards over the past decades has primarily been driven by economic factors and the need to increase orchard efficiency (Fereres et al., 2008; Robinson et al., 2007). Increasing the productivity of orchards to get higher yields of good-quality fruit at a minimum cost, as well as the use of scarce water, is a priority for sustainability, given the rising production costs and pressure on water resources. Many factors determine the yield and quality of pear orchards. These include, among others, the genetic potential of the cultivars and rootstocks planted, as well as the water stress, soils, environmental factors, management practices and nutrition. However, no single factor or resource controls the variations in the yield and quality of the fruit. Instead, it is the complex interplay between these factors that is important, and this report will describe the role of a few selected key factors. Important fruit quality attributes for pears include: 1) the fruit size; 2) the skin colour; 3) the flesh firmness; 4) the total soluble solids; 5) the titratable acidity; 6) the aroma volatiles; 7) the physiological disorders; 8) the dry matter content; and 9) the fruit mass, among others (du Plooy & van Huyssteen, 2000; Zerbin, 2002).

2.3.1 Cultivars and rootstocks

Cultivar evaluation trials have shown that different pear cultivars have different yield potentials, even under similar growing conditions (Kappel & Quamme, 1988; Reginato & Messa, 2021). However, pear orchards are kept for a long time, probably longer than any other kind of deciduous fruit. Rootstocks are one of the most important factors that influence orchard productivity, as they affect the tree growth, leaf nutrition, yield and fruit quality, and they differ in their resistance to soil-borne pests and diseases and response to environmental factors (Ferrandi et al., 2002; North et al., 2015). Selecting the wrong rootstock may therefore adversely affect productivity throughout the lifetime of an orchard. In South Africa, as elsewhere in the world, the trend in pear-growing is to plant more trees per hectare than in the past (Ferrandi et al., 2002). The careful selection of rootstocks is critical for ensuring early returns on the investment, given the high costs associated with establishing high-density

orchards and for controlling excessive vigour. In this regard, rootstocks that produce the desired growth habit (dwarfing or semi-dwarfing) of the trees and promote high yields early in the orchard's life are ideal.

2.3.2 Soil water availability and water stress

The imbalance between water demand and supply is a common cause of yield decline in orchards (Volschenk et al., 2003; Dzikiti et al., 2018; Gush et al., 2019). This imbalance can be a result of not enough, or too much, water. Water stress can be detrimental to fruit production, by reducing growth and net photosynthesis per unit leaf area (Flore & Lakso, 1989; Landsberg & Jones, 1981). The amount of light intercepted by the canopy, the leaf photosynthesis rate, as well as the allocation of assimilates to fruits, controls the actual fruit yield of orchards (Renquist et al., 1994). In pears, as with other fruit types, the partitioning of assimilates to fruit, as opposed to vegetative sinks, is strongly dependent on the light distribution in the canopy and the crop load (Wünsche, 1993; Marsal et al., 2008). Advanced foliar damage and/or leaf senescence caused by water stress could limit carbohydrate availability for growth and development, which, in turn, has an adverse effect on the fruit bud formation, fruit set and fruit size (Naor et al., 2006).

Yield is a function of the number of fruits on the trees, as well as the fruit size. The critical processes to achieve the yield potential of the current year are therefore initial and final fruit set, as well as the fruit growth, assuming that there is adequate fruit bud formation and flower density (Wand et al., 2008). Early season water stress in pome fruit, such as apples and pears, reduces the fruit set, which leads to less fruit per cluster, and it interferes with flower bud morphogenesis (Landsberg & Jones, 1981), while limiting the irrigation water increases the fruit drop (Assaf et al., 1974; Assaf et al. 1975). The effects of water deficit on the yield are more pronounced during budbreak and flowering (Stage 1), the beginning of rapid shoot growth (Stage 2) and the beginning of fruit fill (Stage 3) (Figure 2.3, Boland et al., 2002). Large numbers of flowers and fruit-lets drop, when subjected to water stress, which culminates in low yields at the end of the season. In general, severe water deficits that are imposed by a lack of, or poor, irrigation practices not only reduce the current year's yields, but it also affects production in subsequent years (Ebel et al., 2001; Fereres et al., 2008). Water stress exacerbates alternate bearing, and the intensity of this phenomenon is more pronounced in some cultivars than in

others. According to the Australian Department of Research and Extension, several measures can be taken to minimise the impact of water shortage on pear production during periods of severe water limitations e.g. during droughts (Goodwin et al., 2015). One option is the so-called 'parking the trees'. This approach basically sacrifices the crop and applies minimal irrigation, so that the trees survive and return to full production the following year. With this approach, the trees are managed, in order to minimise the transpiring leaf area and avoid excessive water stress, so that developing fruit buds are not desiccated. Parking the trees can be achieved by withholding irrigation until the root zone (defined as containing 80% of the root system) dries to a minimum soil water tension, around 400 kPa. Deficit irrigation can also be applied, where the trees receive about 30% of the full crop water requirement.



Figure 2.13 The growth cycle of pome fruit (after Boland et al., 2002)

Another option that is used to conserve water in pear orchards during periods of severe water shortages is by removing the fruit (Marsal et al., 2008). Fruits are a strong sink for assimilates and they require higher photosynthetic rates, which can be achieved by opening the stomata more. This leads to a higher stomatal conductance and, hence, higher transpiration rates, which is undesirable during times of water shortages. Removing the fruit also increases

the amount of carbon that is available for developing buds for the next season's crop. Marsal et al. (2008) investigated, in detail, the mechanisms by which pear fruit removal can improve the tree water status and alleviate the effects of drought. In their study, they had control trees that received full irrigation with no fruit thinning. The other treatments included trees with fewer fruit than the control, others were under deficit irrigation, others with root pruning, as well as combinations of these treatments. They observed that fruit thinning reduced the leaf stomatal conductance for at least 30 days, beyond which no further responses were observed. The effects of the reduced crop load on the stem water potential peaked 30-40 days after fruit thinning, and then it tended to decline thereafter.

Removing water shoots is another management practice that can be used to reduce water consumption during periods of limited water. Shoot growth is often quite strong in spring, as the trees utilise residual moisture stored in the soil profile from the winter rains. Therefore, summer pruning to remove water shoots is encouraged, to reduce the transpiration rate of the trees. This also increases fruit initiation, by removing another sink for assimilates. Another more radical step is to de-branch the trees, in order to reduce the transpiring leaf area. While this method definitely reduces the tree water consumption, it has negative repercussions in the long run, through the loss of bearing sites on the trees. Part of the next season's crop is also removed, which is undesirable.

According to Goodwin et al. (2015), reducing the irrigation of pear trees post-harvest can also lead to water savings. A study on the Williams Bon Chretien pear orchards in Australia showed that applying different levels of water deficit postharvest had no effect on the subsequent yield or fruit quality. But similar research is required in South Africa, in order to establish whether there are no negative repercussions on the cultivars that are grown here.

Pears are one of the first fruit crops on which the Regulated Deficit Irrigation (RDI) strategy was applied (Chalmers et al., 1986). The utilisation of this technique has since spread to a wide range of other crop types. RDI is often used to conserve water and to maintain the fruit yield and quality during times of drought. Regulated deficit irrigation has the effect of reducing excessive vegetative growth, with no effects on the fruit size. Generally, RDI is applied during the period when shoot growth is most rapid and fruit growth is slow (Figure 2.4). The timing of the application of RDI is critical to achieve the desired outcome. According to Goodwin and colleagues (2015), the pear trees are irrigated with greatly-reduced volumes of water,

compared to normal irrigation, with irrigation replacements of less than 30% of normal irrigation being required for the slow fruit/ rapid shoot growth phase (Figure 2.4). However, water stress must not occur during the final growth stage, when fruit growth is most rapid. The replacement of 100% of the irrigation water requirements is recommended at this late stage. Given the growing water scarcity in the pear-producing areas of the country, a study on deficit irrigation on pears was done by Volschenk (2014) in the Warm Bokkeveld. The study focused on mature 'Forelle' pear trees on BP3 rootstock, which were subjected to 15 irrigation treatments. These consisted of combinations of 50%, 70% or 90% Plant Available Water (PAW) depletion, or no irrigation during four phenological phases (see Figure 2.3). These included the vegetative growth and cell division, cell enlargement, fruit ripening and post-harvest. According to Volschenk (2014), the response of the trees was evaluated over three seasons (2008/09, 2009/10 and 2010/11), in order to develop guidelines for optimal irrigation management.

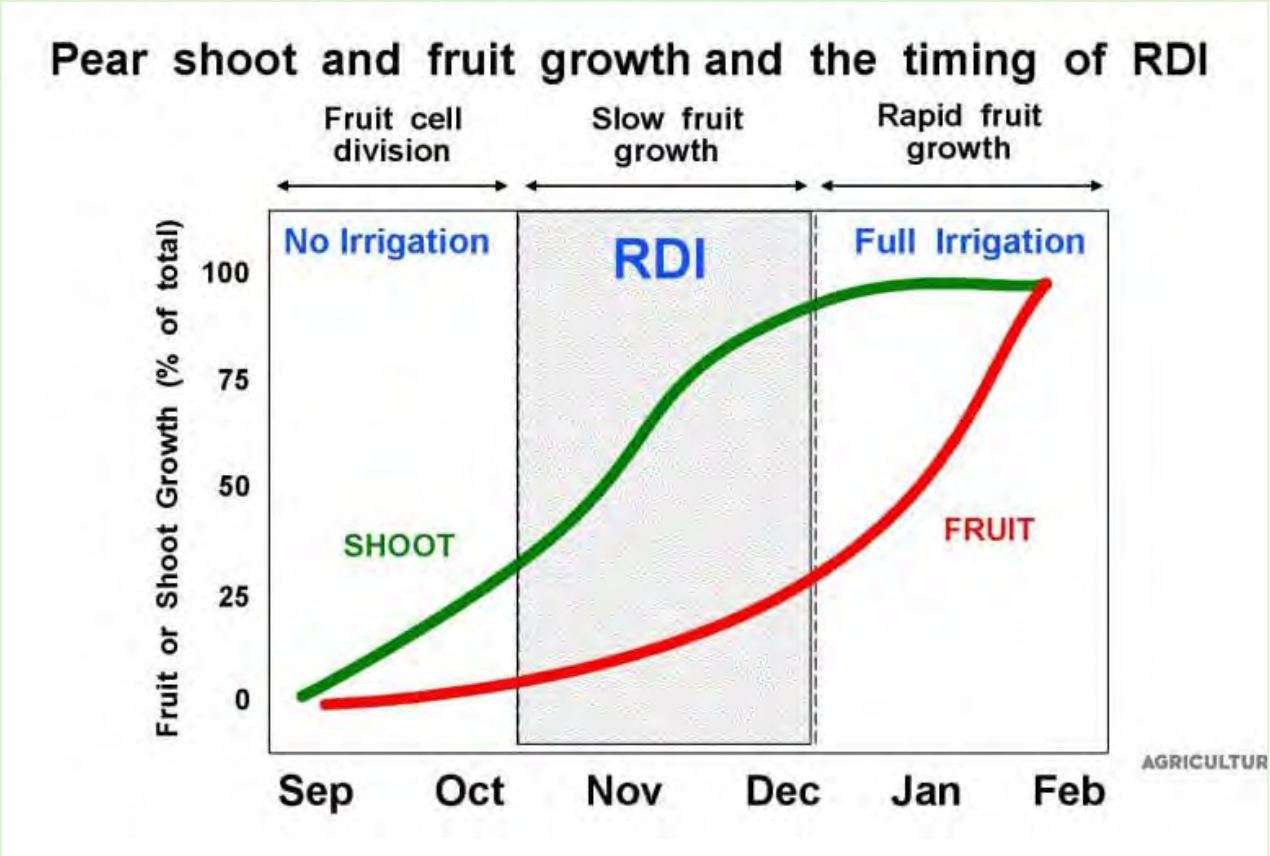


Figure 2.22 Pear shoot and fruit growth and the timing of RDI (after Goodwin et al., 2015)

Trees irrigated at 90% PAW depletion during Phases 2 or 3, or throughout the season, and trees that received no irrigation during Phase 3, had earlier leaf fall, as well as out-of-season bud-break and bloom. Limiting irrigation during ripening or throughout the foregoing season decreased the flower index and the number of flowers per bunch in the following season. Water deficits, particularly in Phases 2 and 3, or throughout the season, reduced the yield by having an effect on the fruit growth, final fruit size and fruit numbers. Limited irrigation during the vegetative growth and fruit cell division phase or post-harvest, which did not decrease the yield significantly, seems to have the potential to save water. Water deficits in Phases 2 and 3 enhanced the fruit maturation in all seasons.

Too much water in the root system is just as damaging to production as a water deficit. Excess soil moisture leads to anaerobic conditions in the soil, which results in the closure of water conducting channels, called aquaporins, as the pH changes (Taiz et al., 2018). The closure of the aquaporins results in the low or poor uptake of water and nutrients, which causes severe injury to the root system and to the tree itself. The roots in waterlogged soils stop growing, the mineral uptake ceases, the leaves turn yellow and remain small, and eventually the roots begin to die. The trees exhibit symptoms that are similar to those induced by water deficit stress. Besides the primary damage to the tree and fruit, the root system becomes more susceptible to infections. Often pear trees in poorly-drained areas are infected by Phytophthora (crown rot), and the condition of the orchard slowly declines over one or more years.

2.4 QUANTIFYING ORCHARD WATER USE

Numerous studies have been conducted in South Africa and elsewhere to quantify the water use of fruit orchards (Gush & Taylor, 2014; Volschenk, 2017; Dzikiti et al., 2018; Taylor & Vahrmeijer, 2018; Taylor et al., 2022). The term ‘orchard water use’ is usually partitioned into components, namely, the plant transpiration component and the orchard floor evapotranspiration component. Plant transpiration refers to the loss of water through the stomata on the leaves or other active plant material e.g. cover crops, weeds, etc. However, in most studies, orchard transpiration has mostly referred to tree transpiration, with transpiration by under-storey vegetation considered to be negligible. A few recent studies have quantified the transpiration dynamics of the under-storey vegetation and found that, at times, these have made a considerable contribution to the orchard transpiration flux, depending on orchard floor

management practices and irrigation type (Ntshidi et al., 2020). Numerous methods have been developed and employed to quantify the water use in fruit orchards. In the next sections, we summarise the key strengths and weaknesses of these methods, as they are applied to individual plants and on a whole orchard scale.

2.4.1 Transpiration measurements

Sap flow monitoring techniques that measure transpiration at a branch, or whole plant, level are the most widely-used methods (Smith & Allen, 1996; Steppe & Dzikiti, 2006; Dzikiti et al., 2022). Individual plant sap flow rates are normally scaled up to whole field water use by using empirical relationships (Gush et al., 2019; Ntshidi et al., 2020). A common feature of all sap flow monitoring techniques is that they involve the injection of heat into the plant and they resolve the resultant temperature gradients to calculate the sap volume flows. According to Smith and Allen (1996), sap flow measuring techniques can be classified into continuous heating and pulsing (non-continuous heating) methods. It is rare to find a sap flow monitoring method that suits all situations. The appropriate sap flow technique depends on the unique circumstances of each study; therefore, when designing experiments, a knowledge of the various methods that are available is essential.

While most sap flow monitoring techniques are easy to understand, install and operate, huge errors can easily creep in if due diligence is not exercised. Data reduction can also be quite complicated and may require various corrections e.g. for wounding created by drilling the trees, determining some parameters to force the closure of the energy balance or to zero temperature gradient signals. Allen et al. (2011a) noted that sap flow monitoring methods, while potentially useful in understanding the actual plant water consumption, can be potential sources of huge errors (as much as 100%) in poorly-designed experiments. In the following sections, we summarise sap flow measurement techniques that have been used to estimate crop water requirements in South Africa.

2.4.1.1 Tissue heat balance sap flow gauges

Tissue Heat Balance (THB) sap flow sensors (Dynamax, Houston. TX, USA) measure the sap flow rate by using the principle of the conservation of energy (Figure 2.5). They are the most direct method for quantifying the sap flow that does not require information on the

anatomy of the plant (van Bavel & van Bavel, 1987). They are a continuous heating sap flow monitoring method that can be used on both woody and herbaceous plants. The THBs can be used on plants with diameters ranging from as small as 2.0 to 130 mm. They have been used in South Africa to quantify the transpiration dynamics of maize crops (Savage et al., 2001), sugarcane (Giteshi et al., 2017), young apple trees (Dzikiti et al., 2018), as well as understorey grass species on orchard floors (Ntshidi et al., 2020). They have been used elsewhere to study complicated the physiological responses of tree crops related to the phenomenon of stomatal oscillations (Steppe et al., 2006; Dzikiti et al., 2007). Because the sensors are wrapped around the plant organ of interest, they are also called the collar method.

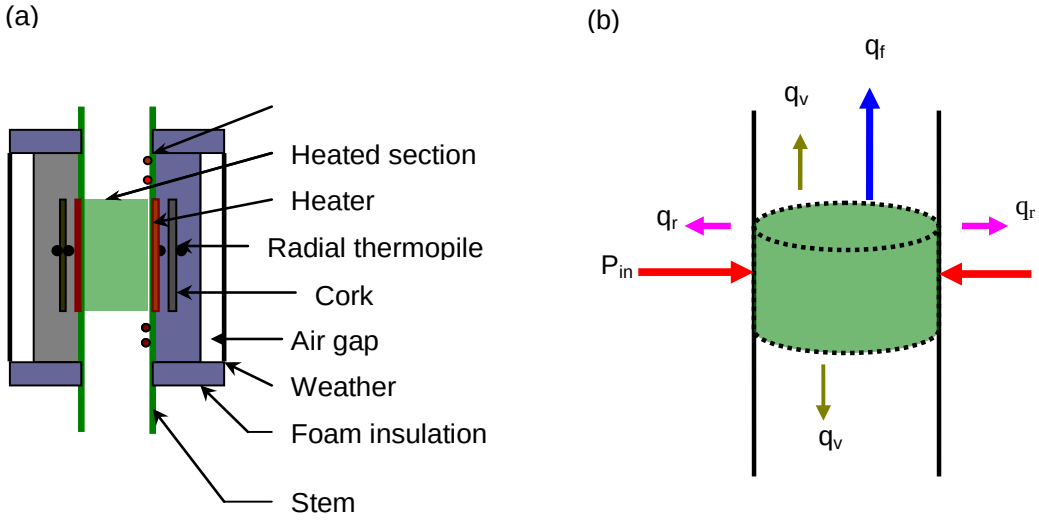


Figure 2.31 Schematic representation of the heat balance sap flow gauge (Dynamax, Houston, TX, USA): (a) Vertical section through the stem heat balance sap flow gauge; (b) Energy balance components of the heat balance sap flow sensor

In this technique, a known constant power, P_{in}, is applied to the plant segment encircled by a small flexible heater (Figure 2.5a), typically a few centimetres in width, wrapped around the organ where sap flow is to be measured (Smith & Allen, 1996). The energy balance equation for that segment is solved for the amount of energy taken up by the moving sap stream under steady-state conditions. This energy is then used to calculate the mass flow of sap in g h^{-1}. With this method, it is essential that the heater is the sole source of energy, so that all the input and output energy fluxes can be accounted for. Thus, it is crucial to insulate the gauge, in order to cut out energy inputs from the environment and to maintain steady-state conditions in the gauged area. Suppose the power input to the plant organ (e.g. the stem in Figure 2.5b) is P_{in},

then, according to Sakuratani (1981) and Baker & van Bavel (1987), the heat balance of the stem can be written as:

$$P_{in} = q_v + q_r + q_f \qquad \text{(W)} \qquad (2.1)$$

where q_v is the rate of vertical heat loss by conduction, q_r is the radial heat loss by conduction through the sensor, and q_f is the heat uptake by the moving sap stream (Figure 2.5b). The value of q_f is obtained by subtracting q_v and q_r from P_{in} which can all be measured. If ΔT_a and ΔT_b are the temperature gradients measured by the axial thermocouples above and below the heater, and ΔT_r is the radial temperature gradient, then applying Fourier's law for one-dimensional heat flow, q_v is calculated by using:

$$q_v = A_{st} k_{st} \left(\frac{\Delta T_b - \Delta T_a}{x}\right) \qquad \text{(W)} \qquad (2.2)$$

where A_{st} is the cross-sectional area of the heated section, k_{st} is the thermal conductivity and x is the distance between the two thermocouple junctions on each side of the heater. The radial component of the stem heat balance, q_r, is determined from ΔT_r by using:

$$q_r = K_{sh} \Delta T_r \qquad \text{(W)} \qquad (2.3)$$

where K_{sh} is the effective thermal conductance of the sheath of materials surrounding the heater. The value of K_{sh} is unknown and depends on the thermal conductivity of the insulating sheath and stem diameter. This is determined from the energy balance equation during periods when q_f is zero. This condition is approached at pre-dawn.

The disadvantages and sources of error in THB sap flow gauges arise from: 1) the effects of the stored energy in the gauged area which are not taken into account, and 2) the thermal gradients e.g. early in the morning, when the sun shines on the exposed parts of the plant tissues. Therefore, the thorough insulation of the gauge with shiny reflective material is mandatory. In addition, the gauges must be installed at least 1.0 m above the ground, in order to minimise the sharp changes in the temperature gradient caused by cold sap from the soil into the warmed plant organs (Steppe & Lemeur, 2004). Thirdly, the Ksh factor may change over time, and this must be constantly recalculated. Lastly, the tissue heat balance sap flow method is a continuous heating method that requires a lot of power. Therefore, it is not suitable for use

in remote sites. The prolonged exposure of plant tissues to the sensors may lead to constriction in fast-growing plant parts, having a girdling-like effect, and the plant may die as a result.

The THB sensors can be installed on the stem of the plant in which the transpiration of the whole plant can be measured. They can also be used to measure transpiration by the fruit. When installed on tree branches, additional data are required to scale up the branch sap flow to the equivalent water depth units in mm per unit time, which is required for the calculation of the water consumption or crop factors. For example, if SF_i is the sap flow (in cm^3/h) of a single plant branch whose leaf area is A_i, then the total transpiration (T_c, in mm) by the field can be calculated as:

$$T_c = \sum_i \frac{SF_i}{A_i} \times LAI_c \qquad (\text{mm d}^{-1}) \qquad (2.4)$$

where LAI_c is the leaf area index (m^2 of leaf area per m^2 of ground area) of the crop.

In situations where both evapotranspiration (ET) and orchard transpiration T are measured simultaneously, orchard floor evaporation (E_s) can be estimated as:

$$E_s = ET - T \qquad (\text{mm d}^{-1}) \qquad (2.5)$$

This relationship can allow the distinction between the beneficial (e.g. transpiration used to grow the crop) and the so-called non-beneficial water uses lost as field-floor evaporation (Gush & Taylor, 2014; Dzikiti et al., 2018; Ntshidi et al., 2020). The tissue heat balance sap flow method will only be used either on small trees (where other methods are not appropriate) or to measure the transpiration fluxes into fruit, the root water uptake patterns or the understorey vegetation transpiration rates.

2.4.1.2 Thermal dissipation probes

Thermal Dissipation Probes (TDPs, also called Granier probes) are probably the cheapest type of sap flow probes (Granier et al., 1985). These are comprised of a pair of thermocouples installed about 4.0 cm apart (Figure 2.7), and commercial versions can be purchased from companies like Dynamax Inc., Houston, USA, although custom-made versions are frequently used. The lower probe is just a thermocouple that measures the sapwood temperature, while the upper probe comprises a thermocouple and a heater. Therefore, a temperature difference (ΔT) exists between the two probes at any given time. As in the THB

method, heat is also applied continuously by using a voltage in the range 3 to 8 V, depending on the size of the probes. The longer the probes, the higher the voltage is required to apply heat uniformly along the probe length. The ΔT at a given time is a function of the sap flow rate.



Figure 2.40 Measurement of transpiration on young trees using Granier probes

When the sap flow rate is high, which is what happens during the daytime, the ΔT is small, and vice versa. Therefore, the time series of the ΔT signal over the course of a day is the inverse of the sap flow. To swap the signal around, Granier (1981) defined an empirical parameter K as:

$$K = \frac{\Delta T_{max} - \Delta T}{\Delta T} \qquad (2.6)$$

where ΔT_{max} is the maximum temperature difference between the probes. This is recorded during periods when the sap flow is low or zero, typically at pre-dawn. Using data from a range of plant species, Granier (1981) related K to the sap velocity (V_s, in cm h^{-1}) by using the relationship:

$$V_s = 0.0119K^{1.231} \quad (2.7)$$

V_s is equivalent to the sap flux density expressed in cm^3 of water cm^{-2} of sapwood area per unit time. The use of Equation 2.7 is often cited as a major source of uncertainty for this method (Steppe et al., 2010; Dzikiti et al., 2011; Pasqualotto et al., 2019). Steppe et al. (2010) noted that the sap flow rate can be underestimated by up to 70% by using this method, partly due to the empirical nature of the equations that are used. As a result, most researchers prefer to independently calibrate the TDPs and to derive species-specific parameters in which Equation 20 can be rewritten as:

$$V_s = aK^b \quad (2.8)$$

where 'a' and 'b' are parameters that can be obtained by linearising Equation 2.8 as a function of the known sap flux density. If the sap velocity is known, the sap flow volume (SF, in $cm^3\ h^{-1}$) can then be calculated as:

$$SF = A_s \times V_s \times 3600 \quad (2.9)$$

where A_s is the sapwood area and 3600 is the number of seconds in an hour.

The advantages of the TDPs are that they are cheap, easy to construct and to operate. They can be used on both woody and non-woody plant species. Their major disadvantage is their low accuracy, compared to other methods, as detailed by Steppe et al. (2010). Heat is applied continuously, so they have high power requirements, which makes it expensive to operate them in remote sites. Solar panels can help as a source of power, but they are prone to theft. The TDP method is invasive, as it involves drilling the plants. However, readings from the TDPs are typically not corrected for wounding, because the sap velocity is calculated from the ratio of the temperatures.

2.4.1.3 Heat Ratio Method

The Compensation Heat Pulse velocity (CHP) technique (Green et al., 1986) is by far the most widely-used pulsing sap flow monitoring method. Early research in South Africa on the water use of tree species used this technique (Dye et al., 1996; 1999). In recent years however, a modification of the CHP, called the Heat Ratio Method (HRM) has gained prominence (Burgess et al., 2001). This has, in many instances, replaced the CHP and over 90%

of the sap flow data on tree crops in the country were collected by using this technique. The HRM comprises of two thermocouples that are installed into the sap wood of the stem at equal distances (~ 0.5 cm) up and downstream of a central heater (Figure 2.7). These thermocouples are marked as T_1 and T_2 in Figure 2.7. This method is suitable for use on woody species with a diameter of at least 4.0 cm (Allen et al., 2011a).

In a typical measurement cycle, all the thermocouples are read to record the reference sapwood temperatures, say T_1 and T_2. This is immediately followed by the injection of a pulse of heat (~ 30 – 50 W) for between 1 and 2 seconds. Thereafter a waiting period in the region of 60 to 90 s is observed, in order to allow the heat to distribute within the tissues. The manner of the heat distribution depends on the rate of sap flow. In the last stage of the measurement cycle, the post-heating temperatures of the thermocouples (e.g. T_1' and T_2') are read and recorded. These measurements are usually repeated a few times per sensor, in order to ensure that the peak temperature is recorded. According to Burgess et al. (2002), the heat pulse velocity (V_h, in cm h^{-1}) is then calculated as:

$$V_h = \frac{k}{x} ln\left(\frac{\Delta T_1}{\Delta T_2}\right) \quad (2.10)$$

where k is the thermal conductivity of the wood, x is the distance of each thermocouple from the heater (~0.5 cm), and ΔT_1 and ΔT_2 are the changes in temperature recorded by the upper and lower thermocouples, respectively. The additional data that are required include the wood density, the moisture fraction and the wound width to correct for the effects of wounding created by drilling and the presence of probes in the transpiration stream. Details of the wounding corrections can be found in Burgess et al. (2002).

The advantage of the HRM technique is that it is a pulsing method. Therefore, it has low power requirements, which make it ideal for use in remote sites. It is accurate for both low and high flows and it can measure reverse sap flows. As a result, it is a valuable tool for ecohydrological studies to understand processes, such as the hydraulic redistribution in plants (Dzikiti et al., 2013; 2017). The sources of error arise from probe misalignments; therefore, drilling and the installation of the thermocouple probes must be done as carefully as possible. The wounding correction and wood density have a very large effect on the outputs of the method. These corrections must be implemented as carefully as possible. Sap velocity varies radially, from the bark to the heartwood (Wulschleger & King, 2000). The flow is fastest in the

younger xylem that is located close to the cambium, and it is slowest towards the heartwood, where there are old collapsed, cavitated and/or occluded vessels (Lambers et al., 2006). Therefore, measurements at several locations along the radial stem cross section are needed, in order to obtain a representative average of the sap velocity.

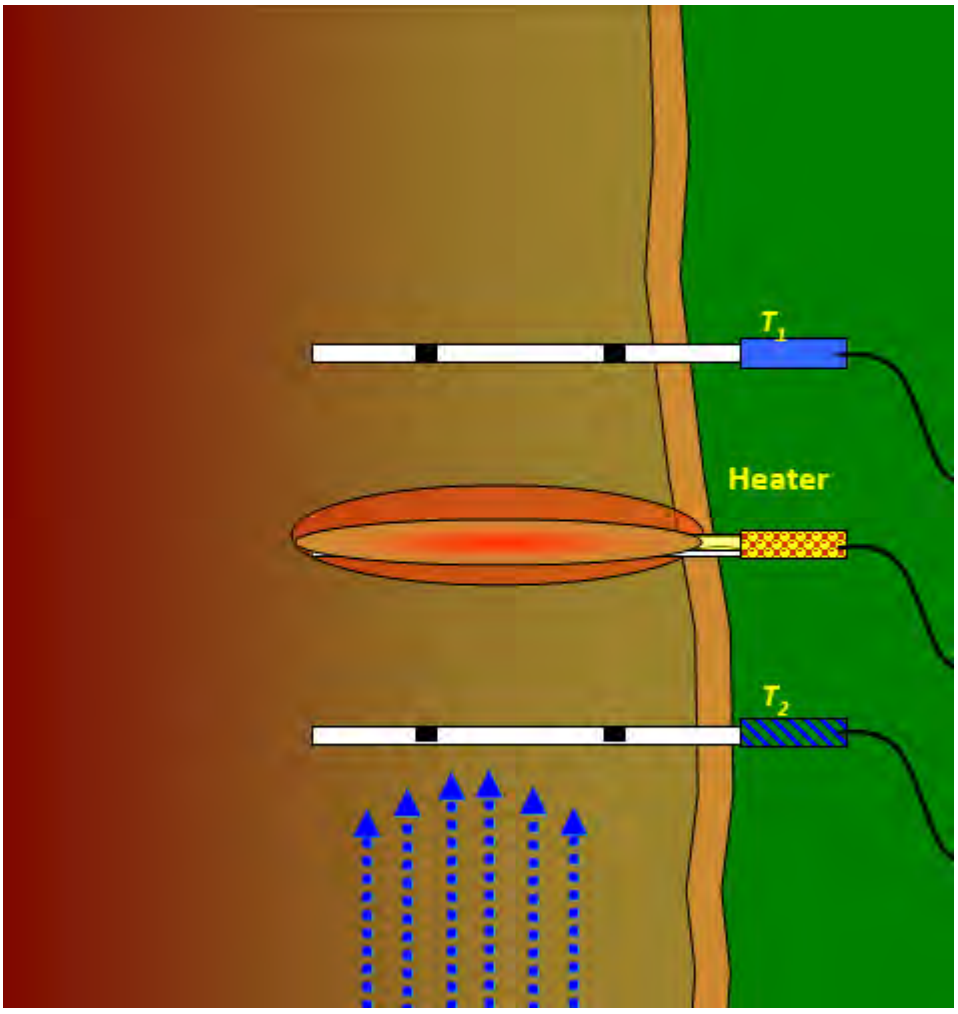


Figure 2.49 Schematic diagram of the heat ratio method (HRM) of monitoring sap flow (after Rafael Oliveira)

This requires more sensors, which may raise the costs. Lastly, the method requires a knowledge of the extent of the sapwood area where the xylem vessels are actively involved in water transport. Inaccurate estimates of the sapwood area can be a source of significant uncertainty in the water use data that are measured by this method.

2.4.2 Determining whole orchard evapotranspiration

Accurate measurements of the crop evapotranspiration (ET) are key for the derivation of accurate crop coefficients ($K_c = ET_c/ET_o$), which are used for irrigation planning. Earlier estimates of the water requirements of irrigated crops in South Africa were done mostly by using Class A evaporation pans and lysimeters (Green, 1985; Dent 1988). However, significant uncertainties were observed, especially with the Class A pan (Annandale et al., 2011). This has necessitated further research to update the crop water use information by using more recent measurement and modelling techniques (Gush & Taylor, 2014). Several methods have been developed in recent years to quantify evapotranspiration in crop fields and the natural environment. The most widely-used techniques include micrometeorological methods, such as the eddy covariance (also called eddy correlation), scintillometry, surface renewal and the Bowen Ratio methods.

Remote sensing methods have also been developed and tested on various crops in South Africa, with products such as the Surface Energy Balance for Land (SEBAL) (Bastiaansen et al., 1998) and ETLook (Bastiaansen et al., 2002) being the most popular with farmers. The soil water balance method, using a range of soil moisture sensors that include neutron probes, time domain reflectometers and capacitance probes, still remains widely used, both in research and for practical irrigation management. A detailed review of the advantages and disadvantages of the various ET estimation methods was published by Allen et al. (2011a). They provided further details on critical information for the reporting of ET data, in order to allow users to discern between good and bad quality data (Allen et al., 2011b). These techniques differ in their level of complexity, their operating principles and the assumptions behind them. In the next section, we summarise only those methods that have been used on South African crops. More complete details can be found in the references that are cited. The most widely-used methods include the eddy covariance, surface renewal, soil water balance and remote sensing approaches.

2.4.2.1 Eddy Covariance Method

The eddy covariance method (Figure 2.8) is the most widely-used micrometeorological technique for quantifying evapotranspiration over large fields (Dzikiti et al., 2018; Paco et al., 2019; Ntshidi et al., 2020). It also measures the atmospheric CO_2 concentration and other trace

gases, such as ozone and methane. Therefore, it is a valuable tool for studying ecosystem exchanges and climate change studies. The eddy covariance method is based on the principle that fluxes of momentum, heat and mass over crop canopies are due to the swirling movement of small pockets of air called eddies, which cause air turbulence (Campbell & Norman, 1998). These fluxes can be determined by taking measurements of the air temperature (T_a) and vertical wind speed (ω) at high frequencies, typically 10-20 Hz, and by calculating the covariance between them:

$$H = \rho C_p \sum(\omega - \bar{\omega})(T_a - \overline{T_a}) \qquad (2.11)$$

where H is the sensible heat flux (in W m^{-2}), ρ is the density of air, C_p is the specific heat capacity of air at a constant pressure, and T_a is the air temperature. The wind speed ω and T_a are measured by using sonic anemometers, and there are various types that are commercially available. The latent heat flux (LE), which is the energy-equivalent of evapotranspiration (ET), can be calculated in two ways. Firstly, as a residual of the surface energy balance equation, if all the other terms are known. The disadvantages of this approach are that: (a) the calculation assumes energy balance closure (Burba & Anderson, 2010), which is often problematic, and (b) the net radiation (R_n) and soil heat flux (G) must be measured accurately (Allen et al., 2011a).

Secondly, the direct measurement of ET using the eddy covariance method can also be done through the covariance of the vertical wind speed and the atmospheric water vapour concentration (e) that is measured by using an Infrared Gas Analyser (IRGA) as:

$$LE = \lambda \frac{M_w/M_a}{P_a} \rho_a \overline{\omega' e'} \qquad (2.12)$$

where M_w and M_a are the molar masses of water vapour and air (g mol^{-1}), P_a is the atmospheric pressure, (kPa), ω' is the instantaneous deviation of the vertical wind speed, e' is the air's vapour pressure and λ is the latent heat of vaporisation. The eddy covariance equipment is quite complex; it requires personnel that are trained in biophysics, atmospheric sciences and electronics for its proper operation. According to Allen et al. (2011a), the inappropriate use of the equipment can lead to misleading information, with errors in the range 30-50%. Therefore, great care is required in the installation of the equipment, as well as in the data collection and processing.

A major requirement for the appropriate use of the eddy covariance are fields that are large in spatial extent, in order to ensure an adequate fetch (Monteith & Unsworth, 1990). Typically for every one-metre height of the infrared and sonic sensors above the crop, an upwind fetch of at least 100 m is required. The use of this method on small fields can lead to errors associated with the so-called clothes-line effect, which may produce unrealistically high ET values, thus producing very high crop coefficients. The theoretical limit for crop coefficients is around 1.4. In addition, the atmospheric boundary layer in small fields is unlikely to have developed to the equilibrium layer, which may influence the results. The sensors must also be a considerable distance above the canopy roughness sublayer, in order to reduce the direct effects of the canopy artefacts on the turbulent fluxes (Pereira et al., 2021b).

Another major requirement for the eddy covariance method is that the IRGA and the sonic anemometer should measure the same air parcel. Therefore, the sensors must be as close to each other as possible, otherwise a correction for sensor separation must be implemented. The post-processing of the high frequency data is critical, in order to reduce the measurement errors.



Figure 2.58 Schematic representation of an eddy covariance micrometeorological method

Mandatory corrections include corrections for air density fluctuations (Webb et al., 1980), as well as coordinate rotations to account for the lack of sensor levelness, spectral corrections etc., as detailed by Burba and Anderson (2010). Another source of error are the disturbances to the normal air patterns, due to the presence of the flux tower and other artefacts e.g. solar panels, data loggers, etc. These generate extra turbulence, which is not related to the natural evaporative process.

2.4.2.2 Surface renewal

Another micrometeorological technique that has been used to quantify crop water use in South Africa and elsewhere is the surface renewal method (Paw U et al., 1995). The method is based on estimating the turbulent exchange of the sensible heat flux (H) between the crop canopy and the atmosphere, which is caused by the instantaneous replacement of air parcels that are in contact with the surface.

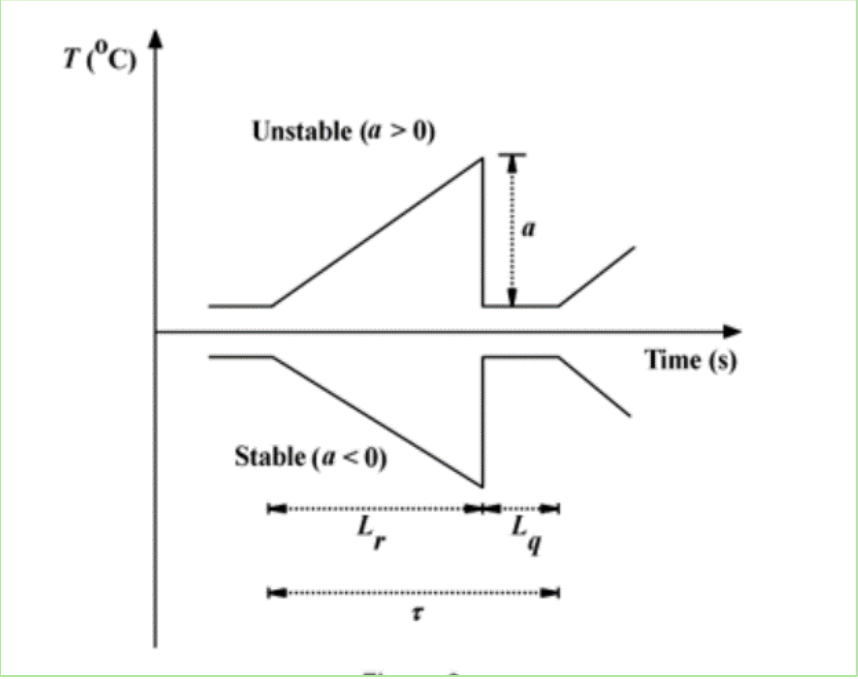


Figure 2.67 An ideal surface renewal analysis ramp model with ramp amplitude for stable (a>0) and unstable (a<0) conditions, ramp period Lr, quiescent period Lq – during which there is no change in air temperature (after Mengistu & Savage, 2010). τ = Lr + Lq is the total ramp period

For this, only the air temperature measured at a high frequency at a single point using unshielded and naturally-ventilated fine-wire thermocouples is required. The theory behind the method is that the air in contact with a crop surface exchanges heat energy with that surface. The air becomes warm, expands, becomes less dense and rises (Mengistu & Savage, 2010; Hu et al., 2018). It is subsequently replaced by cooler and dense overlying air, thereby changing the temperature characteristics of the surface. Air temperature measurements taken at between 2 and 10 Hz shows characteristics which resemble ramp events, as illustrated in Figure 2.9.

According to Paw U et al. (1995) the sensible heat flux can be calculated from the single temperature measurement as:

$$H = \rho C_p \alpha \frac{dT}{dt} \frac{V}{A} \tag{2.13}$$

where α is a correction factor that is derived from independent calibration of the surface renewal method, usually with the eddy covariance method. V/A is the ratio of the air volume to area, which is essentially the height 'z' of the temperature sensor above the ground. Therefore, Equation 2.13 can be written as:

$$H = \rho C_p \alpha \frac{dT}{dt} z \tag{2.14}$$

Therefore, H measured using the surface renewal method is strongly influenced by the placement height (z) of the sensors above the canopy. This parameter must be measured as accurately as possible. If the temperature is measured at canopy height, then z will be equal to the crop height. Pau U et al. (1995) replaced dT/dt with a/τ, so that Equation 2.14 becomes:

$$H = \rho C_p \alpha \frac{a}{Lr+Lp} z \tag{2.15}$$

Complex functions have been developed to accurately determine the ramp amplitude 'a' and total period 'τ'. Details of these can be found in Paw U et al. (1995), Mengistu and Savage (2010) and Hu et al. (2018), among others.

The advantages of the surface renewal method are that the method is: 1) cheaper, as very little instrumentation is needed, 2) very economic on power, so it is ideal for use in remote sites, and 3) it can be accurate, if it is carefully calibrated. The disadvantages of the method are that: 1) it requires a large fetch, like the other micrometeorological techniques, 2) data

reduction and analysis are very complex, 3) it requires the accurate measurement of the vegetation height, which can be a problem in fast-growing plants, 4) it requires calibration with the eddy covariance method, and v) it measures only one component of the surface energy balance (i.e. H). Therefore, accurate measurements of the net radiation (R_n) and soil heat flux (G) are critical for ET to be calculated as the residual in the surface energy balance equation. In South Africa, this method has been used on maize (Savage et al., 2006), sugarcane (Jarmain et al., 2012) and fruit trees (Gush & Taylor, 2014).

2.4.2.3 Soil water balance

The soil water balance method (Figure 2.10) is one of the most widely-used methods for estimating crop water requirements. It is the basis for some of the irrigation scheduling models developed in South Africa, such as the SWB model (Annandale et al., 1999).

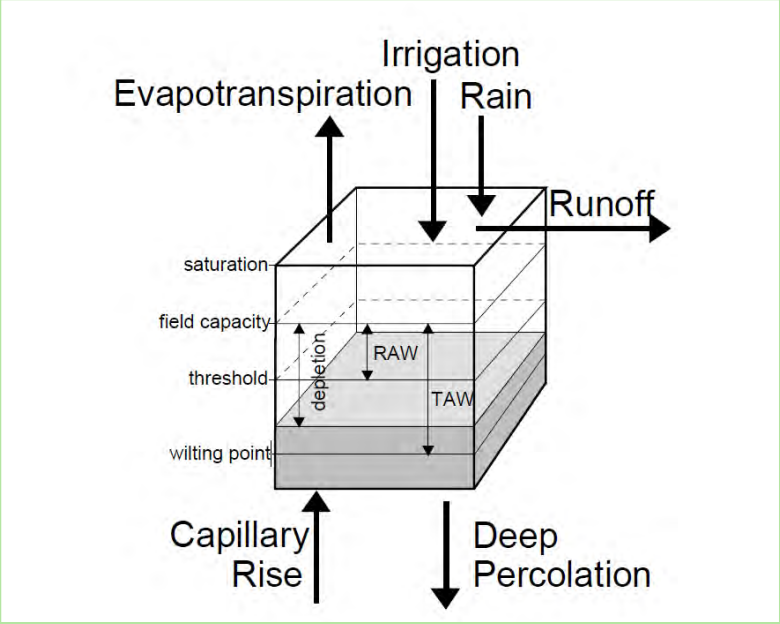


Figure 2.74 Components of the soil water balance in the root zone of plants (after Allen et al., 1998)

The widespread use of the method has mostly been spurred on by the advent of numerous soil moisture measuring devices, such as neutron probes, time-domain reflectometers and capacitance probes (Allen et al., 2011a; Volschenk, 2017). Using the principle of the conservation of mass, rainwater and/or irrigation are lost from the field through

evapotranspiration (ET), Deep Percolation (DP), surface Run Off (RO), and changes in the water stored within the soil profile (±Δθ) (Figure 2.10).

For simplicity, runoff is often assumed to be zero, especially for fields on flat terrain with predominantly sandy soils. The method can be inaccurate e.g. in fields where deep percolation or capillary rise from a shallow water table cannot be account for. For accurate results, fields in which the water table is substantially lower than the root depth is often recommended. Other sources of uncertainty for the soil water balance method include the use of non-calibrated sensors. According to Allen et al. (2011a), some types of soil moisture sensors, e.g. capacitance probes, work best in sandy soils, but they may require calibration in clayey soils. Typical error margins for the soil water balance approach are in the range 10-30%, although they may rise to about 40%, if due care is not taken in the installation, operation and data reduction processes.

CHAPTER THREE

MODELLING WATER USE AND YIELD OF PEAR ORCHARDS

3.0 INTRODUCTION

This study seeks to investigate the water use-yield relationships of two pear cultivars by using data from specific orchards in various production regions in the Western Cape Province. However, in order to scale these data to orchards elsewhere in the country, and beyond, it is necessary to develop models that are not only accurate, but that also use readily-available input data to produce information that growers can use for decision-making. Model outputs that can be useful to fruit growers include: 1) orchard evapotranspiration (ET) and how it varies among pear cultivars, with the crop load and with the seasons; 2) accurate information on the partitioning of ET into actual tree transpiration and orchard floor evaporation, to explore opportunities to save water; and 3) the impact of water deficit on the yield quality and quantity, among others. In the previous WRC/Hortgro funded project (WRC K5 2398//4) on the 'Water use of high-performing apple orchards', a dual source ET model was developed and tested in a range of orchards. This model partitioned the orchard evapotranspiration into its constituent components, namely, tree transpiration and orchard floor evapotranspiration (Dzikiti et al., 2018). Other variants of this model were subsequently developed to include more detail on the contribution of the active vegetation cover on the orchard floor to ET (Ntshidi et al., 2020). Another extension of the modelling work focused on the spatialisation of ET in apple orchards by integrating *in situ* and remote sensing data (Mobe et al., 2021).

Given the physiological similarities between apples and pears, both being pome fruit, a starting point in modelling the water use of pear orchards was to evaluate the ET model that was developed for apples. The ET model for apples is based on a modified version of the Shuttleworth and Wallace (1985) (S-W) Model, as modified and improved by Li et al. (2010) and Dzikiti et al. (2018), among others. For the completeness of this report, we provide the full details of the S-W model (Figure 3.1), as well as the modifications that were made to the original model and those that are proposed for pears. An important extension to this model was the addition of a pear yield sub-model, so that the new model can now produce water productivity (Yield / ET) as another output.

3.1 DESCRIPTION OF THE PEAR ORCHARD WATER USE MODEL

The S-W model is based on a relationship similar to the Penman-Monteith equation, but it is applied separately to the tree canopies and on the orchard floor. The Penman-Monteith approach treats the entire orchard as a single big leaf (Rana et al., 2005), which is not accurate, given the heterogeneity of the orchard surface. According to the S-W approach, the orchard evapotranspiration (λE, in W/m^2) is instead calculated as the algebraic sum of the fluxes from the tree canopies and from the orchard floor:

$$\lambda E = \lambda E_c + \lambda E_s \tag{3.1}$$

where λE_c is the latent heat flux from tree canopies (transpiration) and λE_s is evaporation from the orchard floor. The fluxes are calculated at a reference height x above the orchard (Figure 3.1) and the transpiration (T) and soil evaporation (E_s) components are given by:

$$\lambda E_c = C_c \frac{\Delta A + \left\{ \dfrac{\rho c_p D - \Delta r_a{}^c A_s}{r_a{}^a + r_a{}^c} \right\}}{\Delta + \gamma \left\{ 1 + r_s{}^c / (r_a{}^a + r_a{}^c) \right\}} \tag{3.2}$$

and

$$\lambda E_s = C_s \frac{\Delta A + \dfrac{\left\{ \rho c_p D - \Delta r_a{}^s (A - A_s) \right\}}{r_a{}^a + r_a{}^s}}{\Delta + \gamma \left\{ 1 + r_s{}^s / (r_a{}^a + r_a{}^c) \right\}} \tag{3.3}$$

where C_c is a dimensionless canopy resistance coefficient, C_s is the substrate resistance coefficient, also dimensionless, Δ is the slope of the saturation vapour pressure-temperature curve (kPa K^{-1}), c_p is the specific heat at constant pressure (J kg^{-1} K^{-1}), ρ is the density of air (kg m^{-3}), λ is the latent heat of vaporisation (J kg^{-1}), and D is the vapour pressure deficit of the air at the reference height (kPa). This variable is presented as VPD elsewhere in this report, $r_a{}^a$ (s m^{-1}) is the aerodynamic resistance between canopy source height and the reference level, $r_a{}^c$ (s m^{-1}) is the boundary layer resistance of the canopy, $r_s{}^c$ (s m^{-1}) is the canopy resistance, $r_s{}^s$ (s m^{-1}) is the surface resistance of the substrate, $r_a{}^s$ (s m^{-1}) is the aerodynamic resistance between the

substrate and the canopy source height, and γ is the psychrometric constant (kPa K^{-1}). *A* is the available energy (W m^{-2}) absorbed by the orchard calculated as the difference between the net radiation and the soil heat flux, and A_s (W m^{-2}) is the available energy at the orchard floor calculated from *A* by using Beer's law.

Orchard floor management practices vary among orchards. Therefore, in this model we did not differentiate between evaporation from the bare ground, mulches or transpiration from the cover crops. Rather, we combined total evaporation from all these sources into a single soil evaporation (E_s) for simplicity. The total available energy (*A*, in W m^{-2}) can be calculated as:

$$A = R_n - G \tag{3.4}$$

where (R_n, W m^{-2}) is the net radiation, which can be calculated as:

$$R_n = (1-\alpha)S_d + (\varepsilon_a - \varepsilon_s)\delta(T_a + 273.15)^4 \tag{3.5}$$

where α is the surface albedo of the orchard. Albedo values can be measured by using the four-component net radiometer (Model: CNR4, Kipp & Zonen, The Netherlands). S_d is the downward solar radiation (W m^{-2}), which can be measured by a pyranometer at the weather station located outside the orchards, and T_a is the air temperature (in °C). Sigma (δ) is the Stefan-Boltzmann constant, while ε_a and ε_s represent the emissivity of the atmosphere and the orchard surface, respectively. These were calculated according to Mu et al. (2011) and Bastiaansen et al. (2002) as:

$$\varepsilon_a = 1 - 0.26e^{(-7.77x10^{-4} xT_a^2)} \tag{3.6}$$

and

$$\varepsilon_s = 0.95 + 0.01xLAI \tag{3.7}$$

where LAI is the orchard level leaf area index. The soil heat flux, *G* (in W m^{-2}) in Equation 2.4 was estimated as 20% of the net radiation incidence on the orchard floor ($R_{ns,}$ in W m^{-2}).

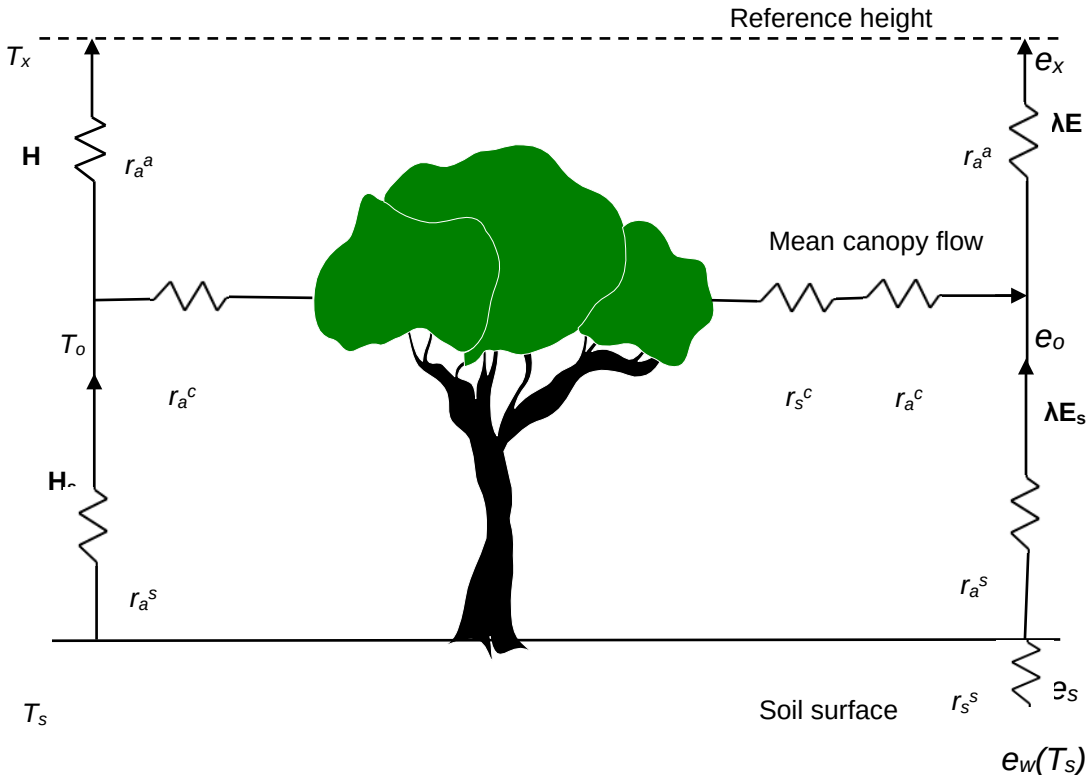


Figure 3.1 Schematic diagram of the S-W model for evaporation from a sparse crop (Shuttleworth & Wallace, 1985)

According to Shuttleworth and Wallace (1985), as well as Li et al. (2010), R_{ns} can be calculated by using Beer's law as:

$$R_{ns} = R_n \bullet e^{-kLAI_o} \tag{3.8}$$

The available energy at the soil surface (A_s, W m^{-2}) can then be given by:

$$A_s = R_{ns} - G \tag{3.9}$$

The extinction coefficient (k) in Equation 3.8 can be taken as a constant at 0.6, according to Impens and Lemeur (1972). According to Shuttleworth and Wallace (1985), the dimensionless constants C_c and C_s in Equations 3.2 and 3.3 are given by the expressions:

$$C_c = \left\{1 + R_c R_a / R_s (R_c + R_a)\right\}^{-1} \tag{3.10}$$

$$C_s = \left\{1 + R_s R_a / R_c (R_s + R_a)\right\}^{-1} \tag{3.11}$$

where:

$$R_a = (\Delta + \gamma) r_a^{\ a} \tag{3.12}$$

$$R_s = (\Delta + \gamma) r_a^{\ s} + \gamma r_s^{\ s} \tag{3.13}$$

$$R_c = (\Delta + \gamma) r_a^{\ c} + \gamma r_s^{\ c} \tag{3.14}$$

The mean boundary layer resistance of the canopy r_a^c and the bulk stomatal resistance of the canopy r_s^c are both surface resistances that are influenced by the surface area of the vegetation present, and can be given by:

$$r_s^{\ c} = \frac{r_{ST}}{2LAI} \tag{3.15}$$

$$r_a^{\ c} = \frac{r_b}{2LAI} \tag{3.16}$$

where r_{ST} is the mean stomatal resistance and r_b the mean boundary layer resistance. The original equations are given in Shuttleworth and Wallace (1985) and these used a constant stomatal resistance (r_{sT}) of 400 s m^{-1}, while the soil surface resistances (r^s_s) were fixed at 0, 500, and 2000 s m^{-1} for wet, moderately wet and dry soils. In this study, as in others, a variable stomatal conductance ($g_{sT} = 1/r_{ST}$) was proposed, following Jarvis (1976). According to this method, if $g_{s\ max}$ is the maximum stomatal conductance for pears, then the stomatal conductance at any given time (in m s^{-1}) is moderated by environmental stress factors according to:

$$g_{ST} = g_{s\max} \times f(R) \times f(T) \times f(VPD) \times f(\theta) \tag{3.17}$$

where *f(R), f(T), f(VPD)* and *f(θ)* are the solar radiation (*R*), air temperature (*T*), vapour pressure deficit of the air (*VPD*) and soil water content (*θ*) stress factors with values between 0 and 1. The stress factor expressions took the following forms:

$$f(R) = \frac{R}{R + k_r} \tag{3.18}$$

$$f(T) = \left(\frac{T - T_{\min}}{T_{opt} - T_{\min}}\right) \times \left(\frac{T_{\max} - T}{T_{\max} - T_{opt}}\right)^{\left((T_{\max} - T_{opt})/(T_{opt} - T)\right)} \quad (3.19)$$

$$f(VPD) = e^{-k_{vpd} * VPD} \quad (3.20)$$

$$f(\theta) = \begin{cases} 1 & \theta \geq \theta_{FC} \\ \left(\frac{\theta - \theta_{WP}}{\theta_{FC} - \theta_{WP}}\right)^{\beta} & \theta_{WP} < \theta < \theta_{FC} \\ 0 & \theta \leq \theta_{WP} \end{cases} \quad (3.21)$$

where k_r, k_{vpd}, and β are parameters obtained by model optimisation and are defined in Table 3.1. Equation 3.18 has been applied on maple trees (*Acer rubrum*) by Bauerle et al. (2002), while Equations 3.19 and 3.20 were used in a sugarcane ET model in South Africa by Bastidas-Obando et al. (2017). Equation 3.20 was adopted from Egea et al. (2011), where θ_{FC} and θ_{WP} represent the volumetric soil water content at field capacity and permanent wilting point in the root zone.

The soil surface resistance can be derived from the soil water content in the top 15 cm (θ_{15}) by fitting a power function proposed by Poyatos et al. (2007) as:

$$r^s_s = \begin{cases} 0 & \theta \geq \theta_{FC} \\ b_1\left(\frac{\theta_{15}}{\theta_{15FC}}\right)^{b_2} & \theta_{WP} < \theta < \theta_{FC} \\ 2000 & \theta < \theta_{WP} \end{cases} \quad (\text{s m}^{-1}) \quad (3.22)$$

b_1 and b_2 are model parameters, which can be obtained from hourly soil evaporation measurements, using micro-lysimeters. The symbol θ_{15} represents the hourly average soil water content of all the soil moisture sensors at a 15 cm depth, and θ_{15FC} is the volumetric water content at field capacity at a 15 cm depth.

Table 3.1 Parameter values for the modified Shuttleworth and Wallace model applied to pear orchards

Parameter	Description	Value
$*b_1$	Value of soil surface resistance when $\theta_{15} = \theta_{FC}$ (in s/m)	200
$*b_2$	Describes the non-linear changes in surface resistance with soil moisture (-)	-5.83
β	Describes the curvature of f(θ) (-)	1.231
K	Extinction coefficient	0.6
k_{vpd}	Describes the influence of the VPD stress factor - f(VPD) (-)	1.33
k_r	Describes the curvature of $f(R_s)$ (in W m^{-2})	302
r_{ST}	Minimum stomatal resistance (in s m^{-1})	116
r_b	Boundary layer resistance (s m^{-1})	26.6
T_{max}	Maximum temperature for complete stomatal closure (in °C)	45
T_{min}	Minimum temperature at which stomata close (in °C)	3
T_{opt}	Optimum temperature for growth of the trees (in °C)	23

3.2 MODELLING YIELD OF PEAR ORCHARDS

Yield data (in kg per tree and converted to tons per ha) were harvested from 10 tagged trees per orchard and compared with that from the farm at the end of each growing season. We modelled the yield by using the approach proposed by Stewart et al. (1977). According to this method, the relative yield reduction ($1 - Y_a/Y_m$) is related to the relative evapotranspiration deficit ($1 - ET_a/ET_m$) by:

$$1 - \frac{Y_a}{Y_m} = K_y \left(1 - \frac{ET_a}{ET_m}\right) \quad (3.23)$$

where Y_a is the actual yield (ton ha^{-1}), Y_m is the maximum yield (ton ha^{-1}), ET_a is the actual annual total evapotranspiration (mm), ET_m is the maximum annual evapotranspiration (mm), and K_y is a water use-yield response function for pears. One approach to determine the water use-yield relationship (Ky) for pear orchards is to use the long-term Fruitlook data for selected high-performing pear orchards and the associated yields from the farms. Ky can be determined as the slope of the $1 - Y_a/Y_m$ vs $1 - ET_a/ET_m$ graph, so a large data-set of the annual ET and yield is required for accurate estimates. Given that the model being developed here will estimate both the yield and water use, it can therefore provide information on the water productivity (WP = Yield/ET) of the pear orchards.

However, given that ET incorporates non-beneficial evaporation from the orchard floor, which may not be directly correlated to the tree yield, we used the modified Stewart model instead, according to the Paredes et al. (2018). According to this model, the crop yield (Ya) is estimated from the actual crop transpiration (Ta), with a transpiration reduction (not ET) occurring due to water stress as:

$$Y_a = Y_m - \frac{Y_m K_y (T_c - T_a)}{T_c} \quad (3.24)$$

T_c is the maximum seasonal transpiration for pears, which was taken as 900 mm, according to the measured data. K_y is the yield response factor, which indicates the sensitivity of the yield reduction to transpiration reduction. K_y <1, for crops whose yield is less sensitive to transpiration reduction. K_y =1 means the reduction in yield varies in direct proportion to the transpiration reduction, and K_y > 1 if crop yields are highly sensitive to transpiration reduction (Paredes et al., 2018). The Ky values obtained with the actual measured yield and transpiration data from the 'Forelle' and 'Packham's Triumph' orchard over multiple seasons are shown in Table 3.2.

Table 3.2 Derivation of the yield response factors (Ky) for 'Packham's Triumph' and 'Forelle' pear cultivars

Year	Site	Cultivar	Ym	Tc	Ta	Ya	Ky
			(t/ha)	(mm/y)	(mm/y)	(t/ha)	
2022/23	Ceres	'Forelle'	90	900	721	69.8	1.13
2023/24	Ceres	'Forelle'	90	900	773	59.1	2.43
2024/25	Ceres	'Forelle'	90	900	768	70.5	1.48
2022/23	Wolseley	Packham	110	900	635	59	1.57
2023/24	Wolseley	Packham	110	900	559	55	1.32
2023/24	Vyeboom	Packham	110	900	526	72.4	0.82
2024/25	Vyeboom	Packham	110	900	648	75.7	1.11
2023/24	Elgin	'Forelle'	90	900	701	45	2.26
	Packham's						1.21(±0.42)
	'Forelle'						1.83 (±0.30)
	Average						1.52

CHAPTER FOUR

'FORELLE' ORCHARD, CERES

4.0 INTRODUCTION

Ceres is a prime pear-producing region in the Western Cape, mostly because of the ideal climate that is characterised by cold winters and warm summers. It has the largest area planted to pears, namely, about 4 734 ha (Hortgro Tree Census, 2022). The main cultivars that are grown include 'Packham's Triumph', Williams Bon Chrétien and the blushing 'Forelle' variety. The climate of Ceres is classified according to the Köppen-Geiger climate classification as Csb, with a warm summer Mediterranean climate. The average maximum daily temperatures range between 28° and 30°C. Winters are colder, with minimum daily temperatures averaging 2° to 4°C, with occasional snow falls on higher ground. Pears, like apples, require considerable cold conditions to accumulate sufficient chill units to exit dormancy in spring. According to Ogundeji and Jordaan (2017), widely-planted pear cultivars like 'Forelle' and 'Packham's Triumph' require between 850 and 900 Richardson Chill Units, respectively. These conditions are easily met in the Ceres and Koue Bokkeveld regions where more than 1 000 chill units can be realised each season.

The dominant soil types in the Ceres region include a mix of sandy silts, clayey silts and shale-derived, often red/yellow-brown soils (Hutton forms). The soils are generally suitable for crop production, although they often have a low-fertility and lack certain important minerals. The pears are grown under irrigation, with the major water sources being dams that are fed by mountain runoff, such as the Koukedouw Dam and several small streams. The groundwater in most parts of the Ceres Valley is not suitable for irrigation due to its high salinity (Dzikiti et al., 2011). Given that pears in this region are produced entirely under irrigation, key questions exist regarding their water requirements and how drought stress influences the fruit yield and quality. This chapter provides quantitative information on the actual water use of a high-yielding 'Forelle' orchard, which was measured over multiple seasons. The focus is only on the unstressed water use of the trees, although we also provide background information that informed an entire PhD study, which is summarised in Appendix A. This supplementary study sought to provide insights on how the trees performed under drip-deficit irrigation applied

during different times of day, following the initial findings on the deficit irrigation of pears reported by Volschenk et al. (2012).

4.1 SITE DESCRIPTION

The 'Forelle' orchard was a mature, full-bearing block at the Buchuland Farm (33° 22'42.90" S: 19° 21'29.24" E, 512 m asl). The farm was located about four kilometres to the east of the town of Ceres (Figure 1.0 and 4.1). The orchard was 22 years old when the study commenced, and it was originally planted in 1994 on the BP1 rootstock. The orchard was one of the largest in the area; it measured about 6.5 ha and was planted with a north-south row orientation (see the yellow boundary in Figure 4.2). Terrain of the orchard was gently-sloping in the northern sections, becoming steep towards the southern parts. The tree density was about 1 481 trees per ha and the trees were irrigated with a micro-sprinkler system that delivered about 32 L/h. There was one micro-sprinkler per tree. Irrigation scheduling was done by using the Irricon profile soil moisture probes (Irricon Pty Ltd), the locations of which are shown by the blue cones in Figure 4.2. On average, the trees received two to three irrigations per week, depending on the weather conditions. Water for irrigation was pumped from a nearby river into a farm storage dam.

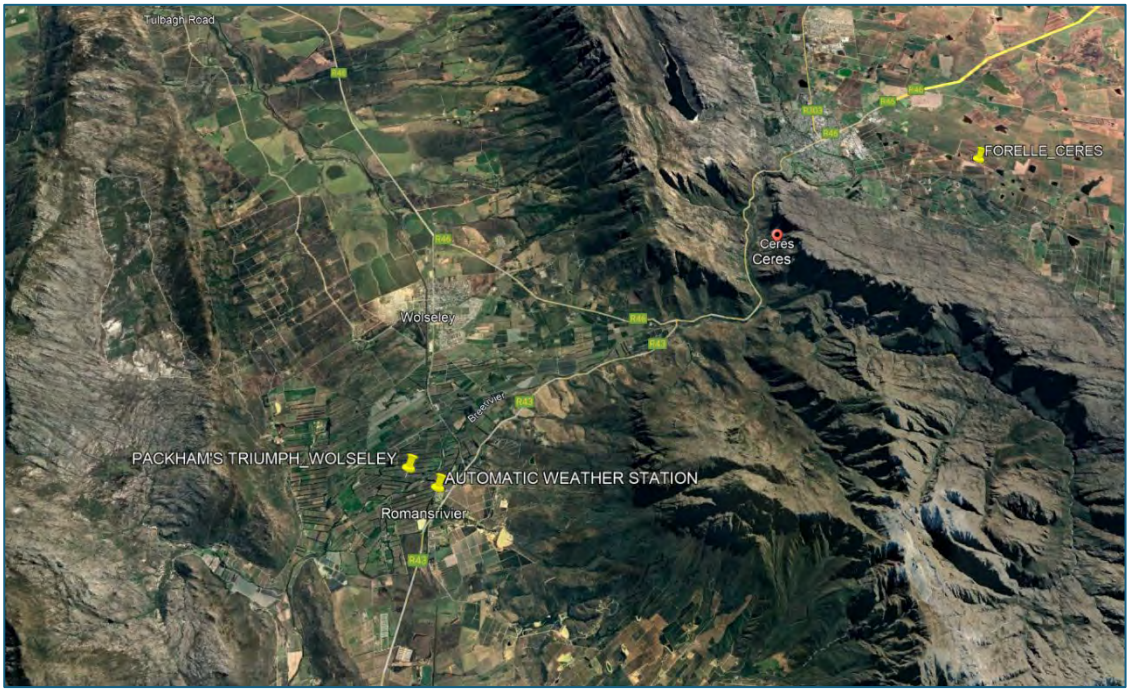


Figure 4.1 Location of the study sites where data were collected in the Wolseley and Ceres production regions

According to the farmer, the water allocation to the farm was inadequate and deficit irrigation was practised outside of the sensitive fruit growth phases. Despite this potential challenge, experts from the pear industry strongly recommended this orchard for this study, as it is one of the consistently high-performing orchards in the region, producing 70 t/ha on average, which is higher than the industry standard.



Figure 4.2 Location of the IrriCheck irrigation probes (blue cones) used for irrigation scheduling in the 'Forelle' orchard in Ceres. The area bounded in yellow is the 'Forelle' orchard

Details of the orchard are summarised in Table 4.1. The interrow region had a thin strip of weeds spanning about 70 cm across, and the rest of the orchard floor was bare ground. Early in the growing season, a dense cover of weeds usually formed between the rows, and these were supported by residual moisture from the winter rains. The heavy soils in most of the orchards were prone to waterlogging. The removal of the weeds was therefore often delayed until late October to early November, in order to facilitate the draining of the soils.

Table 4.1 Properties of the 'Forelle' orchard in Ceres

Age	22 years
Block size	6.5 ha
Coordinates	33° 22'42.90" S: 19° 21'29.24" E, 512 m asl
Planting density	1 481 trees per ha
Cultivar	'Forelle'
Rootstock	BP1
Height	4.5 m
Irrigation	Micro sprinkler (32 L h^{-1})
Soils	Clayey loam
Average yield	70 t ha^{-1}

4.2 SOIL PROPERTIES AT BUCHULAND

The 'Forelle' orchard was established on clay soil, with the highest concentration of clay being found in the 300 to 500 mm layer, as summarised in Table 4.2. The soil particle analysis showed that the top layer of the soil (0 to 300 mm) had a large fine sand fraction which, together with the moderate clay percentage (*ca.* 10%), contributed to a high soil water-holding capacity. Deeper down in the soil profile, the sand fraction got coarser, and a higher stone percentage existed (*ca.* 20%). The total available water within the profile was 87.95 mm, with the field water capacity being 0.187 mm mm^{-1} and the permanent wilting point being 0.088 mm mm^{-1}.

Table 4.2 Physical properties of the soils at Buchuland, Ceres

Soil depth (mm)	Clay (%)	Silt (%)	Fine sand (%)	Medium sand (%)	Coarse sand (%)	Sand grade	Soil texture class[1]
0 – 300	24.0	20.0	35.5	3.2	17.3	Fine	Sandy clay loam
300 - 500	40.0	24.0	13.5	3.7	18.8	N/A	Clay
500 - 1000	34.0	20.0	13.8	5.8	26.4	Coarse	Sandy clay loam

[1]According to the soil texture classification of the USDA

4.3 TREE, FRUIT GROWTH AND SOIL MOISTURE MEASUREMENTS

The growth of the canopy (Figure 4.3) was monitored by measuring the canopy dimensions (base area and height) and the Leaf Area Index (LAI - m^2 of leaf area per m^2 of ground area). These data were collected over three growing seasons, from September 2022 to March 2025. The LAI was measured fortnightly, at the start of the season, and monthly during the rest of the season by using the LAI – 2000 leaf area meter (LiCOR – Lincoln, Nebraska, USA). The LAI curves for each growing season were developed by linear interpolation between the neighbouring measured data points. The LAI data were collected either on overcast days, or at sunset, when the leaves behaved like black bodies, with little light being transmitted through the leaf. The LAI-2000 was programmed to measure the radiation at the top of the canopy at the start of the reading cycle, followed by seven readings under the canopies. The last reading was taken again at the top of the canopy. The LAI was calculated by using Beer's law, using an extinction coefficient of about 0.6 for deciduous trees. The volumetric soil water content was measured hourly by using three-time domain reflectometer probes (Model CS616- Campbell Scientific, USA) installed at a 30 cm, 60 cm and 90 cm depth in the rootzone (Figure 4.4).



Figure 4.3 The 'Forelle' orchard in Ceres in early spring (September) and at full canopy cover in mid-December



Figure 4.4 Installation of soil moisture monitoring equipment in the 'Forelle' orchard in Ceres

The fruit growth in all three seasons was monitored hourly on two fruit, using dendrometers (Figure 4.5a) to get an insight into the growth dynamics and how this was influenced by environmental factors and by management practices. Additional fruit growth data were collected on 20 tagged fruits by using digital callipers at regular intervals throughout the season. The dendrometers were deployed after the fruit set around late October, and the measurements continued until harvest. Irrigation was measured by using water flow meters that were installed in the irrigation lines (Figure 4.5b).

Weather data were collected by using an automatic weather station (Figure 4.6) which was installed about 500 m from the study orchard at Buchuland. The station measured the basic weather variables, namely, the solar radiation, wind speed and direction, air temperature and relative humidity and rainfall. All the data were collected hourly. The weather station was located over a short grass reference, according to the FAO 56 recommendations (Allen et al., 1998).



Figure 4.5 Monitoring fruit growth with a DEX 70 dendrometer (Dynamax Houston, USA) and irrigation, using a water flow meter installed along an irrigation line



Figure 4.6 Automatic weather station at Buchuland in Ceres installed during the 2023-2024 season

4.4 QUANTIFYING ORCHARD TRANSPIRATION

The transpiration by individual trees was measured by using the Heat Ratio Method (HRM) for monitoring the sap flow (Burgess et al., 2001). The HRM system comprised three boxes, with one box assigned per tree. Each box contained four T-Type thermocouple pairs that measured the sapwood temperature at different depths, to account for the radial variation in the sap velocity (Wulschleger & King, 2000). A heater probe was inserted in the middle of the two thermocouples. The electronics inside the tree box (Figure 4.7) were powered by using a 12V 7 Ah battery. The thermocouple pairs were installed in the four cardinal directions around the stem, to account for the circumferential variations in the sap velocity (Lopez-Benal et al., 2010). A metal template was used to drill the three 2 mm diameter holes along the axis of the stem, about 0.50 m from the ground (Figure 4.7). This was done to minimise potential errors, due to the misalignment of the probes, which can be quite substantial (Ren et al., 2017). The top and bottom holes were spaced at 5 mm from the central hole, into which the heater probe was inserted. A new set of holes were drilled at the beginning of each season to avoid poor quality data, as result of the wood around the probes becoming necrotic. Each tree box was connected to a datalogger (Model: CR1000, Campbell Scientific, UT, USA) via a 25-core plain cable. To expand the number of channels for the thermocouples, a multiplexer (Model: AM16/32B, Campbell Scientific, UT, USA) was used. The pulsing of the heat was done through the control ports on the datalogger, and the duration of each pulse was 1.0 s. The sap flow data were collected at hourly intervals over three growing seasons.

The calculation of the transpiration rates (in L per tree) from the HRM technique requires information on the wound width (created by the drilling and insertion of probes), the wood moisture fraction, the wood density and an estimate of the sap wood depth. The wound width data were derived from a wood sample collected from several pairs of probes, in order to get representative averages at the end of each growing season. The wounding correction was done according to the approach described by Burgess et al. (2001). The sapwood area was determined by injecting methylene blue dye into the stem and collecting samples by using a stem corer above the injection point, to visually distinguish between the various parts of the stem's cross section (i.e. sapwood, heartwood and bark).

The volume of sap flow by each instrumented tree (in litres per tree) was calculated as a weighted sum of the products of the sap velocity represented by each probe and the sapwood

area assigned to that probe. The orchard-level transpiration (T, in mm/d) was calculated as the sum of the products of the sap flux density (U) and the stand Sapwood Area Index (SAI: m^2 active xylem m^{-2} ground area) for trees in four stem diameter classes, so that:

$$T = \sum_{i=1,4} SAI_i \times U_i \qquad (4.1)$$

where U_i is the average sap flux density in each size class and each of the instrumented trees was assigned to an appropriate stem size class.

The actual evapotranspiration (ET) of the 'Forelle' orchard in Ceres was measured by using an open path eddy covariance system (Figure 4.8) for the period 15 December 2023 to 06 February 2024. The fluctuations in the concentration of water vapour and CO_2 above the orchard were measured by using a combined infrared gas analyser and a 3D sonic anemometer (Model: IRGASON, Campbell Scientific, UT, USA). The IRGASON was installed on a flux tower that was located in the middle of the orchard at a height of about 2.5 m above the tree canopies (Figure 4.8). This height ensured that the device was above the surface roughness sublayer and that there was adequate fetch around the tower. The IRGASON was installed pointing in the direction of the prevailing wind, which was generally south-easterly.



Figure 4.7 (a) Drilling holes for inserting probes into the tree stem across the four cardinal directions using a drilling jig; (b) Tree boxes monitoring sap flow of mature 'Forelle' trees in Ceres

Other measurements included the net radiation (R_n), which was measured by using a one-component net radiometer (Model CNR1: Kipp & Zonnen, The Netherlands), which was installed at a height of about 8.0 m from the ground. The heat transfer into and out of the ground was measured by using soil heat flux plates (Model: Hukse Flux, The Netherlands) that were installed at a depth of 8.0 cm from the soil surface. A pair of soil averaging thermocouples (Model: TCAV -L, Campbell Scientific, UT, USA) were installed above the soil heat flux plates, to correct the soil heat flux values (G) for the energy stored by the soil above the plates. The data were collected at a frequency of 10 Hz, and the signals were processed at 30 min intervals. The high-frequency signals were processed by using the online EasyFlux programme.

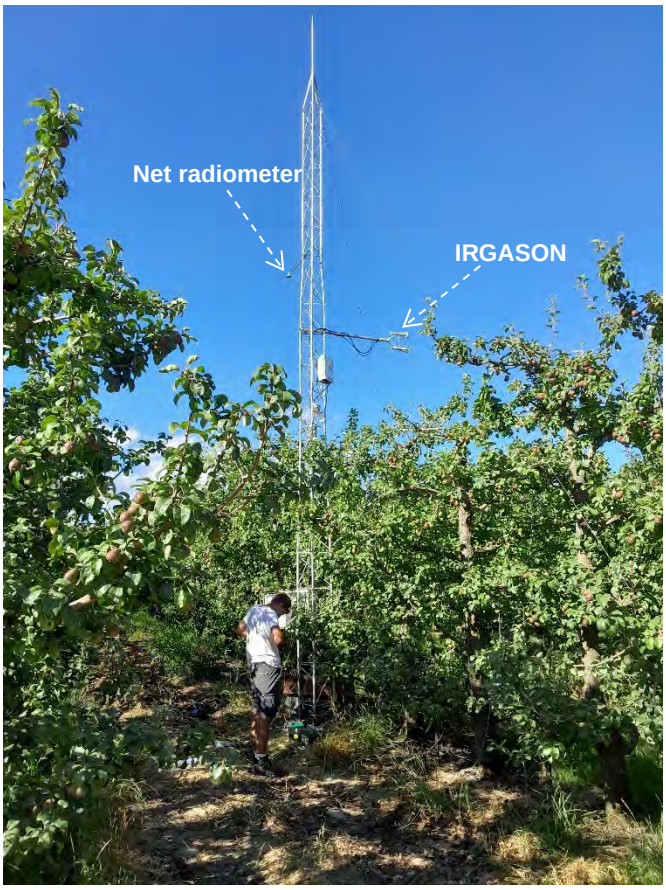


Figure 4.8 Open path eddy covariance system measuring orchard evapotranspiration in the 'Forelle' orchard in Ceres

4.5 TREE WATER STATUS AND LEAF GAS EXCHANGE MEASUREMENTS

The goal of this study was to quantify the maximum unstressed water use of the pear orchards. For this reason, the tree water status data was monitored by using two approaches. Firstly, the pressure chamber was used to measure the midday xylem/stem water potential of the trees (Figure 4.9a). Data were collected monthly on five randomly-selected trees in the orchard. Measurements were taken on two healthy, mature and fully-expanded leaves located close to the stems of the trees. Prior to the measurements, the selected leaves were bagged in zip-lock plastic bags that were padded with aluminium foil. The equilibration periods ranged from one-and-half to two hours prior to measurements. To understand the dynamic flow of water through the vascular system of the pear fruit, additional data were collected on the leaf-stem-fruit water potential gradients from sunrise (0600) to sunset (18 00) on selected dates during the 2023-2024 and 2024-2025 seasons.

The second method of quantifying stress was to also measure the leaf gas exchange (i.e. transpiration/photosynthesis/stomatal conductance) at midday. These data were collected by using an infrared gas analyser (Model Li 6800 – LiCOR, Nebraska, USA), as shown in Figure 4.9(b). The measurements were taken on leaves from four different trees, on two leaves per tree, which means there were eight leaves for each measurement cycle. The leaves chosen for measurement were in the outer part of the canopy at a height of 1.2-1.5 m from the ground (slightly lower than shoulder height). Whenever possible, healthy, fully expanded, mature leaves were measured that were located in the medial section of current-year shoots (at times we had to measure spur leaves, because there were no good current-year shoots in a proper position). Before each round of measurements, the temperature and relative humidity in the chamber were set to ambient values. The light intensity in the cuvette was also adjusted to match the ambient light, which was measured with an external PAR sensor. The leaves used for measurement were tagged, so that the same set of leaves were measured on the east side in the morning (0600-1200) and on the west side in the afternoon (1300-1800). The measurement conditions were set as follows: The air flow rate was set at 500 μmol s^{-1}, and this was kept constant for all campaigns with a fan speed of 10 000 rpm. The CO_2: was set at 400 ppm; the light was adjusted manually to a value close to that of ambient light (measured by external PAR sensor), before measuring each leaf. The temperature and relative humidity were set close to ambient, at the beginning of each cycle. If the VPD became too high, following

ambient conditions (i.e. on most days after midday), the VPD_{leaf} was set to 2.5 kPa. Consequently, RH% in the chamber was much higher than the ambient air relative humidity.

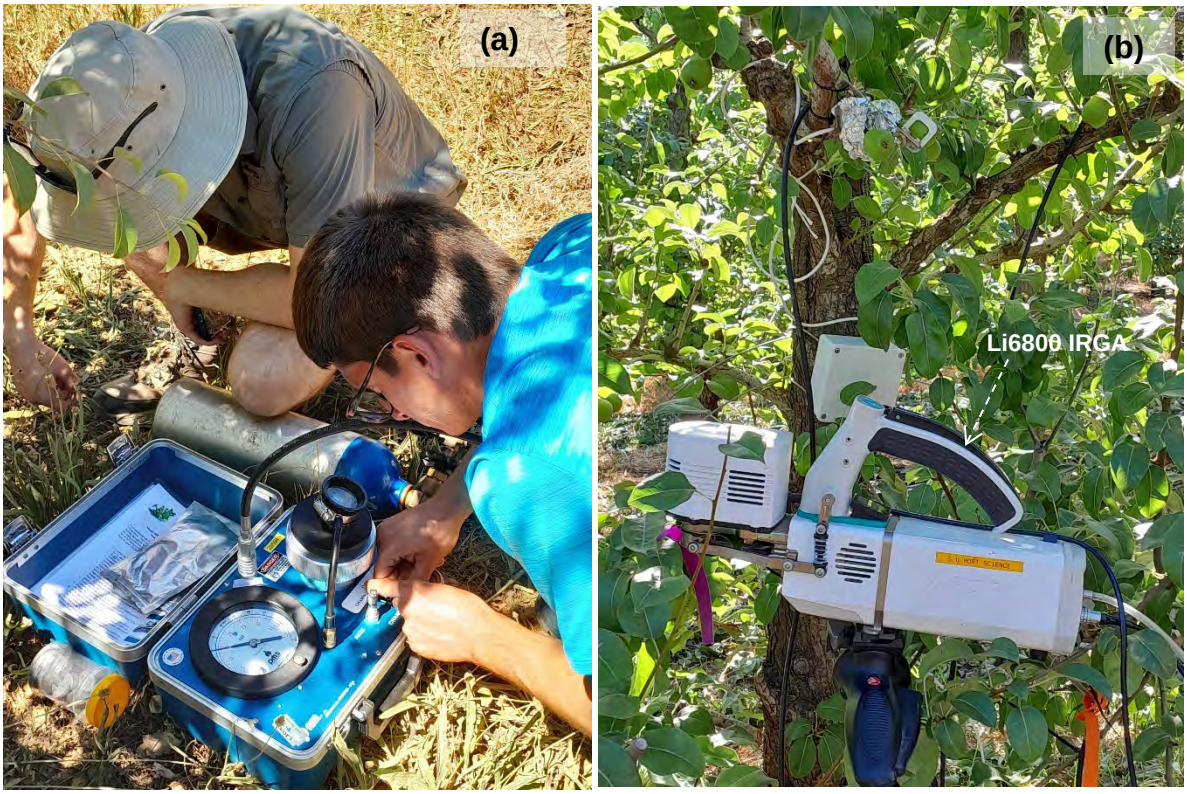


Figure 4.9 (a) Measuring the midday stem water potential of the 'Forelle' trees using a pressure chamber; (b) Leaf gas exchange measurements (photosynthesis and transpiration) using the LI 6800 infrared gas analyser

4.6 YIELD FOR THE 'FORELLE' ORCHARD IN CERES

In each orchard, ten trees were selected for harvesting, by ensuring that they were located at least five trees away from the orchard edge, with a spacing of one or two trees between them. The selected trees were spread across three adjacent rows. In addition, the trees monitored by the sap flow equipment were included in the selection. The total yield per tree was determined by using strip harvesting, where the filled harvest bags (with a predetermined average bag weight) were weighed by using a UWE NBK check weighing scale (UWE Scales South Africa, Cape Town, South Africa). The summed values provided the total tree yield. The average yield for the ten sampled trees was then used to estimate the orchard yield (tons per hectare), based on the tree density. In addition to the yield data, the trunk

circumferences of the selected trees were measured at a height of 30 cm above the orchard floor. The harvest dates were 03 March in 2023, 28 February in 2024 and 05 March in 2025.

4.7 FRUIT QUALITY

The method of sampling fruits and measuring the fruit quality parameters was done on 40 fruits per tree that were picked from the same ten selected trees. The 40 fruits comprised four samples of ten fruits, where each sample was collected from one of four canopy positions, namely, the top, bottom, inside and outside:

- the top and bottom fruits were picked from the very top (only accessible with a ladder) and bottom of the canopy, respectively;
- the inside fruits were selected from shaded areas near the trunk, while the outside fruits were picked from the sun-exposed periphery of the canopy; and
- the outside sample consisted of five fruits from the eastern side and five from the western side of the canopy.

A total of 400 fruits (40 samples) were transported to the Horticultural Sciences Department at Stellenbosch University for a fruit quality determination. Unlike the previous season, where sampling was conducted mostly on the same day as the commercial harvest, the 2024/25 season followed a different approach. Sampling was conducted at the optimal Maturity Index (MI), which is determined by an average firmness of 6.9 kg, rather than strictly adhering to the farm's harvest date. This resulted in a shift in sampling dates, which reflected variations in fruit maturity between the two seasons. However, as in the previous season, the 'Forelle' at Ceres in 2023/24 was sampled slightly earlier than the harvest date on 21 February. The observed shift in the sampling dates for the 2024/25 season suggests a later maturity trend, compared to the previous season. This could indicate differences in the seasonal climatic conditions that influenced the fruit development and ripening. A further analysis of fruit quality parameters will provide insights into these variations. The MI test parameters were the following:

- Background colour – using an industry colour chart (Figure 4.10) by Unifruco Research Services (Bellville), the background colour for two opposite cheeks of each pear was

determined. For a ‘Forelle’ pear, the background colour was only determined on the side opposite to the blushed cheek (Side A).

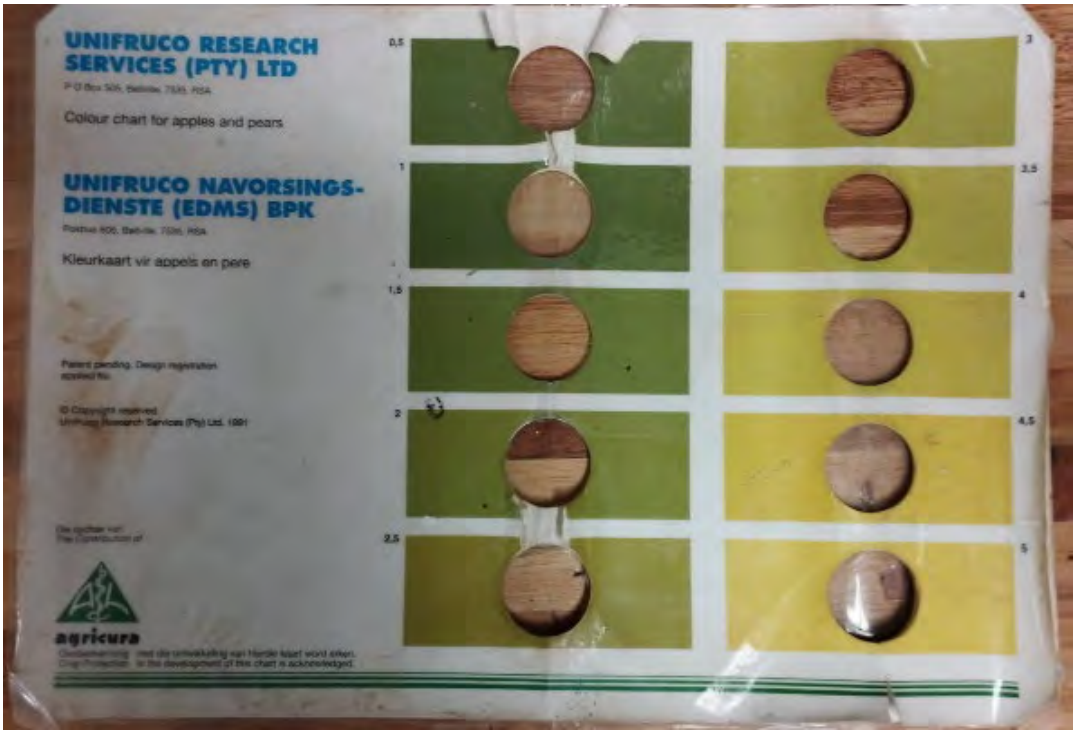


Figure 4.10 Background colour chart

- Firmness (kg) – This was determined on two opposite cheeks on each fruit from the blushed- and opposite cheek. The firmness was measured with a Fruit Texture Analyser (FTA), with a 7.9 mm tip. The FTA is a penetrometer by Guss Instruments (Strand, South Africa) which directly connects to a personal computer with a Windows operating system, and it includes ports to which several supplementary instruments can be attached. The data are digitally captured and stored in a Microsoft Excel sheet.
- Diameter (mm) – An Electronic Fruit Size Measure (EFM) instrument was used, which is an attachment to the above-mentioned FTA.
- Mass (g) – The scale attachment of the Guss Instruments FTA was used.
- Height (mm) – The height was measured with Mitutoyo digimatic callipers (Mitutoyo Corporation America, Aroura, Illinois, United States), which were also connected to the FTA.
- Starch conversion (%) – An iodine test was conductedby using the starch conversion chart (Figure 4.11) by Unifruco Research Services (Bellville).

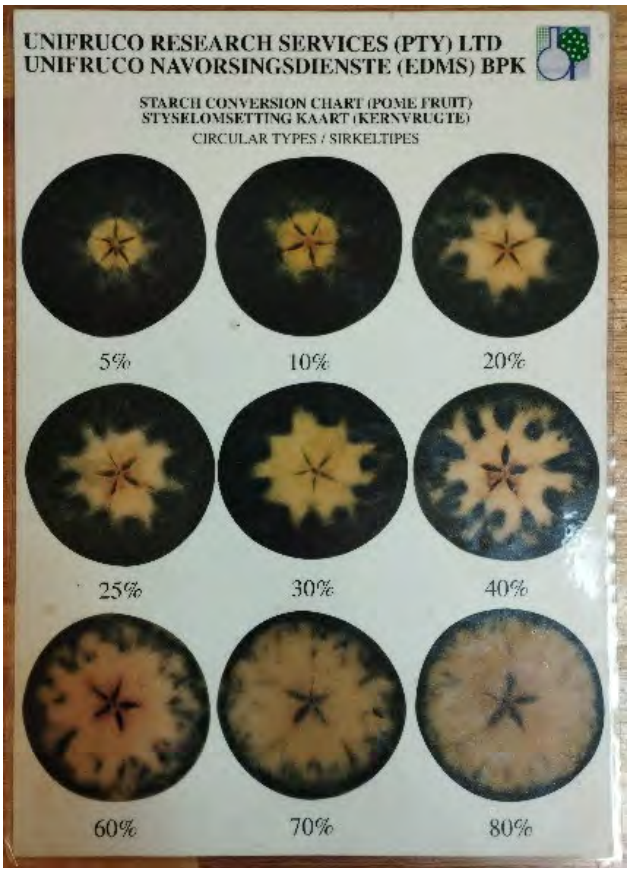


Figure 4.11 Starch conversion chart

- Total Soluble Solids (TSS) (%) – A composite juice sample of each sample of 10 fruits were obtained by blending one cross-sectional slice per fruit together in a common kitchen blender. A small amount of this juice sample was then extracted and used for the TSS measurement with a calibrated electronic refractometer (TSS 0-32%, Model N1, Atago, Tokyo, Japan).
- Titratable Acidity (TA) (% Malic acid) – The remaining juice (not used for TSS test) was poured into vials and left overnight at room temperature for the 'Forelle' pears. This allowed the separation of the solid particles from the juice through sedimentation. After the particles had settled, the TA was determined by using a Metrohm Tritrator, along with an 815 Sample Changer (Titrator model: 888 Titrando, Software: Tiamo, Herisau, Switzerland).

4.8 WATER PRODUCTIVITY OF 'FORELLE' PEARS IN CERES

4.8.1 Physical water productivity

Firstly, we calculated the physical Water Productivity (WP) of the orchard as kg of fruit produced per m^3 of water transpired during the season. The calculation was based on the yield (t ha^{-1}) of (i) ten trial trees, and (ii) the whole orchard block, and the seasonal transpiration (T) was calculated as the average of three representative monitored trees (Eq. 4.2). The water productivity of modelled seasonal total evapotranspiration (ET) was similarly calculated (Eq. 4.3).

$$WP_T \text{ (kg m}^{-3}) = \text{(Yield*1000) / Seasonal transpiration} \quad (4.2)$$

$$WP_{ET} \text{ (kg m}^{-3}) = \text{(Yield*1000) / Seasonal evapotranspiration} \quad (4.3)$$

Secondly, we presented the Water Use Efficiency (WUE) of T (Eq. 4.4) and ET (Eq. 4.5) as m^3 ton^{-1} (equivalent to L kg^{-1}), since this value is also sometimes presented in the literature.

$$WUE_T \text{ (m}^3 \text{ ton}^{-1}) = \text{Seasonal transpiration / Yield} \quad (4.4)$$

$$WUE_{ET} \text{ (m}^3 \text{ ton}^{-1}) = \text{Seasonal evapotranspiration / Yield} \quad (4.5)$$

4.8.2 Economic water productivity

Thirdly, we calculated the Economic Water Productivity (EWP) as the gross income of the harvest (R ha^{-1}) per m^3 of water transpired (Eq. 4.6) or evapo-transpired (Eq. 4.7) per ha. This factors in the overall quality and marketability of the fruit. The calculations were based on the orchard block data.

$$EWP \text{ (R m}^{-3}) = \text{Orchard gross income / Seasonal transpiration} \quad (4.6)$$

$$EWP \text{ (R m}^{-3}) = \text{Orchard gross income / Seasonal evapotranspiration} \quad (4.7)$$

4.9 RESULTS AND DISCUSSION

4.9.1 Climatic conditions

Monthly climatic conditions at Ceres during the three growing seasons, stretching from September 2022, when the trial started, to June 2025 are summarised in Figure 4.12. As expected, the daily solar irradiance showed clear seasonality, peaking in the summer months, and reaching about 35.5 MJ/m^2/d in January 2024. The 2023-2024 season appears to have been substantially warmer than the other two seasons. It had 18 days with maximum daily temperatures exceeding 35°C, compared to only one during 2022-2023 and zero days in the 2024-2025 season. The maximum temperature reached in the 2023-2024 season was 39°C, compared to 34.5°C in the previous season (2022-2023) and 33.6°C in the preceding (2024-2025) season. The 2022-2023 growing season (September to May) was significantly colder, with 27 days recording the lowest temperatures below 3°C, compared to only two days in the other two seasons. The average temperatures for the growing seasons were 15.8°C for 2022-2023, 19.8°C for 2023-2024 and 17.6-°C for 2024-2025.

The warmer conditions in the summer of 2024 led to a higher Vapour Pressure Deficit (VPD) of the air, which peaked above 2.5 kPa, compared to around 1.6 kPa in the previous and preceding seasons. These VPD levels are low, compared to those that have been recorded in the Koue Bokkeveld in previous studies, which reached up to 4.0 kPa during the 2014/15 season (Dzikiti et al., 2018). Consistent with the VPD and temperature data, the atmospheric evaporative demand, depicted by the reference evapotranspiration (ETo) varied from under 2.0 mm/d to around 7.8 mm/d in summer in the 2022-2023 season, compared to 3.0 to 8.1 mm/d in the 2023-2024 season.

During the 2022-2023 growing season, the annual total rainfall (September 2022 to August 2023) in Ceres was 820.5 mm, with less than half the amount (334.5 mm) falling during the growing season (September to April). The 2023-2024 season had a much drier growing season, receiving only 225.6 mm, while the annual total rainfall was 830.1 mm. In the 2024-2025 season, Ceres received 244.6 mm during the fruit-growing season. The total reference evapotranspiration for the same period far exceeded the rainfall, namely 1126, 1200 and 1186 mm, respectively, for the 2022-2023, 2023- 2024 and 2024-2025 seasons (Table 4.4).

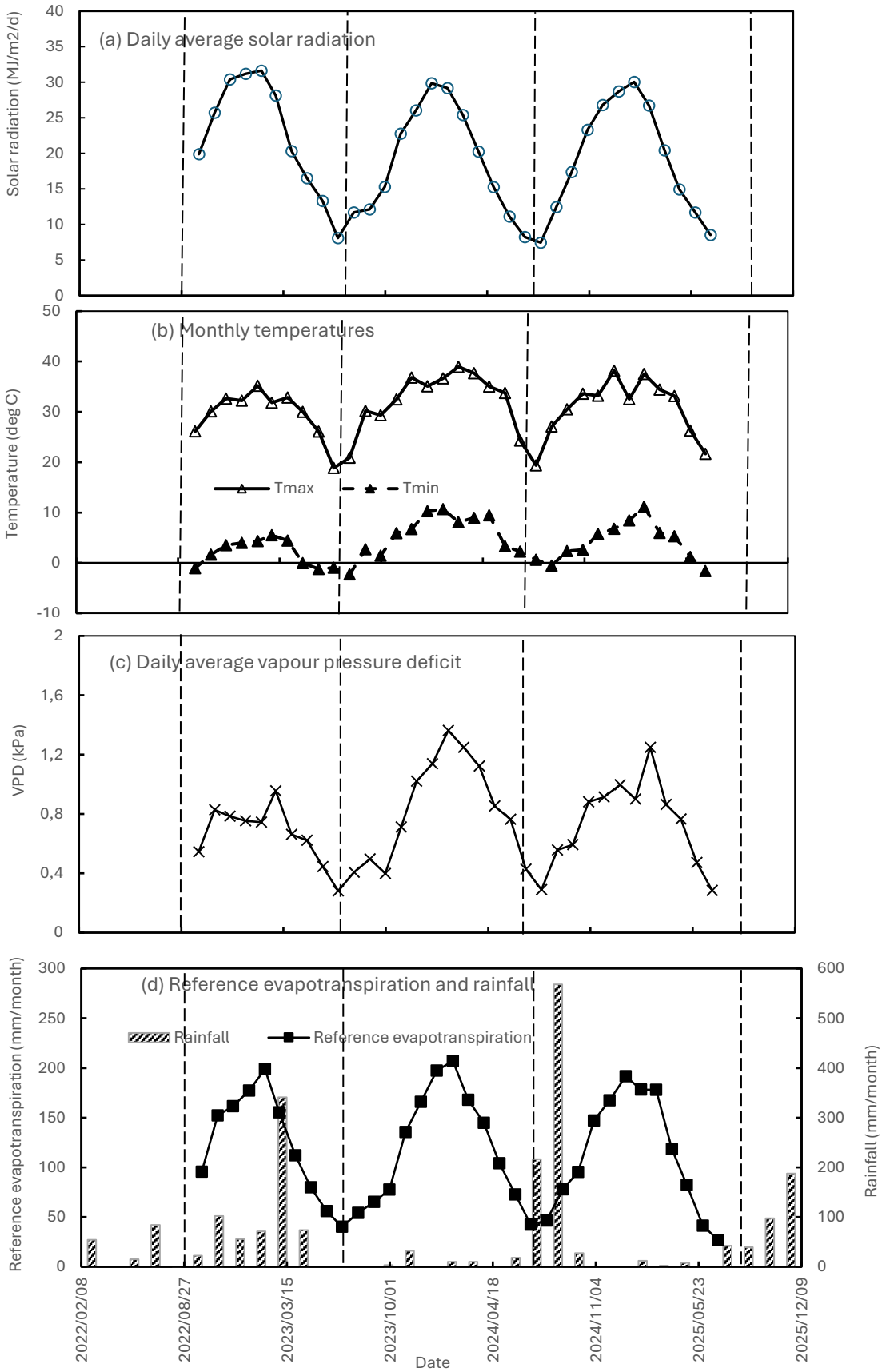


Figure 4.12 Monthly average daily solar radiation, (b) maximum and minimum temperatures, (c) vapour pressure deficit of the air, and (d) monthly total rainfall and reference evapotranspiration over three growing seasons from September 2022 to June 2025.

The winter rainfall was higher than the long-term average for Ceres; this can be attributed to the wetter rainy season in the winter of 2023, which saw about 59% of the total falling between 01 May and 31 July 2023.

Table 4. 4 Monthly climatic conditions averaged over three years between September 2022 and May 2025

	R_s	T_{max}	T_{min}	RH_{max}	RH_{min}	U_2	Rain	ET_o	VPD
Date	($MJ/m^2/d$)	(°C)	(°C)	(%)	(%)	(m/s)	(mm)	(mm)	(kPa)
September	17.5	28.7	0.9	98.9	15.5	1.7	18.1	89.6	0.5
October	23.9	32.1	3.4	98.8	15.8	1.5	0.0	145.0	0.8
November	27.8	34.2	5.3	97.7	12.5	1.8	10.3	165.0	0.9
December	29.9	35.2	7.0	98.3	12.6	1.9	39.5	188.7	1.0
January	30.3	34.8	7.8	97.4	11.0	1.7	2.8	194.7	1.0
February	26.8	36.1	8.2	96.2	11.3	2.0	10.8	167.1	1.2
March	20.3	35.0	6.5	98.7	16.7	1.4	51.6	125.0	0.9
April	15.6	32.7	4.9	98.9	14.2	1.4	31.8	88.8	0.7
May	12.0	28.7	1.1	98.9	14.4	1.1	62.5	56.7	0.6
June	8.3	21.6	-0.1	99.2	27.9	1.4	248.4	36.5	0.3
July	6.4	13.4	-0.6	66.6	12.2	1.2	214.0	33.6	0.2
August	8.2	19.1	0.7	66.7	9.4	0.9	9.1	47.7	0.4
			Total				698.8	1338.1	

4.9.2 Soil water content dynamics and leaf area index

Data for the earlier parts of the campaign are missing, due to the datalogger overwriting the data records, when the downloading intervals were too long. Given the heavy soils on the farm and the high residual soil moisture from the wet winter seasons, irrigation normally commenced in late October to early November. A thick layer of weeds was maintained between the tree rows, in order to assist with draining the excess water. The downslope parts of the orchard were usually waterlogged at the end of the winter season. However, the delay in the commencement of irrigation in the upper sections of the orchard, where our equipment was installed, resulted in substantial soil drying, especially in the shallow soil layers.

At the start of the 2023/2024 growing season, the profile showed signs of saturation, with a maximum amount of water of 340 mm (Figure 4.13). The first irrigation maintained the soil water content at the field water capacity. It was noted that all irrigation amounts under 17 mm contributed positively to the total soil water content. The irrigation did not penetrate up to 900 mm. Irrigation of less than 17 mm per day could lead to water loss through evaporation from the soil surface, as water is mainly located in the top part of the profile. Irrigation amounts per day that equated to more than 17 mm positively increased the soil water content. One important aspect to note is that the soil profile was kept wet, well above the field water capacity from 18 December 2023 to 18 February 2024. Irrigating above the field water capacity could have led to the unnecessary surface runoff of water and caused anaerobic conditions.

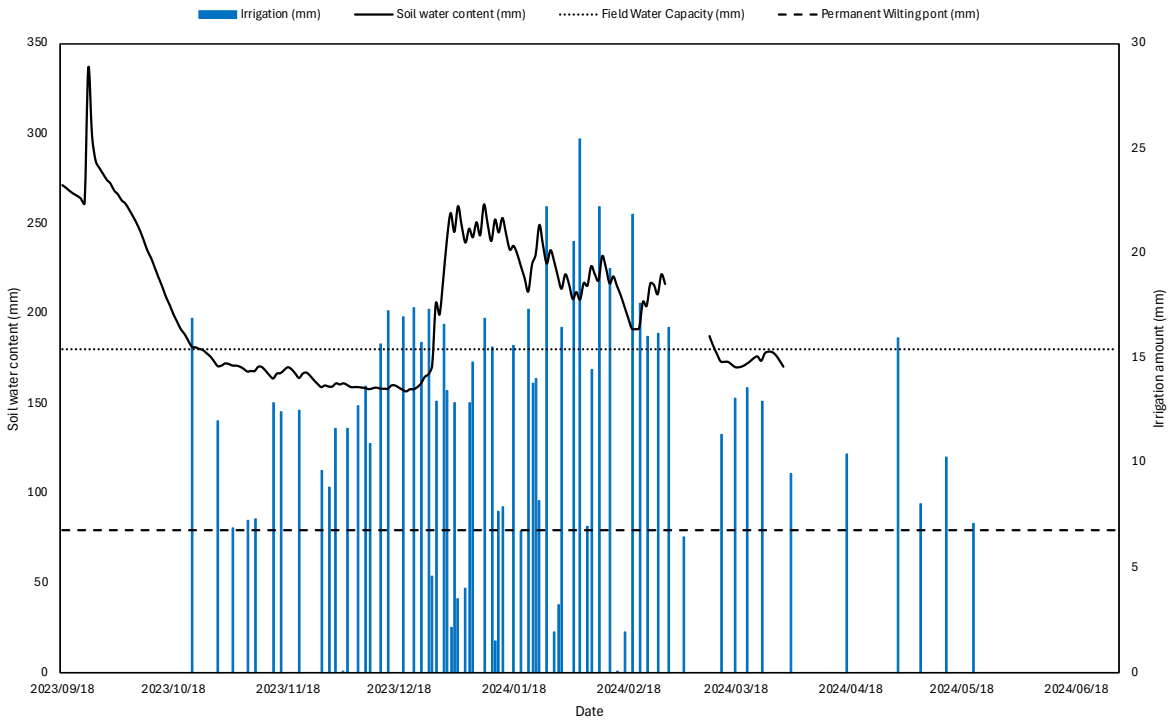


Figure 4.13 Total soil water content (mm) fluctuations (0 – 900 mm depth), along with irrigation amounts and timing over the 2023/2024 season for a 'Forelle' pear orchard situated close to Ceres.

The 2024/2025 season started with less soil water in the profile than the previous season (Figure 4.14). Irrigation started at approximately the same time as in 2023. However, the orchard received larger irrigation amounts (≥ 17 mm) earlier in the season. The soil water content for the 2024/2025 season was again higher than that of the field's water capacity. The

higher soil water content may have contributed to anaerobic conditions for roots and surface runoff, leading to water wastage.

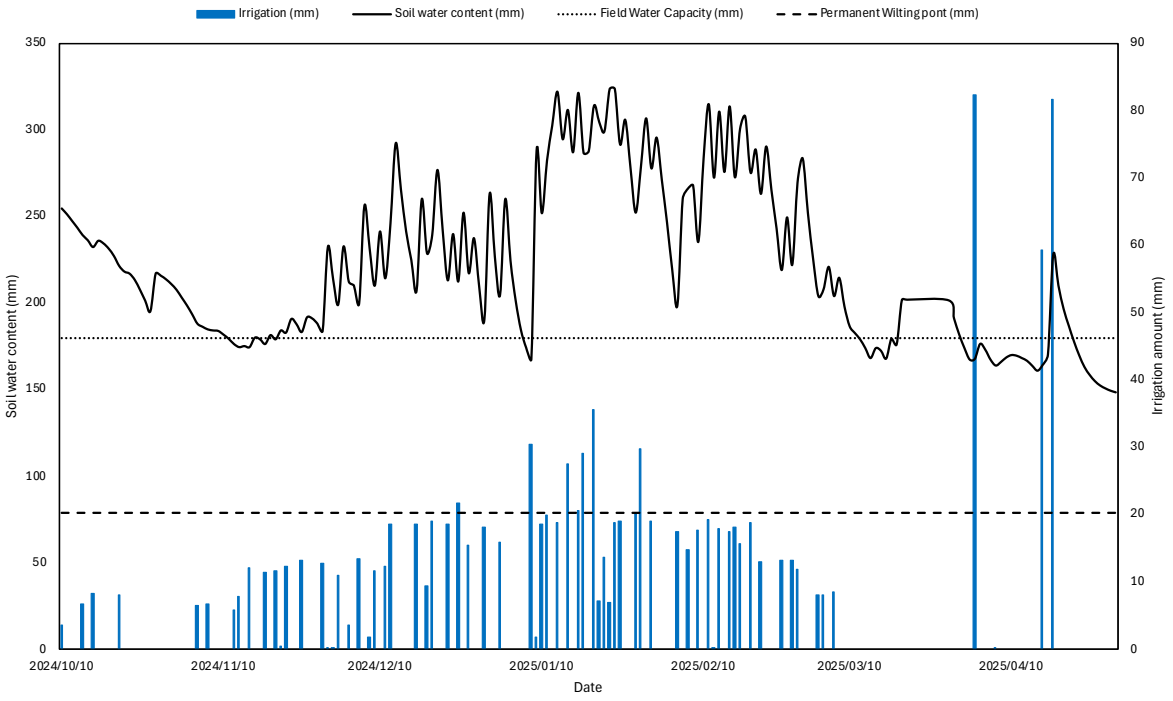


Figure 4.14 Total soil water content (mm) fluctuations (0 – 900 mm) depth), along with irrigation amounts and timing over the 2024/2025 season for a 'Forelle' pear orchard situated close to Ceres.

The 'Forelle' trees in this orchard were not pruned during the 2022-2023 season, due to labour issues leading to large canopy sizes, the leaf area index of which peaked at close to 4.0 (Figure 4.15). Being a blushed cultivar, we would have expected the trees to have more open canopies to promote fruit colour development. However, this was not the case during all three seasons. In the 2023-2024 and 2024-2025 seasons, the peak LAI was slightly lower than in the first year, due to summer pruning (Figure 4.15). These canopy management practices impacted the observed water consumption rates.

During the 2023-2024 season, the orchard was pruned around 11 December 2023, which led to a decline in the leaf area index from a peak of around 3.8 to about 3.0. Thereafter, only a marginal increase in LAI was observed, due to limited shoot growth in summer. The peak LAI during the 2024-2025 season was about 3.7.

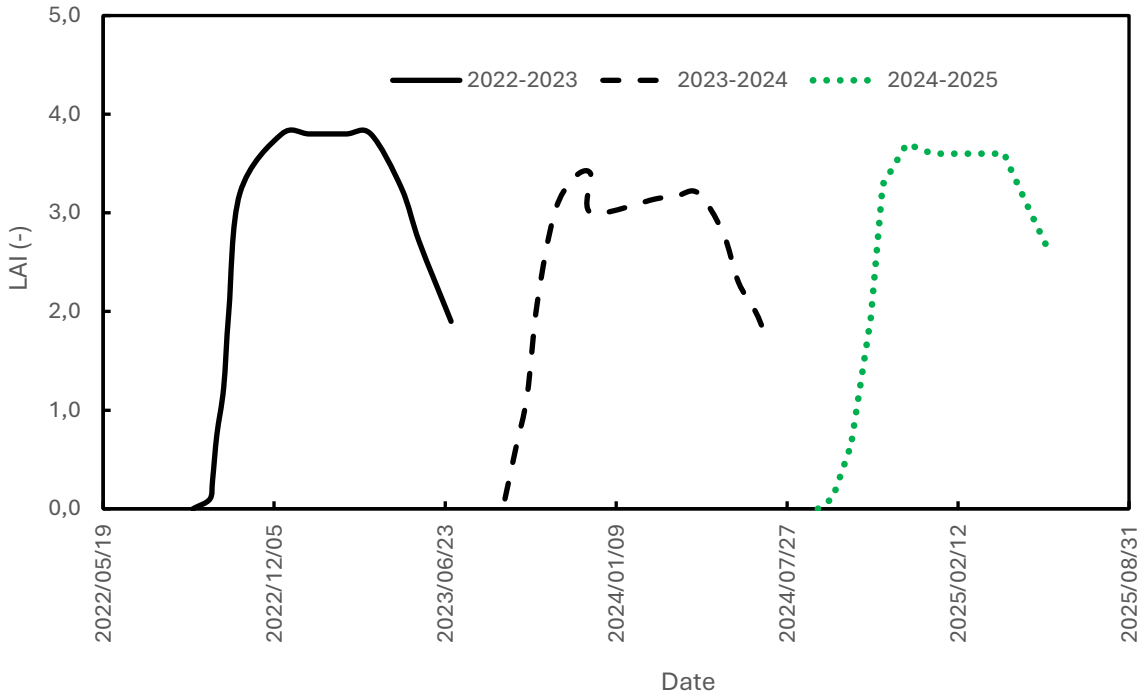


Figure 4.15 Leaf area index of the 'Forelle' orchard at Buchuland during the 2022-2025 growing seasons

4.9.3 Diurnal and seasonal dynamics in the tree water status and leaf gas exchange

4.9.3.1 Leaf gas exchange and tree water status

It has been suggested that water use efficiency in fruit production can be enhanced through late afternoon irrigation, when water in flows are energetically more favourable into the fruit than leaf transpiration (Scalisi et al., 2021; Luca Correlli Grappadelli & Stephano Musachi, pers. comm). In this section, we sought to quantify the diurnal and season dynamics in the leaf-stem-xylem-fruit water potential differences (Figure 4.16) of 'Forelle' pears. Appendix A gives a detailed description of a PhD study which examined this hypothesis, in detail, for drip-irrigated 'Forelle' pears.

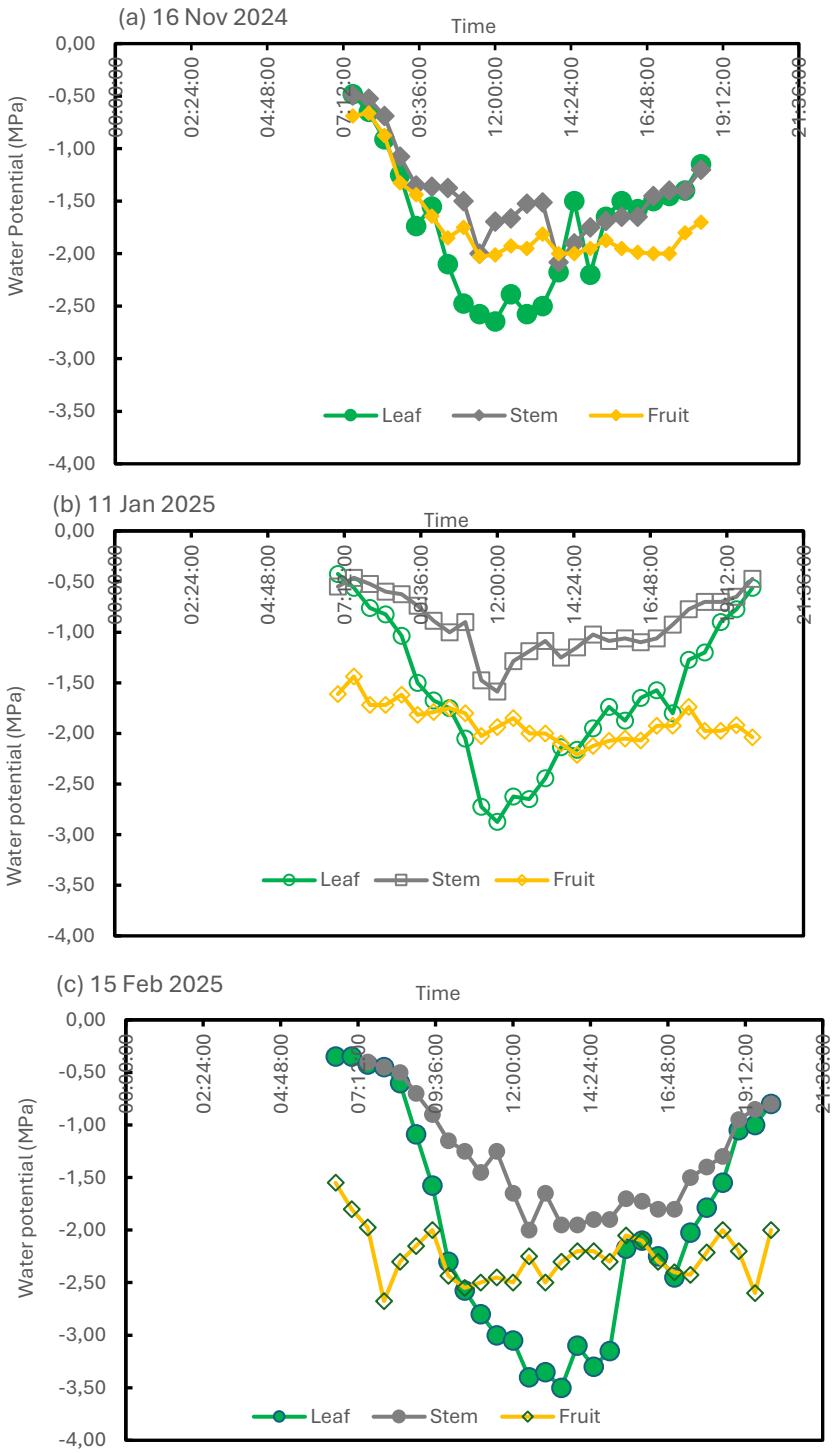


Figure 4.16 Hourly changes in the relationship between the leaf, the trees' xylem and fruit water potential during the (a) early, (b) mid- and (c) late season for the 'Forelle' pears measured from sunrise to sunset on typical clear days

Data for the 'Forelle' trees were collected hourly, from pre-dawn until sunset. The data in Figure 4.16a suggest that from pre-dawn to about mid-morning, the leaf, the stem's xylem and the fruit

water potential were similar early in the season (in November), when the fruit was still young. This is not surprising, given that the fruit's xylem is still functional early in the growing season (Morandi et al., 2014) and the stomata still actively regulate the fruit peel transpiration. However, at midday, the leaf water potential in Figure 4.16a was far larger than the potential of the stem's xylem and the fruit water. Therefore the leaves were a stronger sink of water, which implies that water flowed from both the stem's xylem and the fruit towards the leaves. In the late afternoon, the stem's xylem water potential quickly equilibrated with the leaf water potential (Figure 4.16a). The fruit water potential remained low after sunset, which suggests that the fruit was a stronger sink for water. This implies that water most likely flowed from the tree into the fruit, thereby driving growth through cell expansion.

In mid-January and towards harvest (February), the pre-dawn leaf water potential was equal to the stem water potential, but the fruit water potential remained lower than both of them, as shown in Figures 4.16b & c. This trend is likely because of the more negative osmotic water potential in the fruit, due to the accumulation of sugars. However, it is not clear whether there was a direct water flows into the fruit, as the xylem vessels were likely dysfunctional by this time. Therefore, an MSc study was designed to investigate the vascular flow patterns for pears, as reported in Appendix B.

The stem and leaf water potentials had a strong non-linear relationship with the VPD, as shown in Figure 4.17. High VPDs caused a slight increase in the water potentials, possibly because the stomata close at high VPDs, in order to avoid the excessive desiccation of the plant.

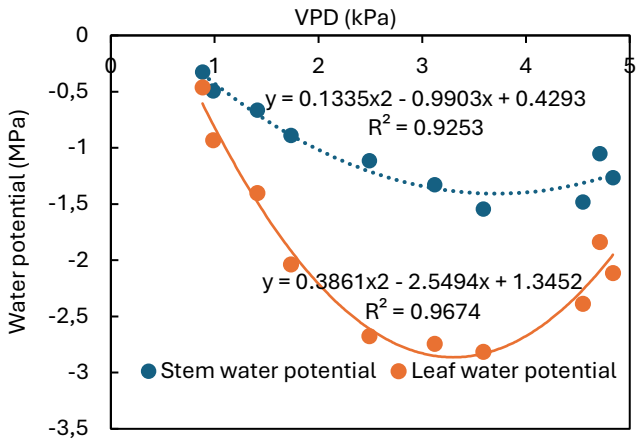


Figure 4.17 Relationship of stem and leaf water potential of the 'Forelle' trees with VPD on typically-clear days

An albeit weak linear relationship was observed between the stem water potential and the soil water content at various depths in the rootzone (Figure 4.18). The stem water potential had the strongest correlation with the soil water content in the 0 to 30 cm depths, which suggests that this soil depth had the greatest impact on the tree water status.

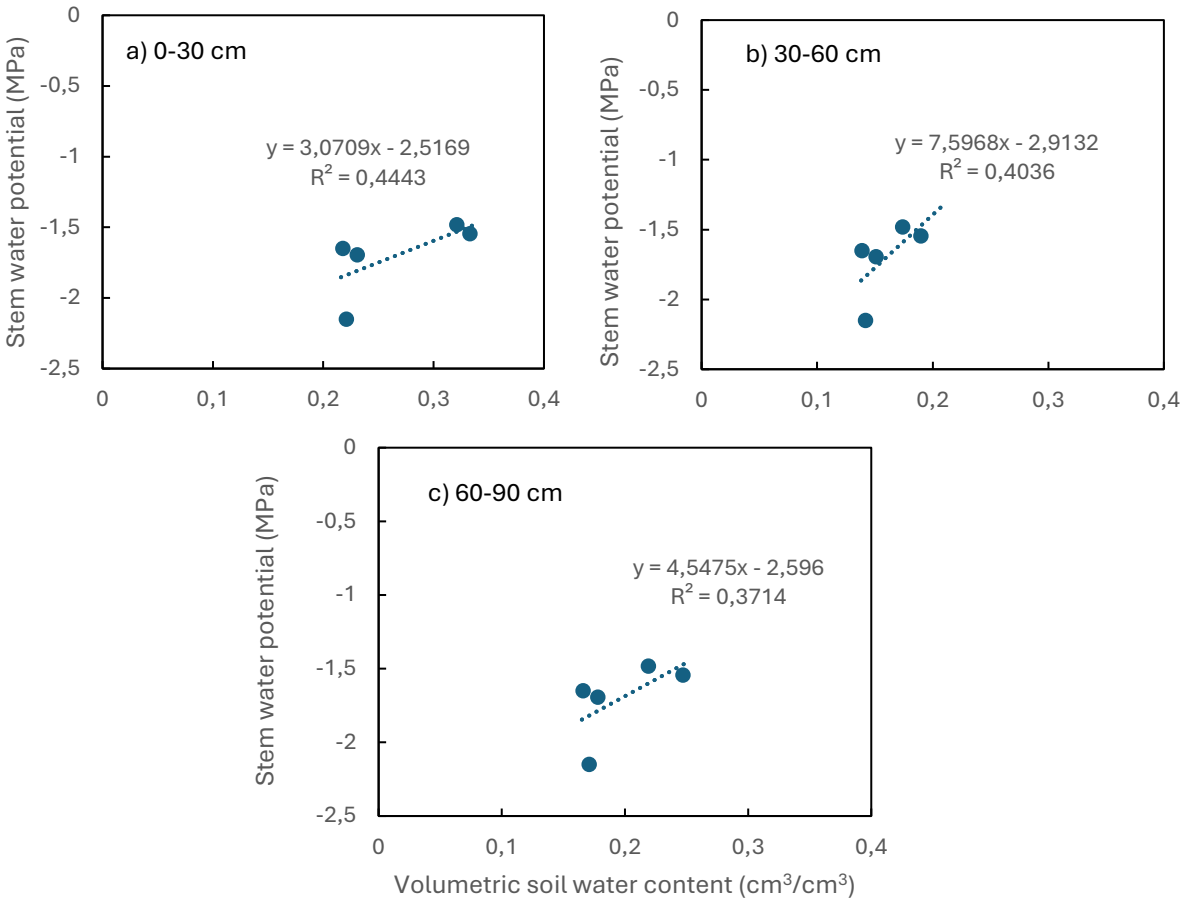


Figure 4.18 Relationship of midday stem water potential with the volumetric soil water content at midday in the depth intervals of 0-30 cm, 30-60 cm, and 60-90 cm in the rootzone over the season of 'Forelle' trees

Figure 4.19 shows the diurnal pattern of the leaf stomatal conductance (g_s), leaf transpiration (E_{leaf}) and net photosynthesis (A_{leaf}) of 'Forelle' trees early in the season on 30/11/2023 (on Panels a, c and e, respectively) and around mid-season on 19/12/2023 (b, d and f). The daily pattern of the VPD on a particular date is also presented on the same plots as g_s and E_{leaf}, while the daily pattern of solar radiation (R_s) is presented alongside A_{leaf}.

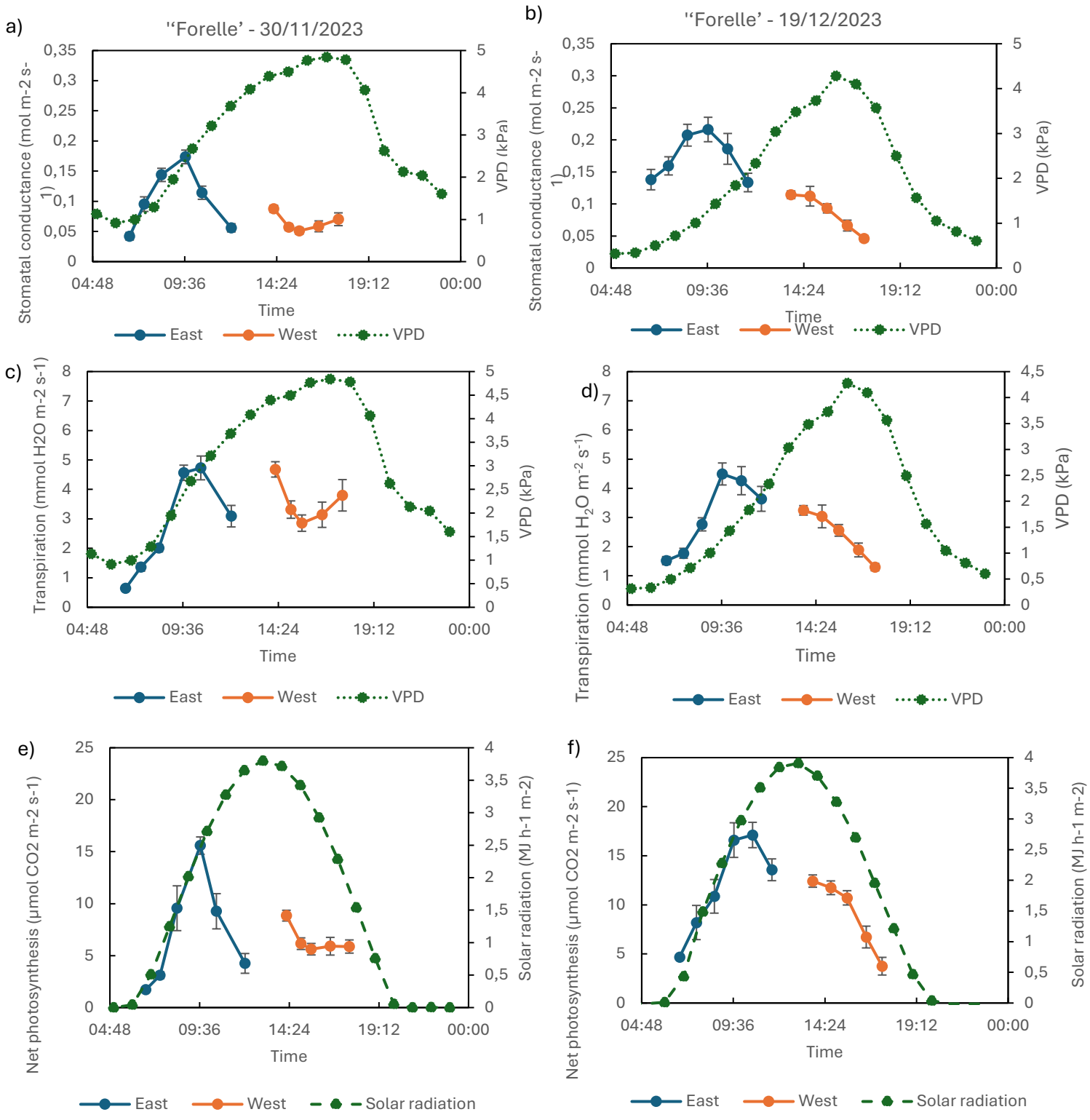


Figure 4.19 Timeseries of daily VPD of the air and stomatal conductance (a & b), leaf transpiration (c & d), and of daily solar radiation and net photosynthesis (e & f) of leaves of 'Forelle' trees. Each data point represents the mean (±SE) of eight leaves. Measurements were taken firstly from the eastern and then the western side of the canopy on 30/11/2023 (a, c & e) and on 19/12/2023 (b, d & f)

A general pattern among the daily g_s was observed where stomatal conductance increased in the morning, alongside the rising VPD, until around 09:30 to 10:00 am, but it decreased afterwards, while the VPD still rose to its maximum in the afternoon at around 16:00 pm. A similar pattern was followed by E_{leaf} and A_{leaf}. Solar radiation reached its peak at around 13:00 pm on all the measurement dates.

4.9.3.2 Seasonal changes in tree water status

The midday stem water potential is a widely-used indicator of the tree water status (Intrigliolo & Castel, 2006; Dzikiti et al., 2011; Blanco et al., 2025). The leaf water potential, on the other hand, is rarely used for irrigation decision-making, because it is not stable (Dzikiti et al., 2010). It is highly sensitive to rapid changes in environmental conditions, irrespective of the actual tree water status (Jones, 2004). For example, the leaf water potential may increase by a significant margin when a dense cloud passes overhead, even if the water status of the plant has not changed. We measured the stem water potential on six different occasions during the 2024-25 growing season, as shown in Figure 4.20. Several stress thresholds for the midday stem water potentials of pears have been reported in the literature, ranging from -1.25 MPa (Blanco et al., 2025) to around - 1.8 MPa (Miras- Avalos & Araujo, 2025). In this study, we used a midday stem water potential stress threshold of -1.50 MPa and - 1.8 MPa as severe stress. Irrigation must be triggered when the stem water potential approaches this value. It is apparent that some stress occurred in this 'Forelle' orchard early and late in the growing season. The early season stress can be explained by the delay in the commencement of irrigation at the farm. According to the farm manager, there was inadequate water at the farm, so the commencement of irrigation was delayed as much as possible, to stretch the limited resource. This strategy ensured that adequate water was available for the late growth stage, although its effectiveness was unclear. Before harvesting, irrigation was withheld, in order to improve the internal quality of the fruit. This likely explained the late season water stress observed in Figure 4.20.

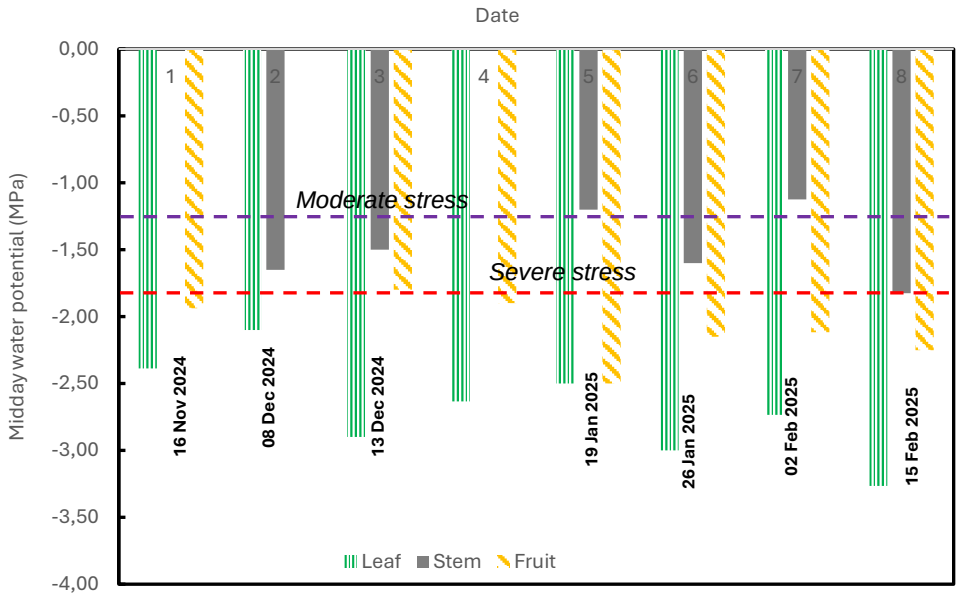


Figure 4.20 Seasonal changes in the leaf, xylem and fruit water potentials of the 'Forelle' orchard over the 2024-2025 season

The accumulation of water stress over the course of the season can be depicted by a Water Stress Integral (WSI), as explained by Meyers et al (1988). According to this approach

$$WSI = \sum_{i=1}^{n} (\psi_{xi} - \psi_0)\, n \qquad (4.8)$$

where ψ_{xi} is the midday stem water potential on day i, ψ_0 is the maximum stem water potential that was set at -1.0 MPa, and n is the number of days between measurements, which was approximately two weeks (14 days). Figure 4.21 shows that the cumulative stress in the 'Forelle' orchard was building up at a lower pace than the cumulative threshold stress that is represented by the orange line. Therefore, we can conclude that the 'Forelle' orchard at Ceres did not experience severe stress over the course of the season.

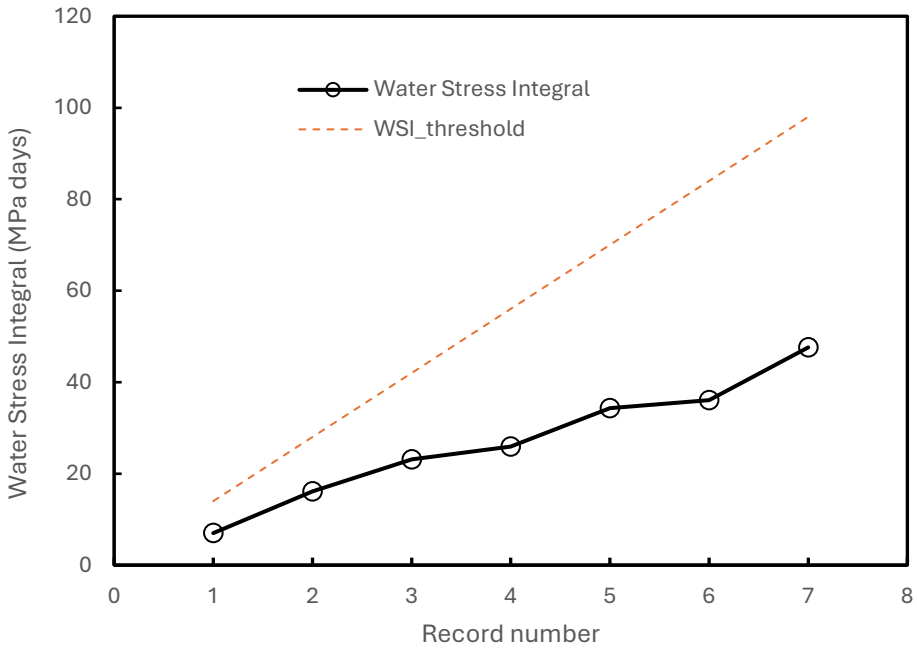


Figure 4.21 Accumulation of water stress in the 'Forelle' orchard over the 2024-2025 growing season in Ceres

4.9.4 Orchard water use

4.9.4.1 Transpiration dynamics

The relationship between the atmospheric evaporative demand and tree transpiration that was measured with sap flow gauges over three growing seasons, is shown in Figure 4.22. For all three seasons (2022-2025), the peak transpiration approached 43 litres per tree per day, which translated to about 6.4 mm/d in equivalent depth units (Figure 4.23). Although the atmospheric evaporative demand was slightly lower in 2022-2023, the high transpiration rates can be attributed to the lack of summer pruning. In 2023-2024, the trees were pruned, but still produced a high peak transpiration, due to the comparatively higher atmospheric evaporative demand, given the strong positive correlation between transpiration and the reference evapotranspiration, as shown in Figure 4.24. Another notable feature of the seasonal tree water use graph is its asymmetric nature in all three seasons. The rapid increase in the leaf area caused a sharp increase in transpiration during the transition from spring to summer. However, the later parts of the growing season, from autumn to winter, was characterised by a slow decline, as the leaves aged and senesced gradually.

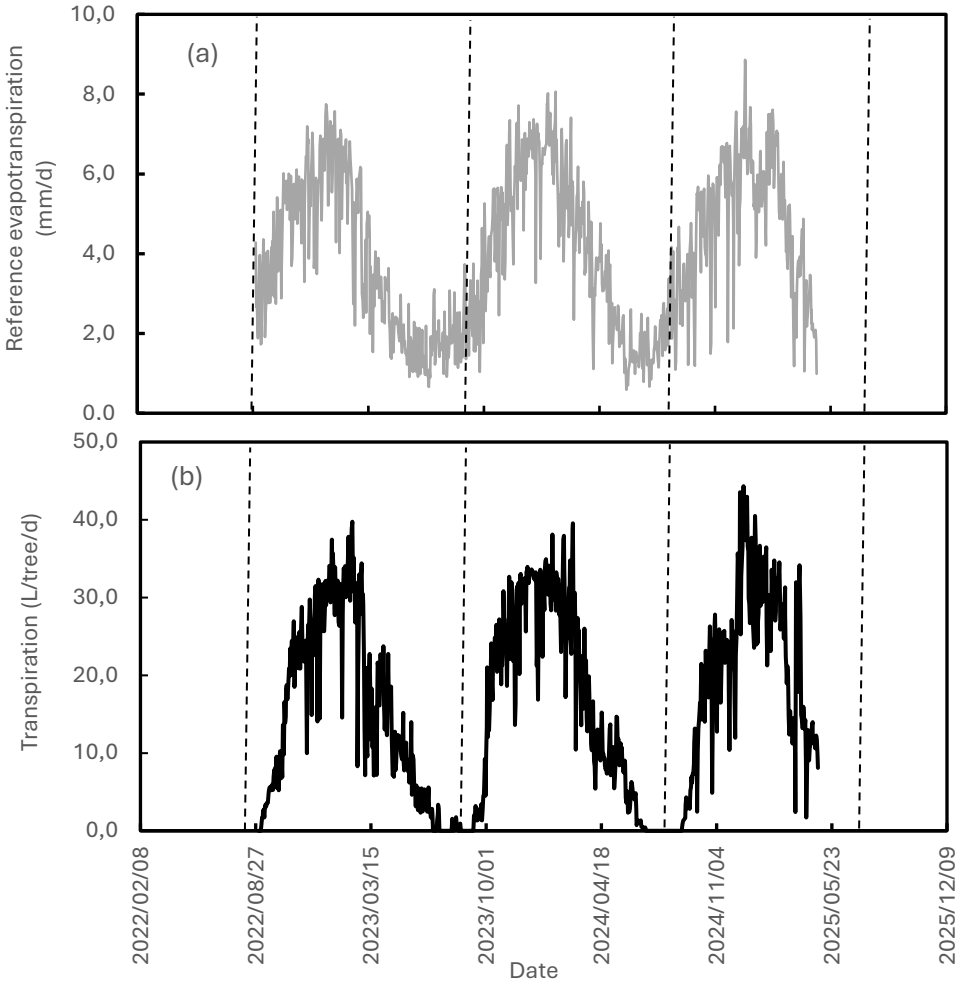


Figure 4.22 (a) Reference evapotranspiration, and (b) actual tree transpiration (in L/tree/day) from October 2022 to February 2024

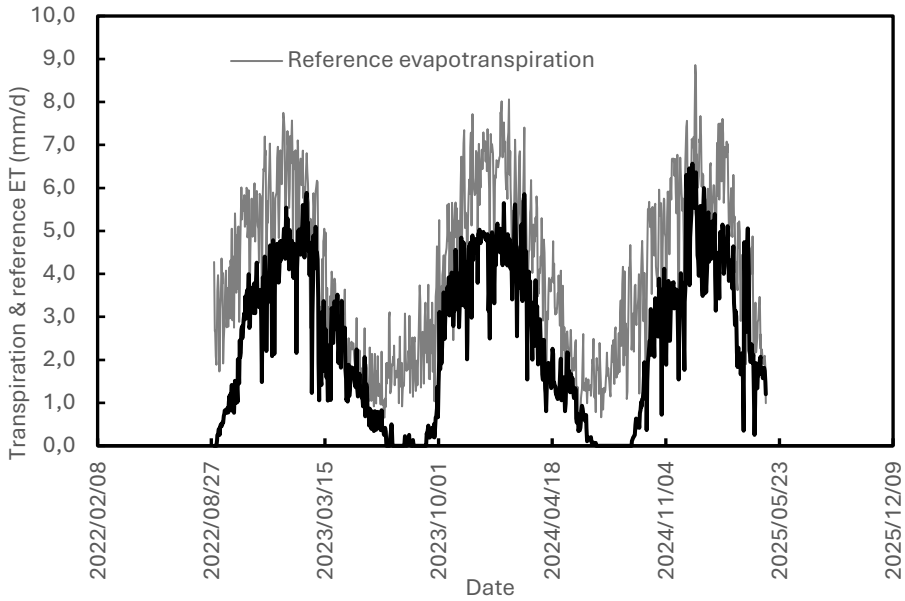


Figure 4.23 Reference evapotranspiration and transpiration expressed in mm/day over three growing seasons

According to Figure 4.23, the tree transpiration was consistently lower than the reference evapotranspiration throughout much of the season. More than 71% of the variation in transpiration of the trees was explained by changes in the atmospheric evaporative demand, as shown in Figure 4.24. The daily transpiration peaked at 5.6, 5.9 and 6.4 mm for the first, second and third season, respectively. The seasonal total transpiration (September to April) was high, at 721 mm during the 2022-2023 season, 773 mm during 2023-2024 and 757 mm during the 2024-2015 season. This translated to 7 210, 7 730 and 7 570 m^3 of water transpired per hectare per season. These transpiration rates are high compared, for example, to those measured on apple orchards with a similar LAI, as reported in previous studies (e.g. Dzikiti et al., 2018; Gush et al., 2019), which suggests a likely higher transpiration per unit leaf area for pear trees than apple trees, which was also reported by Girona et al. (2011).

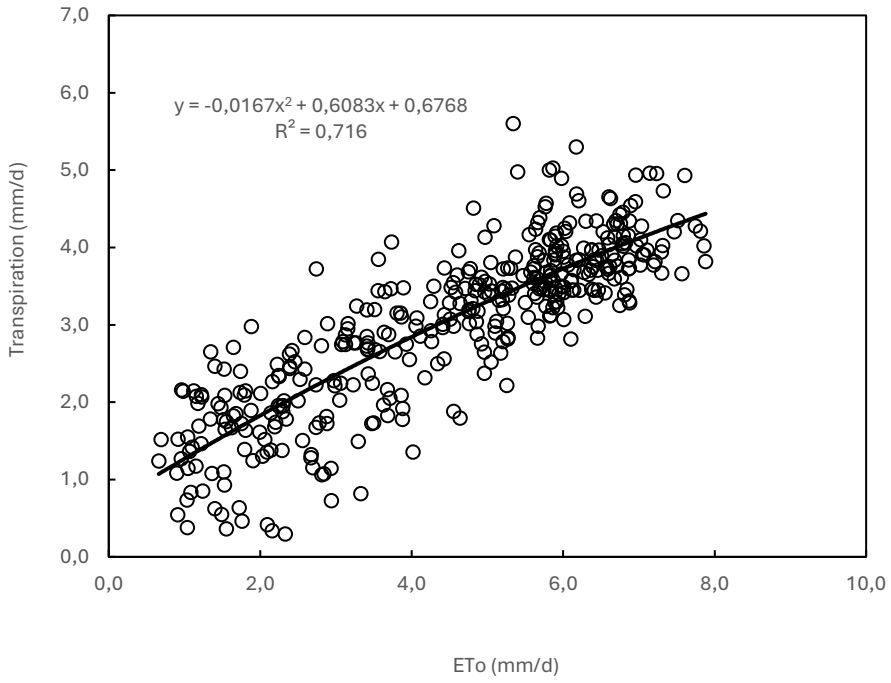


Figure 4.24 Transpiration response of the 'Forelle' orchard to the daily atmospheric evaporative demand over two growing seasons

4.9.4.2 Tree water use and radiation interception

The amount of radiation intercepted by tree canopies is one of the variables that is easy to measure. Some studies have attempted to relate light interception to tree water use by using

complex modelling approaches (e.g. Casadesus et al., 2011; Volschenk et al., 2025). Figure 4.25 shows a strong linear relationship between tree transpiration and the amount of light intercepted only during the active leaf expansion phase, from September to late November. At full canopy cover, the daily transpiration was poorly correlated to the light intercepted. This suggests that light interception is a poor predictor of tree water use at full canopy cover, which varies very little during most of the season. In Figure 4.25, the linear relationship between these variables broke at a LAI value of between 3 and 3.3. This approach may still be useful in young orchards where the mutual shading of leaves is less.

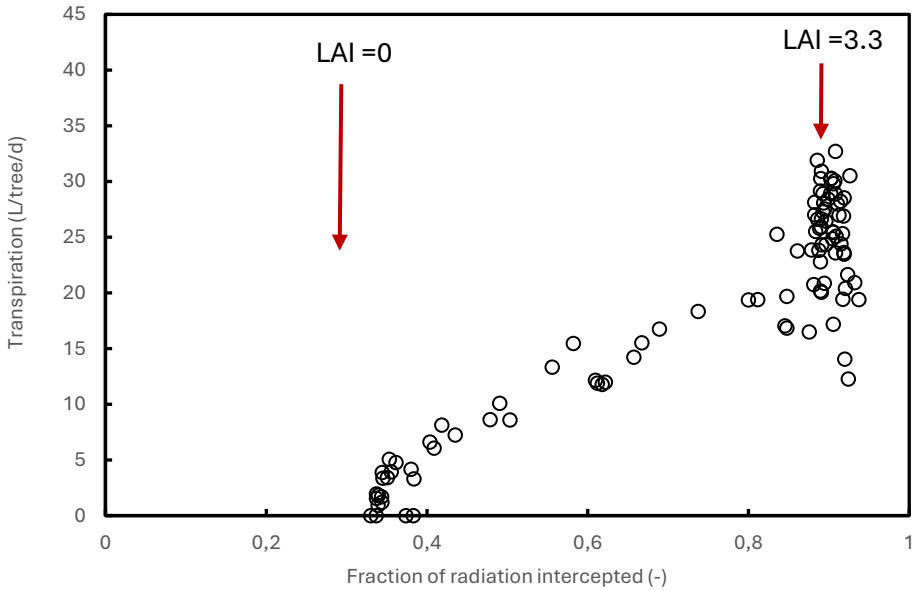


Figure 4.25 Effect of intercepted radiation on tree water use from bud-break to full canopy cover

4.9.5 Orchard evapotranspiration

The actual daily orchard evapotranspiration was measured in the 'Forelle' orchard at Buchuland from 15 December 2023 to 06 February 2024. Micrometeorological techniques, such as the eddy covariance, scintillometry, surface renewal, Bowen Ratio, etc., are based on the assumption that the surface of interest is a flat, extensive and homogenous surface. The orchard surface is heterogenous, and is characterised by distinct tree rows and wide interrow spacings. In addition, the specific orchard at Buchuland was on sloping terrain, which caused the surface to deviate from the ideal surface. To correct for this, an energy balance closure analysis was undertaken, in the available energy ($R_n - G$) was compared against the sum of the major fluxes lost from the orchard, as the latent heat flux (the energy equivalent of

evapotranspiration - LE) and the sensible heat (H – energy used to warm the air). Figure 4.26 shows a substantial energy imbalance in which less than 50% of the available energy was converted into LE and H, despite the strong correlation. This energy imbalance was corrected by using the Bowen ratio approach, as described by Dzikiti et al. (2018), among others.

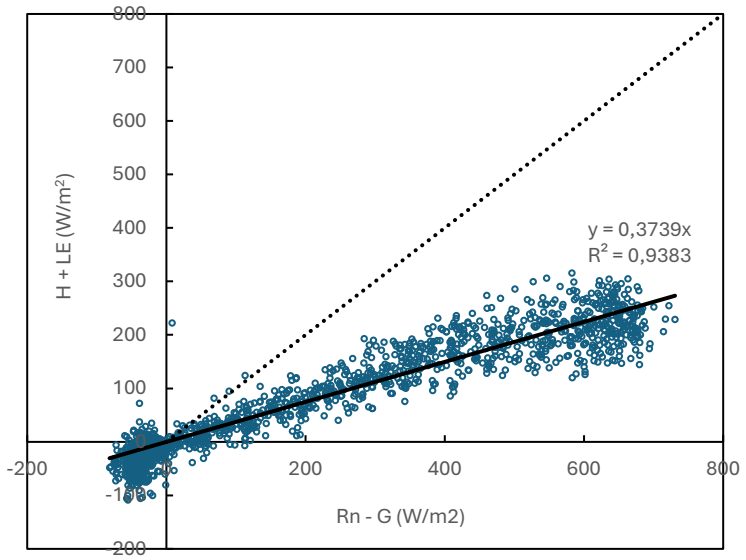


Figure 4.26 Energy balance closure for the 'Forelle' orchard

The relative magnitudes of the reference evapotranspiration, orchard transpiration and actual evapotranspiration (ET) are shown in Figure 4.27. The actual evapotranspiration was close, but slightly lower than, the reference evapotranspiration during the measurement period, which suggests mid-season crop coefficients of around 1.0, if not slightly lower.

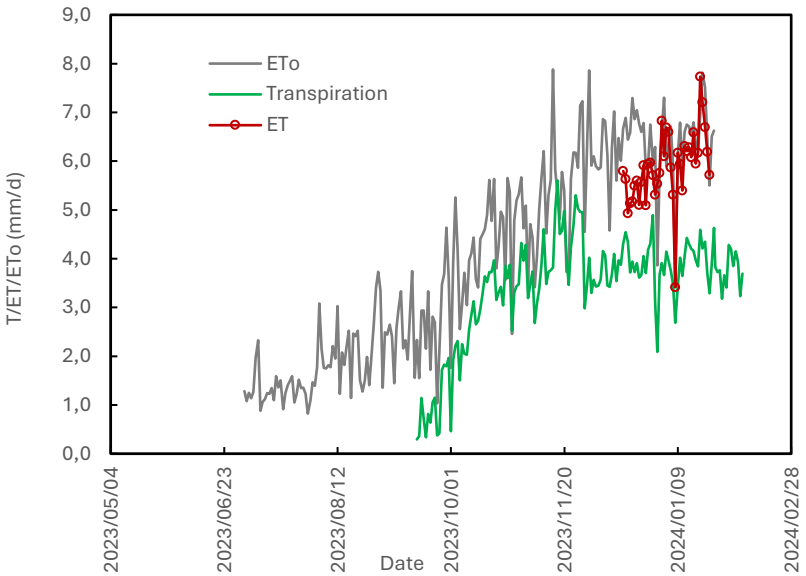


Figure 4.27 Comparison of the measured ET_o, actual evapotranspiration and orchard transpiration

Detailed estimates of the crop coefficients are presented in the water use modelling section. As expected, the orchard transpiration was lower than the actual evapotranspiration, which suggests a substantial contribution of the orchard floor evaporation to the water use of the whole orchard.

4.9.6 Modelling water use and its partitioning in the 'Forelle' orchard

The dual source model accurately predicted the orchard water use and its components, namely, the tree transpiration and orchard floor evaporation. Changes made to the water use model parameters, relative to the original ones used on apple orchards, are the minimum stomatal resistance of 56.2 s/m; Kr = 0.1 MJ/m^2/d; k_{vpd}= 0.08 kPa^{-1}; T_{max} = 50°C; T_{opt} = 25°C and T_{min} = 0°C. In this study, we assumed that the soil water content was not limiting, as the orchards were generally well watered. Therefore Equation 3.21 = 1. The measured and modelled whole orchard transpiration were similar over two growing seasons (Figure 4.28a). Similarly, the modelled orchard ET was not significantly different from the measured values (Figure 4.28b). Detailed statistics of all the data are presented in Chapter Seven, when the last orchard is discussed.

When applying the model to estimate the daily orchard water use and its partitioning, the trend emerges, as shown in Figure 4.29. Orchard floor evaporation dominated the ET flux early in the season. However, as the canopy cover developed and much of the orchard floor was shaded, transpiration contributed the most to the daily orchard ET. The higher LAI during the 2022-2023 season, due to the orchard not being pruned, resulted in a lower rise in orchard floor evaporation than in the second season, when the canopy was relatively more open. The contribution of the orchard floor to the daily ET varied from almost 100% in early September to around 20% in mid-January.

The modelled total ET (01 September to 30 April) of the 'Forelle' orchard, averaged over the three seasons, was around 916 mm (9 160 m^3/ha). Of this, 7 500 m^3/ha was from tree transpiration and about 1 660 m^3/ha from orchard floor evaporation. This means that beneficial water use (transpiration) amounted to close to 80% of the total orchard water consumption, and the balance was from orchard floor evaporation. The low orchard floor evaporation was likely a result of the high canopy cover in this orchard, the narrow range micro-sprinklers that

wetted a small orchard floor area, and the reduced irrigation at certain times of the season, due to the water shortage experienced by the farm.

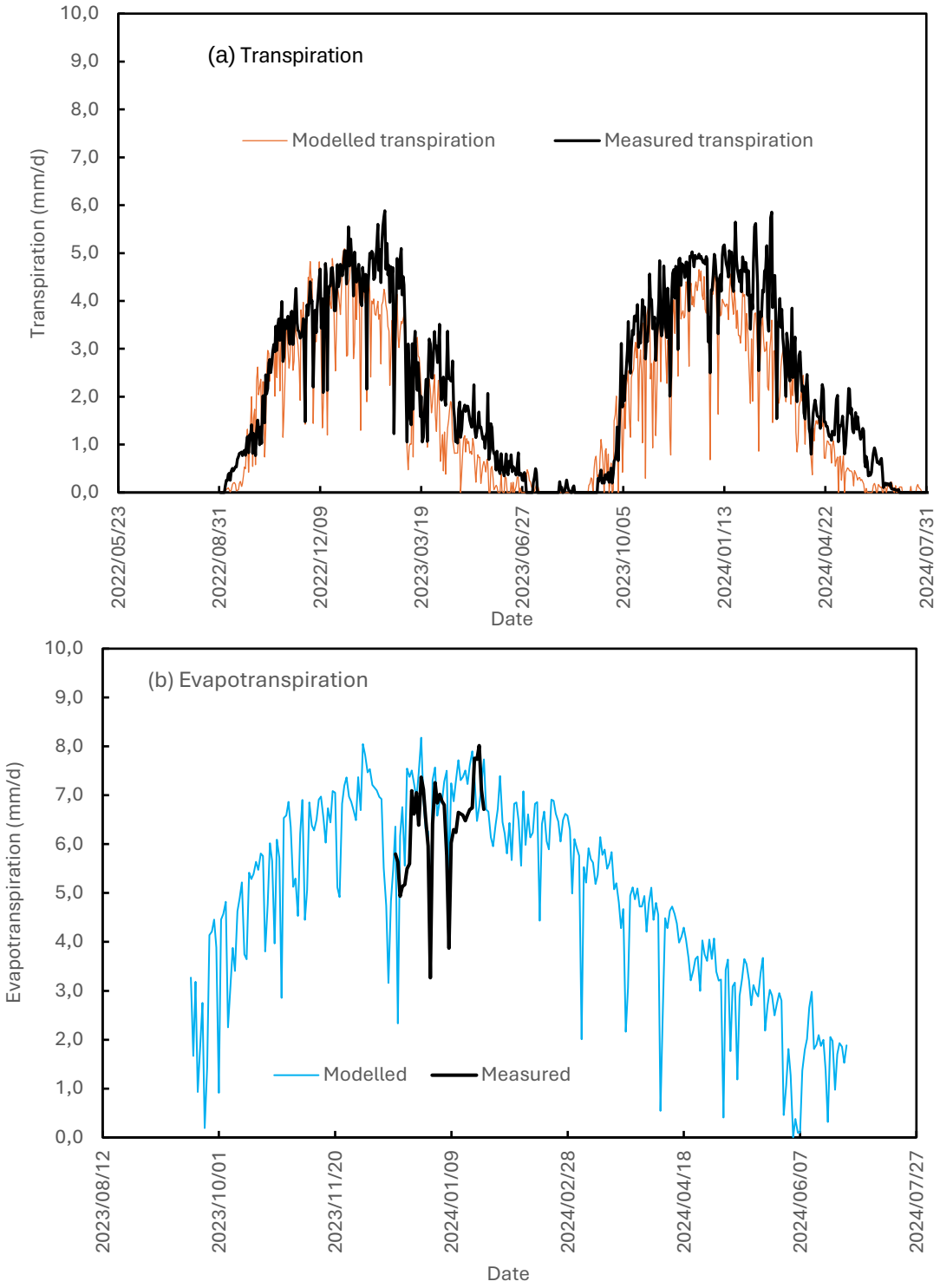


Figure 4.28 Comparison of measured vs modelled (a) daily transpiration, and (b) orchard evapotranspiration.

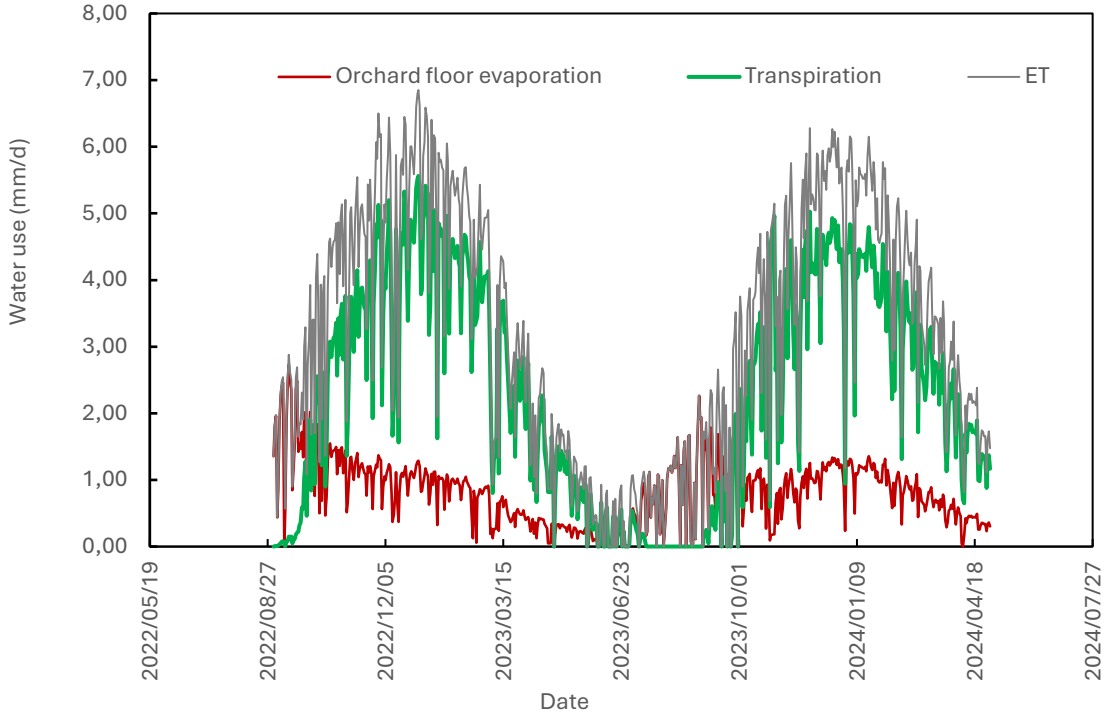


Figure 4.29 Partitioning of daily evapotranspiration (ET) into the transpiration and orchard floor evaporation components over the 2022 to 2024 growing seasons

We applied the model to illustrate how the cumulative orchard ET compared with the other water fluxes. We used the 2023-2024 growing season as an example in Figure 4.30.

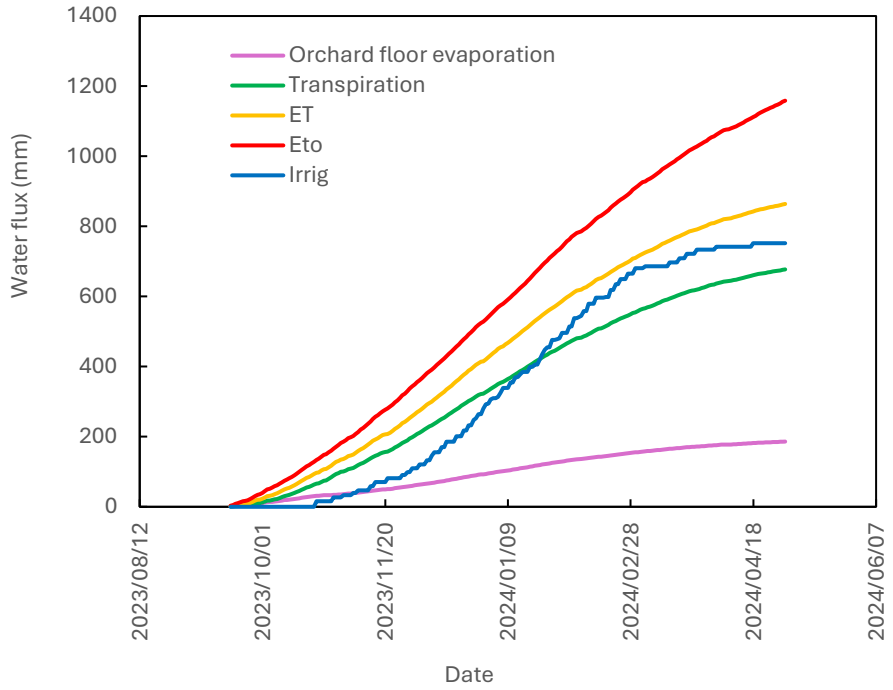


Figure 4.30 Cumulative transpiration, actual evapotranspiration, reference evapotranspiration and irrigation for the 'Forelle' orchard during the 2023-2024 season

The late start to the irrigation is evident (blue line) in which light irrigation was applied from late October to the first week of December during the 2023-2024 season. The cumulative irrigation only matched the transpiration on 16 January 2024, but it never matched the ET. About 250 mm of rainfall was received during the season and this likely made up for the deficit in the crop water requirement. Figure 4.31 shows the weekly measured and modelled basal crop coefficient (K_{cb} = T/ET_o) and the orchard crop coefficient (K_c = ET/ET_o). The mid-season crop coefficients (Kc) derived in this study (~ 0.90 – 1.09) were consistent with the FAO 56 tabulated value for pears averaging ~ 0.95 (Allen et al., 1998), as well as with those derived in Spain by Girona et al. (2011) (Kc ~ 1.0).

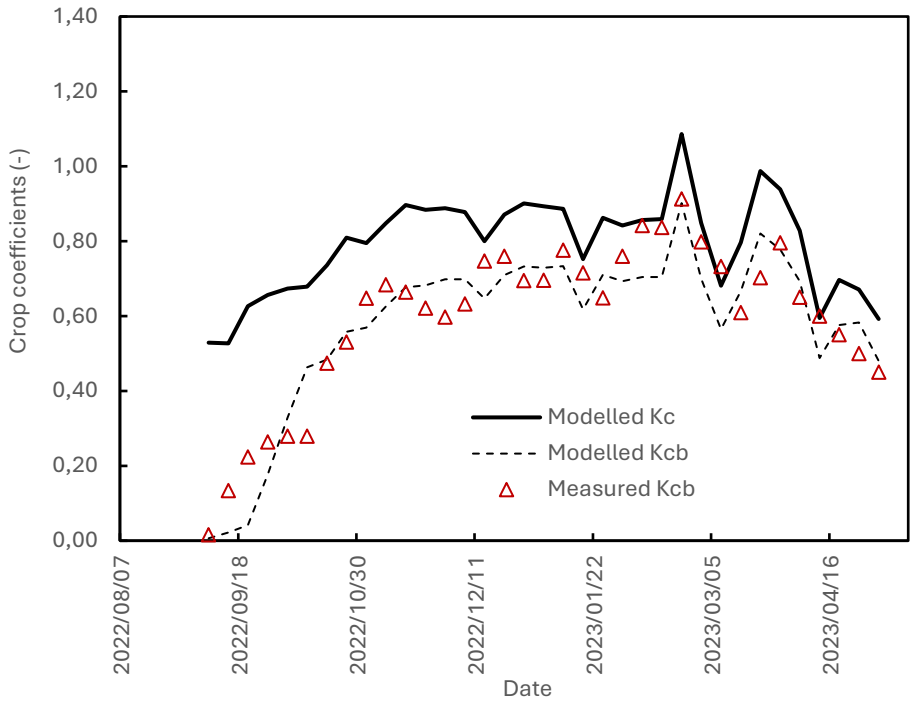


Figure 4.31 Crop coefficients for a mature 'Forelle' orchard in Ceres over the course of the 2023-2024 growing season

4.9.7 Fruit growth and quality for the 'Forelle' orchard in Ceres

The typical seasonal growth trend for the 'Forelle' fruit that is measured using dendrometers hourly during the 2022-2023 growing season, is shown in Figure 4.32. Over the 111-day measurement period, the fruit grew by about 31.8 mm, giving an average growth rate of about 0.28 mm/d, or roughly 2 mm per week. An initial detailed description of the growth

dynamics of the pear fruit, in relation to the phenological stage and environmental factors, were described in a paper published in the Water SA Journal (Dzikiti et al., 2024).

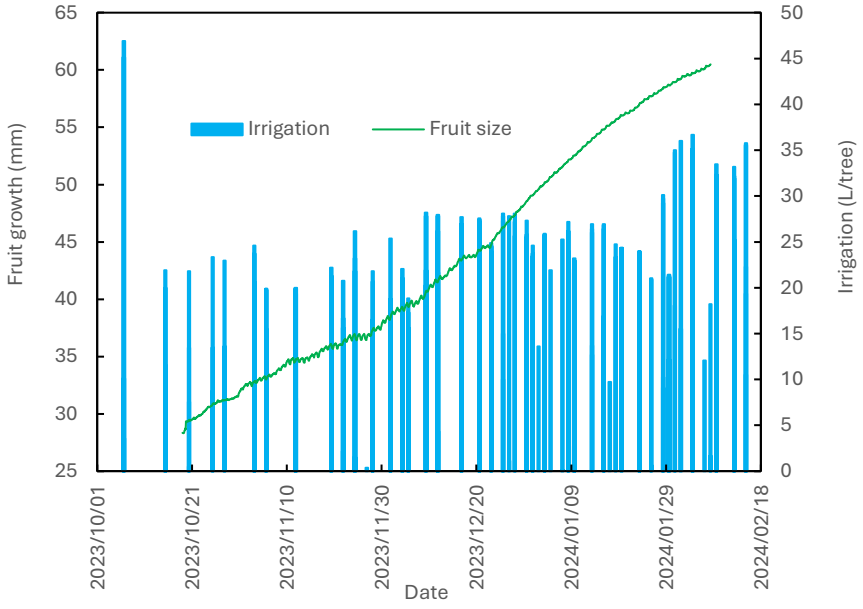


Figure 4.32 Fruit growth trends in relation to irrigation received an individual 'Forelle' tree

Details of the yield and the mean sizes for the harvested trees are shown in Table 4.5 for the three seasons.

Table 4.5 Average yield, fruit number and trunk circumference per tree for 'Forelle' trees

Season	Cultivar	Yield (kg/tree)	Number of fruits/tree	Trunk circumference (cm)	Yield efficiency (kg/cm2)
2022-2023	'Forelle'	26.8	147	63.62	0.08
2023-2024	'Forelle'	39.8	271	62.7	0.13
2024-2025	'Forelle'	47.6	338	64.4	0.14

With a tree density of 1 481 plants per hectare, the 26.8 kg/tree translated to an estimated yield of about 39.7 t/ha. In the 2023/24 season, the average yield increased to 39.8 kg per tree, which translates to approximately 58.9 t/ha. The average yield per tree in 2024/25 was much higher at 47.6 kg, which amounted to 70.5 t/ha. The yield values for all the seasons were compared with those obtained by the packhouse. The yield efficiency (yield in kg per

square centimetre of stem area) was very low in the first season, corresponding to the smaller yield at 0.08 kg/cm^2, and increasing to 0.14 kg/cm^2 in the final year.

4.9.8 Fruit quality

Table 4.6 shows that the fruit mass on the top- and outside of the canopy had similar values. There were appreciable differences in mass for the inside and bottom fruits (which themselves had similar values). The 'Forelle' pears showed almost no starch breakdown at the time of the fruit quality assessment.

Table 4.6 Averages of the quality parameters, per position – and overall, for the 'Forelle' pears

Season	Cultivar	Position	Firm A (kg)	Firm B (kg)	Diameter (mm)	Mass (g)	Height (mm)	BG A	BG B	Starch (%)	TSS (%)	TA (%)
	'Forelle'	Top	6.7	6.5	64.0	173.1	83.2	2.3	-	0.0	14.7	0.3
		Outside	6.3	6.4	63.3	173.2	84.5	2.3	-	0.0	14.2	0.3
2022-2023		Inside	6.2	6.2	60.5	151.7	80.7	2.3	-	0.0	13.5	0.4
		Bottom	6.2	6.2	61.0	152.7	80.3	2.3	-	0.6	13.3	0.4
		Average	6.3	6.3	62.2	162.7	82.2	2.3	-	0.15	13.9	0.3
2023-2024	'Forelle'	Outside	6.6	6.6	60.1	144	-	2.1	-	0.0	16.1	-
		Inside	6.4	6.6	60.4	143.7	-	2.3	-	0.0	15.9	-
		Average	6.5	6.6	60.3	143.9	-	2.2	-	0.0	16	-
2024-2025	'Forelle'	Outside	6.5	6.5	58.0	147.6		2.6		0.0	13.5	

Additional fruit quality variables, taking into account the position of the harvested fruit in the canopies, were also included, as reported in Table 4.7.

Table 4.7 Averages of the additional quality parameters, per position – and overall, measured on the 'Forelle' pears

Cultivar	Position	Red Intensity	Red %	Cork spot	Sunburn
'Forelle' (2022-23)	Top	5.5	40.8	0.0	1.5
	Outside	6.6	35.9	0.0	2.2
	Inside	10.5	10.5	0.0	0.6
	Bottom	10.1	12.4	0.0	0.4
	AVERAGE	8.2	24.9	0.0	1.2
2023-2024	Outside	7.2	32.2	0.0	0.6
	Inside	8.1	10.1	0.0	0.0
	AVERAGE	7.7	21.2	0.0	0.3
2024/25	Outside	5.8	30.6	0.0	1.0

Even though no statistical analysis has been done yet, clear differences are apparent between the different canopy positions for all the parameters, except for cork spot incidence, which remained zero throughout the canopy. These differences are expected, since they reflect the effect of the sunlight distribution pattern throughout a tree canopy.

4.9.9 Water productivity for the 'Forelle' orchard in Ceres

The mean T-based WP of 'Forelle' pear in the Ceres region (Table 4.8) was 7.65-9.67 kg m^{-3} across the first two seasons, when calculated for the trial trees. The transpiration data for the third season was problematic, and therefore, it was left out of the calculations. When using the yield data for the whole orchard block, it was 6.79-9.3 kg m^{-3} for the 2022 to 2024 seasons. The small difference between trial trees and the orchard block can be ascribed to the slightly lower yield in the whole orchard. WP was the highest in 2024-2025, but we suspect this was due to the poor quality of the sap flow data, due to the trees reacting to prolonged exposure to the probes over multiple seasons. In contrast, the value was lowest in 2023-2024, when the yield was lower and transpiration was higher, as the trees were not pruned during that season. The T-based EWP was 79.2-115.3 R m^{-3} for the two seasons – these high values are linked to a high crop gross value of 'Forelle'. The relatively lower value for 2023-2024 was due to both the lower crop gross value and the higher seasonal transpiration.

Table 4.8 Physical Water Productivity (WP), Water Use Efficiency (WUE), and Economic Water Productivity (EWP), based on seasonal transpiration for the 'Forelle' pear orchard in Ceres in 2022-2023, 2023-2024 and 2024-2025

	2022-2023	2023-2024	2024-2025
Planting density (trees/ha)	1481	1481	1481
Seasonal transpiration (mm)	721.4	772.8	597.1
Seasonal transpiration per hectare (m^3/ha)	7214.2	7727.6	5971.1?
Trial trees:			
Yield (t/ha)	69.8	59.1	78.3
Water Use Efficiency (m^3/ton)	103.4	130.8	76.2
Physical Water Productivity (kg/m^3)	9.67	7.65	13.1?
Whole orchard block:			
Yield (t/ha)	66.7	52.5	65.0
Water Use Efficiency (m^3/ton)	108.2	147.2	91.9
Physical Water Productivity (kg/m^3)	9.3	6.8	10.9
Orchard gross income (R/ha)	R831 732	R612 234	R809 214
Economic Water Productivity (R/m^3)	R115.29	R79.23	R135.52

When calculated, based on the ET (Table 4.9), the WP values of the trial trees were 6.63-8.87 kg m^{-3} for the three seasons. For the whole orchard, the corresponding values were 5.89-7.36 kg m^{-3}. The differences were due to a higher yield for the whole orchard. The ET-based EWP was 68.69-91.56 Rand m^{-3}. The high gross value of the 'Forelle' crop yielded a high EWP, especially in the first and third seasons, with a slightly lower value in the second season, because of the lower yield and lower gross value. Seasonal ET values were relatively similar across the three years.

Table 4.9 Physical Water Productivity (WP), Water Use Efficiency (WUE), and Economic Water Productivity (EWP) based on seasonal evapotranspiration for the 'Forelle' pear orchard in Ceres in 2022-2023, 2023-2024 and 2024-2025

	2022-2023	2023-2024	2024-2025
Planting density (trees/ha)	1481	1481	1481
Seasonal evapotranspiration (mm)	923.2	891.4	883.6
Seasonal evapotranspiration per hectare (m^3/ha)	9232.0	8913.6	8835.7
Trial trees:			
Yield (t/ha)	69.76	59.09	78.33
Water Use Efficiency (m^3/ton)	132.4	150.8	112.8
Physical Water Productivity (kg/m^3)	7.56	6.63	8.87
Whole orchard block:			
Yield (t/ha)	66.7	52.5	65.0
Water Use Efficiency (m^3/ton)	138.4	169.8	135.9
Physical Water Productivity (kg/m^3)	7.22	5.89	7.36
Orchard gross income (R/ha)	R831 732	R612 234	R809 214
Economic Water Productivity (R/m^3)	R90.09	R68.69	R91.58

4.10 CONCLUSIONS

We collected three years of detailed data for the 22-year-old 'Forelle' orchard at Ceres. The results suggest that this orchard had high seasonal water use rates, with the total measured transpiration averaging 750 mm (750 m^3/ha) over two irrigation seasons (2022-2024). The modelled seasonal total evapotranspiration averaged 9 160 m^3/ha. Early in the season, orchard floor evapotranspiration accounted for 100% of the orchard ET, and this contribution declined to around 20% at the mid-season stage. The modelled single crop coefficient (K_c) for the orchard was around 1.0. The average transpiration-based physical water productivity was about 8.7 kg/m^3, while the ET based physical water productivity was lower, averaging 7.1 kg/m^3. The transpiration based economic water productivity averaged R97/m^3, while the ET based value was lower, at R79/m^3.

CHAPTER FIVE

'PACKHAM'S TRIUMPH' ORCHARD, WOLSELEY

5.0 INTRODUCTION

According to the Hortgro Tree Census of 2022, Wolseley and Tulbagh are the fourth-largest growing regions for pears in the Western Cape. They have approximately 1 429 ha under pears, which are dominated by cultivars such as 'Forelle', 'Packham's Triumph' and William Bon Chrétien. In this Chapter, we report on the data collected over two growing seasons in a mature high-performing 'Packham's Triumph' orchard in Wolseley. The climate of Wolseley, as classified according to the Köppen-Geiger classification, was Csa, which is characterised by warm dry summers and cool wet winters. The high summer temperatures in Wolseley are like those in Ceres, but the winters are warmer, averaging 9° to 10°C.

The soils in the Wolseley area are predominantly sandy loam, which is often mixed with gravel clay. The alluvial nature of the soils in the Breede River Valley makes them fertile, well-drained and suitable for planting a wide range of crops, with vineyards, pear orchards and nectarines orchards being the dominant crop types. These crops are also grown under irrigation, often with water drawn from the Breede River. The water requirements of the pear orchards in this region are not known. Therefore, this study sought to close this important information gap for trees that were well-watered, by using the actual water use, yield and environmental measurements. These data were used to calibrate and validate the dual source ET model described in Chapter 3.

Climate change is a huge concern for the fruit industry in the Western Cape Province, where the frequency and severity of droughts is expected to increase in future. We obtained daily climate change data for the period 01 January 1961 to 31 December 2099 for six global circulation models for a 50 km x 50 km grid that included the Wolseley area (Dzikiti et al., 2022). The data were used to run the dual source ET model, in order to obtained estimates of changes in the water requirements of pear orchards under future harsher growing conditions. The simulations were performed for the worst-case business-as-usual scenario (RCP 8.5), where the trapped energy within the atmosphere is projected to increase by 8.5 W/m^2 by 2100, causing significant warming.

5.1 STUDY SITE AND PLANT MATERIAL

The ‘Packham’s Triumph’ orchard (Figure 5.1) was at the Romansrivier Farm (33°27’37.51” S; 19°11’40.44” E, 258 m asl) in Wolseley, which flanks the banks of the Breede River on either side of the river channel. The orchard was 16 years old when the study commenced, having been planted in 2009 in rows with a north-south orientation. The rootstock was the BP1 rootstock, and the orchard size was about 2.75 ha. The tree spacing was 4 m x 1.5 m, giving a tree density of 1 667 trees per hectare (Table 5.1). The orchard was on flat terrain, and the trees were planted on low ridges. The soils were deep sandy loams of the Fernwood soil form, the physical properties of which are summarised in Table 5.2. There was a thick layer of clay soil at a depth of about 60 to 70 cm, which most likely limited the depth of the root system. Irrigation was via a micro-sprinkler system, with one micro-sprinkler per tree and with each micro sprinkler delivering about 32 L/h. Irrigation was scheduled by means of soil moisture probes (IrriCheck Pty Ltd). According to the farm manager, the irrigation season started in about the first week of October, where the trees received water roughly twice per week. During the warm summer months, and during the fruit growth stages that are sensitive to water deficits, irrigation was applied up to three times per week.



Figure 5.1 ‘Packham’s Triumph’ orchard at the Romansrivier Farm in Wolseley, showing the late spring and summer images

According to the pear industry experts, this 'Packham's Triumph' orchard was ranked as one of the highest-yielding orchards, as it consistently produced close to 80 t/ha, on average. The orchard was bounded to the south by tall windbreaks, which most likely affected the turbulent air fluxes over the orchard.

Table 5.1 Properties of the 'Packham's Triumph' orchard in Wolseley

Age	13 years
Block size	2.75 ha
Coordinates	33°27'37.51" S; 19°11'40.44" E. 258 m asl
Planting density	1 667 trees per ha
Cultivar	'Packham's Triumph'
Rootstock	BP1
Height	4.0 m
Irrigation	Micro sprinkler (35 L h^{-1})
Soils	Clayey loam
Average yield	80 t ha^{-1}

5.2 SOILS AND CLIMATE DATA

The orchard was planted in a uniform fine sandy loam soil, with a low percentage of stone present throughout the soil profile. Although the soil particle analysis showed low clay percentage values (*ca.* 9%), there was a high percentage of fine sand present. Fine sand has been known to act similarly to clay particles, in terms of their soil water-holding capacity. This is reflected in the total available soil water content of *ca.* 135.1 mm. The field water capacity and permanent wilting point amounted to 0.195 $mm.mm^{-1}$ and 0.044 $mm.mm^{-1}$, respectively.

Table 5.2 Soil physical properties for the 'Packham's Triumph' orchard in Wolseley

Soil depth (mm)	Clay (%)	Silt (%)	Fine sand (%)	Medium sand (%)	Coarse sand (%)	Sand grade	Soil texture class[1]
0 - 300	8.0	20.0	53.3	15.2	3.5	Fine	Sandy loam
300 - 600	10.0	16.0	61.3	10.5	2.2		
600 - 900	10.0	24.0	45.5	16.8	3.8		

[1]According to the soil texture classification of the USDA

Similar data on the tree growth, soil water content and transpiration were collected in the 'Packham's Triumph' orchard in Wolseley, as described for the 'Forelle' orchard in Ceres. In the 'Packham's Triumph' orchard in Wolseley, data were collected over two growing seasons, from 01 September 2022 to 30 April 2024, and at the same intervals as the 'Forelle' orchard in Ceres. Weather data were measured by using an automatic weather station (Figure 5.2). The station was located next to the ''Packham's Triumph' orchard'. The station was installed over a uniform short grass surface, the attributes of which resemble the grass reference crop (Allen et al., 1998). The equipment used for the weather station was comprised of pyranometers (Model: SP 212 Apogee Instruments, Inc., Logan UT. USA), which measured the solar irradiance, and the air temperature and relative humidity probe (Model: HMP60 Campbell Scientific, Inc., Logan UT, USA), which was installed about 2.0 m above the ground. A three-cup anemometer and wind vane (Model RM Young Wind Sentry Set Model 03001, Campbell Scientific, Inc., Logan UT, USA) was used to measure the wind speed and direction, respectively at a 2.0 m height, while the rainfall was recorded by using a tipping bucket rain gauge (Model: TE525-L; Campbell Scientific, Inc., Logan UT, USA). All the sensors were connected to a data logger (Model: CR1000 Campbell Scientific, Inc., Logan UT, USA), which was programmed with a scan interval of 10 s. The output signals were processed at hourly and daily intervals.

5.3 WATER USE MEASUREMENTS

The actual evapotranspiration (ET) of the 'Packham's Triumph' orchard was measured by using an open-path eddy covariance system (Figure 5.3). The flux tower was located downstream to the prevailing winds in the orchard, on account of the small orchard size. The fluctuations in the concentration of water vapour and CO_2 above the orchard were measured by using a combined infrared gas analyser and a 3D sonic anemometer (Model: IRGASON, Campbell Scientific, UT, USA). The installation height of the sensors was about 2.5 m above the tree canopies (Figure 5.3). This height ensured that the device was above the surface roughness sublayer and that there was adequate fetch around the tower. The IRGASON was installed, pointing in the direction of the prevailing wind, which was generally south-easterly.



Figure 5.2 Automatic weather station at the Romansrivier Farm, Wolseley



Figure 5.3 Eddy covariance system measuring the whole orchard evapotranspiration in Wolseley

Other measurements included the net radiation (Rn), which was measured by using a one-component net radiometer (Model CNR1: Kipp & Zonen, The Netherlands) and which was installed at a height of about 8.0 m from the ground. Heat transfer into and out of the ground was measured by using soil heat flux plates (Model: Hukse Flux, The Netherlands), which was installed at a depth of 8.0 cm from the soil surface. A pair of soil-averaging thermocouples (Model: TCAV -L, Campbell Scientific, UT, USA) were installed above the soil heat flux plates, in order to correct the soil heat flux values (G) for the energy stored by the soil above the plates. The data were collected at a frequency of 10 Hz and the signals were processed at 30-minute intervals. The high frequency signals were processed online by using the EasyFlux software. The software corrected the signals for the lack of levelness of the equipment (coordinate rotation), fluctuations in air density, according to the Webb-Pearman-Leuning approach, as well as other corrections.

The transpiration was measured on three trees of different stem sizes, as in the 'Forelle' orchard. Therefore, we will not repeat the full details of the methodology.

5.4 WATER USE MODELLING: IMPACT OF CLIMATE CHANGE ON ORCHARD WATER USE

Climate change simulations were performed by using daily climate data for the period 01 January 1961 to 31 December 2099. The data were used in the dual source ET model described in Chapter Three, assuming that the trees were always well irrigated. All changes in the tree physiology were due to climatic conditions. The climate change data were derived for a 50 km x 50 km horizontal grid close to the Wolseley study area, by using the Conformal-Cubic Atmospheric Model (CCAM) developed by CSIRO (Commonwealth Scientific and Industrial Research Organisation) in Australia (McGregor & Dix, 2001). The CCAM model is a variable-resolution Global Climate Model (GCM) that was used to realistically simulate the climate system teleconnection to southern Africa (Dzikiti et al., 2022). The present study used six GCMs, namely: the Community Climate and Earth-System Simulator (ACS 1-0); the National Centre for Meteorological Research Coupled Global Climate Model, Version 5 (CNR-CM5); the Geophysical Fluid Dynamics Laboratory Coupled Model (GFD-CM3); the Max Planck Institute Coupled Earth System Model (MPI-ESM-LR); the Norwegian Earth System Model (NOR-ESM1-M); and the Community Climate System Model (CCS-M4).

All model runs to generate the climate change data were performed under the Representative Concentration Pathway 8.5 (RCP 8.5). This scenario is commonly referred to as the 'business-as-usual' scenario, which represents the 90th percentile of the policy scenarios used in the Coupled Model Intercomparison Project Phase Five (CMIP5). RCP 8.5 is also associated with high baseline emissions and low mitigation for the 21st century.

The extraction of site-specific meteorological data, including the near air surface (2 m) maximum and minimum temperatures, the maximum and minimum relative humidity, and the daily average windspeed and precipitation from gridded modelled fields, was achieved through an inverse distance weighted remapping, by using the Climate Data Operator (CDO) (Lötter & le Maitre, 2014). The missing daily total solar radiation (R_s) was calculated from the temperature data, following the approach by Allen et al. (1998):

$$R_s = k_{Rs}\sqrt{T_{max} - T_{min}}R_a \qquad (5.1)$$

where T_{max} and T_{min} (in °C) are the daily maximum and minimum temperatures, R_a (MJ/m_2/d) is the extraterrestrial radiation, k_{Rs} is a constant equal to 0.16 for 'interior' locations, where land mass dominates and air masses are not strongly influenced by a large water body (Allen et al., 1998). The extraterrestrial radiation was calculated, as described in the FAO 56 (Allen et al., 1998). The validation of the simulated daily solar radiation with the actual measured values over close to two years, from September 2022 to July 2024, is shown in Figure 5.4.

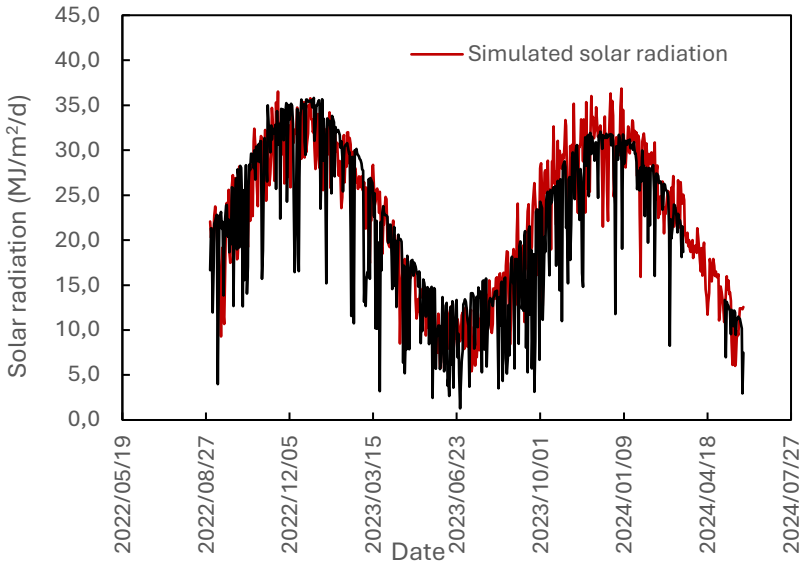


Figure 5.4 Comparison of the observed (black line) and the simulated daily solar radiation over two years from September 2022 to July 2024 for the Wolseley weather

station.

The climate change data were subsequently used as inputs to the pear orchard water-use model that was developed, and they were calibrated and validated by using the actual measured data collected in this study. These data were used to simulate future changes in the crop water requirements between the current (2020- 2030), near-term (2050-2065) and the far-future periods (2090-2099) for each of the six GCMs.

5.5 YIELD AND FRUIT QUALITY

The harvest date for the 2022/2023 season was 02 February 2023, and for the 2023/2024 it was 31 January 2024. The method of sampling fruits and measuring the fruit quality parameters was similar for both the 'Packham's Triumph' and 'Forelle' cultivars, as described in Chapter 4. The 'Packham's Triumph' fruits were picked before midday and placed in a Regulated Atmosphere (RA) cold room at 10°C, upon their arrival at the University. The following morning, the fruits were removed from storage and left for two hours to warm to room temperature, before the Maturity Indexing (MI) procedure began. The MI parameters common to all the cultivars, were described in Chapter 4.

5.6 RESULTS AND DISCUSSION

5.6.1 Climatic conditions for 2022-24 in Wolseley

As expected, the seasonal trend in most climatic variables at Wolseley were like that at Ceres over the two seasons, although the magnitudes of some variables differed. For instance, the daily maximum solar irradiance in summer was slightly low in Wolseley, peaking at about 33 MJ/m^2/d, while the wintertime maximum was a little higher at 12.5 MJ/m^2/d (Figure 5.5a). Wolseley recorded maximum temperatures of 40.3° and 40.6°C, respectively, during the 2022-2023 and 2023-2024 seasons, which were higher than those recorded in Ceres. The minimum winter temperatures were 1.7°C in 2022-2023 and -1.0°C in 2023-2024 (Figure 5.5b). The average temperature for the entire study period was higher in Wolseley, at about 18.6°C, compared to 14.5°C in Ceres. The relatively high temperatures at Wolseley led to a somewhat higher VPD during the first two seasons, which peaked at 2.1 kPa, which suggests a somewhat higher atmospheric evaporative demand in Wolseley (Figure 5.5c). The average daily wind varied between 1.9 and 2.1 m/s.

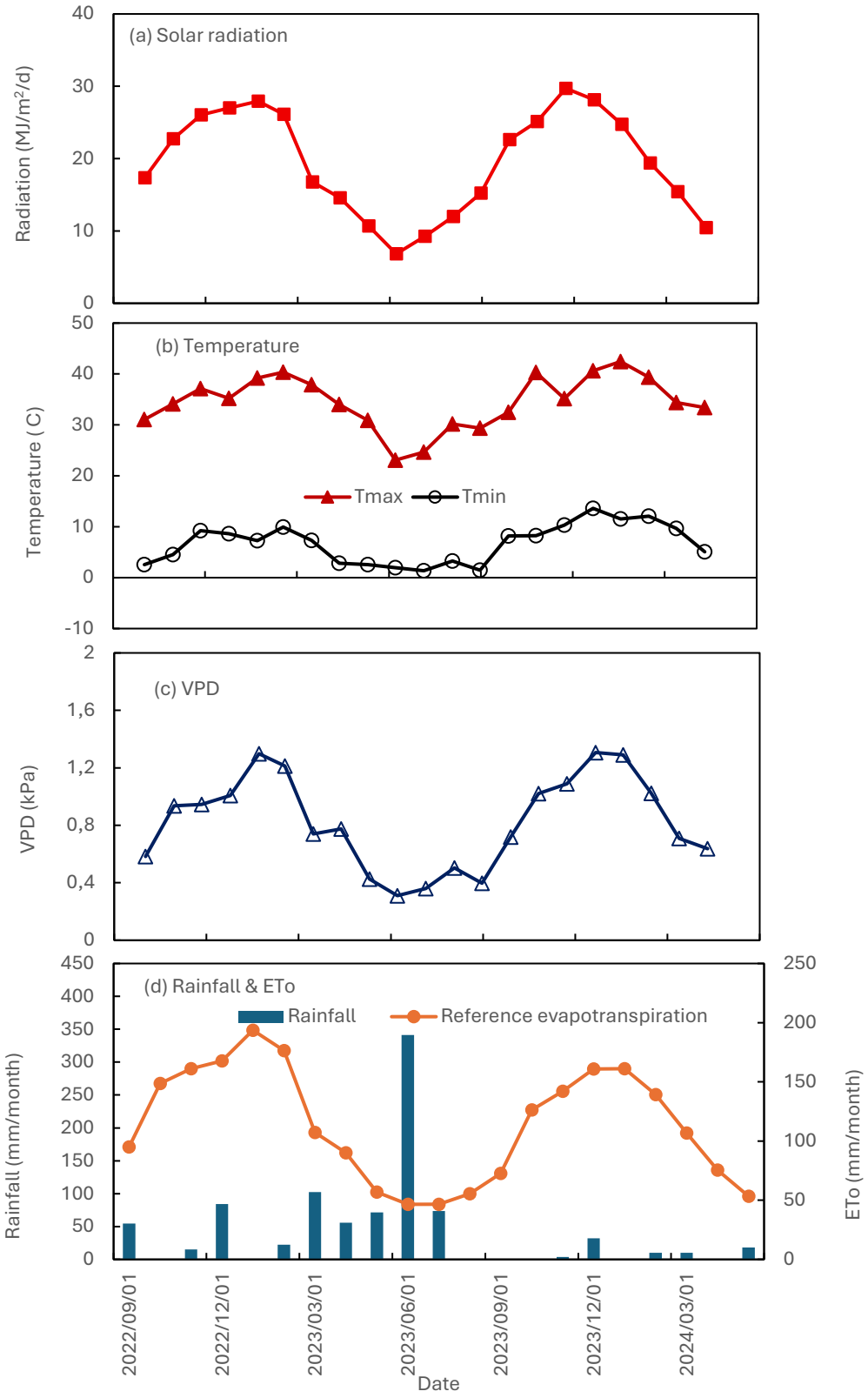


Figure 5.5 Monthly climatic conditions in Wolseley from 01 September 2022 to 31 May 2024 including (a) the average daily solar radiation for the month, (b) air temperature, (c) vapour pressure deficit of the air, (d) rainfall and the reference evapotranspiration

The daily total reference evapotranspiration varied from around 1.0 mm/d on cloudy days in winter, to a peak of around 8.0 mm/d in both seasons (Figure 5.5d). The total rainfall for the period 01 September 2022 to 31 July 2023 was about 740 mm, compared to the reference evapotranspiration of about 1 247 mm over the same period (Table 5.3). Rain that fell during the fruit-growing period, from September to the end of April, was only 238 mm in 2022-2023. More than 60% of the 740 mm rain fell during the winter months, from May to July. June 2023 was the wettest month, receiving rainfall of 340 mm, which was more than the total rainfall for the entire fruit-growing season.

Table 5.3 Two-year average summary of the monthly weather conditions in Wolseley from September 2022 to May 2024

	R_s	T_{max}	T_{avg}	T_{min}	RH_{max}	RH_{min}	U	Rain	ET_o	VPD
	($MJ/m^{2/}d$)	(°C)	(°C)	(°C)	(%)	(%)	(m/s)	(mm/month)	(mm/month)	(kPa)
September	16.3	30.2	16.1	2.0	99.7	20.0	1.5	27.2	83.8	0.5
October	22.7	33.3	19.8	6.4	97.0	15.8	1.5	0.0	137.4	0.8
November	25.6	38.7	23.7	8.7	98.4	12.4	1.1	9.4	151.7	1.0
December	28.4	35.2	22.3	9.5	99.4	16.6	0.9	58.2	164.2	1.0
January	28.0	39.9	25.2	10.4	98.4	13.8	1.1	0.3	177.4	1.3
February	25.4	41.4	26.1	10.8	99.3	11.9	1.0	16.1	157.8	1.3
March	18.1	38.6	24.2	9.7	99.1	16.3	0.9	56.1	106.9	0.9
April	15.0	34.2	20.2	6.3	98.6	16.8	0.9	27.8	82.8	0.7
May	10.6	32.1	18.0	3.8	100.0	20.1	0.9	44.8	55.1	0.5
June	3.4	23.1	12.5	2.0	100.0	30.6	2.1	341.1	46.6	0.3
July	4.6	24.7	13.0	1.4	100.0	24.6	1.1	73.7	46.6	0.4
August	6.0	30.2	16.7	3.3	100.0	18	1.2	0.0	55.4	0.5
Total								655	1266	

5.6.2 Tree water status and soil moisture dynamics

The typical trends in the leaf, stem xylem and fruit water potentials for the 'Packham's Triumph' trees are shown in Figure 5.6a. These data were collected on a typical clear day on 16 January 2024, a few days before harvest. The water potential gradients determine the direction of the water within the trees, and this idea is being exploited in a trial with 'Forelle' trees, as reported later in this report. During the daytime, the leaf water potential is lowest, which implies that the leaf is the strongest sink for water. Water is therefore expected to flow from the other

tree organs to the leaves during the daytime. The data-set in Figure 5.6 is quite limited and the water potential gradients in the late afternoon to evening are not clear. However, it seems as if the stem xylem and fruit water potential were similar for the 'Packham's Triumph', compared to the same time in the season for the 'Forelle', as shown in Chapter 3. The small water potential gradients imply that small quantities of water were most likely drawn into the fruit in the evening, which is consistent with the theory that the fruit xylem were probably dysfunctional by this stage in the growing season. The Vapour Pressure Deficit of the air (VPD) seemed to influence the leaf and stem water potential of the 'Packham's Triumph' trees in a similar way to the 'Forelle' trees, as reported in Chapter 3 (Figure 5.6b).

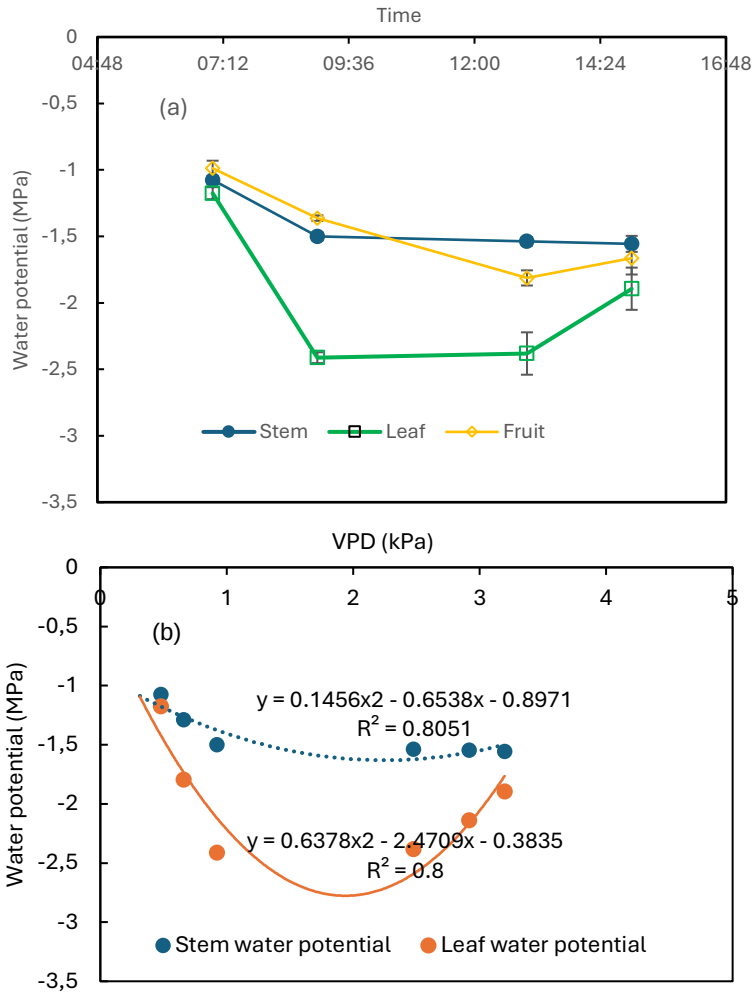


Figure 5.6 Diurnal trends in the leaf, fruit and stem water potential (a) and their relationship with the VPD (b) on a typical clear day on 06/12/2023

The midday stem water potential was measured on three occasions (once a month) during the 2023-2024 season, as shown in Figure 5.7. Data were collected on 08 November

2023, 06 December 2023 and 16 January 2024. Irrigation in this orchard commenced earlier than in the 'Forelle' orchard in Ceres, and this is shown by the high midday stem water potential in November. However, as the season progressed and the atmospheric evaporative demand increased, the midday stem water potential progressively declined to values that approached the severe stress thresholds (Figure 5.7).

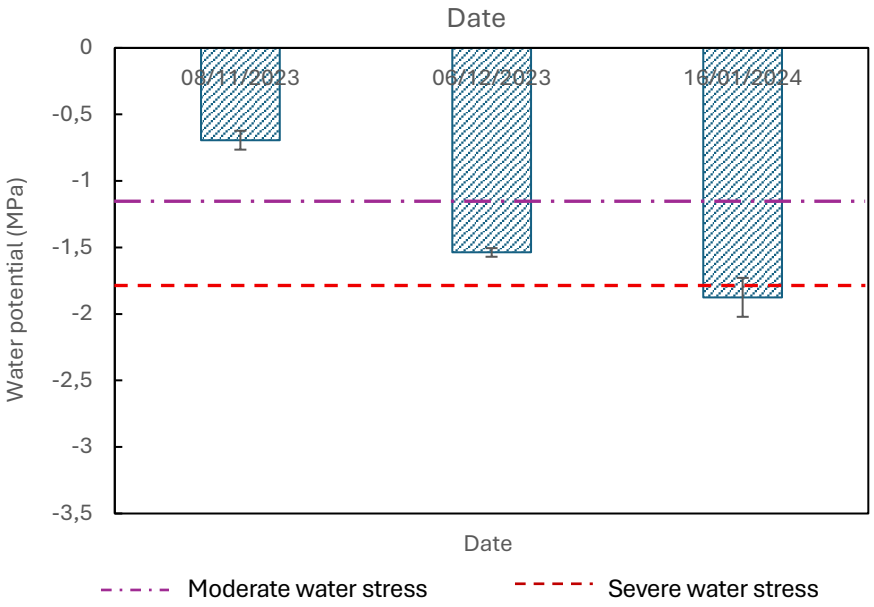
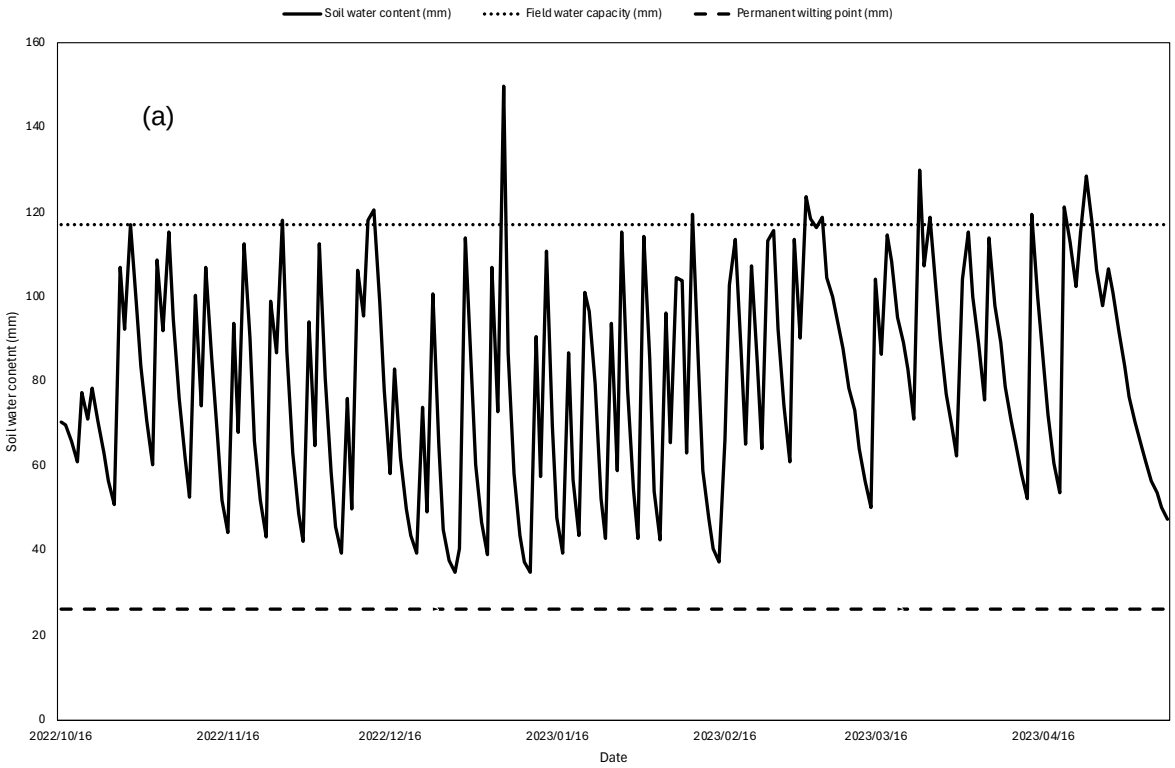


Figure 5.7 Average midday stem water potential on three different dates over the 2023/2024 season. The thresholds of moderate water stress (-1.3 MPa) and severe water stress (-1.8 MPa) are indicated, respectively, by the purple and red dashed lines

A possible explanation for this trend is that the duration of irrigation was not changed with the increasing atmospheric evaporative demand, which led to stress. Unfortunately, our water flow meter data for this orchard was unreliable, so we cannot confirm if the irrigation duration was increased during the warm summer months. Another possible reason could be related to the low hydraulic efficiency of the transpiration stream that resulted in canopy transpiration far exceeding the root water uptake, thereby creating transient internal water deficits, even when soil water was abundant. A third, and most likely reason, that explains the severe water stress after 17 January 2024 is that irrigation was reduced towards harvest, which was end of January 2024. This is confirmed by the soil water content data in Figure 5.8b, where infrequent irrigation was evident from the changes in the soil water content.



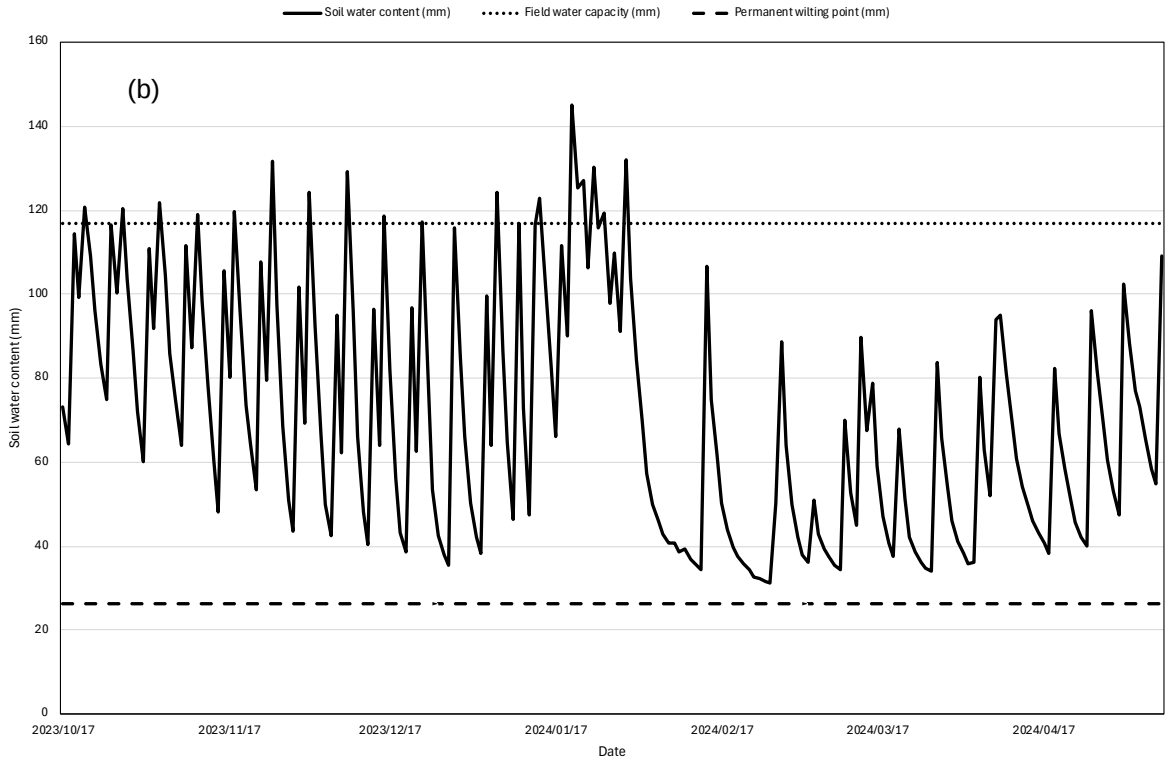


Figure 5.8 Changes in the total soil water content in the root zone (0 – 900 mm) of the 'Packham's Triumph' orchard at Wolseley; (a) during the 2022 – 2023 season, and (b) 2023 – 2024 season.

The soil water content graphs (Figure 5.8) for both seasons showed the same trend. Around the beginning of the season, the grower used a soil water depletion level of *ca.* 40%. This was presumably due to the lower atmospheric demand. As the season progressed, shifts to a soil water depletion level of *ca.* 60% were made. This forced the trees to use the soil water deeper in the profile, as the atmospheric evaporative demand increased. The soil water content dynamic graphs for both seasons followed the same trend. It is important to note that only the first 600 mm was analysed because of gaps in the data from sensors lower down in the profile.

The data for the leaf gas exchange for the 'Packham's Triumph' at Wolseley over the two measurement dates, 06 December 2023 and 16 January 2024, respectively, are shown in Figure 5.9. The diurnal trend in the stomatal conductance is similar for the 'Forelle' trees, peaking early in the morning and declining throughout much of the day. The sun-lit leaves on the western part of the canopy had a much lower stomatal conductance the late afternoon in December 2023, than in January 2024. The mid-morning peak stomatal conductance for the 'Packham's Triumph' was higher, approaching 0.25 mol m^{-2} s^{-1}, compared to that of the 'Forelle' reported in Chapter 4, which peaked at around 0.20 mol m^{-2} s^{-1}. It is not clear whether this reflected the cultivar differences or whether it was due to management issues, as the 'Forelle' trees tended to be somewhat stressed. The net photosynthesis trend of the 'Packham's Triumph' trees was symmetrical around midday, reaching a maximum of close to 20 µmol m^{-2} s^{-1}. Again, this was higher than that of the 'Forelle' trees that peaked at around 17 µmol m^{-2} s^{-1}. There was no evidence of the up-regulation in photosynthesis late in the season, when the demand for assimilates was highest, due to the high crop load. The same trend was observed for the 'Forelle' trees. The photosynthetic diurnal trend was in phase with that of the solar radiation, both reaching the maximum values around midday. However, the peak VPD occurred in the late afternoon, after 16h00 (Figure 5.9 e and f).

The leaf transpiration data early in the season (06 December) was not linearly related to the VPD in Figure 5.10, which is consistent with the stem sap flow-derived transpiration presented in Figure 5.10b. As the VPD increased beyond 1-2 kPa, the stomata closed, in order to prevent the desiccation of the trees. This is evident from both the leaf gas exchange (Figure 5.10 a) and the stem sap flow (Figure 54.10b) measurements. However, both leaf transpiration and stem sap flow were linearly related to the VPD just before harvest on 16 January 2024 (Figure 5.10a & b). This observation is unexpected, as it suggests that the transpiration pattern

of pear trees responds differently to VPD during different stages of the growing season. The restricting effect of VPD on the stomata seems to diminish in the later stages of pear fruit growth, which is quite interesting. A closer look at the relationship between these variables throughout the season is warranted, in order to gain more insights into the effects of VPD on the water use of pear trees.

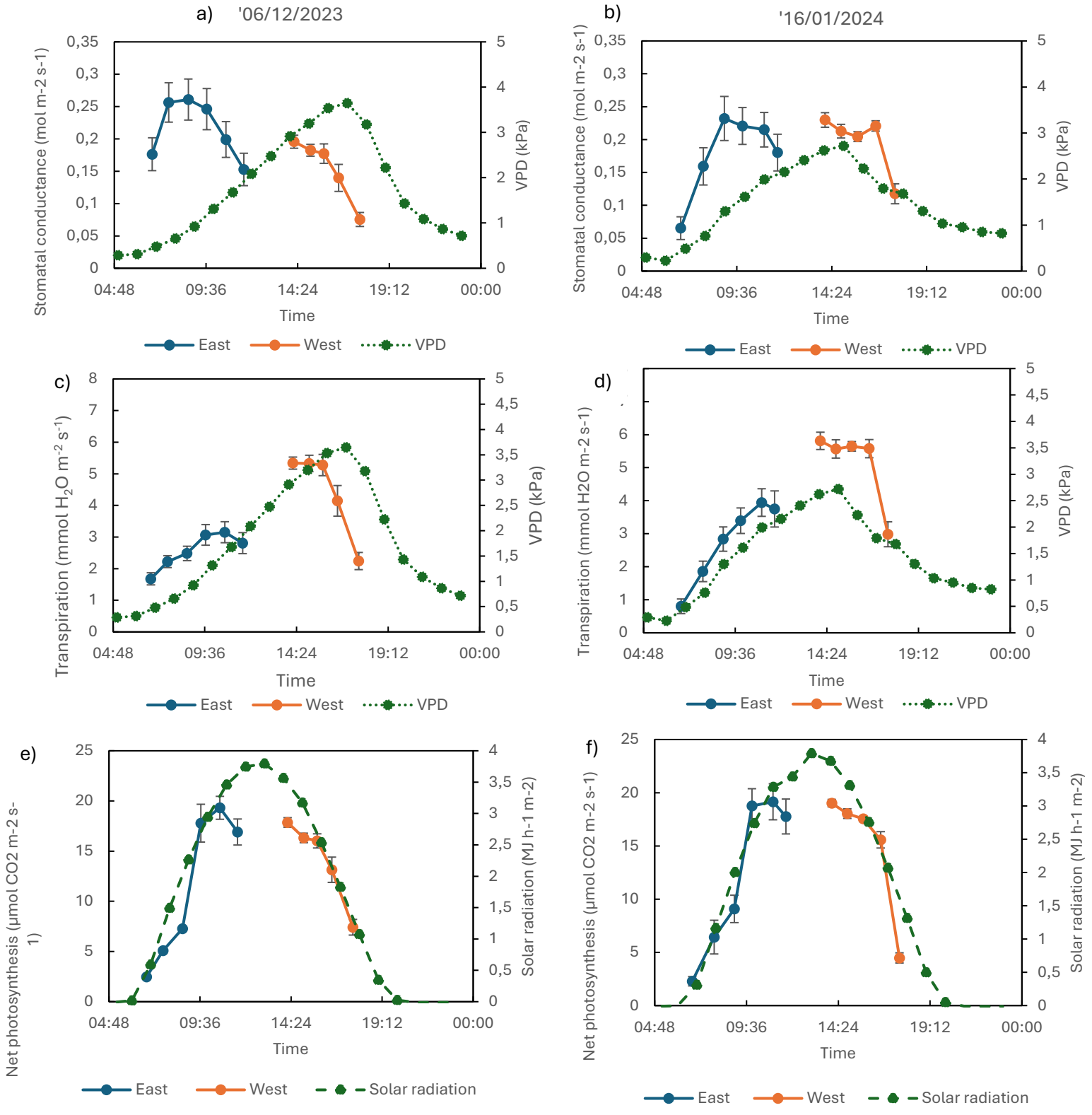


Figure 5.9 Time-series of daily VPD of the air and stomatal conductance (a & b), leaf transpiration (c & d), and of daily solar radiation and net photosynthesis (e & f) of leaves of ‘‘Packham’s Triumph’’ trees. Each data point represents the mean (±SE) of eight leaves. Measurements were taken from firstly the eastern- and then western side of the canopy on 06/12/2023 (a, c, e) and on 16/01/2024 (b, d, f).

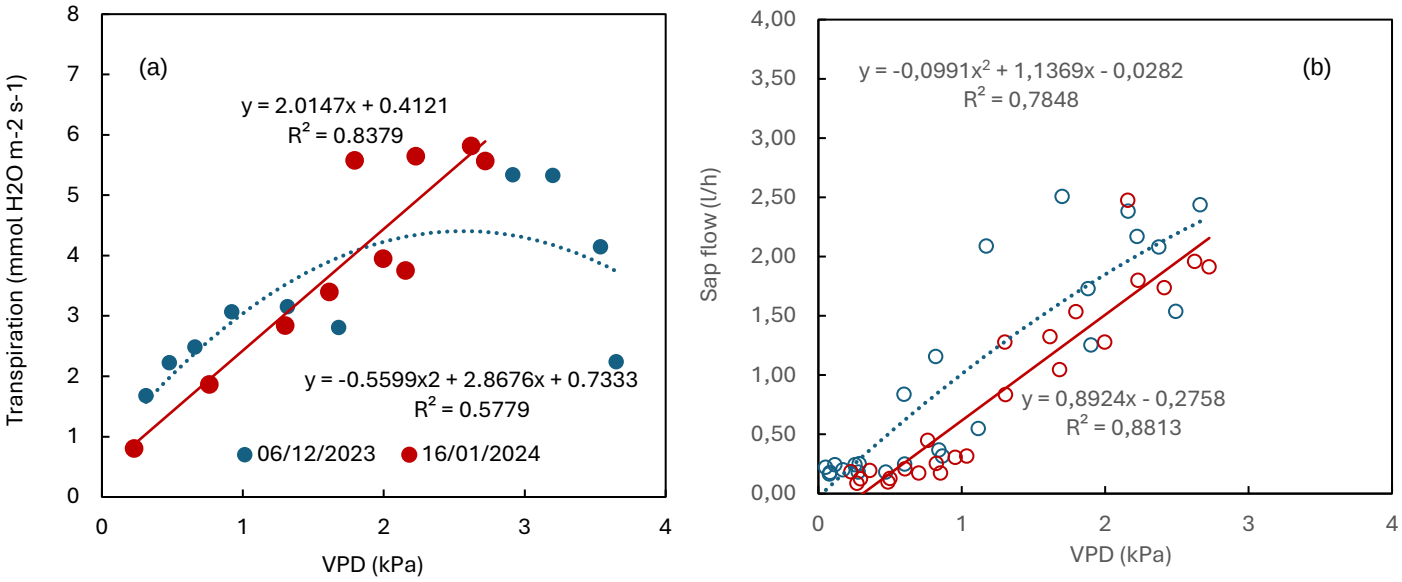


Figure 5.10 Relationship between (a) the hourly leaf transpiration rate and VPD of the air, and (b) hourly stem sap flow mid-season on 06/12/2023 and before harvest on 16/01/2024

The reason for the observed change in transpiration response to the VPD is unclear. However, it is probable that the presence of mature fruit towards harvest, which are a strong sink for assimilates, likely upregulated the photosynthesis, which necessitated the stomata to remain open for long periods. The product of the VPD and the stomatal conductance was however, strongly linearly related to leaf transpiration, irrespective of the time of year, as shown in Figure 5.11

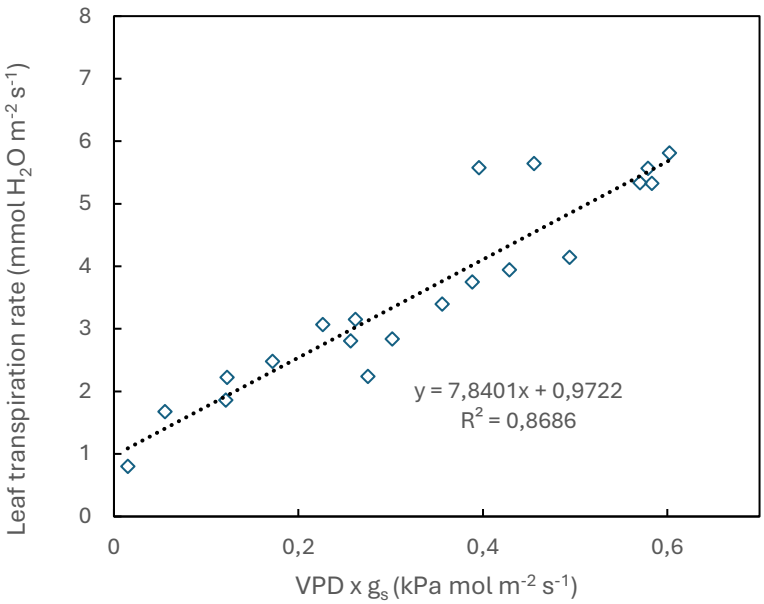


Figure 5.11 Effect of the product of VPD of the air with stomatal conductance on leaf transpiration rate, using hourly values from 06:00 to 17:00 on two dates of measurement i.e. 06/12/2023 and 16/01/2024.

Photosynthesis, on the other hand, was poorly correlated with the stomatal conductance, as shown in Figure 5.12. This is because the stomatal conductance reached a peak in the morning, when photosynthesis followed the diurnal course of the solar radiation. This is illustrated in Figure 5.13, where there is a strong linear relationship between the net photosynthesis and the solar radiation over the course of a clear day.

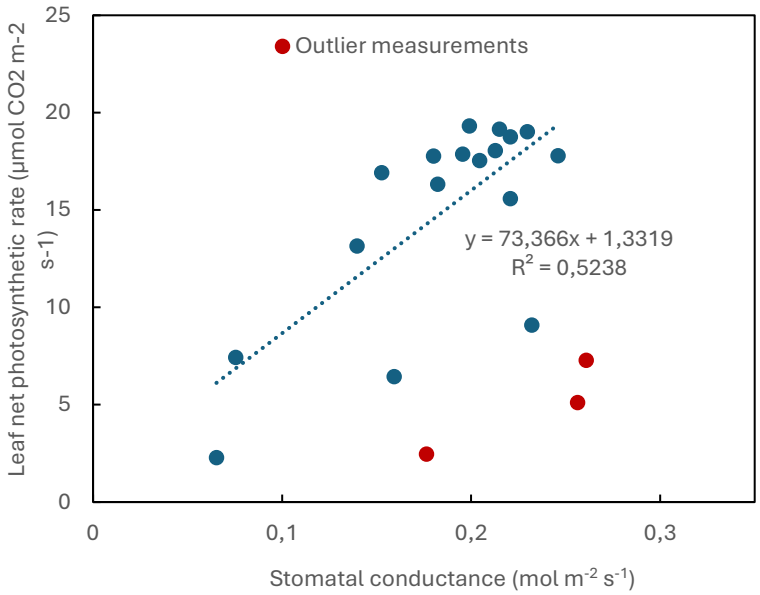


Figure 5.12 Effect of leaf stomatal conductance on leaf net photosynthetic rate, using hourly values from 06:00 to 17:00 on two dates of measurement: 06/12/2023 & 16/01/2024. Three outlier data points (at 06:00, 07:00 and 08:00 on 06/12/2023) were excluded from the calculation of the linear trendline; these points are indicated in red

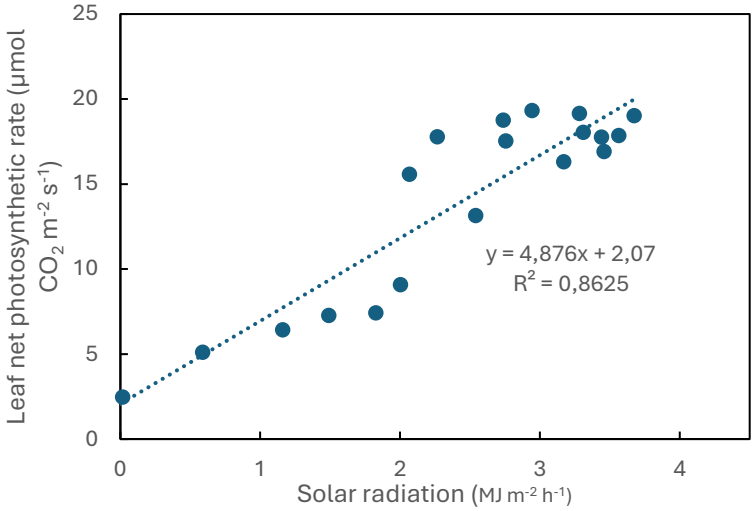


Figure 5.13 Effect of solar radiation on net photosynthesis using hourly values from 06:00 to 17:00 on two dates of measurement i.e. 06/12/2023 and 16/01/2024

5.6.3 Canopy development and orchard transpiration

Changes in the tree leaf area index (m^2 of leaf area per m^2 of ground area) over two growing seasons, namely the 2022-2023 and the 2023-2024 seasons, are shown on Figure 5.14. Vegetative growth commenced early- to mid-September and the quickest rate of canopy development was in October. The peak canopy size, with an LAI around 3.4, was reached by end of November in each season. This corresponded to a fractional vegetation cover of around 0.87, assuming an extinction coefficient of 0.60. After the mid-season peak canopy size, the decline in LAI was less steep, compared to the early season increase, due to the gradual ageing and senescing of the leaves. No significant canopy growth that was observed during the growing season, probably due to the low frequency of visits to the study site. As expected, the trees had no leaves in winter, with complete leaf fall occurring in early- to mid-July.

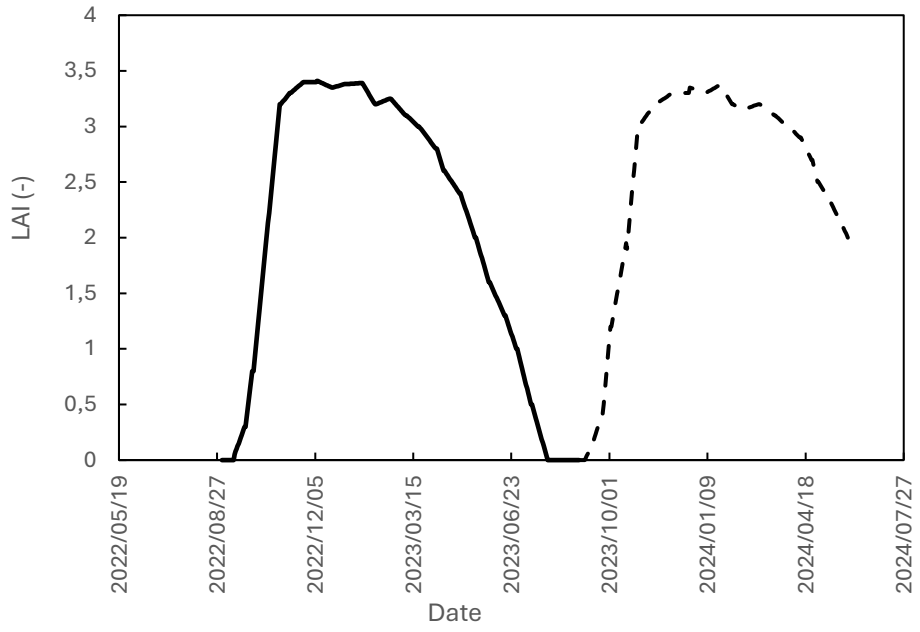


Figure 5.14 Leaf area index of the 'Packham's Triumph' orchard in Wolseley during the 2022-2023 and 2023-2024 seasons

The daily and seasonal transpiration patterns of the 'Packham's Triumph' trees in Wolseley over the 2022-2023 and 2023-2024 seasons in litres per tree per day, and in mm per day, are shown in Figure 5.15. The individual tree transpiration peaked at about 32 litres on a typical clear day in summer, which translated to 5.3 mm/d. These values were lower than those reported for the 'Forelle' trees that had much larger canopy sizes. The average seasonal total water transpired by a typical 'Packham's Triumph' tree during the 2022-2023 season was about 3 760 litres, from 01 September 2022 to 31 May 2023, which corresponded to 626.7 mm (or 6 267 m^3/ha). During the second season, the average tree transpiration from 01 September 2023 to 31 May 2024 was slightly lower at 3 318 litres per tree, which translated to 553 mm in equivalent depth units.

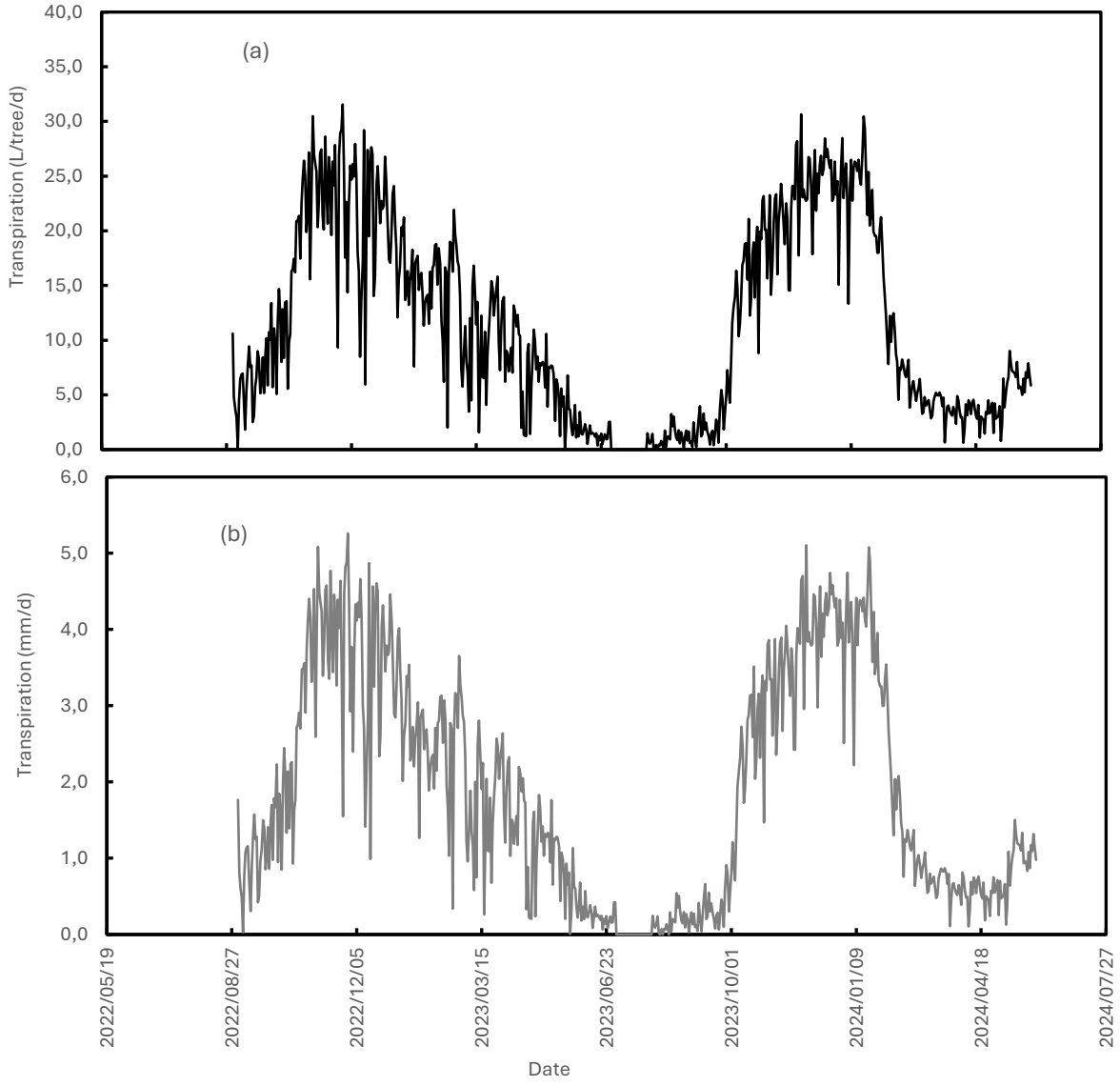


Figure 5.15 Seasonal changes in (a) the individual tree transpiration (in litres per tree per day); and (b) tree transpiration expressed in equivalent water depth units

The daily transpiration was strongly driven by the solar radiation (see Figure 5.16), with a coefficient of determination of 0.82. This means that the changes in daily solar radiation explained up to 82% of the variations in the tree transpiration. This was greater than that reported for the 'Forelle' orchard (71%), most likely because of the differences in the water management strategies of the two orchards. There tended to be some water stress in the 'Forelle' orchard, as seen from the soil water depletion data presented in Chapter 4. A high soil water deficit tends to weaken the influence of climatic factors, as the stomata close in response to the drought stress, rather than in response to the atmospheric evaporative demand.

The daily average VPD over the entire season had a strong non-linear relationship with the daily total transpiration (Figure 5.16b), with an R^2 of 0.71. From the daily data, the VPD threshold, beyond which the stomata began to close, was between 1.0 and 1.5 kPa. The exact physiological mechanism by which the VPD causes stomatal closure is unknown, although it is widely believed that this occurs to reduce excessive water loss, in order to avoid hydraulic failure. Because the reference evapotranspiration is calculated by using both the solar radiation and the VPD, it is therefore not surprising that a non-linear relationship also existed between transpiration and the ET_o (Figure 5.16c). The ET_o explained up to 82% of the variation in transpiration, but with a large scatter at high, rather than at low, ET_o values.

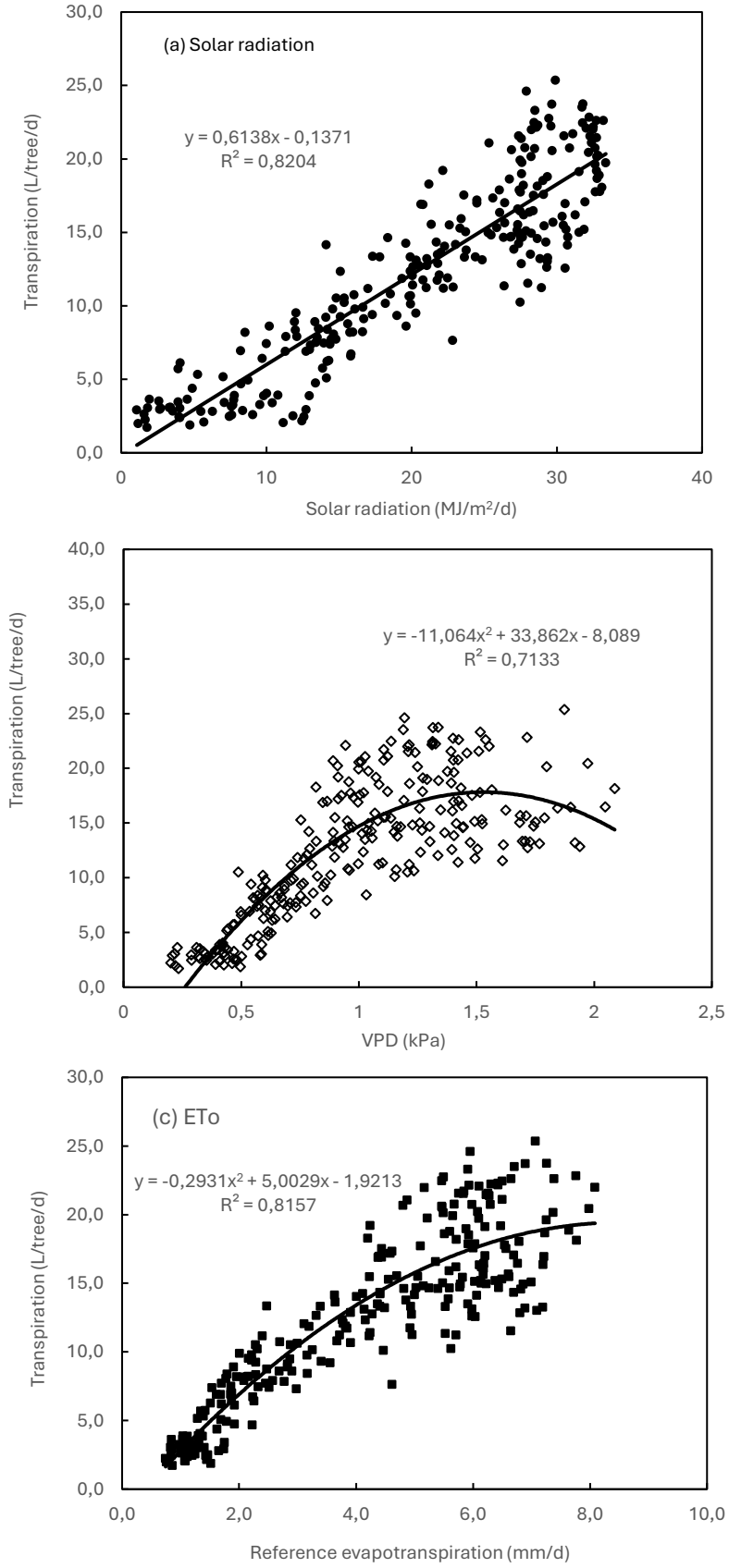


Figure 5.16 Effect of different climate drivers: (a) solar radiation, (b) VPD and (c) reference evapotranspiration on transpiration by 'Packham's Triumph' trees in Wolseley

5.6.4 Orchard evapotranspiration

A comparison of the relative magnitudes of the measured reference evapotranspiration, orchard transpiration and actual evapotranspiration over the two seasons is shown in Figure 5.17. The actual evapotranspiration was measured during short window periods (see brown line), due to the unavailability of equipment, since it was being used on other projects. There were also technical issues with the eddy covariance system at certain times, which rendered some of the data unusable. The measured whole orchard ET varied between 0.4 and 7.0 mm/d. The ET data for the 'Packham's Triumph' orchard in Wolseley were measured over 41 days in winter, from 09 to 18 May 2023, and in summer, from 19 October to 09 November 2023. A strong linear relationship existed between the actual measured orchard evapotranspiration and the reference evapotranspiration for the 'Packham's Triumph' orchard (Figure 5.18). The slope of this line represents an average crop coefficient of about 0.91 for the orchard, which is consistent with the Kc values reported in literature for pears (Allen et al., 1998; Girona et al., 2011). The dotted line depicts the 1 to 1 line. In practice however, the crop coefficient should be adjusted, with the crop growth stage being low during the early phases, and rising to a peak at the mid-season stage, according to Allen et al. (1998). This will be covered in the following sections of this Chapter.

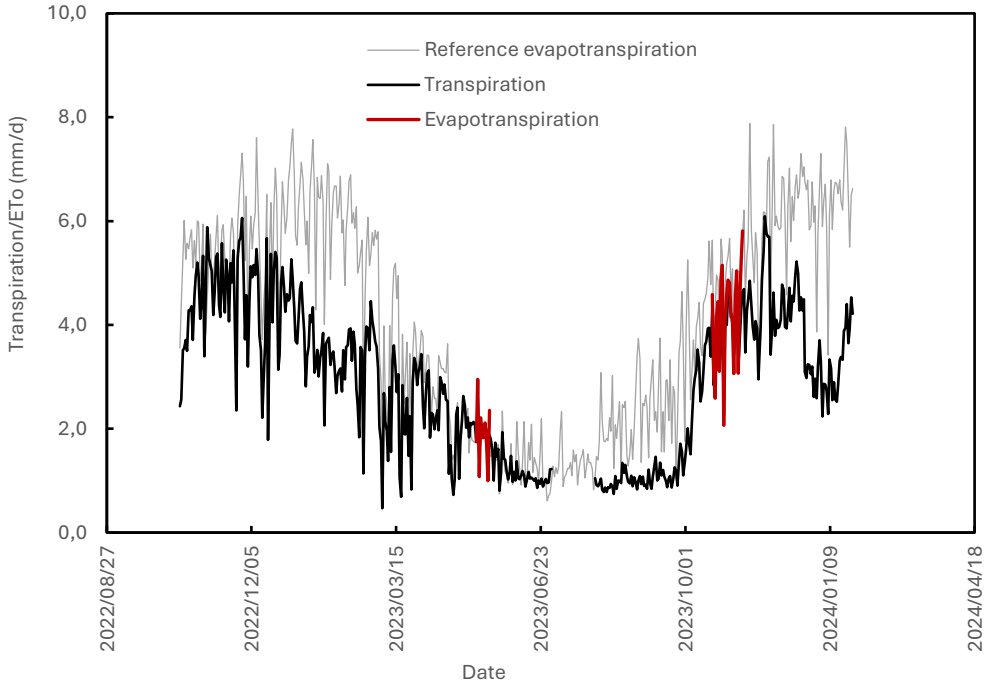


Figure 5.17 Seasonal course of the tree transpiration in equivalent water depth units and the reference evapotranspiration over two growing seasons

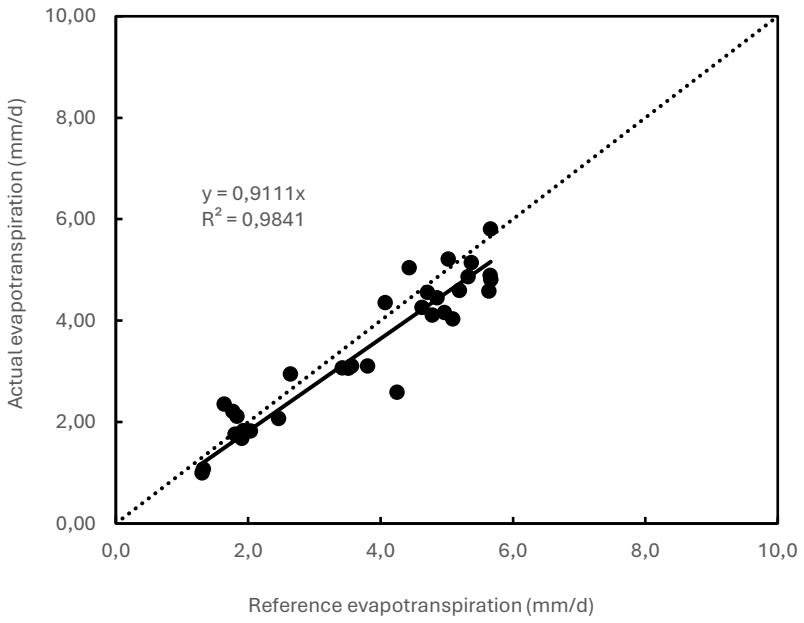


Figure 5.18 Effect of the atmospheric evaporative demand on the evapotranspiration of the 'Packham's Triumph' orchard in Wolseley. The slope of the line depicts the average crop coefficient for the orchard

5.6.5 Water use modelling and crop coefficients

The dual source evapotranspiration (ET) model was applied to 'Packham's Triumph' orchard in Wolseley and the typical daily transpiration simulations over multiple seasons are shown in Figure 5.19. Both the orchard transpiration and ET were accurately predicted by the model. Detailed statistics are presented in Chapter 8, when the ET data are pooled together for all the sites, due to the limited measured data. The model explained a variation of up to 83% in the transpiration. The Nash-Satcliffe Efficiency (NSE) was positive at 0.68, which indicates an acceptable of the performance model (Moriasi et al., 2007). The RMSE for transpiration was low, at ±0.75 mm/d. The R^2 for the orchard ET at Wolseley, which had the longest measurement record, was 0.89. The NSE for Wolseley was very high at 0.85 (Figure 5.20) which showed a very high urem (8 030 m^3/ha). This water use value is for the period that covers most of the irrigation season, from 01 September to 30 April.

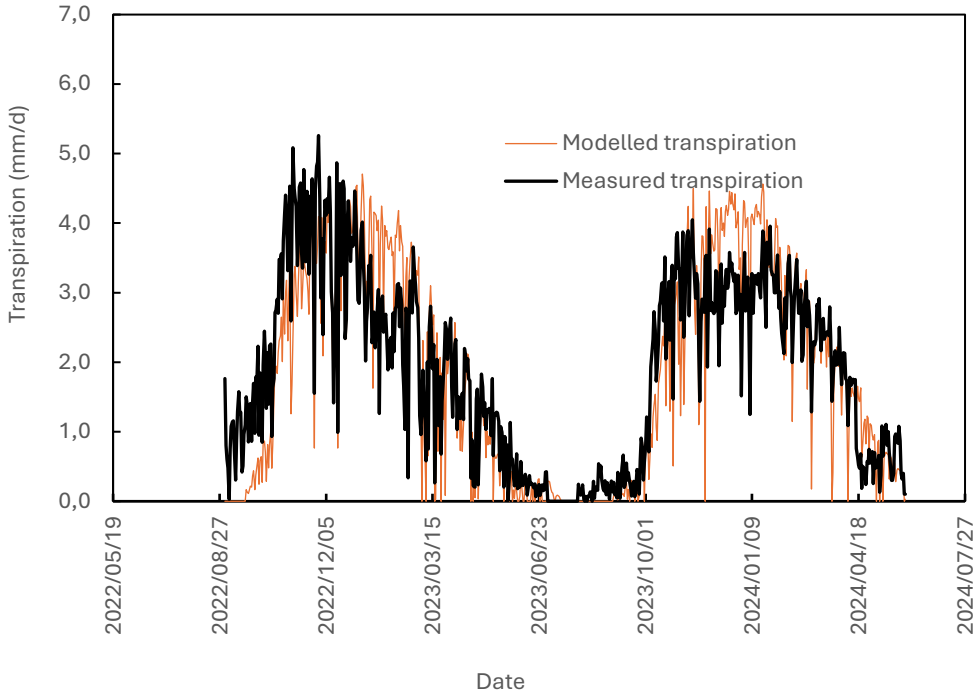


Figure 5.19 Comparison of the measured and modelled (a) transpiration and (b) evapotranspiration for the 'Packham's Triumph'

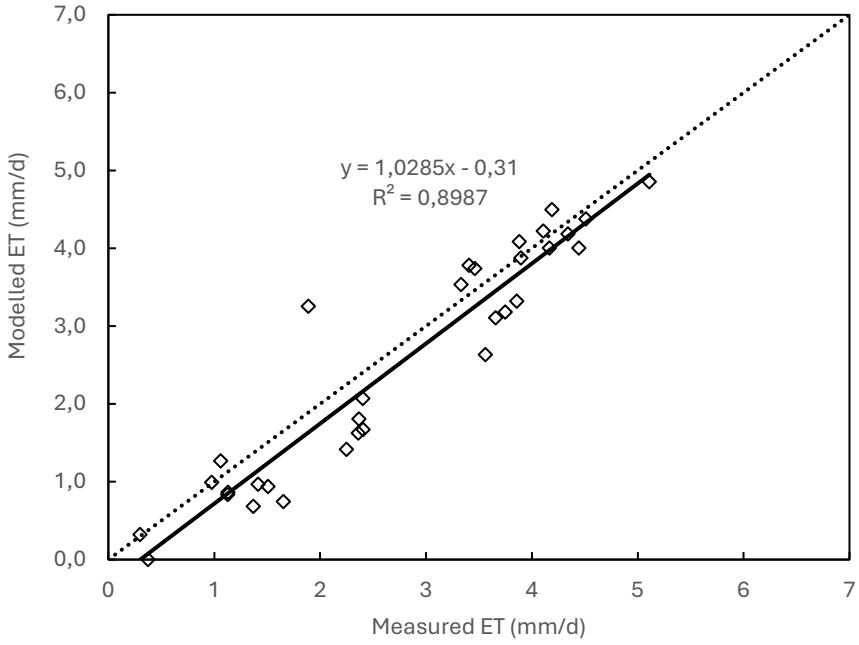


Figure 5.20 Comparison of the measured and modelled actual evapotranspiration of the 'Packham's Triumph' orchard at Wolseley

The detailed partitioning of the water use components for the 'Packham's Triumph' orchard in Wolseley is shown in Figure 5.21. Early in the season, the orchard floor evapotranspiration flux constituted almost 100% of the orchard ET, due to no canopy cover in September. The contribution of the orchard floor ET diminished as the season progressed, to between 20 and 22% of ET at full canopy cover during the mid-season stage.

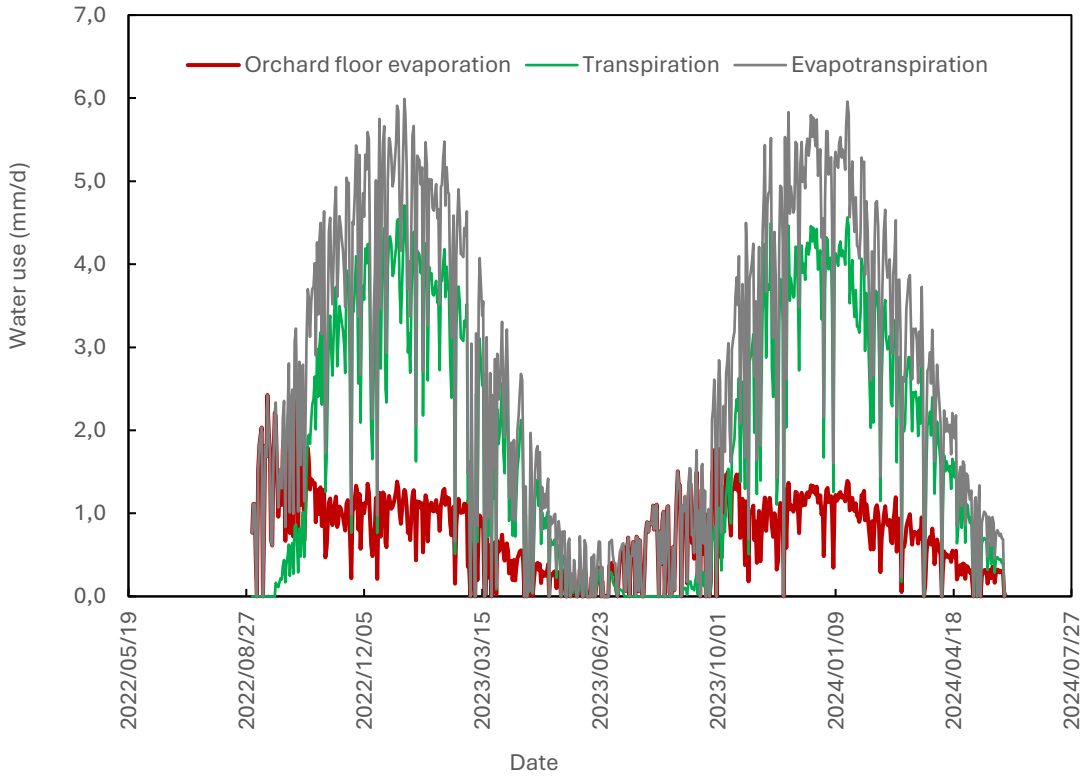


Figure 5.21 Modelled partitioning of evapotranspiration of the 'Packham's Triumph' orchard at Wolseley over two growing seasons from September 2022 to May 2024

The measured and modelled basal ($K_{cb} = T/ET_o$) and crop coefficients ($K_c = ET/ET_o$) over a typical growing season for the 'Packham's Triumph' orchard in Wolseley, are shown in Figure 5.22. The measured Kcb values were obtained from the ratio of the measured weekly total orchard transpiration to the weekly reference evapotranspiration. The crop coefficients were presented as weekly values, in order to reduce the noise in the daily data. The weekly peak Kcb ranged from 0.67 and 0.74 during the mid-season stage, which was slightly lower than that of the 'Forelle' orchard in Ceres, as reported in Chapter 4. The modelled values closely matched the measured values. The maximum crop coefficients were up to 0.94 during the maximum canopy cover in January and February. These values are close to the average value of 1.0

observed from the lysimeter measurements by Girona et al. (2011), under Mediterranean conditions in Spain.

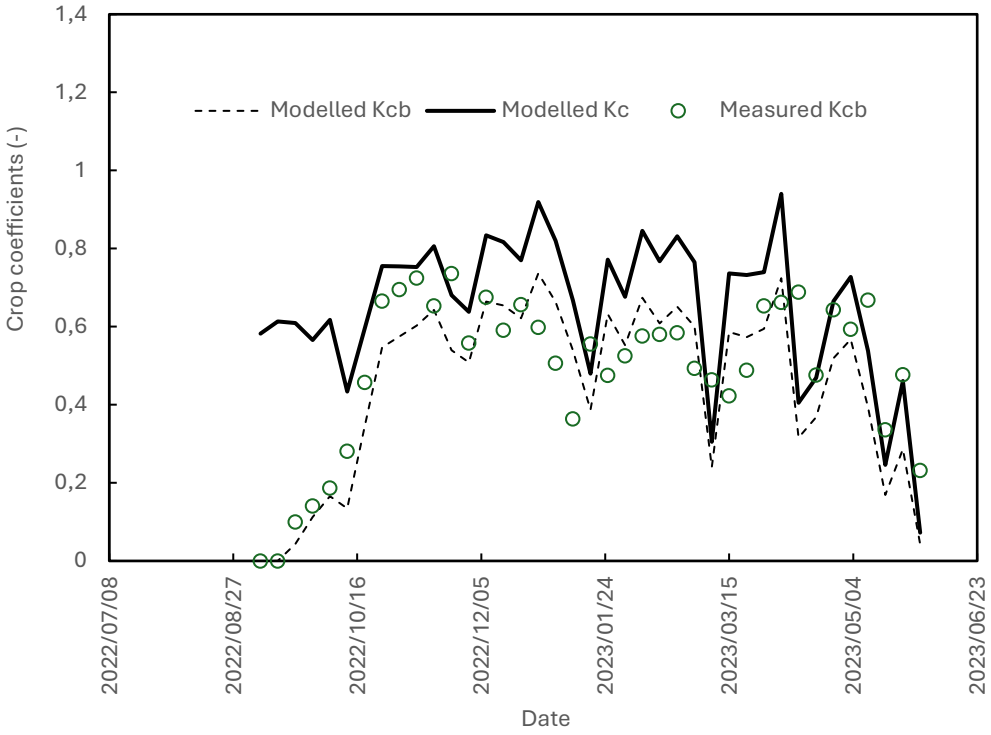


Figure 5.22 Weekly crop coefficients for the 'Packham's Triumph' orchard at Wolseley during the 2023-2024 growing season

5.6.6 Climate change impacts on the water use of pear orchards

Most Global Climate Models (GCM) predict future warmer and drier conditions in the Western Cape and other fruit-growing areas in the Mediterranean region (Jack et al., 2022). The projected trajectory of the transpiration-constraining factors, namely the solar irradiance and VPD stress factors described by Equations 3.18 and 3.20 for the period 1961 to 2099, is shown in Figure 5.23. These trends in the stress factors suggest that potential increases in the solar radiation intensity are unlikely to constrain transpiration, while potential changes in the VPD are likely to cause significant transpiration reductions under the warmer and drier conditions in future. Because the VPD accounts for both the temperature and humidity, the trend in the temperature stress factor is not shown independently.

The six GCM models suggest that the reference evapotranspiration (ETo) will increase by about 2.6% between the current period (2020-2030) and the mid-century (2045-2065) (Figure 5.24a and Table 5.4). An increase of up to 6.6% is projected for ETo between the current period and the end of the century (2090-2099). Assuming that the orchards will always be well-

watered, and that all the stress will be due to climatic factors, the orchard ET is projected to increase by 3.5% between the current period and mid-century, while a cumulative increase of 9.7% is projected between the current period and the end of the century (Table 5.4). The orchard transpiration is projected to increase by a somewhat smaller margin, at 3.1% between the current and mid-century, and 9.1% by end of century. The orchard floor evaporation is however, projected to increase by a larger margin of 4.4% between the current and mid-century, and up to 10.9% by the end of the century.

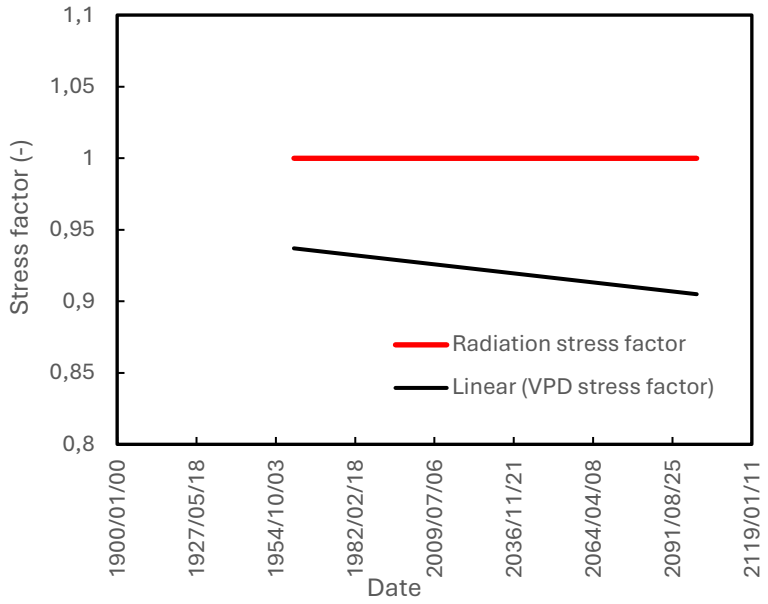


Figure 5.23 Time series of the solar radiation and vapour pressure deficit stress factors for the period 01 January 1961 to 31 December 2099 for 'Packham's Triumph' trees

There are serious concerns about the impact of climate change on resource availability, especially in key fruit-producing regions in the Mediterranean climatic regions that are expected to get drier and warmer in the future (Masia et al., 2021). Various estimates have been made on the likely impacts on the crop water requirements, especially for perennial fruit-tree orchards. For example, Ogundeji and Jordaan (2017) performed a simulation study on various fruit-tree species in the Ceres area of the Western Cape, using the FAO 56 approach, in which crop water use is estimated to be the product of the reference evapotranspiration and a crop coefficient. This approach assumes that the crops do not react to the stressful environment. However, the reality of climate change is that crops are likely to experience physiological stress under the extreme warm and dry future conditions, and no studies have accounted for this stress in pear orchards.

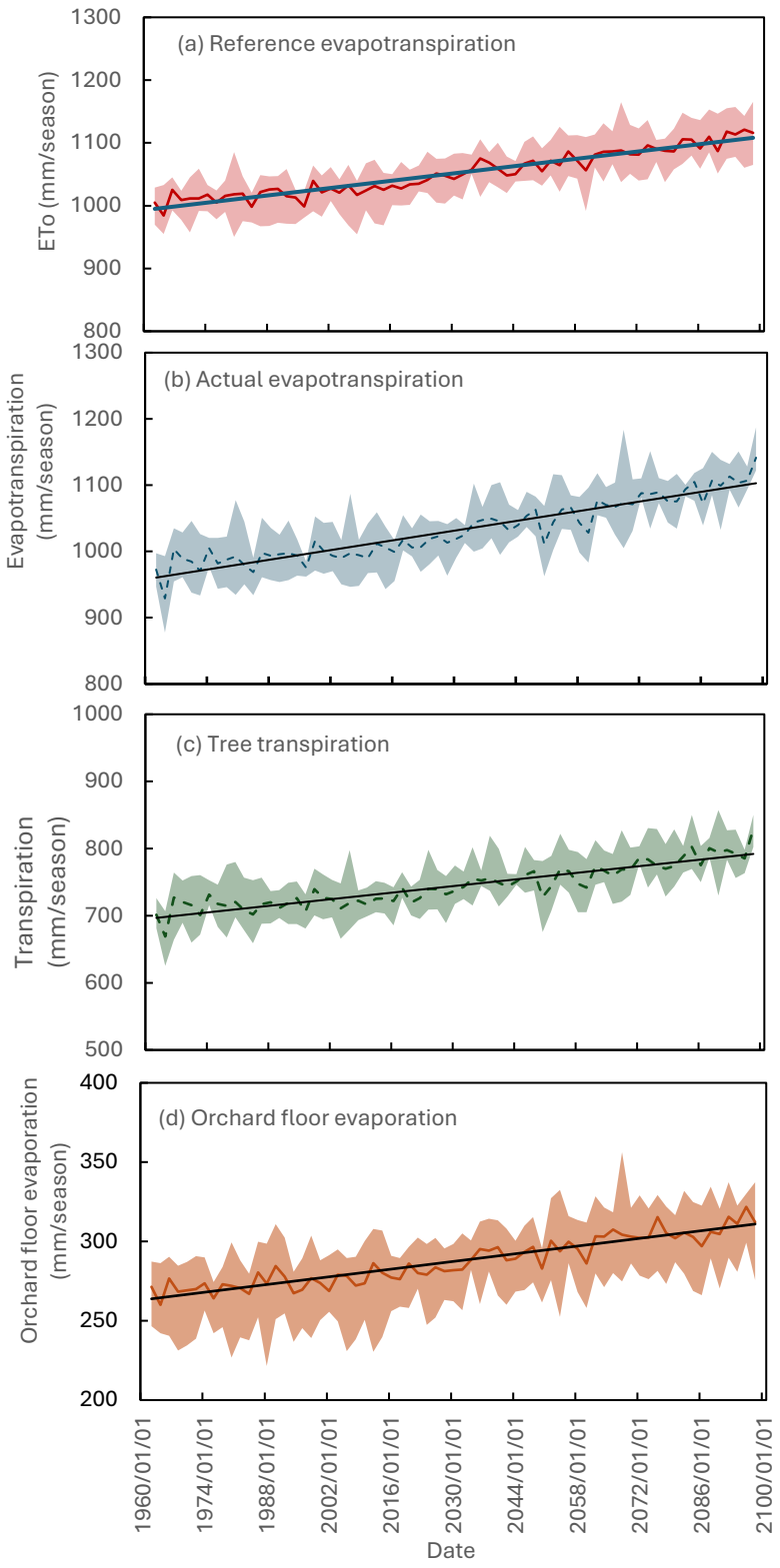


Figure 5.24 Time series prediction of changes in (a) the atmospheric evaporative demand represented by the reference evapotranspiration, (b) actual orchard evapotranspiration, (c) orchard transpiration, and (d) orchard floor evaporation for 'Packham's Triumph' pear orchards in Wolseley for the period 01 January 1961 to 31 December 2099

Table 5.4 Projected future changes in orchard water use fluxes from the current (2020-2030), to mid (2050-2060) and end of century (2090-2099). A full growing season is defined as the period from 01 September to 30 April

	Climate change model	Orchard floor evapouration	Transpiration	Evapotranspiration	ETo
		(mm/season)	(mm/season)	(mm/season)	(mm/season)
Current	NOR	283	720	1004	1039
	ACS	259	765	1024	1013
	CCS	293	729	1022	1054
	CNR	284	722	1005	1041
	GFD	291	737	1028	1067
	MPI	283	720	1004	1039
	Mean	282.2	732.2	1014.5	1042.2
2050	NOR	302	739	1041	1075
	ACS	270	785	1055	1039
	CCS	290	749	1039	1063
	CNR	294	749	1043	1062
	GFD	309	770	1079	1101
	MPI	302	739	1041	1075
	Mean	294.5	755.2	1049.7	1069.2
2099	NOR	317	778	1095	1107
	ACS	283	831	1114	1069
	CCS	315	792	1106	1116
	CNR	318	802	1120	1116
	GFD	328	817	1145	1152
	MPI	317	778	1095	1107
	Mean	313.0	799.7	1112.5	1111.2

In addition, changes in the individual water balance components in the future have rarely been investigated. Ogundeji and Jordaan (2017) predicted an increase in the ET for pears in the Ceres area of 17.8% between a baseline period (1971 to 1990) and the mid-century (2045-2065). However, the dual-source ET model, which was validated with experimental

data, shows a much lower future increase in the orchard ET of about 6.4% over the same period. According to the dual-source ET model, orchard floor evaporation will have the greatest contribution (~ 8.2%), while the tree transpiration component will increase by only 5.8%, because of the increasing VPD-induced stress on stomatal conductance. However, if we redefine the baseline period to the current decade (2020-2030), keeping the mid-century period the same, the orchard ET will increase by less than 5% within this period. Masia et al. (2021) followed a similar K_cET_o approach for various crops, namely maize, wheat and grapes, in the Mediterranean region over an even shorter period (1976-2005) to (2036-2065). Their study suggested an increase of 13%, 16% and 10% in the water use of each crop type in the future. There is a possibility that the actual future increases could be lower, if the environmental stress factors are included, especially in the transpiration model.

5.6.7 Fruit yield and quality

5.6.7.1 Fruit yield

The harvest and fruit quality quantification procedures are like those reported for the 'Forelle' orchards in Ceres, so we will not repeat it here. Only the harvest dates differed. In the 2022/23 season, the average yield was approximately 33.7 kg per tree. Given a tree density of 1 667 plants per hectare, this translated to a yield of around 56.2 tons per hectare. For the 2024/25 season, the average yield increased to 35.6 kg per tree, resulting in approximately 59.3 tons per hectare (Table 5.5).

Table 5.5 Average yield: fruit number and trunk circumference per tree for 'Packham's Triumph' trees

Cultivar	Season	Yield (kg/tree)	Number of fruits/tree	Trunk circumference (cm)
'Packham's Triumph'	2022-23	33.7	-	39.8
'Packham's Triumph'	2023-24			
'Packham's Triumph'	2024-25	35.63	-	36.7

5.6.7.2 Fruit quality

Table 5.6 shows that no clear differences appeared between the different positions for any of the fruit quality parameters that were measured. The presence of significant differences is yet to be confirmed by an appropriate statistical analysis test, such as ANOVA.

Table 5.6 Averages of the quality parameters, per position – and overall, for the 'Packham's Triumph' pears

Cultivar	Position	Firm A (kg)	Firm B (kg)	Diameter (mm)	Mass (g)	Height (mm)	BG A	BG B	Starch (%)	TSS (%)	TA (%)
Packham's Triumph (2022/23)	Top	7.5	7.5	67.8	157.0	72.0	2.3	2.3	41.7	13.7	0.2
	Outside	7.5	7.5	65.9	145.2	72.2	2.0	2.1	38.1	14.0	0.3
	Inside	7.3	7.2	67.5	153.0	73.0	2.2	2.3	39.9	13.5	0.3
	Bottom	7.5	7.5	65.6	140.9	68.4	2.1	2.3	40.1	13.3	0.3
	Average	7.5	7.4	66.7	149.0	71.4	2.1	2.2	39.9	13.6	0.3
Packham's Triumph (2024/25)	Top	7.6	7.5	66.4	183.2	76.8	-	-	-	-	-
	Outside	7.6	7.5	67.2	190.3	77.8	-	-	-	-	-
	Inside	7.4	7.3	66.7	187.3	78.9	-	-	-	-	-
	Bottom	7.7	7.9	65.8	184.0	78.0	-	-	-	-	-
	Average	7.6	7.6	66.5	186.2	77.9	-	-	-	-	-

5.6.7.3 Water productivity of the 'Packham's Triumph' orchard in Wolseley

The yield data of 'Packham's Triumph' pear trial trees in the Wolseley region were not available for the 2022-2023 season. The T-based WP for the trial trees in 2023-2024 was 10.11 kg m^{-3} (Table 5.7). For the whole orchard block, the T-based WP was 9.88 and 9.97 kg m^{-3} for the two seasons, respectively. The difference between the trial trees and orchard block was thus small. In 2022-2023, the seasonal water use and yield were both higher than in 2023-2024, so that the WP was similar in the two seasons. The T-based EWP was 44.83 and 45.71 R m^{-3} in 2022-2023 and 2023-2024, respectively. Both the gross value and seasonal T were slightly higher in the first season, compared to the second season, resulting in a comparable EWP.

Table 5.7 Physical Water Productivity (WP), Water Use Efficiency (WUE), and Economic Water Productivity (EWP) based on seasonal transpiration for the 'Packham's Triumph' pear orchard in Wolseley in 2022-2023 and 2023-2024

	2022-2023	2023-2024
Planting density (trees/ha)	1667	1667
Seasonal transpiration (mm)	597.4	554.8
Seasonal transpiration per hectare (m^3/ha)	5973.8	5548.0
Trial trees:		
Yield (t/ha)		56.09
Water Use Efficiency (m^3/ton)		98.90
Physical Water Productivity (kg/m^3)		10.11
Whole orchard block:		
Yield (t/ha)	59.0	55.3
Water Use Efficiency (m^3/ton)	101.3	100.3
Physical Water Productivity (kg/m^3)	9.88	9.97
Orchard gross income (R/ha)	R267 788	R253 593
Economic Water Productivity (R/m^3)	R44.83	R45.71

The ET-based WP for the trial trees was 7.05 kg m^{-3} in 2023-2024, and for the whole block it was 7.59 and 6.95 kg m^{-3} for 2022-2023 and 2023-2024, respectively (Table 5.8). The transpiration was slightly higher and the yield slightly lower in the second season, compared to the first. The EWP for ET was 34.43 and 31.88 R m^{-3} for the two seasons, respectively. The lower value in the second season can be ascribed to both a slightly lower gross value and a slightly higher seasonal ET.

Table 5.8 Physical Water Productivity (WP), Water Use Efficiency (WUE), and Economic Water Productivity (EWP) based on seasonal evapotranspiration for the 'Packham's Triumph' pear orchard in Wolseley in 2022-2023 and 2023-2024

	2022-2023	2023-2024
Planting density (trees/ha)	1667	1667
Seasonal evapotranspiration (mm)	777.8	795.4
Seasonal evapotranspiration per hectare (m^3/ha)	7777.6	7953.6
Trial trees:		
Yield (t/ha)		56.09
Water Use Efficiency (m^3/ton)		141.79
Physical Water Productivity (kg/m^3)		7.05
Whole orchard block:		
Yield (t/ha)	59.0	55.3
Water Use Efficiency (m^3/ton)	131.8	143.8
Physical Water Productivity (kg/m^3)	7.59	6.95
Orchard gross income (R/ha)	R267 788	R253 593
Economic Water Productivity (R/m^3)	R34.43	R31.88

5.7 CONCLUSIONS

In this Chapter, we reported on the water use-yield relationships of the 'Packham's Triumph' orchard in Wolseley for the 2022-2023 and 2023-2024 growing seasons. The seasonal total transpiration of this orchard was 5 974 m^3/ha for the first season and 5 548 m^3/ha for the second season. The average for the two seasons was 5 761 m^3/ha, which was lower than that for the 'Forelle' orchard in Ceres, which was around 7 500 m^3/ha. The lower transpiration of the 'Packham's Triumph' orchard in Wolseley can be attributed to the smaller size of the trees canopies. In general, these differences are not expected, as 'Forelle' trees that produce blushed fruit are expected to have more open canopies, and hence a lower LAI, to promote colour development. This was not the case in the present study. The modelled seasonal total ET was 7 778 m^3/ha in the first season and 7 954 m^3/ha in the second season, with a mean of 7 866 m^3/ha. This water use figure can be rounded off to 8 000 m^3/ha for the 'Packham's Triumph' orchard. The yield for the two seasons was low, at 59.0 t/ha for the first season and 55.3 t/ha for the second season. The transpiration-based water productivity averaged 9.9 kg/m^3, while the ET-based water productivity was lower, at 7.3 kg/m^3. These

values are higher than those of the 'Forelle' orchard, as reported in Chapter 4, because of the lower transpiration of the Packham's trees. The transpiration-based economic water productivity was R 45.3/m^3, while the ET-based economic water productivity was lower, at R31.2 /m^3. These values are lower than those reported for the 'Forelle' orchard in Ceres in Chapter 4, because of the high gross value of the blushed 'Forelle', compared to that of the 'Packham's Triumph'. All six GCM models suggest an increase in the reference evapotranspiration (ETo) by about 2.6%, between the current period (2020-2030) and the mid-century (2045-2065). An increase of up to 6.6% was projected for the ETo between the current period and end of the century (2090-2099). Assuming that the orchards will always be well-watered, and that all the stress will be due to climatic factors, the orchard ET was projected to increase by 3.5% between the current period and mid-century, while a cumulative increase of 9.7% was projected between the current period and end of the century. The orchard transpiration was projected to increase by a somewhat smaller margin, at 3.1%, between the current and mid-century, and 9.1% by end of the century. However, orchard floor evaporation was projected to increase by a larger margin of 4.4% between the current and mid-century, and up to 10.9% by the end of the century. These results suggest that it is critical to adopt irrigation strategies that reduce orchard floor evaporation, in order to adapt to future climate changes.

CHAPTER SIX

'PACKHAM'S TRIUMPH' ORCHARD, VYEBOOM

6.0 INTRODUCTION

The dominant land use in Vyeboom are fruit orchards that are planted to apples, pears, stone fruit, wine grapes and berries. Pome fruit are the most widely-planted crop type and occupied more than 4 000 ha in 2014. According to the Western Cape Department of Agriculture report in 2014, grapes (192 ha) and stone fruit (178 ha) were the second- and third-highest planted crops, with small amounts of berries (41 ha) and citrus (10 ha). The soil types in the Vyeboom area varies greatly across the region. They are highly erodible because of the prevalence of shale-derived material. There are also sandstone-derived soils, as well as podsols. Most soils are deep, red or yellow-brown, and they are often weathered and acidic because of the region's high rainfall. Most of the soils are suitable for agriculture and they support numerous fruit orchards. A prominent feature in the study area is the Theewaterskloof Dam, which is the largest dam in the Western Cape Water Supply System, with a capacity of about 480-483 million cubic meters. The dam supplies water for irrigation to most of the surrounding farms in the Vyeboom and Villiersdorp regions.

The climate of Vyeboom is of the Mediterranean-type (Köppen-Geiger classification: Csb), which is characterised by warm dry summers and cool wet winters. The maximum daily growing season temperatures in Vyeboom tend to be lower than those in Ceres and Wolseley. The area receives higher rainfall than the other study sites, due to orographic effects of the surrounding mountain ranges. This chapter describes data that were collected in one of the many commercial orchards in the area that are owned by Fruitways company. This orchard had consistently higher yields than the other three orchards, due to its favourable growing conditions, which included a milder microclimate and deep fertile clayey-loam soils. The milder orchard microclimate was because of the orchard being in the vapour blanket of the Theewaterskloof Dam, which was less than 400 m away.

We will report on the water use, soil water content, growth, yield and environmental data, as in previous chapters. Given the long history of yield data, from the planting of the orchard in 2012 until the full-bearing age, combined with the availability of climate data for this

period, this chapter reports, in detail, on the development and testing of the yield model for pear orchards. The data from the other orchards were leveraged to develop the water use-yield response functions that are required in the yield model.

6.1 DESCRIPTION OF THE STUDY SITE

The Vyeboom study site was a full-bearing, high-performing 'Packham's Triumph' orchard at the Graymead Farm (- 34°1' 44.39"; 19°8' 10.98"; 318 m asl). The orchard was block G26F planted in 2012 on 2.63 ha. The tree spacing was 4 m x 1.5 m, giving a tree density of 1 667 trees per hectare. The rootstock was the BP1 rootstock. One-in-10 trees were the Rosemarie and Abate Fetel pollinator cultivars, arranged in a diamond pattern. The trees were planted on raised beds on a gentle sloping north-southerly terrain with a north-easterly orientation. Irrigation was via a micro-sprinkler system with one sprinkler per tree delivering 32 L/hr. Irrigation was managed by means of an automated soil moisture monitoring IrriCheck system. The orchard was planted on sandy clay-loam soils with a high lime content.



Figure 6.1 'Packham's Triumph' orchard (marked in red) at the Graymead Farm, Vyeboom

The orchard was bounded by pine trees, which were used as wind breakers on the north-west side, a 'Cape Rose' pear orchard on the east side, another 'Packham's Triumph' orchard to the south and a small farm dam on the western side of the orchard (Figure 6.1). The orchard was situated less than 400 m from the eastern margins of the Theewaterskloof Dam. The orchard was one of the consistently high-yielding orchards, which has often produced more than 100 t/ha per year when the orchard reached full-bearing age. There was a dense cover of tall fescue (*Festuca arundinacea*) between the rows, which grew all year round.

6.2 SOIL TYPE

Soils in the orchard were predominantly of the deep sandy, clay loam type. A uniform clay percentage, *ca.* 22% throughout the whole soil profile, contributed to the high total soil water content of 127.65 mm (Table 6.1). The high soil water content and a relatively low stone percentage aided the orchard in producing exceptionally high yields, which exceeded 120 t/ha in some years. A soil particle analysis also indicated that a high percentage of fine sand was also present throughout the profile. The field capacity was 0.212 mm mm^{-1} and the permanent wilting point was 0.07 mm mm^{-1}.

Table 6.1 Physical characteristics of the soils at the 'Packham's Triumph' orchard in Vyeboom

Soil depth (mm)	Clay (%)	Silt (%)	Fine sand (%)	Medium sand (%)	Coarse sand (%)	Sand grade	Soil texture class[1]
0 – 300	25.2	14.0	54.4	3.7	2.7	Fine	Sandy clay loam
300 – 600	25.2	16.0	52.6	3.7	2.5		Sandy clay loam
600 – 900	17.2	20.0	55.2	3.9	3.7		Sandy loam

[1]According to the soil texture classification of the USDA

6.3 TRANSPIRATION, SOIL MOISTURE, GROWTH AND CLIMATIC MEASUREMENTS

As with the other orchards, the leaf area index of the orchard was monitored regularly by using the leaf area meter (Model: LAI – 2000, Licor, Nebraska, USA). Fruit growth was monitored continuously by using electronic dendrometers that were attached to two fruits. The

volumetric soil water content was measured at 30, 60 and 90 cm depths, using time domain reflectometer probes (Model: CS616, Campbell Scientific, Texas, USA). Irrigation was monitored using a water flow meter connected to the irrigation line. Equipment from this site was vandalised during the winter of 2024, when all the cables of the sensors were cut. The system was re-established before the onset of the 2024-2025 season in September.

Transpiration was measured on three trees with varying stem sizes that represented the small, median and large size categories (Table 6.2). The heat ratio method described in the previous chapters was used to monitor the whole tree sap flow rate, in litres, per tree. The whole orchard transpiration in equivalent water-depth units was calculated, based on the procedure described in Chapter 4. Orchard evapotranspiration was not measured at this site, due to equipment limitations. The values reported in the next sections were derived by using the dual source ET model, which was validated at the other study sites.

Table 6.2 Installation details for the sap flow probes in the 'Packham's Triumph' orchard at Vyeboom

Tree no	Probe no	Diameter (cm)	Depth (mm)
1	1	12	10
	2		20
	3		20
	4		40
2	1	9	10
	2		20
	3		20
	4		40
3	1	14	10
	2		20
	3		20
	4		40

Weather data were obtained from the automatic weather station operated by the Graymead Farm. The weather station was situated less than one kilometer from the study orchard. The station measured the basic weather variables, namely the solar irradiance, maximum and minimum air temperatures, maximum and minimum relative humidity, wind speed and direction, and rainfall. According to Allen et al. (1998), the evapotranspiration was

calculated for a short grass reference. The weather station was located on the banks of the Theewaterskloof Dam. The data were collected at hourly and daily time intervals.

6.4 WATER PRODUCTIVITY

6.4.1 Seasonal transpiration

The transpiration was derived as L tree^{-1} d^{-1} and as mm d^{-1} from the daily sap flow data, as described in Chapter 2 of this report. The total seasonal transpiration was then summed for the period 01/09/2023 to 30/04/2024 for the first season, and 01/09/2024 to 30/04/2025 for the second season. Since there were most likely small amounts of transpiration after 31 May 2024 that were not measured, the calculation of the total seasonal transpiration is very slightly underestimated, and the water productivity is slightly overestimated for the 2023-2024 season.

6.4.2 Yield, pack out and gross income

The methods used to harvest the fruit and estimate the yield of the trial trees are presented in Chapter 2 of this report. The pack-house supplied the data on the orchard yield, the grading of the fruit (ton grade^{-1}), the market price per grade (R ton^{-1}) and the gross orchard income (R ha^{-1}).

6.4.3 Physical and economic water productivity

The methods used to calculate water productivity are detailed in Chapter 4 of this report. The calculation of WP_p was based on the yield of (i) ten trial trees, and (ii) the whole orchard block, and the seasonal transpiration (m^3 ha^{-1}) was calculated as the average of three representative monitored trees. The WP_e was calculated for the whole orchard block.

6.5 FRUIT YIELD AND QUALITY

6.5.1 Fruit yield

The orchard yield for ‘Packham’s Triumph’ in the 2023/24 and 2024/25 seasons was determined by using the same method, where the total fruit weight of ten randomly-selected trees was measured. Among these, three trees were also monitored for their sap flow. In the 2023/24 season, the harvest in Vyeboom took place on the 24th of January 2024, with the

sampling for maturity and quality assessment being conducted on the same day. The remaining fruit were stripped and weighed on the 30th of January 2024, to determine the total fruit mass per tree. In the 2024/25 season, a shift in maturity was observed, which led to changes in sampling and harvest dates. The harvest in Vyeboom occurred on the 24th of January 2025, while the sampling for maturity and quality assessment took place on the 27th of January 2025. The remaining fruit were stripped and weighed on the 2nd of February 2025. In addition, the stem circumference of the ten selected trees was measured at 20 cm above the graft union, for both seasons. These adjustments in the harvest and sampling dates indicate seasonal variations that may have influenced fruit ripening.

6.5.2 Fruit quality assessment

The 'Packham's Triumph' fruit samples were harvested in the morning, as described above, and they were stored overnight at the Wet Laboratory in the Department of Horticultural Science at Stellenbosch University in regular atmosphere storage at 10^{0}C for an assessment of their maturity and quality. After the overnight storage, the fruits were removed from storage and allowed to gain room temperature for three hours, before the assessment began. The following parameters were measured as per commercial standard practice:

- the diameter (mm);
- the height (mm);
- the mass (g);
- the firmness (kg), determined on opposite cheeks using a penetrometer (Fruit texture Analyzer, Guss Instruments, Strand, South Africa) with a 7.9 mm tip;
- the background colour (also background Colour 2 for the green cheek in the case of 'Packham's Triumph'), using the industry colour chart by Hortgro, Paarl;
- the sunburn severity, using the 'Packham's Triumph' and 'Forelle' sunburn colour chart set P. 13 and P.25;
- the starch conversion, using the iodine test with the starch conversion chart by Hortgro, Paarl;
- the Total Soluble Solids (TSS): for each group of pears, a combined juice sample was prepared by using one slice per fruit (i.e. a disk-shaped slice cut along the fruit diameter), which were blended together in a kitchen blender, and the TSS (%) was

measured from a small sub-sample of the juice by using a calibrated electronic refractometer (TSS 0-32%, Model N1, Atago, Tokyo, Japan); and

- Titratable Acidity (TA): after extracting a sub-sample for TSS testing, the remaining juice was tested for the TA content (reported as % malic acid) by using a Metrohm Tritrator, along with the 815 Sample Changer (Titrator model: 888 Titrando, Software: Tiamo, Herisau, Switzerand).

The fruits were packed by Elgin Orchards (Pty) Ltd., which will provide the pack-out information at a later stage, as well as the prices obtained for different quality classes. These data will be included in future deliverables.

6.6 RESULTS AND DISCUSSION

6.6.1 Weather conditions

The climatic conditions at Graymead Farm from September 2023 to July 2025 are summarised in Figure 6.2. The daily average solar radiation for each month was quite low, compared to the other sites, peaking at less than 28.6 MJ/m^2/d for both seasons (Figure 6.2a). The reasons for this are unclear, although the presence of the tall mountain ranges to the west of the study site may have cut out a lot of the diffuse radiation incidence on the orchard. The high incidence of cloud cover may also have played a part in reducing the radiation intensity. As expected, clear seasonal variations in the air temperature were evident, with the maximum peaking at about 39°C and the minimum at 13°C in summer. In winter, the monthly average maximum temperature reached 22.3°C and the minimum was -0.92°C. According to Figure 6.2b, the minimum temperature was zero degrees Celsius, or lower, for three months, namely August, September and October 2024. The monthly peak vapour pressure deficit was low during 2023, reaching around 0.83 kPa. It rose in 2024 to roughly double that in 2023, at about 1.43 kPa (Figure 6.2c). These VPD values are lower than those recorded at the other three study sites, most likely because of the proximity to the dams i.e. the Theewaterskloof Dam and a smaller holding dam adjacent to the study site (Figure 6.1) that created a humid environment over the study site.

Rain fell in all months of the year, varying in amounts from as low as 1.6 mm to more than 440 mm in July 2024 (Table 6.3). The annual rainfall at Vyeboom was very high during the

2023-2024 season, reaching 1 125 mm, compared to 1 019 mm in the reference evapotranspiration.

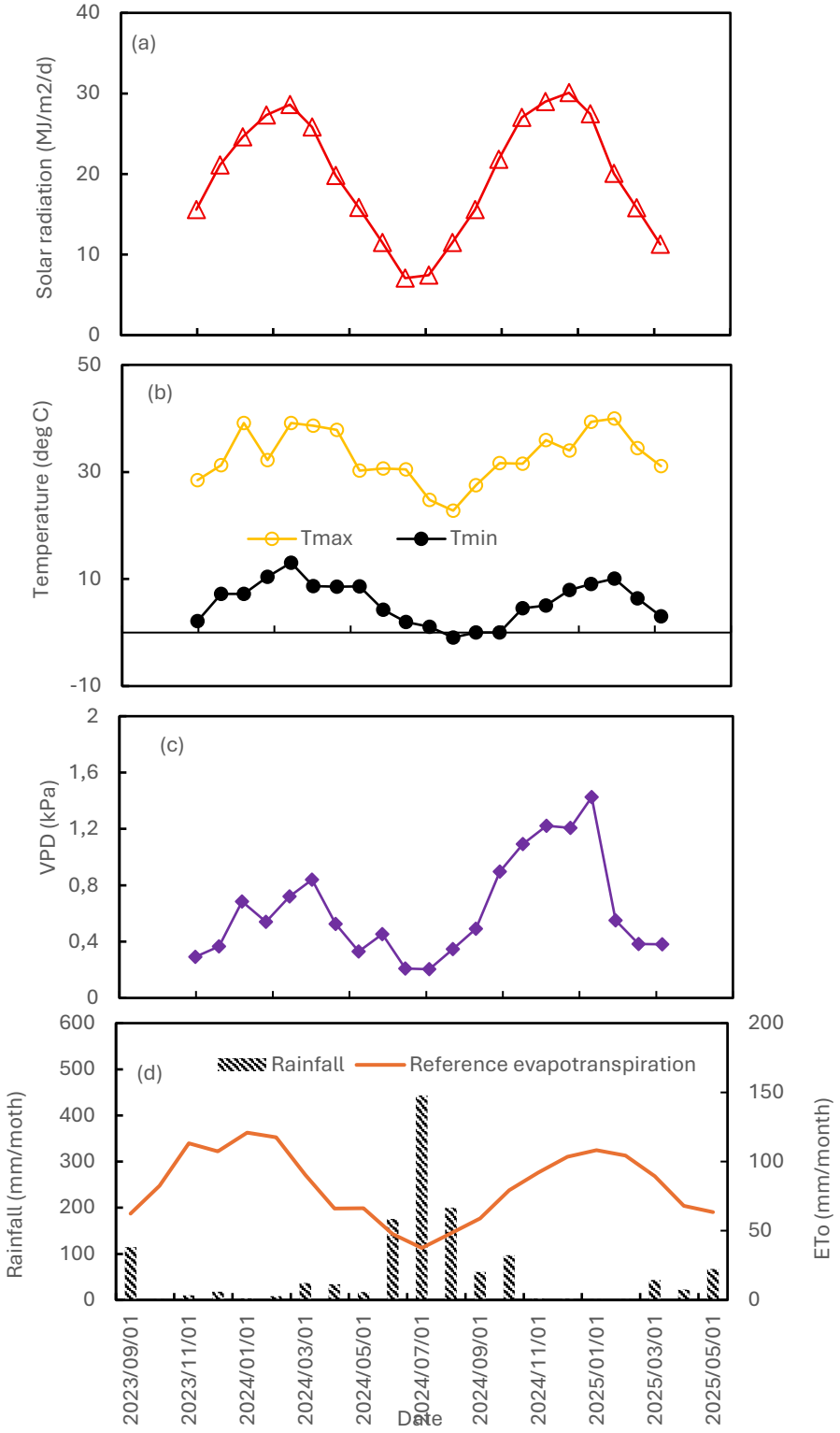


Figure 6.2 Average monthly climatic conditions at Vyeboom over two growing seasons including (a) the solar radiation, (b) maximum and minimum temperatures, (c) vapour pressure deficit of the air, (d) monthly total rainfall and the reference evapotranspiration

Of this amount, 74% (836 mm) of the rain fell during the winter months, from May to August. During the fruit-growing season (September to April), the total rainfall was very low, namely 228 and 231 mm, respectively, for the two seasons. The total reference evapotranspiration during the growing season was 760 and 704 for the 2023-2024 and 2024-2025 growing seasons, respectively.

Table 6.3 Summary of monthly climatic conditions at Vyeboom from September 2023 to May 2025

	Solar radiation	Tmax	Tmin	RHmax	Rmin	VPD	u	Rainfall	ETo
	(MJ/m2/d)	(°C)	(°C)	(%)	(%)	(kPa)	(m/s)	(mm)	(mm)
2023/09/30	7.8	28.4	2.1	99.0	17.0	0.3	2.6	114.8	62.5
2023/10/31	10.6	31.2	7.2	99.0	20.0	0.4	2.4	1.6	82.6
2023/11/30	12.3	39.1	7.2	99.0	8.0	0.7	2.1	10.4	113.2
2023/12/31	13.7	32.2	10.4	99.0	25.0	0.5	2.1	18.2	107.4
2024/01/31	14.3	39.2	13.1	99.0	9.0	0.7	2.1	4.0	120.9
2024/02/29	12.9	38.6	8.7	99.0	12.0	0.8	1.9	8.0	117.5
2024/03/31	9.9	37.9	8.6	99.0	13.0	0.5	1.9	37.0	90.4
2024/04/30	7.9	30.3	8.6	99.0	19.0	0.3	2.2	34.0	66.0
2024/05/31	5.7	30.7	4.3	99.0	15.0	0.5	2.1	17.2	66.3
2024/06/30	3.5	30.5	2.0	99.0	15.0	0.2	2.3	175.6	47.7
2024/07/31	3.7	24.8	1.1	99.0	6.0	0.2	1.8	443.2	37.6
2024/08/31	5.7	22.8	-0.9	99.2	14.0	0.3	1.5	200.4	48.2
2024/09/30	7.8	27.5	0.0	99.2	0.0	0.5	1.3	60.6	58.9
2024/10/31	10.9	31.6	0.0	99.2	10.1	0.9	1.1	96.8	79.4
2024/11/30	13.5	31.5	4.5	98.1	11.2	1.1	1.0	2.8	92.1
2024/12/31	14.5	35.9	5.1	98.1	8.1	1.2	1.1	2.4	103.4
2025/01/31	15.0	34.0	7.9	97.6	11.8	1.2	1.1	1.8	108.3
2025/02/28	13.7	39.4	9.1	96.8	9.2	1.4	1.0	1.6	104.2
2025/03/31	10.0	40.0	10.1	99.9	11.4	0.6	1.9	43.0	89.5
2025/04/30	7.9	34.4	6.4	99.9	17.2	0.4	1.8	22.6	68.1
2025/05/31	5.6	31.1	3.0	99.9	7.9	0.4	2.2	67.0	63.6

6.6.2 Canopy growth and development

The seasonal trend in the Leaf Area Index (LAI) followed a similar trajectory to that of the other three orchards; it was characterised a more rapid early season growth in spring, reaching peak values in mid-summer, before a more gradual decline in autumn and into the winter season. The peak LAI for this orchard was the lowest of the four orchards, reaching a

value around 3.0 for both seasons. The tree height (~ 3.5 m) and canopy size ~ 3.0 m x 2.6 m were also generally lower in this orchard, than in the other orchards. The orchard floor maintained a short (~ 10-15 cm height) cover of a tall fescue cover crop over a 60 to 70 cm strip width throughout the growing season. The wide range of micro-sprinklers kept the cover crop healthy during the dry season. Irrigation occurred roughly two to three times per week, except during exceptionally hot weather when the irrigation frequency was increased. Irrigation amounts varied from 1.0 to 6 mm per event in the early season, and increased to as much as 12 mm during the peak summer season. Total seasonal irrigation was low, at 300 mm, during the 2024-2025 season. The irrigation data for the 2023-2024 season were unreliable, due to a high frequency of data loss because of power problems to the station.

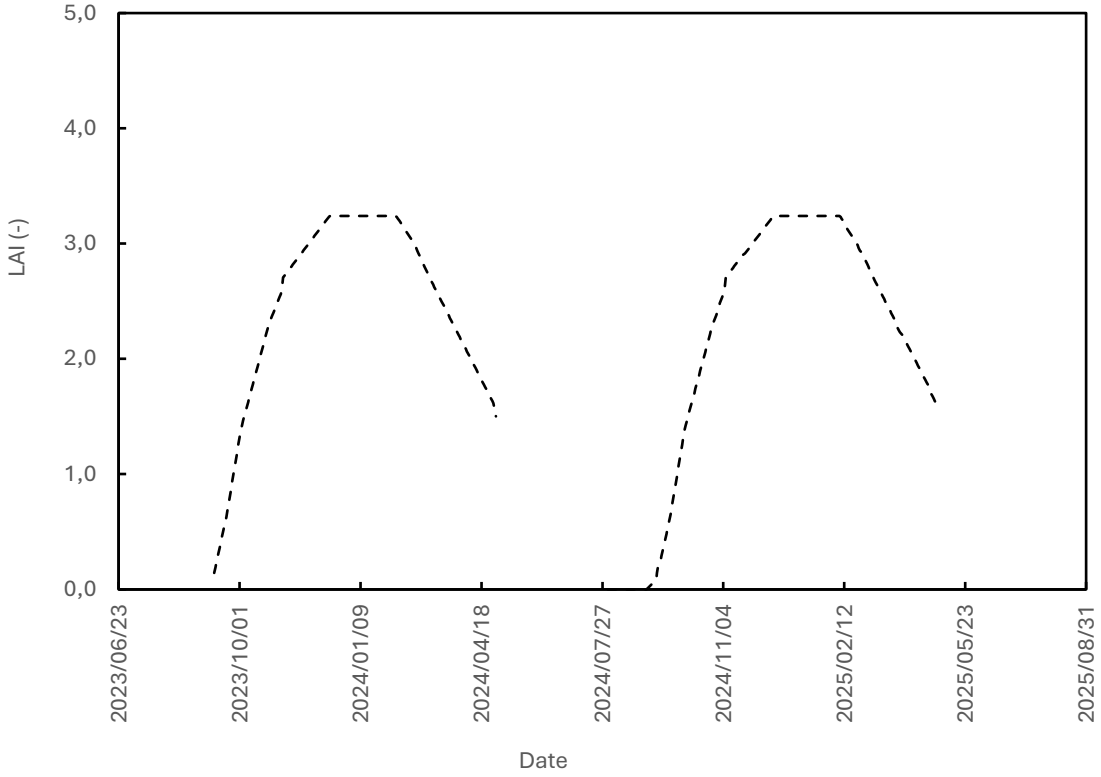


Figure 6.3 Leaf area index of the 'Packham's Triumph' orchard at Vyeboom for the 2023-2024 and 2024-2025 seasons

6.6.3 Transpiration and soil water content dynamics

The soil water content data in the rootzone of the trees are not continuous because they were not downloaded regularly. A lot of the data were lost when the memory of the datalogger got full. For this reason, the soil water content data for the Vyeboom orchard are not presented in this report. As at the other sites, orchard transpiration was strongly related to the

atmospheric evaporative demand, which is depicted by the reference evapotranspiration (Figure 6.4). The maximum water use of an individual tree was around 26 litres per tree per day during the 2023-24 season and 32 L/tree/day during the 2024-2025 season. These water use rates were somewhat lower than those reported for the 'Packham's Triumph' in Wolseley. At equivalent water depth units, the maximum daily transpiration reached 4.4 mm during the 2023-2024 season. It was higher during the 2024-2025 season, when it reached 5.5 mm/d.

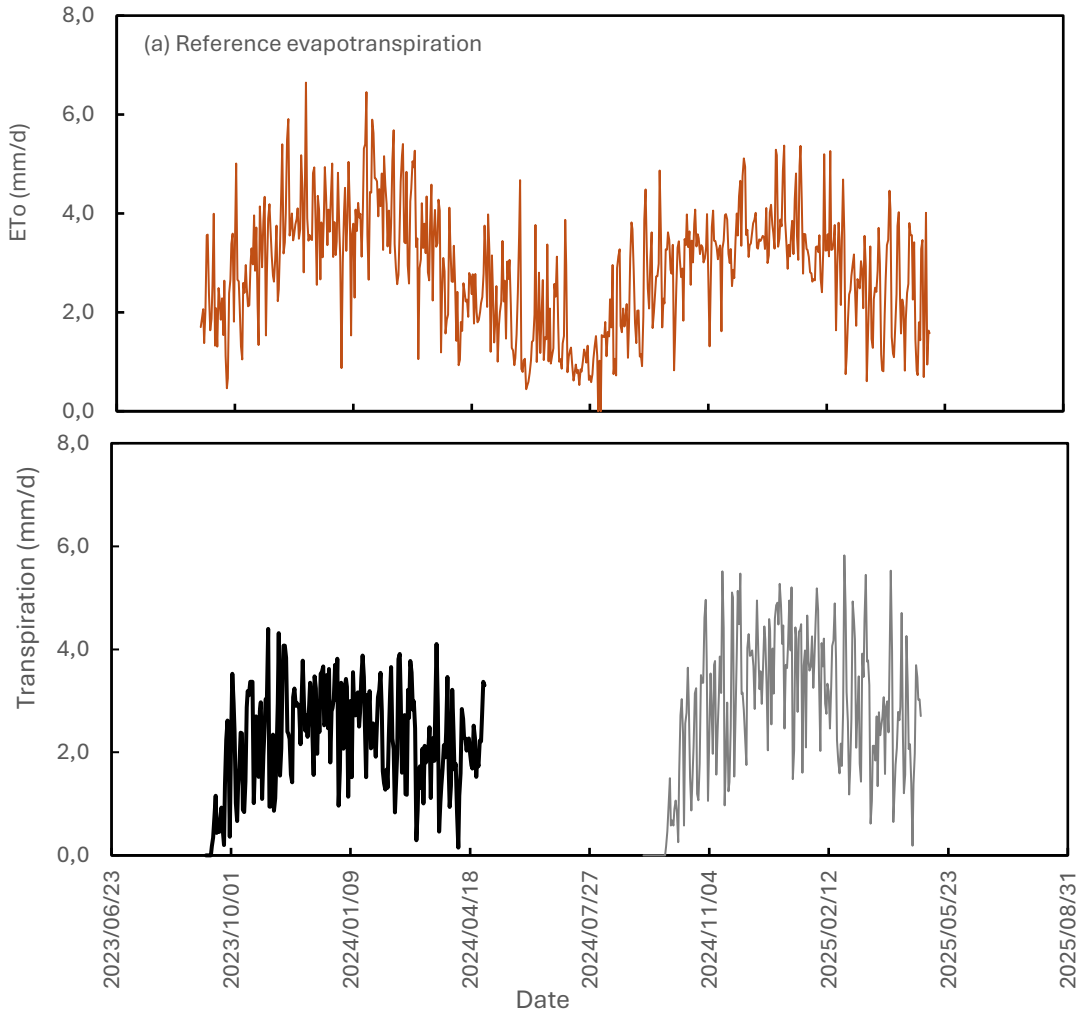


Figure 6.4 (a) The reference evapotranspiration, and (b) transpiration dynamics for the 'Packham's Triumph' trees at Vyeboom over two growing seasons.

The seasonal total transpiration was 500.2 mm from 01 September 2023 to 30 April 2024, which translated to a water consumption of 5 000 m^3/ha. From 01 September 2024 to 30 April 2025, the total orchard transpiration was higher, at 497.7 mm (i.e. 4 970 m^3/ha). The average seasonal transpiration for the two years was therefore around 498.9 mm (4 989 m^3/ha/season).

6.6.4 Water use modelling and orchard water balance

The dual source water-use model described in Chapter 3 was applied to the full-bearing 'Packham's Triumph' orchard in Vyeboom for the 2023-2024 and 2024-2025 seasons. Figure 6.5 shows that the simulated transpiration rates were of a similar order of magnitude to the measured values. A comparison of the measured and modelled daily transpiration data showed an R^2 of 0.47, an RMSE ~ ± 0.87 mm/d, an MAE ~ ± 0.68 mm/d and a Nash-Sutcliffe efficiency of 0.30. The somewhat low level of predictive accuracy can be attributed to the low quality of the sap flow data that had many gaps in it, due to the equipment malfunctioning and gap filling being required. The predicted seasonal transpiration was 470 mm during the 2023-2024 season and 602.9 mm for the 2024-2025 season. The predicted average seasonal transpiration for the two seasons was 536.5 mm, which was 8% higher than the measured value (498.8 mm). The predicted seasonal total orchard evapotranspiration was 686.9 mm in 2023-2024 and 796.5 mm in 2024-2025. The average seasonal ET for the 'Packham's Triumph' orchard in Vyeboom for the two seasons was therefore 741 mm, which amounts to a crop water requirement of 7 410 m^3/ha/season. This water requirement rate is lower than the 8 030 m^3/ha that was estimated for the full-bearing 'Packham's Triumph' in Wolseley.

The partitioning of the orchard water use into the transpiration and evapotranspiration components is shown in Figure 6.6, which is based on the model simulations. As expected, in late winter – early spring, orchard floor evapotranspiration accounted for 100% of the orchard total water use.

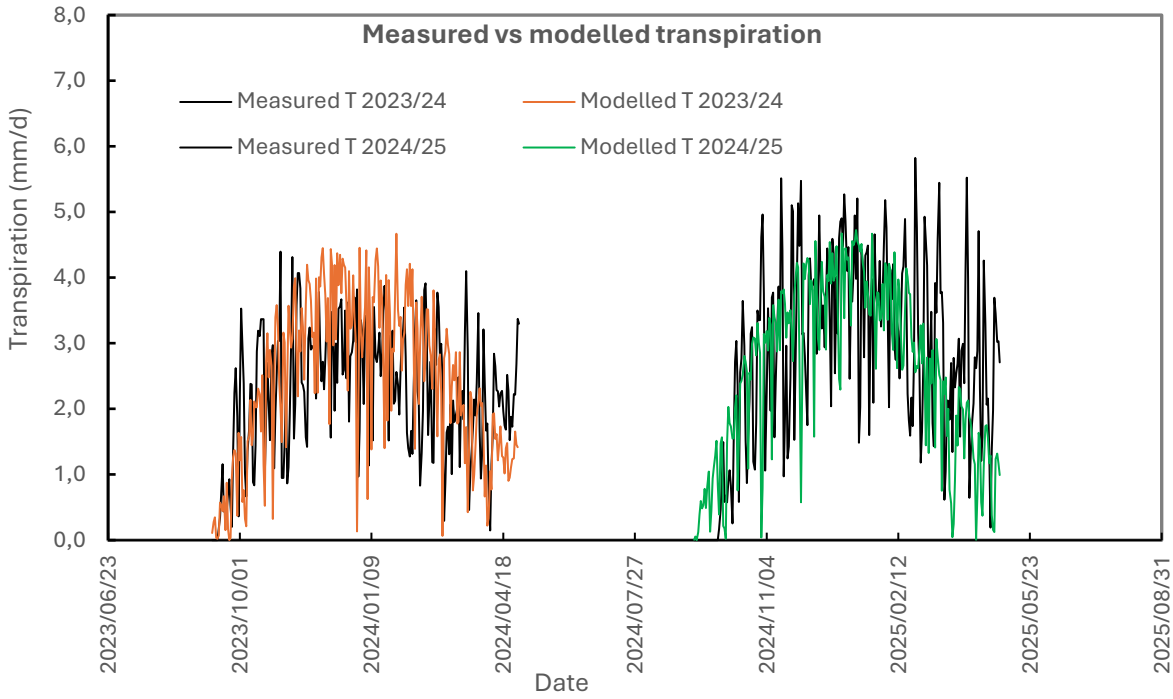


Figure 6.5 Trends in the measured and modelled transpiration for the 'Packham's Triumph' trees at Vyeboom over two growing seasons

As the canopy cover developed, increasing both the tree transpiration component and shading of the orchard floor, the contribution of the orchard floor evaporation to the total orchard water use decreased. For the 2023-2024 season, the orchard floor evaporation contributed ~ 31% to the seasonal orchard ET, while it contributed 24% in the 2025-2026 season, respectively. On average, the orchard floor contributed 28% to the total orchard water use during the two growing seasons at Vyeboom. The orchard floor water use was higher at the Vyeboom site, compared to the other three orchards, because of the comparatively low canopy cover of the trees.

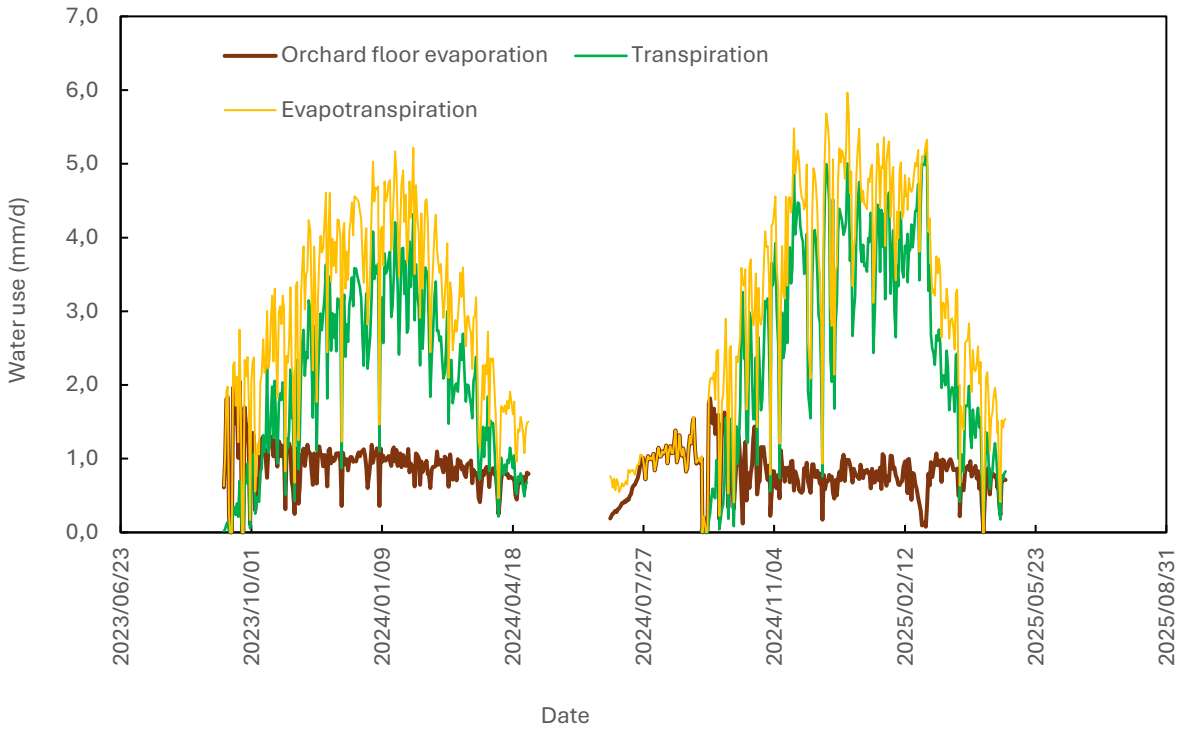


Figure 6.6 The measured transpiration and modelled evapotranspiration trends for the 'Packham's Triumph' trees at Vyeboom over two growing seasons

An illustration of the water balance components of the 'Packham's Triumph' orchard for the 2024-2025 growing season is shown in Figure 6.7. Even though the annual rainfall was high (>1 000 mm), less than 25% of this fell during the fruit growing season. The seasonal (September to April) total rainfall plus irrigation matched the orchard transpiration, namely, 625 and 603 mm, respectively. The actual orchard evapotranspiration was close to the reference evapotranspiration, with values of 738.6 mm for ETo and 796.5 mm for ET. Based on the yield from the orchard (see later in this Chapter), this was one of the best-managed orchards with very high yields. However, its water use was the least among the four orchards that were studied. The trends in the monthly water use amounts are shown in Figure 6.8.

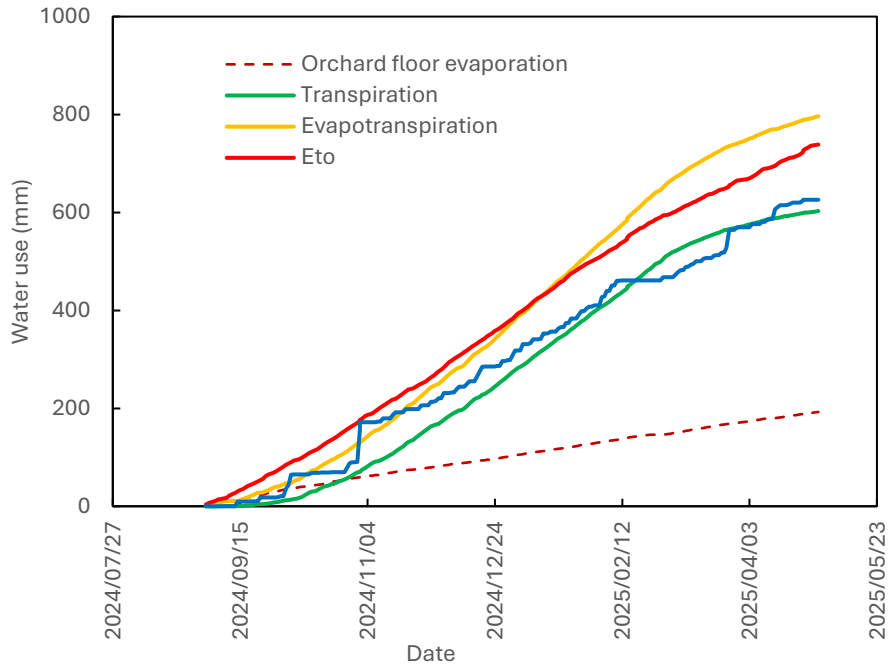


Figure 6.7 Water balance of the 'Packham's Triumph' orchard in Vyeboom for the 2024-2025 growing season

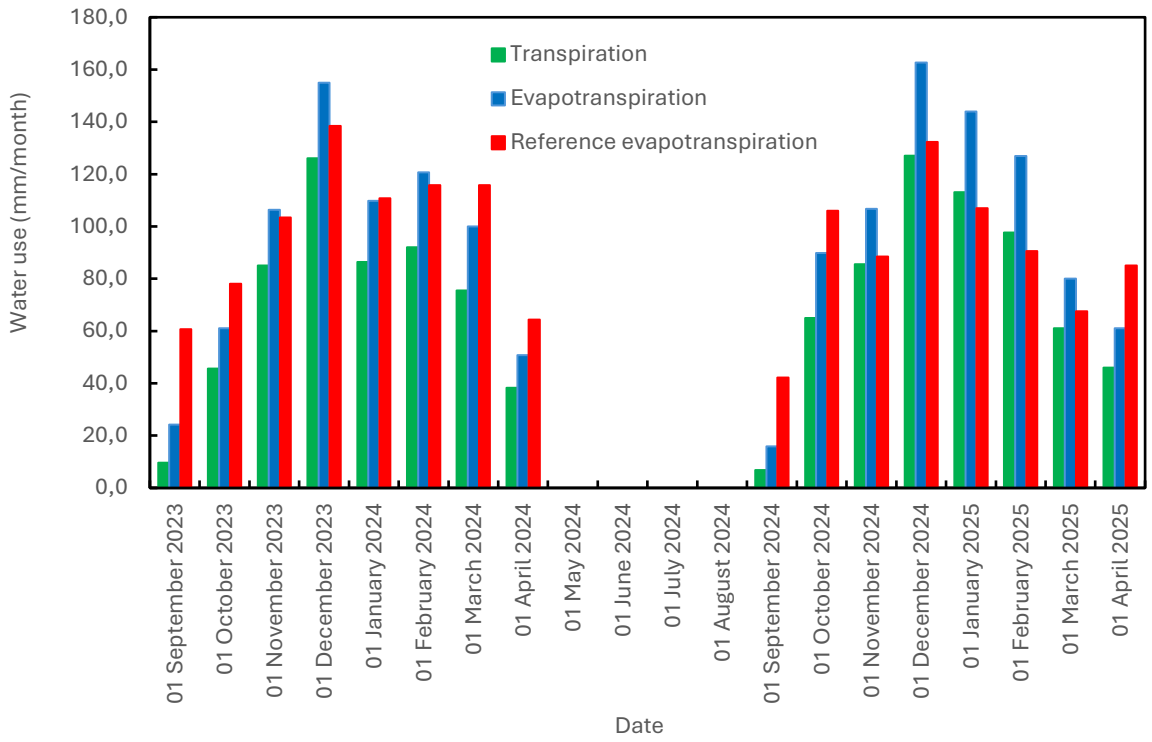


Figure 6.8 Monthly total water use partitioned into the actual transpiration (green bar), reference evapotranspiration (red bars) and actual evapotranspiration (blue bars) for the full-bearing 'Packham's Triumph' orchard in Vyeboom over two growing seasons

The measured and modelled basal (K_{cb}) and crop coefficients (K_c) for the 'Packham's Triumph' orchard in Vyeboom over a typical growing season are shown in Figure 6.9. The peak weekly K_{cb} ranged from 0.68 to 0.78, while the maximum crop coefficient was similar to that observed in the other orchards, namely, in the range of 0.97 to 1.14.

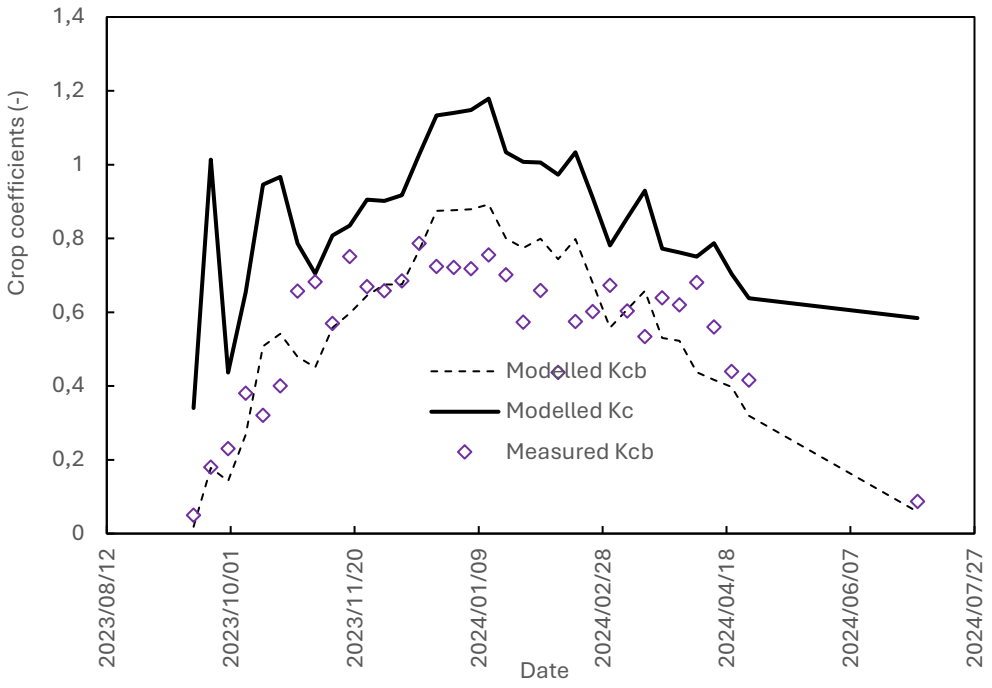


Figure 6.9 Weekly changes in the crop coefficients for the 'Packham's Triumph' orchard at Vyeboom over the 2023-2024 growing season

6.6.5 Modelling the yield of 'Forelle' and 'Packham's Triumph' orchards

The modified yield model by Doorenbos and Prutt (1977) is described in Chapter 3. We set the theoretical maximum seasonal transpiration for pears to 900 mm, for both the 'Forelle' and 'Packham's Triumph' cultivars. However, using a common theoretical maximum yield for both cultivars yielded unrealistically-high Ky values for the 'Forelle' orchards. Therefore, we defined different maximum yields as 90 t/ha for 'Forelle' and 110 t/ha for 'Packham's Triumph', which was consistent with the observed yield trends for these two cultivars. 'Forelle' tends to produce smaller yields than 'Packham's Triumph'. Using the measured yields and the measured seasonal total transpiration values produced distinct average Ky values of 1.14 ± 0.42 for the 'Packham's Triumph' orchards and 1.83 ± 0.31 for the 'Forelle' orchards (Table 6.3). High Ky values imply a greater yield reduction, due to a reduction in transpiration e.g. due to water stress.

Table 6.4 Deriving of the yield response factor (Ky) for the 'Forelle' and 'Packham's Triumph' pear cultivars under South African conditions

Year	Site	Cultivar	Ym	Tc	Ta	Ya	Ky	Ky SEM
			(t/ha)	(mm/y)	(mm/y)	(t/ha)		
2022/23	Ceres	'Forelle'	90	900	721	69.8	1.13	
2023/24	Ceres	'Forelle'	90	900	773	59.1	2.43	
2024/25	Ceres	'Forelle'	90	900	768	70.5	1.48	
2022/23	Wolseley	Packham	110	900	635	59	1.57	
2023/24	Wolseley	Packham	110	900	559	55	1.32	
2023/24	Vyeboom	Packham	110	900	470	72.4	0.82	
2024/25	Vyeboom	Packham	110	900	603	75.7	1.11	
2023/24	Elgin	'Forelle'	90	900	701	45	2.26	
	Packhams						1.14	0.42
	'Forelle'						1.83	0.31
	Average						1.48	0.30

The average Ky values that combine the 'Forelle' and 'Packham's Triumph' datasets was 1.48 ± 0.30. The significance of these Ky values is that the yield reduction in the 'Forelle' orchards appears to be more sensitive to water deficits, which causes transpiration reduction, compared to that of 'Packham's Triumph'. To validate the accuracy of the yield response factors, we used historical weather and yield data for the 'Packham's Triumph' data from Vyeboom in 2013, when the orchard was planted, to 2020, when the orchard reached its full-bearing age. The historical yield data is shown in Figure 6.10.

We then applied the water use model to estimate the seasonal total transpiration, with the following assumptions:

1) The orchards were well-watered at all times, so the water stress function was given a value of 1.0 (which means no transpiration reduction, due to water shortage); and
2) The peak leaf area index increased by similar proportions to the yields in subsequent years, from planting until full-bearing.

With these assumptions, the yield model produced good simulations of the yield, as shown in Figure 6.11. The second assumption above is the greatest weakness of the model; it should

be refined in future studies, where the LAI is tracked from planting until the orchards reach their full-bearing age.

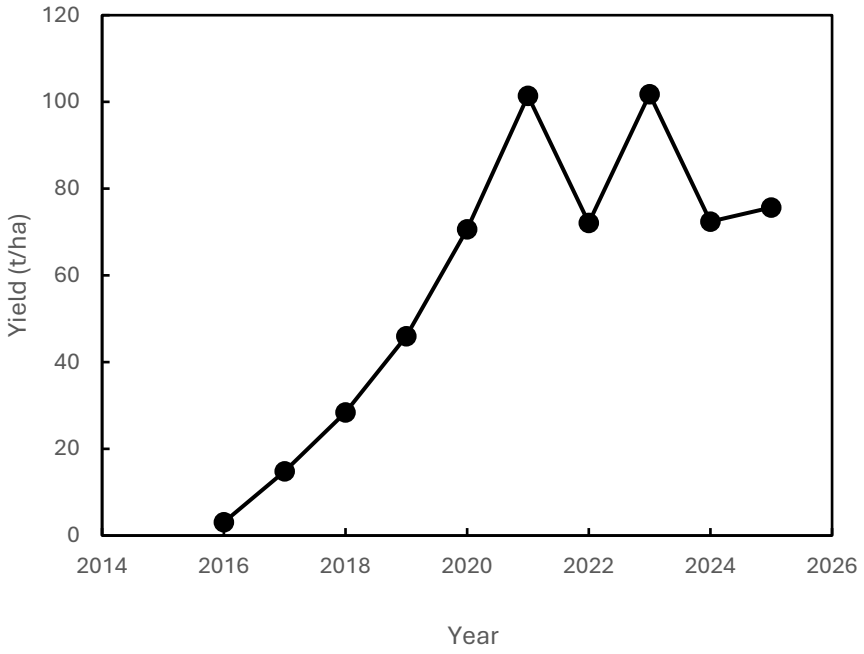


Figure 6.10 Yield trends for the 'Packham's Triumph' orchard from planting (2012) until the 2024/25 growing season

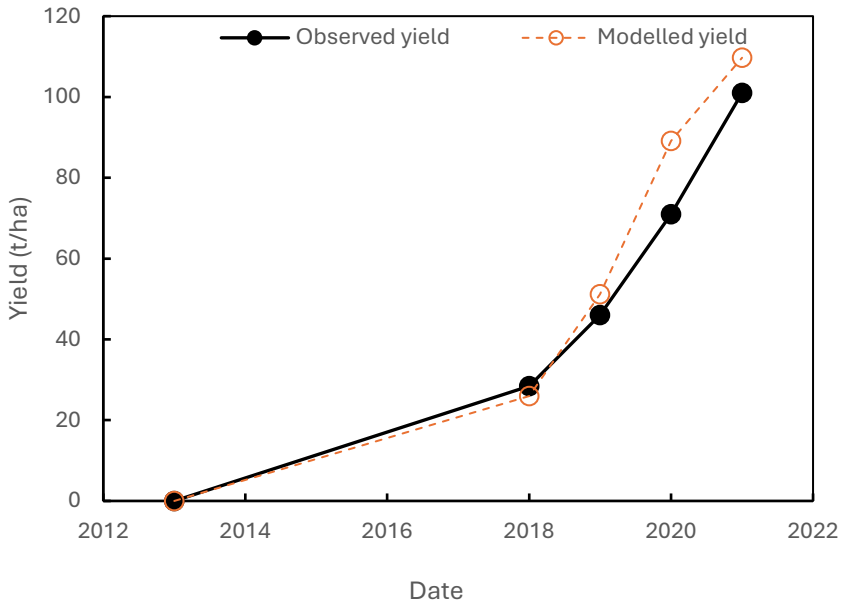


Figure 6.11 Comparison of the actual and modelled yield of a 'Packham's Triumph' orchard at Vyeboom, from planting in 2013 until its full-bearing age at around 2020-2022

6.6.6 Fruit yield and quality

This section presents the data on the yield quantity (Table 6.5) and quality (Table 6.6) for the 'Packham's Triumph' cultivar for the 2023/24 and 2024/25 growing seasons.

Table 6.5 Average yield and main stem circumference

Cultivar	Average Yield (kg/tree)	Yield (t/ha)	Average stem circumference (cm)
'Packham's Triumph' (2023-24)	44.81	74.69	40.53
'Packham's Triumph' (2024-25)	67.2	112.02	39.04

The average yield determined from 10 trees was about 44.8 kg during the 2023-2024 season. The yield was much higher during the 2024-2025 season, at about 67 kg per tree. These data translated to yields of 74.7 t/ha during the 2023-2024 season and 112 t/ha during the 2024-2025 season, as summarised in Table 6.5. The yield in the current season is much higher than the industry average.

Table 6.6 represents the average values obtained by the quality analyses on the fruit samples of the 'Packham's Triumph' in Vyeboom. The samples were picked when optimum firmness was reached. Both cultivars were stored overnight at a regular atmosphere (10^0C) storage and evaluated a day after sampling.

Table 6.6 Fruit maturity and quality in for the 'Packham's Triumph' orchard in Vyeboom

Cultivar	Diameter (mm)	Height (mm)	Mass (g)	Firmness A (kg)	Firmness B (kg)	Blush Colour (Chart set P.16)	Background colour A (Chart)	Background colour B (Chart)	Sunburn (relevant Chart)	Starch conversion (%)	TSS (%)
'Packham's Triumph' (2023-24)	71.74	74.62	180.93	7.47	7.52		2.08	2.23		37.46	11.52
'Packham's Triumph' (2024-25)	57.31	68.56	121.95	7.31	7.37		2.14	2.24	-	-	-

6.6.7 Water productivity of 'Packham's Triumph's at Vyeboom

The T-based WP of 'Packham's Triumph' pears in the Vyeboom region was 15.01 and 19.92 kg m^{-3} in 2023-2024 and 2024-2025, respectively, when calculated for the trial trees (Table 6.7). The large difference was due to the substantially higher yield in the second season. For the whole orchard block, it was 16.07 and 17.68 kg m^{-3}, respectively. While the difference between the two seasons was still there, it was smaller, based on a smaller yield difference. The T-based EWP was 69.20 and 104.91 R m^{-3} in the first and second seasons, respectively. Since the seasonal T was similar between the seasons, the higher gross value in 2024-2025 led to the higher EWP.

Table 6.7 Physical Water Productivity (WP), Water Use Efficiency (WUE), and Economic Water Productivity (EWP) based on seasonal transpiration for the 'Packham's Triumph' pear orchard in Vyeboom in 2023-2024 and 2024-2025

	2023-2024	2024-2025
Planting density (trees/ha)	1667	1667
Seasonal transpiration (mm)	497.8	576.1
Seasonal transpiration per hectare (m^3/ha)	4978.1	5761
Trial trees:		
Yield (t/ha)	74.70	99.12
Water Use Efficiency (m^3/ton)	66.6	50,2
Physical Water Productivity (kg/m^3)	15.01	17.21
Whole orchard block:		
Yield (t/ha)	80.0	88.0
Water Use Efficiency (m^3/ton)	62.2	65.47
Physical Water Productivity (kg/m^3)	16.07	15.28
Orchard gross income (R/ha)	R344 499	R522 122
Economic Water Productivity (R/m^3)	R69.20	R90.63

Table 6.8 Physical Water Productivity (WP), Water Use Efficiency (WUE), and Economic Water Productivity (EWP), based on seasonal evapotranspiration for the 'Packham's Triumph' pear orchard in Vyeboom in 2023-2024 and 2024-2025

	2022-2023	2023-2024
Planting density (trees/ha)	1667	1667
Seasonal evapotranspiration (mm)	692.1	797.1
Seasonal evapotranspiration per hectare (m^3/ha)	6920.9	7970.9
Trial trees:		
Yield (t/ha)	74.70	99.12
Water Use Efficiency (m^3/ton)	92.65	80.42
Physical Water Productivity (kg/m^3)	10.79	12.44
Whole orchard block:		
Yield (t/ha)	80.0	88.0
Water Use Efficiency (m^3/ton)	86.5	90.6
Physical Water Productivity (kg/m^3)	11.56	11.04
Orchard gross income (R/ha)	R344 499	R522 122
Economic Water Productivity (R/m^3)	R49.78	R65,50

When calculated relative to the seasonal ET, the WP was 10.79 and 12.44 kg m^{-3} for the two seasons, respectively (Table 6.8). For the whole orchard block, the WP was 11.56 and 11.04, respectively. Both the yield and seasonal ET were higher in 2023-2024, compared to 2022-2023, but the relative yield difference was smaller in the orchard block. The ET-based EWP was 49.78 and 65.50 for the two seasons, respectively. The higher value in 2023-2024 was due to a high gross crop value, while the seasonal ET showed a relatively smaller increase, from the first to the second season.

6.7 CONCLUSIONS

In this Chapter, we have shown that the seasonal water use of the full-bearing 'Packham's Triumph' orchard with a relatively small canopy size (LAI < 3.0), growing in a region with milder climatic conditions, was quite low, compared to the other sites. The total seasonal transpiration was 576.1 and 497.8 mm for the first and second seasons, respectively. The average transpiration for the two seasons was 537 mm, which was lower than that for the 'Packham's Triumph' in Wolseley. However, the yield was higher in Vyeboom at 80 and 88 t/ha for the first and second year, respectively. The transpiration-based physical water productivity

averaged 16.11 kg/m^3 for the two seasons, while the evapotranspiration-based mean value was 11.62 kg/m^3. These values are considerably higher than those for the same cultivar in Wolseley (9.9 and 7.3 kg/m^3), primarily because of the high yields and low water-use rates in Vyeboom. The economic water productivity was also high in Vyeboom, averaging R79.9/m^3 for the transpiration and R57.6/m^3 for the ET-based economic water productivity. In this Chapter, we also investigated the application of a transpiration-based yield model. There is a need to effectively test some of the assumptions made in the calculations, in order to generate confidence in the yield model.

CHAPTER SEVEN

'FORELLE' ORCHARD, ELGIN

7.0 INTRODUCTION

Elgin is one of the key fruit-producing regions in the Western Cape. It is located on a high-altitude valley on the eastern margins of the Atlantic Ocean. Intensive fruit farming is the dominant land use, with the fruit types being mostly apples, pears and greenhouse cut flowers, as well as other crop types. In 2012, the region produced about 60% of the apples produced in the country (Phillipe, 2013*)*. As with the other three orchards studied in this project, the climate of Elgin is also of the Mediterranean-type (Köppen-Geiger: Csb), and it is characterised by mild wet winters and warm dry summers. The climate of the area is influenced by the higher altitude (250-500 m asl), the surrounding mountains and the proximity to the Atlantic Ocean, which produces cooler temperatures and frequent cloud cover. The area receives a much higher rainfall than the Ceres and Wolseley production regions that have been reported in this study. The terrain in Elgin is mostly hilly and the soils are predominantly well-drained, nutrient-poor and clay-loam. The area consists of acidic clay-loam soils with a high water-holding capacity, which are often classified under the Glenrosa or Mispah forms.

In this chapter, we report on the water use-yield relationship of a mature 'Forelle' orchard, the data of which were collected over two growing seasons. The data were used to validate the water use model described in Chapter Three.

7.1 DESCRIPTION OF THE 'FORELLE' ORCHARD IN ELGIN

The Elgin orchard is the fourth orchard where data on the water use-yield relationships for pear orchards was collected on 'Forelle' (-34° 10' 48.48" 19° 1' 30.25"; 319 masl) in the EGVV area (Figure 7.1). The 'Forelle' trees were grafted on the BP2 rootstock and pollinated by the 'Early Bon Chretien' cultivar. The orchard was laid out in alternating three rows of 'Forelle', followed by one row of Early Bon Chretien. The trees were planted in 2003, with a spacing of 4.5 m x 1.5 m. The tree density was therefore 1 481 plants per hectare and the total area of the orchard was approximately 4.2 ha. The rows were planted with a north-south orientation, in order to maximise the light interception. A dense cover of indigenous grasses, together with

patchy sections covered by the exotic kikuyu grass, grew between the tree rows. An automated micro-sprinkler irrigation system was used to water the trees by emitting ~ 32 L/h. The irrigation system was also set to pulse when temperatures reached to 28°C, to cool down the canopies and to reduce the sunburn damage on the fruit. The orchard was surrounded by pine tree windbreaks on the west and eastern sides. There was a dam on the northern side and an apple orchard on the southern side of the study orchard. The average that was yield obtained fluctuated greatly over the past three seasons, namely 48.5, 22.7, and 45.8 tons/ha in 2021, 2022 and 2023, respectively.



Figure 7.1 'Forelle' orchard (marked around in white) at the farm in Elgin

7.2 CHARACTERISING THE SOILS AT THE ELGIN ORCHARD

This 'Forelle' orchard was established on a clayey-loam soil with a high stone percentage (*ca.* 63%) within the first 900 mm. This, together with the high coarse sand fraction (Table 7.1) found from 300 mm downwards, contributed to the low total soil water content of 97.2 mm. The field water capacity of the soil was 0.176 mm mm^{-1} and the permanent wilting point was 0.057 mm mm^{-1}.

Table 7.1 Physical characteristics of the soils at the 'Forelle' orchard in Elgin

Soil depth (mm)	Clay (%)	Silt (%)	Fine sand (%)	Medium sand (%)	Coarse sand (%)	Sand grade	Soil texture class[1]
0 – 300	17.2	22.0	44.2	1.8	14.8	Fine	Sandy loam
300 – 600	13.2	10.0	22.3	2.6	51.9	Coarse	
600 – 900	17.2	20.0	31.1	2.0	29.6	Coarse	

[1]According to the soil texture classification of the USDA

7.3 TRANSPIRATION, SOIL MOISTURE, GROWTH AND WEATHER MEASUREMENTS

As with the other orchards, the leaf area index of the orchard was monitored regularly by using the leaf area meter (Model: LAI – 2000, Licor, Nebraska, USA). The fruit growth was monitored continuously by using electronic dendrometers attached to two sun-exposed fruits. The volumetric soil water content was measured at 30, 60 and 90 cm depths, by using time domain reflectometer probes (Model: CS616, Campbell Scientific, Texas, USA). Irrigation was monitored by using a water flow meter connected to the irrigation line.

Transpiration was measured on three trees with varying stem diameters that represented the small, median and large sizes (Table 7.2).

Table 7.2 Installation details for the HRM sap flow sensors at Elgin

Tree no	Probe no	Stem diameter (cm)	Depth (mm)
1	1	16	10
	2		20
	3		30
	4		40
2	1	15	10
	2		20
	3		30
	4		40
3	1	11	10
	2		20
	3		30
	4		40

The heat ratio method that has been described in the previous chapters was used to monitor the whole tree sap flow rates in litres per hour. The whole orchard transpiration, in equivalent water depth units, was calculated based on the procedure described in Chapter Four. Weather data were obtained from the automatic weather station operated by the farm. The weather station was situated adjacent to the orchard. The station measured the basic weather variables, namely, the solar irradiance, maximum and minimum air temperatures, maximum and minimum relative humidity, wind speed and direction and rainfall. The reference evapotranspiration was calculated for a short grass reference, according to Allen et al. (1998). The data were collected at hourly and daily time intervals. The soil water content data were also discontinuous, due to irregular downloading, which led to a substantial loss of the soil water content data.

7.4 FRUIT YIELD AND QUALITY FOR EGVV ORCHARDS

7.4.1 Fruit yield

The orchard yield for 'Forelle' in Elgin for the 2023/24 and 2024/25 seasons was determined by measuring the fruit weight of ten randomly-selected trees, including three trees that were monitored for sap flow. In the 2023/24 season, sampling for maturity and quality assessment was conducted on the 14th of February 2024, followed by the harvest and weighing of the remaining fruit per tree on the 16th of February 2024. In the 2024/25 season, a shift in maturity was observed, and sampling took place on the 23rd of February 2025 at an optimal maturity index, with an average firmness of 6.9 kg. However, the trees have not yet been harvested, in order to obtain the total yield per tree, as the farm has not proceeded with harvesting. In addition, the stem circumference of the ten selected trees was measured at 20 cm above the graft union, for both seasons.

7.4.2 Fruit quality assessment

The 'Forelle' pear samples were harvested in the morning, as described above, and stored overnight in regular atmosphere storage at 10^{0}C at the Wet Laboratory in the Department of Horticultural Science at Stellenbosch University, for the maturity and quality assessment. After the overnight storage, the fruits were removed from storage and allowed to acquire room

temperature for three hours, before the assessment began. The following parameters were measured and observed, as per commercial practice:

- the diameter (mm);
- the height (mm);
- the mass (g);
- the firmness (kg), determined on opposite cheeks, using a penetrometer (Fruit texture Analyser, Guss Instruments, Strand. South Africa) with a 7.9 mm tip;
- the foreground colour (blush) for 'Forelle' pears, using the 'Forelle' Pears Sel set p.16" chart;
- the background colour (also background Colour 2 for the green cheek in the case of 'Packham's Triumph'), using the industry colour chart by Hortgro, Paarl;
- the sunburn severity, using the 'Packham's Triumph' and 'Forelle' sunburn colour chart set P. 13 and P.25;
- the starch conversion, using the iodine test with the starch conversion chart by Hortgro, Paarl;
- the Total Soluble Solids (TSS): for each group of pears, a combined juice sample was prepared by using one slice per fruit (i.e. a disk-shaped slice cut along the fruit diameter), which were blended together in a kitchen blender, and the TSS (%) was measured from a small sub-sample of the juice by using a calibrated electronic refractometer (TSS 0-32%. Model N1, Atago, Tokyo, Japan); and
- Titratable Acidity (TA): after extracting a sub-sample for TSS testing, the remaining juice was tested for the TA content (reported as % malic acid) by using a Metrohm Tritrator, along with the 815 Sample Changer (Titrator Model: 888 Titrando. Software: Tiamo, Herisau. Switzerand).

The fruit were packed by Elgin Orchards (Pty) Ltd., which will provide the pack-out information, as well as the prices obtained for the different quality classes, at a later stage.

7.5 RESULTS AND DISCUSSIONS

7.5.1 Microclimate and tree growth

A summary of the weather data is shown in Figure 7.2 for the period 01 September 2022 to 08 March 2025. Over the three years of monitoring, the maximum daily solar radiation reached 30.1 MJ/m^2/d during the 2024-2025 season. Fewer than five days each year had maximum temperatures exceeding 35°C. Over the two-year period, a maximum of 39.1°C was reached in January 2024. The lowest temperature recorded was around 0°C in July 2023. The vapour pressure deficit of the air was low, due to the high relative humidity associated with the coastal Elgin region. The average daily ETo during the summer months varied between 4.0 and 5.0 mm/d, with a peak of 6.5 mm being reached in January 2024. The orchard received rainfall throughout the year, as shown in Figure 7.2d. The growing season rainfall amounted to 245.2 mm in 2023-2024, with 1 081.6 mm of the annual rainfall, which was higher than that of the Wolseley or Ceres sites. During 2024-2025, the growing season rainfall was 231.6 mm, while the total reference evapotranspiration was 1 169.3 and 1 037.3 mm for the two seasons.

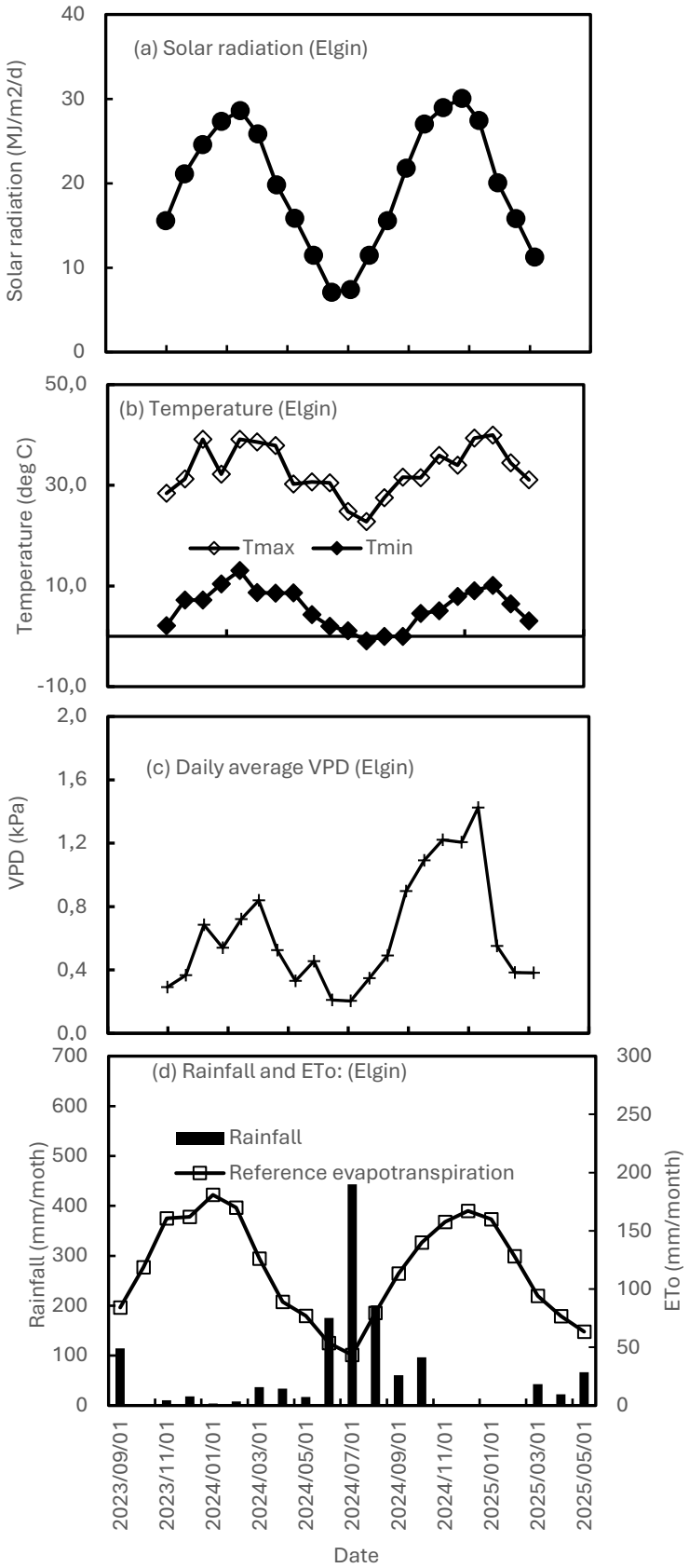


Figure 7.2 Daily changes in orchard microclimatic conditions at Elgin from January 2023 to March 2025 representing (a) the solar radiation, (b) maximum and minimum air temperatures, (c) vapour pressure deficit of the air. (d) reference evapotranspiration and rainfall.

The canopy size of the ‘Forelle’ trees at Elgin was like those in Ceres, with the peak LAI approaching 4.0 during the mid-season stage (Figure 7.3). There was also an asymmetrical growth pattern, which was characterised by a rapid increase in the leaf area early in the season and a gradual decline in autumn into the winter season. The LAI data were derived from the ‘Forelle’ trees only, excluding the pollinator rows.

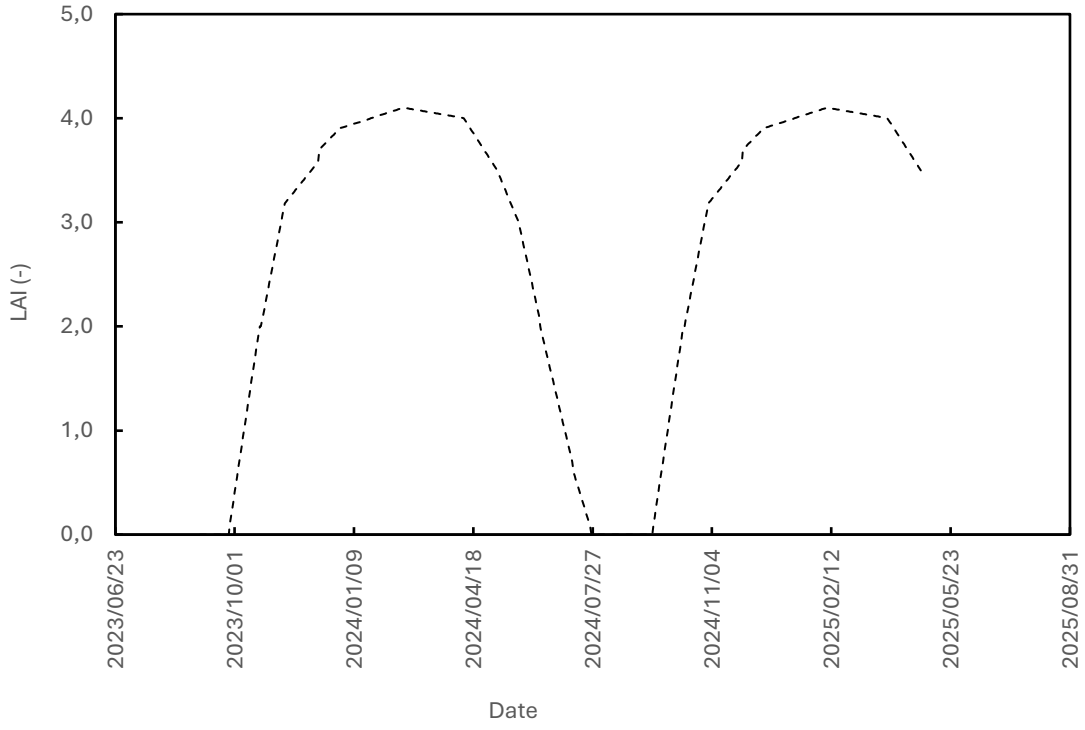


Figure 7.3 Leaf area of ‘Forelle’ trees in Elgin over the 2023-2024 and 2024-2025 seasons

7.5.2 Transpiration dynamics

The transpiration trend of the ‘Forelle’ orchard in Elgin was like that in the other three orchards, being strongly influenced by the atmospheric evaporative demand, which is depicted by the reference evapotranspiration in Figure 7.4. The early season transpiration trend during the 2023-2024 season was not well defined, due to poor data quality as a result of equipment failure. The second season’s data were of a better quality. Daily transpiration peaked at 5.7 mm, which was slightly lower than that recorded for the ‘Forelle’ orchard in Ceres, which was similar in size.

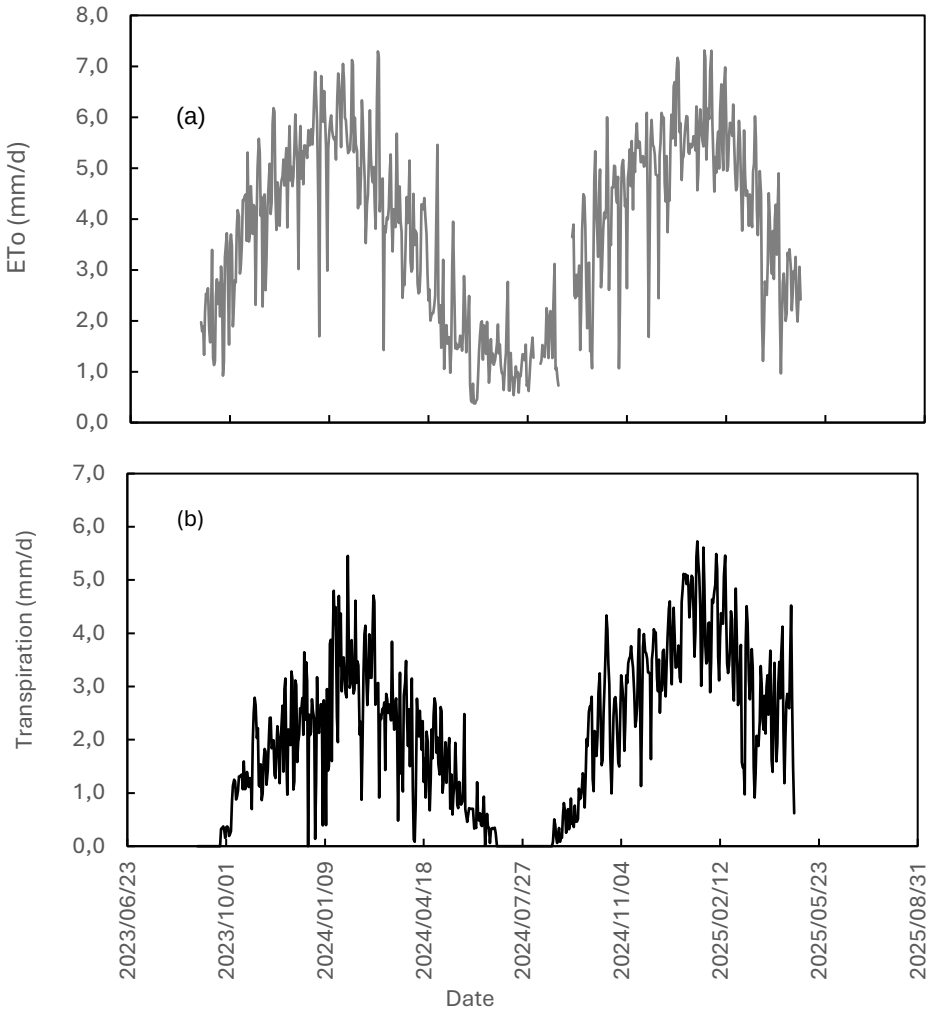


Figure 7.4 Seasonal changes in (a) the reference evapotranspiration and (b) transpiration of the 'Forelle' orchard at Elgin over the 2023-2024 growing season

The seasonal total transpiration for Elgin averaged over two growing seasons, from 2023 to 2025, was 700.6 mm, which was slightly lower than the 750 mm recorded for the 'Forelle' orchard in Ceres. In Elgin, the ET data were collected over 17 days in autumn between 18 March and 23 April 2025 and yielded values in the range 1.1 and 4.9 mm/d. A comparison of the measured and modelled daily transpiration for the 'Forelle' orchard in Elgin is shown in Figure 7.5. The poor model fit for the first year was a result of the poor quality of the measured transpiration data. The two fluxes agreed more strongly in the second season, with the model explaining more than 70% of the measured transpiration. The modelled average seasonal total ET for the 'Forelle' in Elgin was 851 mm (8 510 m^3/ha). The basal crop coefficients varied between 0.79 to 0.90, while the maximum crop coefficients were not significantly different from the other three orchards, namely, 0.83 to 1.08 in Elgin (Figure 7.6).

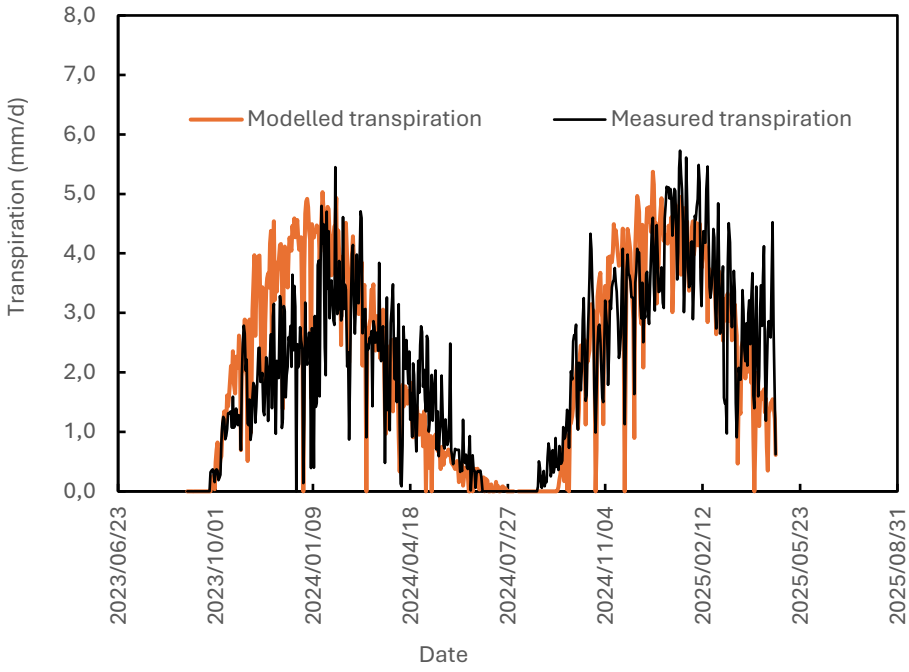


Figure 7.5 Comparison of the measured and modelled transpiration of the 'Forelle' orchard in Elgin for the 2023-2024 and 2024-2025 seasons

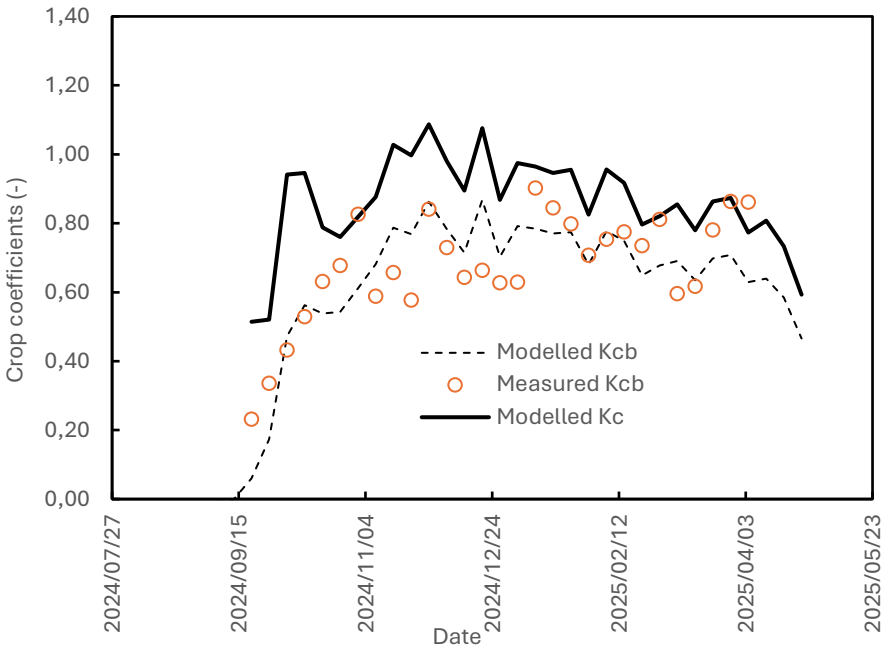


Figure 7.6 Measured and modelled weekly and seasonal single and basal crop coefficients for the 'Forelle' orchard in Elgin

7.5.3 Fruit yield and quality results

This section presents data on the yield quantity (Table 5.2) and quality (Table 5.3) for the two pear cultivars for the 2023-2024 and 2024-2025 growing seasons. The average yield

per tree was very low for both seasons, amounting to 10.49 and 37.92 kg/tree. This translated to about 15.6 t/ha and 56.2 t/ha, respectively.

Table 7.3 Average yield and main stem circumference

Cultivar	Average Yield (kg/tree)	Yield (t/ha)	Average stem circumference (cm)
'Forelle' (2023-24)	10.49	15.55	
'Forelle' (2024-25)	37.92	56.22	54.98

The 2023-2024 season had bigger and heavier fruit than during 2024-2025, due to the lighter crop load in the former.

Table 7.4 Fruit maturity and quality in EGVV

Cultivar	Diameter (mm)	Height (mm)	Mass (g)	Firmness A (kg)	Firmness B (kg)	Blush Colour (Chart [illegible])	Background colour A (Chart)	Background colour B (Chart)	Sunburn (relevant Chart)	Starch conversion (%)	TSS (%)
'Forelle' (2023-24)	67.24	82.30	181.62	6.78	6.67	5.14	2.1		3.65	0.08	14.05
'Forelle' (2024-25)	54.64	81.86	133	6.67	6.5	8.19	1.7		18.77	6.5	-

7.5.4 Water productivity of 'Forelle' pears in Elgin

The T-based WP of the 'Forelle' trial trees in Elgin was 3.27 and 7.96 kg m^{-3} in 2023-2024 and 2024-2025, respectively (Table 7.5). For the whole orchard, the corresponding values were 2.53 and 6.85 kg m^{-3}. The yield of this orchard in 2023-2024 was exceptionally low, resulting in a very low WP. A high proportion of Class 3 fruit (52%) also led to a very low gross orchard value, since Class 3 only fetched a price of 0.42 R kg^{-1}, compared to 14.83 R kg^{-1} for Class 1 (37% pack-out). Consequently, the EWP of this 'Forelle' orchard was very low, at 15.46 R m^{-3}. In 2024-2025, the yield and gross value returned to what would be expected for this orchard, as did the seasonal transpiration. The T-based WP was 7.96 kg m^{-3} and the EWP was 123.2 R m^{-3}. When expressed relative to the seasonal ET (Table 7.6), the WP for the trial trees was 1.87 and 6.39 kg m^{-3}, and for the whole orchard, the values were 1.44 and 5.50 kg m^{-3}, respectively. The EWP values were 8.84 and 98.99 R m^{-3}, respectively.

Table 7.5 Physical Water Productivity, Water Use Efficiency, and Economic Water Productivity based on measured seasonal transpiration for the 'Forelle' pear orchard in Elgin in 2023-2024 and 2024-2025

	2023-2024	2024-2025
Planting density (trees/ha)	1481	1481
Seasonal transpiration (mm)		700.6
Seasonal transpiration per hectare (m^3/ha)	-	7006.4
Trial trees:		
Yield (t/ha)	-	55.74
Water Use Efficiency (m^3/ton)	-	125.7
Physical Water Productivity (kg/m^3)	-	7.96
Whole orchard block:		
Yield (t/ha)	12.0	48.0
Water Use Efficiency (m^3/ton)	-	146.0
Physical Water Productivity (kg/m^3)	-	6.85
Orchard gross income (R/ha)	R73 474	R863 192
Economic Water Productivity (R/m^3)	-	R123.20

Table 7.6 Physical Water Productivity, Water Use Efficiency, and Economic Water Productivity based on measured seasonal evapotranspiration for the 'Forelle' pear orchard in Elgin in 2023-2024 and 2024-2025

	2023-2024	2024-2025
Planting density (trees/ha)	1481	1481
Seasonal evapotranspiration (mm)	831.3	872.0
Seasonal evapotranspiration per hectare (m^3/ha)	8312.7	8719.6
Trial trees:		
Yield (t/ha)	15.54	55.74
Water Use Efficiency (m^3/ton)	535.1	156.4
Physical Water Productivity (kg/m^3)	1.87	6.39
Whole orchard block:		
Yield (t/ha)	12.0	48.0
Water Use Efficiency (m^3/ton)	692.7	181.7
Physical Water Productivity (kg/m^3)	1.44	5.50
Orchard gross income (R/ha)	R73 474	R863 192
Economic Water Productivity (R/m^3)	R8.84	R98.99

7.6 CONCLUSIONS

The data collected in this orchard showed that the seasonal total transpiration for the 'Forelle' trees in Elgin was in the region of 700 mm (7 000 m^3/ha). This was considerably higher than for both the 'Packham's Triumph' orchards, due to the large canopy size of the trees in Elgin. The quality of the sap flow data in the first season was poor, due to technical issues with the equipment. The yield of the orchard was also unrealistically too low, for unclear reasons. Both the yield and transpiration data improved in the second season. The modelled evapotranspiration for the whole season averaged 852 mm, which translated to the crop water requirements of 8 520 m^3/ha per season. This orchard had the least physical water productivity, at 7.90 kg/m^3 for the transpiration-based values and 5.50 kg/m^3 for the ET based values. The economic water productivity was quite high, at R123/m^3 and R99/m^3 for the transpiration and ET based values, respectively, due to the very high gross income from the orchard.

CHAPTER EIGHT

CONCLUSIONS AND RECOMMENDATIONS

8.0 INTRODUCTION

Pears are the second-most widely planted deciduous fruit crop in South Africa, and they contribute about 16% to the gross earnings of the sector (Hortgro, 2024). The fact that more than 90% of the pears produced in the country are grown in the Western Cape, a region that is projected to get warmer and drier in the future, means that they face the considerable risk of climate variability and change projected for the region (Midgley & Lotze, 2011; Jack et al., 2020). This risk is amplified by the fact that all the pears produced in the country are grown under irrigation (Volschenk et al., 2012). However, competition for the scarce water resources is growing, due to the growing population of the Cape Town Metropolitan area, as well as the increasing demand for water by industry, recreation and the high-water consumption by invasive alien plants (Dzikiti et al., 2013; Ntshidi et al., 2015; le Maitre et al., 2016).

In addition, accurate quantitative information on the water use of pear orchards under local conditions has, until now, been lacking. As the saying goes "*You cannot manage what you do not measure*"; this lack of information on the water requirements of pear orchards has led to poor decision-making on water allocation and poor irrigation scheduling, which has caused significant wastage of the limited water resources. Given that the water resources in most pear-growing catchments are almost fully allocated and some farmers grow their crops with very limited water, there is a need to increase their water use efficiency, by producing more fruit per drop of water. The saved water can be used to support more irrigated land, thereby increasing production and the sustainability of the fruit industry.

In this study, detailed water use, growth, climate, soils, yield quality and quantity data were collected from four commercial pear orchards in regions with different microclimatic conditions in the Western Cape province. For clarity of what happens in each orchard, a full description of the study sites, data collection and analytical procedures was presented as individual Chapters in this report. The goal of the present Chapter is to consolidate information from the four orchards and to highlight the key take-home messages from the study. Changes

in the water use of pear orchards under climate change were projected only for the orchard in Wolseley, due to difficulties in acquiring the climate change data in the other production regions. Our assumption is that the conclusions drawn for the Wolseley site will apply to all the other production regions in the Western Cape Province.

8.1 SUMMARY OF THE GROWING CONDITIONS IN THE PRODUCTION REGIONS

The major fruit-producing regions in the Western Cape Province tend to have different microclimatic conditions, due to large variations in their altitude and proximity to the coast. The soil types also vary greatly, from the deep fertile alluvial soils along the river channels, to shallow rocky soils in high-lying areas. These differences in the growing conditions are expected to cause differences in the crop water requirements and crop performance. In this section, we discuss only the differences in the climatic conditions between the sites. As expected, all the climatic variables showed clear seasonal variations that are typical of Mediterranean-type climates. Ceres for example, had the highest daily average solar radiation, peaking at 31.6 MJ/m^2/d in summer in February 2024, with a minimum of 7.5 MJ/m^2/d reached in winter in July 2024. The peak daily average radiation was somewhat lower in Elgin, reaching 28.6 MJ/m^2/d, with a minimum of 7.1 MJ/m^2/d on overcast days. The low radiation levels in Elgin were most likely a result of the high incidence of cloud cover in the coastal region, which is prone to cold fronts and orographic rainfall. The monthly maximum temperature was, however, higher in Elgin, reaching 40.0°C in February 2025, compared to 38.9°C in Ceres, which is likely due to the higher altitude in Ceres. The recorded monthly minimum temperature was lower in Ceres at the – 3.2°C reached in July 2023, while Elgin's minimum temperature over the two seasons was – 0.92°C reached in July 2024. There was no significant difference in the vapour pressure deficit of the air, with peak monthly values hovering around 1.36 and 1.42 kPa for Ceres and Elgin, respectively. During the 2022-2023 growing season, the annual total rainfall in Ceres was 820.5 mm, with less than half the amount (334.5 mm) falling during the growing season (September to April). The 2023-2024 season had a much drier growing season in Ceres, receiving only 225.6 mm, while the annual total rainfall was 830.1 mm. In the 2024-2025 season, Ceres received 244.6 mm during the fruit-growing season. The seasonal (September-April) total reference evapotranspiration was more than five times higher than the rainfall, namely, 1 132.6, 1 200.2 and 1 158.7 mm for the 2022-2023, 2023-2024 and 2024-2025

seasons, respectively. The Elgin area, on the other hand, received similar amounts of growing season rainfall, namely 245.2 mm in 2023-2024, with a much higher annual rainfall of 1 081.6 mm. During 2024-2025, the growing season rainfall was 231.6 mm, while the total reference evapotranspiration was 1 169.3 and 1 037.3 mm for the two seasons. The average total reference evapotranspiration for the growing season was 1163.8 mm for Ceres and 1 103.3 mm for Elgin. Therefore, the Elgin area had a slightly milder atmospheric evaporative demand than Ceres, although the differences were very small. The rainfall during the growing season was similar between these two production regions. We have excluded the climate data from the Wolseley and Vyeboom sites in this analysis, because the data had large gaps, due to equipment failure.

8.2 SUMMARY ON ORCHARD WATER USE

Although cultivar differences in the water-use rates are possible, the daily total transpiration of the pear trees in this study was strongly influenced by the canopy size. The 'Forelle' trees in Ceres and Elgin, which had the largest canopy sizes, had the highest peak transpiration rates of 39.9 and 37.1 L/tree/d. These transpiration rates amounted to 5.9 and 5.5 mm/d. Maximum daily transpiration at Wolseley was 30.6 L/tree/d (5.1 mm/d) and 27.0 L/tree/d (4.5 mm/d) at Vyeboom, with lower peak LAI values. The seasonal total transpiration was 750.3 mm for Ceres, which averaged over two growing seasons from 2022 to 2024, and 700.6 mm for Elgin for the 2024-2025 season. The 'Packham's Triumph' orchards in Wolseley and Vyeboom had the lowest seasonal transpiration of 576.1 and 497.8 mm, respectively, which were the averages for the two growing seasons.

The whole orchard ET, measured with the eddy covariance system, varied between 0.4 and 7.0 mm/d among three of the four orchards (Figure 8.1). The ET data were measured over 41 days for the 'Packham's Triumph' orchard in Wolseley, in winter from 09 to 18 May 2023, and in summer from 19 October to 09 November 2023. In the 'Forelle' orchard in Ceres, the ET data were collected over 40 days, mostly in summer from mid-December 2023 to end of January 2024. This explains the high ET values that had a narrow range between 2.4 and 7.7 mm/d at Ceres. In Elgin, the ET data were collected over 17 days in autumn, between 18 March and 23 April 2025, and the yielding values were in the range 1.1 and 4.9 mm/d.

The dual source ET model was applied to all four pear orchards, and the typical daily transpiration simulations over multiple seasons are presented in Chapters Four, Five, Six and Seven. Because the ET data were limited, due to equipment availability issues, the data for all the sites were pooled in Figure 8.1. The dotted line in Figure 8.1 shows the 1:1 line. Both the orchard transpiration and ET were accurately predicted by the model, and the detailed statistics are shown in Table 8.1.

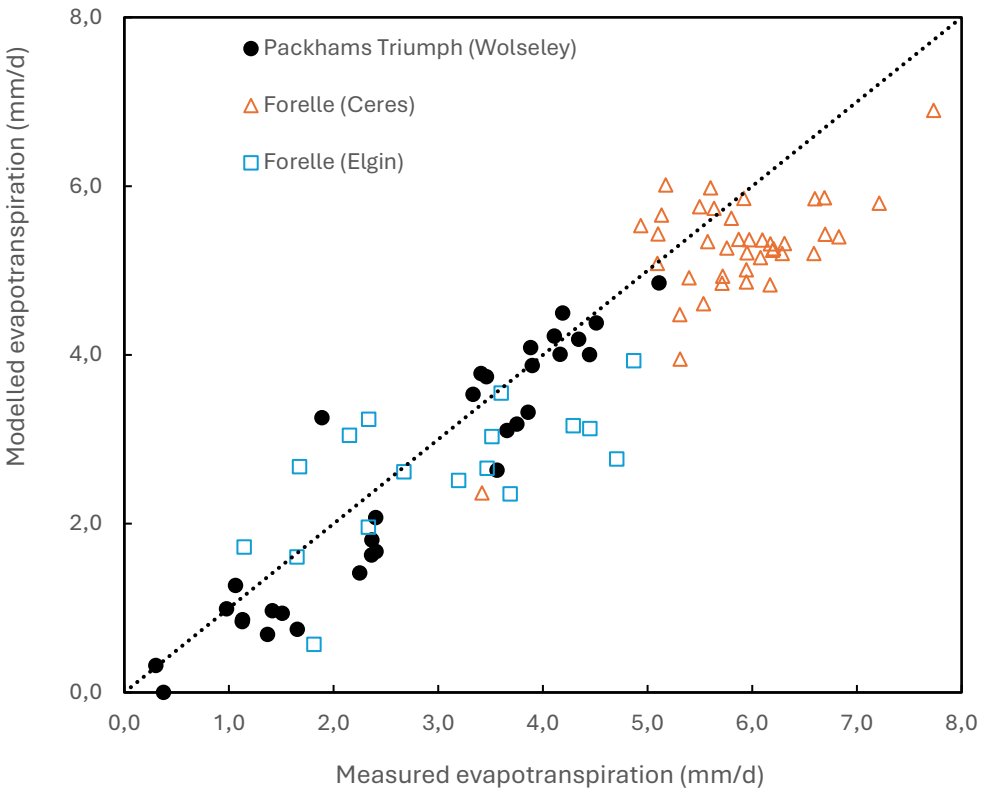


Figure 8.1 Performance of the dual-source ET model in estimating the orchard evapotranspiration across three study sites, namely Ceres, Wolseley and Elgin

Table 8.1 Summary of the statistics comparing the measured and modelled water-use variables for the four pear orchards

Orchard	Cultivar	Variable							
		Transpiration				Evapotranspiration			
		R^2	RMSE	MAE	NSE	R^2	RMSE	MAE	NSE
			(mm/d)	(mm/d)			(mm/d)	(mm/d)	
Ceres	'Forelle'	0.83	0.75	0.59	0.68	0.4	0.87	0.77	0.30
Wolseley	'Packham's Triumph'	0.79	0.88	0.72	0.65	0.91	0.72	0.61	0.85
Elgin	'Forelle'	0.64	0.93	0.75	0.52	0.42	0.95	0.85	0.29
Vyeboom	'Packham's Triumph'	0.47	0.87	0.68	0.30	-	-	-	-

The model explained between 47% and 83% of variations in the transpiration, with the lowest accuracy (R^2 ~ 0.47) being obtained at the Vyeboom orchard, due to the poor data quality because of persistent problems with the sensors. The Nash-Satcliffe Efficiency (NSE) was positive at all sites, ranging from 0.30 to 0.68, which indicates an acceptable model performance (Moriasi et al., 2007). The RMSE varied between ±0.75 mm/d for the Ceres orchard, to ±0.93 mm/d for Elgin. The R^2 for the orchard ET ranged between 0.40 and 0.91, with the highest accuracy obtained for the 'Packham's Triumph' orchard in Wolseley, which had the longest measurement record. The root mean square error was less than 1.0 mm/d, ranging between ±0.72 mm/d for the Wolseley and ±0.95 mm/d for the Elgin site. The NSE ranged between 0.29 and 0.85, with the highest prediction accuracy for the Wolseley orchard.

The modelled average seasonal total ET for 'Packham's Triumph' in Wolseley was 803 mm (8 030 m^3/ha), 916 mm (9 160 m^3/ha) for 'Forelle' in Ceres, 851 mm (8 510 m^3/ha) for 'Forelle' in Elgin, and 741 mm (7 410 m^3/ha) for 'Packham's Triumph' in Vyeboom. Assuming effective seasonal rainfall amounts of 280 mm for Ceres and Wolseley and 238 mm for the Elgin and Vyeboom areas, the irrigation requirements amounted to 6 360 m^3/ha for the 'Forelle' orchard in Ceres, 5 230 m^3/ha for the Packham's, 6 130 m^3/ha for the 'Forelle' in Elgin, and 5 030 m^3/ha for the 'Packham's Triumph' in Vyeboom. The normalisation of these irrigation requirement data to trees with similar canopy sizes may be necessary for a direct comparison

of the effect of the growing region on the water use. This was not done because the selected orchards were mature, full-bearing orchards, the water use of which should be close to the maximum values. However, there does not seem to be a direct correlation between the crop load and orchard water use. For example, the Vyeboom orchard had the highest yield, yet it had the least irrigation requirements. This observation suggests that other factors, especially management factors, played a big role in the high productivity of the orchard in Vyeboom. It is difficult to identify which specific factors, as little else was monitored in the way of management e.g. fertiliser regimes, pesticides etc.

The measured and modelled basal (Kcb) and single crop coefficients (Kc) over a typical growing season were reported for each of the four orchards. Peak Kcb ranged from 0.67 and 0.74 for 'Packham's Triumph' in Wolseley, 0.68 to 0.78 for 'Packham's Triumph' in Vyeboom, 0.68 to 0.84 for 'Forelle' in Ceres, and 0.79 to 0.90 for 'Forelle' in Elgin. The maximum crop coefficients were not significantly different in the four orchards, namely, 0.80 to 0.92 in Wolseley, 0.97 to 1.14 in Vyeboom, 0.90 to 1.09 in Ceres, and 0.83 to 1.08 in Elgin.

The order of magnitude, of the transpiration values recorded in this study were consistent with those measured by Goodwin et al. (2015) in pear orchards in Australia, who recorded peak sap flows of between 20 and 40 L/tree/d. The mid-season crop coefficients (Kc) derived in this study (~ 0.90 -1.09) were closer to the FAO 56 tabulated value for pears averaging ~ 0.95 (Allen et al., 1998) and to those derived in Spain by Girona et al. (2011) (Kc ~ 1.0). However, these were almost double the mid-season Kc for a mature pear orchard (~ 0.50) observed by Conceição et al. (2008) in Portugal for a drip irrigated orchard, with a low average measured ET of only 1.9 mm/d. These results highlight the large variability in water use and crop coefficients for pear orchards growing under different environmental and management conditions.

8.3 WATER PRODUCTIVITY AS INFLUENCED BY CULTIVAR AND GROWING REGION

8.3.1 'Forelle' orchards

Across both 'Forelle' orchards in Ceres and Elgin, the T-based WP was in the range 3.27-13.12 kg m^{-3} (trial trees) and 2.53-10.89 kg m^{-3} (whole orchard). If the 2023-2024 season in Elgin is regarded as an anomaly, the general range (trial and orchard) was 6.79-13.12 kg m^{-3}.

By comparison, the T-based WP of full-bearing apple orchards in the Western Cape was estimated at 17.7-23.1 kg m^{-3} for 'Rosy Glow' in the KBV (Midgley et al., 2024), and 10.8-21.5 kg m^{-3} for 'Golden Delicious' and 'Cripps' Pink' in the KBV and EGVV (Dzikiti et al., 2018). The generally-higher WP of apples, compared to 'Forelle' pears, is due to their higher yields, which can exceed 100 t ha^{-1}.

The mean T-based WP in Ceres was 10.15 kg m^{-3}, compared to 7.96 kg m^{-3} in Elgin (excl. 2023-2024). The difference is due to the higher mean yield in Ceres (61.4 t ha^{-1}), compared to Elgin (48.0 t ha^{-1}), whereas the mean seasonal transpiration was similar at ca. 700 mm. The ET-based WP for 'Forelle' trial trees was, on average, 7.69 kg m^{-3} in Ceres and 6.39 kg m^{-3} in Elgin, and 6.82 kg m^{-3} and 5.50 kg m^{-3}, respectively, for each orchard. The seasonal ET in the two regions was similar, at 899 mm (Ceres) and 872 mm (Elgin), so that the difference in the ET-based WP was due to the higher yield in Ceres.

The T-based EWP (excl. 2023-2024 Elgin) was in the range 79.23-135.52 R m^{-3}, with a mean value in Ceres of 110.01 R m^{-3}, and 123.20 R m^{-3} in Elgin. When expressed in terms of ET, the respective values were 83.45 R m^{-3} and 98.99 R m^{-3}. The values were slightly higher in Elgin, primarily due to the higher gross income (863,192 R ha^{-1}), compared to a mean gross income of 751,060 R ha^{-1} in Ceres. The T-based EWP values for apples in the Western Cape have been quantified as 80.1-86.6 R m^{-3} for 'Rosy Glow' (Midgley et al., 2024), 73.4-93.7 R m^{-3} for 'Cripps Pink' (Dzikiti et al., 2018), 69.2 R m^{-3} for 'Golden Delicious Reinders' (Midgley et al., 2024), and 46.6-49.4 R m^{-3} for 'Golden Delicious' (Dzikiti et al., 2018). Thus, 'Forelle', one of the most lucrative pear cultivars produced in South Africa, has an EWP higher than 'Golden Delicious', and one that is similar to, or higher than, the high-value 'Cripps Pink' and 'Rosy Glow'.

8.3.2 'Packham's Triumph' orchards

In the 'Packham's Triumph' orchards in Wolseley and Vyeboom, the T-based WP was in the range 10.11-19.92 kg m^{-3} (trial trees) and 9.88-17.68 kg m^{-3} (whole orchard). The T-based WP in Wolseley was 10.11 kg m^{-3}, compared to a mean value of 17.46 kg m^{-3} in Vyeboom. The mean seasonal transpiration in Vyeboom was 498 mm, which was 13.6% lower than the 576 mm measured for this cultivar in Wolseley. In addition, the yield was significantly higher in Vyeboom (84.0 t ha^{-1}), compared to Wolseley (57.1 t ha^{-1}). Together, this indicates a significantly higher T-based WP in Vyeboom, compared to Wolseley.

The ET-based WP for 'Packham's Triumph' was in the range of 6.95-7.59 kg m^{-3} (Wolseley) and 10.79-12.44 kg m^{-3} (Vyeboom). This was based on a seasonal ET of 787 mm and 745 mm, respectively, as well as a higher yield in Vyeboom, as described in the previous paragraph. When comparing these results to 'Forelle' pears, 'Packham's Triumph' generally has a higher T- and ET-based WP in the Western Cape, due to a higher yield (Vyeboom) and lower seasonal transpiration (Wolseley and Vyeboom). The estimated WP value for 'Packham's Triumph' in Vyeboom was higher than that for 'Golden Delicious' (10.8 kg m^{-3}) and 'Cripps' Pink' (14.2 kg m^{-3}) apples in the KBV (Dzikiti et al., 2018), but closer to values (17.7-23.1 kg m^{-3}) for 'Rosy Glow' in the KBV, which had a high yield, but also a higher seasonal transpiration (Midgley et al., 2024). The WP for apples in EGVV (18.0-21.5 kg m^{-3}) (Dzikiti et al., 2018) was marginally higher than for 'Packham's Triumph' in Vyeboom.

The T-based EWP of 'Packham's Triumph' pears in Wolseley was 45.27 R m^{-3}, on average, and the corresponding ET-based EWP was, on average, 33.15 R m^{-3}. In Vyeboom, the T-based EWP was estimated at 87.05 R m^{-3}, on average (but with a much higher value in 2024-2025, compared to 2023-2024) and an average ET-based EWP at 57.64 R m^{-3}. These values are generally lower than the EWP of 'Forelle', owing to the higher price fetched by 'Forelle'. However, 2024-2025 was an exceptional season for 'Packham's Triumph' in Vyeboom, where a high yield and orchard gross income were achieved, which led to an EWP value higher than that measured for high value 'Rosy Glow' (80.1-86.6 R m^{-3}) and 'Cripps Pink' (73.4-92.7 R m^{-3}) apples (Dzikiti et al., 2018; Midgley et al., 2024).

8.4 CHALLENGES WITH THE STUDY AND RECOMMENDATIONS FOR FUTURE WORK

A few challenges were experienced in the execution of this study. The first challenge was related to the identification of suitable study sites. The micro-meteorological equipment used in this study requires large homogenous orchards, in order to ensure an adequate fetch around the flux tower. It was difficult to find such orchards, given that pear orchards tend to be smaller in size. The 'Forelle' orchard in Ceres (6.5 ha) was an exception, but the sloping terrain posed a challenge. Numerous amounts of equipment were deployed in the various orchards. Equipment failure, as well as the running down of batteries, led to gaps in the data for some orchards, as detailed in the earlier chapters. There was only one eddy covariance system, which had to be rotated among the study sites. This led to large data gaps, which were filled in

by modelling. We are fortunate to have received a donation of two more eddy covariance systems from the Western Cape Department of Agriculture. However, we could not deploy these systems in this study, due to the lack of the flux towers on which to mount the sensors. Two fluxes were bought and delivered in January 2026. Therefore, future studies will benefit from this equipment. Lastly, we had an incident of theft and vandalism to our equipment at the Vyeboom study site. Fortunately, this happened during the winter season when active monitoring was not happening. Nevertheless, it was a drawback, as some of the cables and sensors had to be replaced.

Several recommendations are made, to improve our understanding of how pear orchard water use is affected by the cultivar, the production region and the crop load. These include the need to understand the following:

1) the orchard water use and productivity under drip irrigation;
2) the cultivar differences in water use and productivity;
3) how the crop load directly influences the tree water status and water use;
4) the contribution of orchard floor evapotranspiration, due to cover crops to orchard ET;
5) the performance of pear orchards under nets; and
6) the effects of different rootstocks on the water use and the resilience to water stress of pear trees

REFERENCES

ALLEN RG, PEREIRA LS, RAES D and SMITH M (1998) Crop evapotranspiration. FAO Irrigation and Drainage Paper 56. Food and Agriculture Organisation (FAO), Rome, Italy.

ALLEN RG, PEREIRA LS, HOWELL TA and JENSEN ME (2011) Evapotranspiration information reporting: I. Factors governing measurement accuracy. *Agric Water Manag* **98** 899-920.

ANNANDALE JG, STIRZAKER RJ, SINGELS A, VAN DER LAAN M and LAKER MC (2011) Irrigation scheduling research: South African experiences and future prospects. *Water SA* **37** 751-763.

BAKER JM and VAN BAVEL CHM (1987) Measurement of mass flow of water in stems of herbaceous plants. *Plant Cell and Environ* **10** 777-782.

BASTIAANSSEN WGM, MENENTI M, FEDDES RA, and HOLTSLAG AAM (1998) A remote sensing surface energy balance algorithm for land (SEBAL). 1: Formulation. *J Hydrol* **212** 198-212.

BOLAND A, ZIEHRI A and BEAUMONT J (2002) Guide to best practice in water management: orchard crops, Murray Darling Basin Commission, State of Victoria, Department of Natural Resources and Environment, Melbourne.

BURGESS SSO, ADAMS MA, TURNER NC, BEVERLY CR, ONG CK, KHAN AAH and BLEBY TM (2001) An improved heat pulse method to measure low and reverse rates of sap flow in woody plants. *Tree Physiol* **21** 589-598.

CHALMERS DJ, MITCHELL PD and VANHEK L (1981) Control of peach tree growth and productivity by regulated water supply, tree density and summer pruning. *J Amer Soc Hort Sci* **106** 307-312.

COOK NC and STRYDOM DK (2000) The South African high-density system. *Acta Hort* **513** 321-327.

COSTA G, BELTRAME E, ECCHER P and PIANEZZOLA A (1997) High density planted pear orchards: effects on yield, performance and fruit quality. *Acta Hort* **451** 505-512.

DRAGONI D, LAKSO AN and PICCIONI RM (2005) Transpiration of pear trees in a humid climate using heat pulse sap flow gauges calibrated with whole-canopy gas exchange chambers. *Agric for Meteorol* **130** 85-94.

DYNAMAX INC (1997) A Thermal Dissipation Sap Velocity Probe for Measurement of Sap Flow in Plants. http://www.dynamax.com/TDP.htm

DZIKITI S, STEPPE K, LEMEUR R and MILFORD JR (2007) Whole -tree level water balance and its implications on stomatal oscillations in orange trees (Citrus sinensis (L.) Osbeck) under natural climatic conditions. *J Exp Bot* **58** 1893-1901.

DZIKITI S, VERREYNNE JS, STUCKENS J, STREVER A, VERSTRAETEN WW, SWENNEN R and COPPIN P (2010) Determining the water status of Satsuma mandarin trees [Citrus Unshiu Marcovitch] using spectral indices and by combining hyperspectral and physiological data. *Agric For Meteorol* **150** 369-379.

EVANS RG and SADLER EJ (2008) Methods and technologies to improve efficiency of water use. *Wat Res Res* **44** 1-15.

FLORE JA and LAKSO AN (1989) Environmental and physiological regulation of photosynthesis in fruit crops. *Hort Rev* **11** 111-158.

FOUCHÉ JR, ROBERTS SC, MIDGLEY SJE and STEYN WJ (2010). Peel color and blemishes in 'Granny Smith' pears in relation to canopy light environment. Acta Hort. **45** 899-905.

GIBSON LA, JARMAIN C, SU Z and ECKARDT FE (2013) Estimating evapotranspiration using remote sensing and the Surface Energy Balance System - a South African perspective. *Water SA* **39** (4) 477-483.

GIRONA J, DEL CAMPO J, MATA M, LOPEZ G and MARSAL J (2011). A comparative study of apple and pear tree water consumption measured with two weighing lysimeters. *Irrig. Sci* **29** 55-63.

GRANIER A (1985) Une nouvelle methode pour la mesure du flux de seve brute dans le tronc des arbres. *Annales des Sciences Forestieres* **42** 193-200.

GRANIER A (1987) Evaluation of transpiration in a Douglas-fir stand by means of sap flow measurements. *Tree Physiol* **3** 309-319.

GREEN SR and CLOTHIER BE (1999) The root zone dynamics of water uptake by a mature pear tree. *Plant and Soil* **206** 61-77.

GREEN S, MCNAUGHTON K, WUNSCHE JN and CLOTHIER BE (2003) Modelling Light Interception and Transpiration of Pear Tree Canopies. *Agron J* **95** 1380-1387.

GUSH MB, DYE PJ, CLULOW AD, TAYLOR NJ, EVERSON CS, DZIKITI S and NAIKEN V (in press) Application of a Heat Pulse Velocity sap flow monitoring system (heat ratio method) for

measuring transpiration rates in woody plant species. In: TAYLOR NJ and GUSH MB (Eds). (in press). The water use of selected fruit tree orchards: Volume 1. Water Research Commission, Pretoria, RSA, WRC Report 1770/1/14, Appendix A.

GUTIÉRREZ MV and SANTIAGO LS (2006) A Comparison of Sap Flow Measurements and Photometry in Two Tropical Lowland Tree Species with Contrasting Wood Properties. *Int J Trop Biol* **54** (1) 73-81.

HANSEN P (1971) The effect of fruiting upon transpiration rate and stomatal opening in pear leaves. *Physiol Plant* **25** 181-183.

IRVING DE and DROST JH (1987) Effects of water deficit on vegetative growth, fruit growth and fruit quality in Cox's Orange Pippin apple. *J Hort Sci* **62** (4) 427-432.

JARMAIN C and KLAASSE A (2012) Fruitlook: An operational service to improved crop water and nitrogen management in grapes and other deciduous fruit trees using satellite technology for the season of 2011-12. Progress Report, Western Cape Provincial Department of Agriculture.

JARMAIN C, EVERSON CS, SAVAGE MJ, MENGISTU MG, CLULOW AD and GUSH MB (2008) Refining tools for evaporation monitoring in support of water resources management. *WRC Report No.* 1567/1/08, Water Research Commission, Pretoria.

JONES HG (1992) Plants and microclimate: a quantitative approach to environmental plant physiology. 2nd Ed. Cambridge University Press.

LAKATOS T (2003) Crop load as a modifying factor in crop evapotranspiration model for irrigation scheduling. *Acta Hort* **618** 379-382.

LÖTZE E and BERGH O (2008) Are chilling unit calculations still relevant for the SA fruit industry? Fruitgro science. http://www.hortgro.co.za/production-techical-information/research-development/climate-information/

LÖTTER J DeV, BEUKES DJ and WEBER HW (1985) Growth and quality of pears as affected by different irrigation treatments. *J Hort Sci* **60** 181-192.

MARSAL J, LOPEZ G, GIRONA J, BASILE B and DE JONG TM (2005) Heterogeneity in fruit distribution and stem water potential variations in peach trees under different irrigation conditions. *J Hort Sci Biotech* **80** 82-86.

MARSHALL DC (1958) Measurement of sap flow in conifers by heat transport. *Plant Physiol* **33** 385-396.

MIDGLEY SJE and LÖTZE E (2011) Climate change in the Western Cape of South Africa: trends, projections and implications for chill unit accumulation. *Acta Hort* **903** 1127-1133.

MIDGLEY G, CHAPMAN R, MUKHEIBIR P, TADROSS M, HEWITSON, WAND S, SCHULZE R, LUMSDEN T, HORAN M, WARBURTON M, KGOPE B, MANTLANA B, KNOWLES A, ABAYOMI A, ZIERVOGEL G, CULLIS R and THERON A (2007) An input into the long-term mittigation scenarios process: Impacts, vulnerability and adaptation in key South African sectors. Department of Environment Affairs and Tourism, South Africa.

MIRÁS-AVALOS JM and ARAUJO ES 2025 Relationships Between Midday Stem Water Potential and Soil Water Content in Grapevines and Peach and Pear Trees. *Agronomy* **15** 1257. https://doi.org/10.3390/agronomy15051257.

MONTEITH JL and UNSWORTH M (1990) Principles of environmental physics. 2nd edition. Antony Rowe Ltd, Eastbourne.

RANA G and KATERJI N (2000) Measurement and estimation of actual evapotranspiration in the field under Mediterranean climate: a review. *European Journal of Agronomy* **13** 125-153.

RENAULT D and WALLENDER WW (2000) Nutritional water productivity and diets. *Agric Wat Man* **45** 275-296.

RÜGER S, EHRENBERGER W, AREND M, GEßNER P, ZIMMERMANN G, ZIMMERMANN D, BENTRUP FW, NADLER A, RAVE E, SUKHORUKOV VL and ZIMMERMANN U (2010) Comparative monitoring of temporal and spatial changes in tree water status using the non-invasive leaf patch clamp pressure probe and the pressure bomb. *Agric Wat Man* **98** 283-290.

SAKURATANI T (1981) A heat balance method for measuring water flux in the stem of intact plants. *J Agric Meteorol* **37** 9-17.

SAVAGE MJ, GRAHAM AND and LIGHTBODY KE (2000) An investigation of stem steady state heat energy balance technique in determining water use by trees. WRC Report No 348/1/00.

SCHOLANDER PF, HAMMEL HJ, BRADSTREET A and HEMMINGSEN EA (1965) Sap pressure in vascular plants. *Science* **148** 339-346.

SMITH DM and ALLAN SJ (1996) Measurement of sap flow in plant stems. *J Exp Bot* **47** 1833-1844.

STEPPE K, DE PAUW DJW, DOODY TM and TESKEY RO (2010) A comparison of sap flux density using thermal dissipation, heat pulse velocity and heat field deformation methods. *Agric For Meteorol* **150** 1046-1056.

SWANSON RH (1994) Significant historical developments in thermal methods for measuring sap flow in trees. *Agric For Meteorol* **72** 113-132.

TAYLOR NJ and GUSH MB (in press) The water use of selected fruit tree orchards (Volume 1): Review of available knowledge. Water Research Commission, Pretoria, RSA, WRC Report 1770/1/14.

VOLSCHENK T, DE VILLIERS JF and BEUKES O (2003) The selection and calibration of a model for irrigation scheduling of deciduous fruit orchards. WRC Report 892.

VIRLET N, MARTINEZ S, LEBOURGEOIS V, LABBE S and REGNARD JL (2012) Contribution of airborne remote sensing to high-throughput phenotyping of a hybrid pear population in response to soil water constraints. *Options Méditerranéennes* **67** 185-191.

YAHYAI RA (2012) Managing irrigation of fruit trees using plant water status. *Agric Sciences* **3** 35-43.

APPENDIX A

CAPACITY BUILDING, CONFERENCE PRESENTATIONS &

PEER- REVIEWED PUBLICATIONS

A1. CAPACITY BUILDING

The following three students have been involved in this study for degree purposes:

1) Mr Anele Sidzumo

Anele registered for a PhD in Agriculture (Horticulture) in the Department of Horticultural Sciences at Stellenbosch University in January 2024. He is currently in the third year of his studies on a project entitled:

Water-use efficiency and postharvest performance of high production pear orchards

Anele expects to hand in his thesis by end of 2026 for graduation in March 2027.

2) Mr Johan Pienaar

Johan registered for his MSc in Agriculture (Horticulture) in the Department of Horticultural Science at Stellenbosch University in January 2023. The title of his thesis is:

Quantifying water use and fruit vascular flows in two pear cultivars grown in the South Africa

Johan graduated in March 2026.

3) Mr Kondwani Ngulube, MSc

Kondwani registered for his MSc in Agriculture (Horticulture) in the Department of Horticultural Sciences at Stellenbosch in January 2025. The title of his thesis is:

Water productivity and water use partitioning in high performing pear orchards in South Africa

Kondwani expects to submit his thesis by end of 2026 for graduation in March 2027.

A2. PEER REVIEWED PUBLICATIONS

The following articles have been published, or are under peer review in journals:

1) Dzikiti S, JC Pienaar, P Dangare, S Whitehead, M Gray, E Crouch, SJE Midgley and WJ Steyn. 2024 Fruit growth and water use of two pear cultivars grown in South Africa: Implications for precision irrigation scheduling. *Water SA* **50** (4) 357-364
2) Giuliani N, Pienaar JC, Sidzumo A, Dzikiti S, Tagliavini M and Midgley SJE. Continuous measurement of fruit size allows the detection of transient water deficit stress in pear. Under review - Scientiae Horticulturae Journal.
3) Dzikiti S, Pienaar JC, Sidzumo A, Ngulube JK, Dangare P, Crouch E, Ntshidi Z, Visser JM, Midgley SJE and Steyn WJ. Assessing water use and yield dynamics of high performing ‘‘Forelle’’ and ‘‘Packham’s Triumph’’ pear orchards under changing climatic conditions in the Western Cape Province, South Africa. Under review - Agricultural Water Management Journal.
4) Ngulube KJ, Crouch E and Dzikiti S. Leaf gas exchange, water use and growth of cover crop species commonly planted in South African pear orchards. (Under preparation for submission to the South African Journal of Botany).
5) Sidzumo A, Crouch E and Dzikiti S. Performance of Forelle pear trees to deficit irrigation applied late afternoon under South African conditions. (Under preparation to be submitted to the Horticulture Journal).

A3. CONFERENCES, WORKSHOPS AND SYMPOSIA

Project team members made the following oral presentations:

1. Sidzumo et al. (2025). Water use efficiency trends and the effect of preharvest water stress on postharvest fruit quality. Hortgro Symposium 2025 (Oral presentation)
2. Sidzumo (2025). Performance of Forelle orchards to irrigation applied at different times of day Fieldsman (Irrigation workgroup) (Oral presentation)
3. Dzikiti et al. (2025). Growth trends of fruit from two pear cultivars grown in South Africa: Implications for precision irrigation scheduling. Fruit tree Crop Responses

to Water deficit and decision support Systems applications (FRUITCREWS) workshop, Naoussa Greece (May 2025).

4. Sidzumo et al. (2026). Effect of soil water deficit on postharvest quality and storability of Forelle pears. Combined Congress (January 2026).

APPENDIX B

DOES DEFICIT IRRIGATION APPLIED LATE AFTERNOON IMPROVE THE PERFORMANCE OF PEAR TREES?

PhD – Mr Anele Sidzumo

B0. INTRODUCTION

Several studies on the deficit irrigation of pear trees have yielded conflicting findings. For example, Volschenk et al. (2012) working on 'Forelle' pears in South Africa showed that deficit irrigation applied at various stages of fruit growth caused yield reduction. On the other hand, Blanco et al. (2025). working on d' Anjou and Bartlett pear cultivars in Washington State in the USA, showed that deficit irrigation reduced vegetative growth. However, it had no significant effect on the yield. The water productivity of the orchards increased by 53%, on average, which highlights the potential significant benefits of the deficit irrigation strategy. Although deficit irrigation has not yielded satisfactory results under local conditions, it could be necessary to utilise this practice in pear orchards in the future, given the increasing water shortages in key production regions, due to climate change-induced droughts and the increasing competition for water.

Research on how deficit irrigation can best be implemented in pear orchards under South African conditions has merit. It is probable that the hot and dry weather conditions during the growing season in the Western Cape could be a prime reason for the unsuccessful implementation of deficit irrigation. This study therefore investigated the possibility of improving the tree performance under deficit irrigation by manipulating the time of day when the irrigation is applied. The idea behind the project was borne out of discussions with visiting Italian and USA horticulturists (Prof Luca Corelli Grappadelli and Prof Steffano Mussachi pers. comm.). The strategy has been implemented by Scalisi et al. (2021) and produced the improved yields of nectarines in Australia.

The physiological basis for the possible benefit of late-afternoon irrigation is illustrated in Figure B1, which shows the water uptake and loss dynamics of a tree on a typical clear day.

Stomata open at sunrise, as soon as light hits the leaves. It is known that blue light, in combination with the utilisation of the internally-stored CO_2, are responsible for the opening of stomata. Transpiration (green line) commences immediately. However, the uptake of water by the roots (blue line) commences much later, due to the hydraulic resistance and capacitance of the trees. For the 'Forelle' trees at Buchuland, we determined that the time lag between the commencement of water loss via transpiration and stem sap flow was between 1.0 and 1.5 hours. We can assume that this is also the time lag between tree transpiration and root water uptake. During the early hours of the day, when transpiration exceeds the root water uptake, the tree uses its internally-stored water (see blue shade in Figure B1), and this leads to the shrinkage of the fruit and stems (Steppe et al., 2006; Dzikiti et al., 2010), as shown in Appendix C.

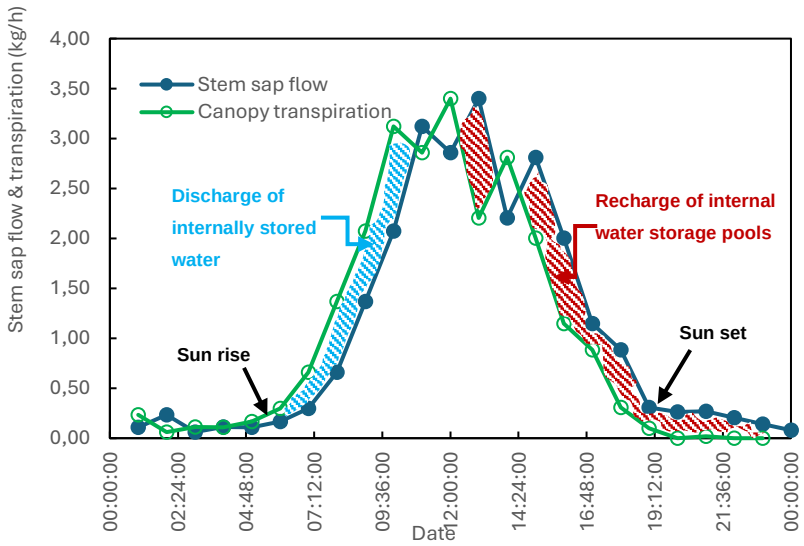


Figure B1. Illustration of the tree water uptake (stem flow – dotted line) and loss (transpiration or gas exchange in circles) over the course of typical day

The implication of this is that irrigation that is applied too early in the day risks being lost via soil evaporation, as the tree water uptake only starts later. However, the amount of soil evaporation will depend on the atmospheric evaporative demand, among other factors. As transpiration continues, the tension in the transpiration stream grows, until the roots begin taking up water. From late afternoon onwards, the atmospheric evaporative demand and light intensity decrease. Transpiration decreases as well, while the root water uptake continues, driven by the strong soil–tree water potential gradient that is created during the day. This leads

to the root water uptake exceeding the tree water loss, which leads to the recharge of the internally-stored water (see the brown shade in Figure B1). The water recharge continues through much of the night, as illustrated in Figure B1.

The benefit of late afternoon irrigation, if it exists, might arise from the fact that the late water application leads to more water recharging the plant organs, rather than being lost as transpiration (which happens early in the day). The recharge of the internal water storage pools leads to an increased turgor pressure in the fruit cells, and this is necessary for cell expansion and growth. A typical example of how the extent of the recharge of internally-stored water pools is used in practical irrigation is through the utilisation of the pre-dawn leaf water potential. If plants are not well-watered, then the recharge of the internal storage pools will be incomplete, which leads to low pre-dawn water potential values. The assumptions that were adopted in this trial, relating to late afternoon irrigation, were as follows:

1) The trees were under drip irrigation, which required daily irrigation during the peak summer season. The proposed approach is not suitable for micro-irrigated orchards, where the irrigation frequency is low;
2) Irrigating in the late afternoon always ensured that the trees had sufficient water to recharge the internally-stored water, even if deficit irrigation was practiced;
3) The sufficient recharge of the internal pools the previous night would ensure that the trees have a sufficient buffer to meet the early morning water requirements, which causes the stomata to open for longer. This is important, given that the stomatal conductance and photosynthesis of pears reach a peak early in the morning, as shown in Chapters Four and Five.
4) Late afternoon deficit-irrigated trees may experience water stress sooner during the daytime, when they exhaust the amount of water available to them. However, this should be beneficial to the trees, as it will only help to create a stronger soil-tree water potential gradient in the late afternoon. There is a high probability of the stomata closing around midday, but this will depend on the severity of the water stress. Mild stress may not severely reduce photosynthesis, given the weak CO_2 gradient across the stomatal pore, compared to the water potential gradient that drives transpiration. In any case, the stress around midday may be beneficial in driving the accumulation of sugars in the fruit.

To test these assumptions, the experiment described in the next section was set up. Detailed eco-physiological yield quality and quantity measurements were collected. We will provide highlights of the key findings in this section.

B1 MATERIALS AND METHODS

B1.1 STUDY SITE AND TREATMENT DESCRIPTION:

This study was carried out during the 2023/24, 2024/25 and 2025/26 growing seasons in the 'Forelle' orchard in Ceres, which is described in Chapter Four. Six irrigation treatments were imposed, as shown in Figure B2. The Micro-sprinkler Control (MC) supplied 32 L h^{-1} per sprinkler every second day, depending on the soil moisture and according to the farmer's standard practice. The Micro-sprinkler Deficit (MD) followed the same schedule, but applied 26 L h^{-1} per sprinkler, which is equivalent to 74% of MC. Under drip irrigation, the Drip Control (DC) applied water daily in the morning at around 0900 by using two lines per row, with emitters spaced at 0.5 m, each delivering 1.6 L h^{-1}. The Drip Deficit (DD) was irrigated at the same time, but with emitter spacing widened to 0.75 m, which reduced the application to 67% of DC. The Drip Control Time-of-Day (DCT) applied the same volume and spacing as the DC, but in the late afternoon (~ 1600). The Drip Deficit Time-of-Day (DDT) followed the same schedule as the DCT through a 0.75 m emitter spacing, but at 67% of the application rate. The trial was laid out as a randomised complete block design to account for the spatial variability in the soil properties, the slope and the microclimate across the orchard. The MC and MD treatments were each allocated to three rows, with only the central row being used for measurements and the outer two serving as buffers. The drip irrigation treatments were assigned to adjacent rows, in order to mimic realistic orchard conditions, while minimising the cross-interference from micro-sprinkler drift and associated microclimate effects.

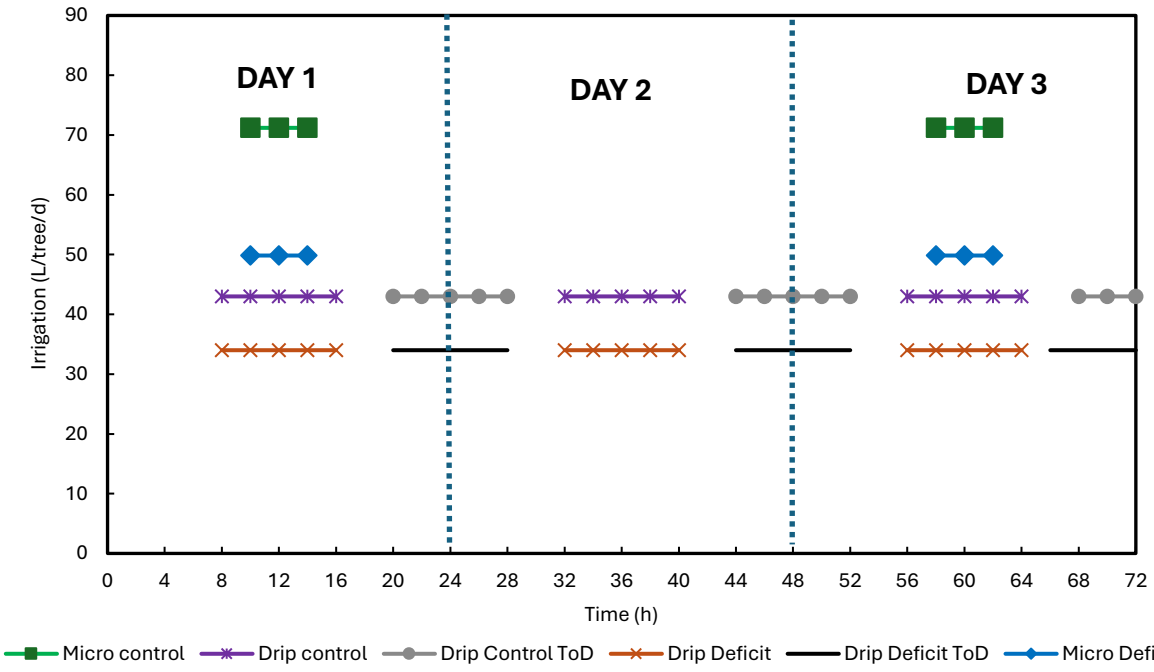


Figure B2. Three days schematic representation of irrigation treatments applied to 'Forelle' pear orchards, detailing micro-sprinkler (MC, MD) and drip (DC, DD, DCT, DDT) system configurations, application volumes and timings

All trees followed the same regular recommended horticultural care practices for the 'Forelle' pear cultivar, which included thinning, pruning and the control of pests and diseases.

B1.2 DATA COLLECTION

The microclimatic conditions were monitored, as described in Chapter Four. The root zone soil water content under the different treatments was monitored by using time-domain reflectometer probes (Model CS616, Campbell Scientific, USA) installed at depths of 0.20, 0.60 and 0.90 m, and covering the effective root zone, which extended to about 0.80 m. Irrigation application was measured by using electronic water flow meters that were installed in one row of each treatment.

Several campaigns were undertaken throughout the growing season to quantify the changes in the tree water status. These included: 1) the pre-dawn leaf water potential; 2) the midday stem water potential; and 3) the stomatal conductance and fluorescence variables. Additional measurements included the whole tree sap flow on at least two trees per treatment, as well as the continuous fruit growth, by using electronic dendrometers on two fruit per treatment. These data were complimented with manual fruit growth measurements on 20 fruit

per treatment. To assess the fruit number and yield under the six irrigation treatments, eight study trees per treatment row per block were strip-harvested at the end of the season. The number of fruits and total fruit mass per tree were recorded, and the trunk circumference was measured, using a soft measuring tape. The average fresh mass per fruit was determined by using a precision mass balance (Model SNUG III, Jadever, Taiwan) to the nearest 0.1 g. The total fruit yield per tree was then estimated as the product of the average fruit mass and the total number of fruits.

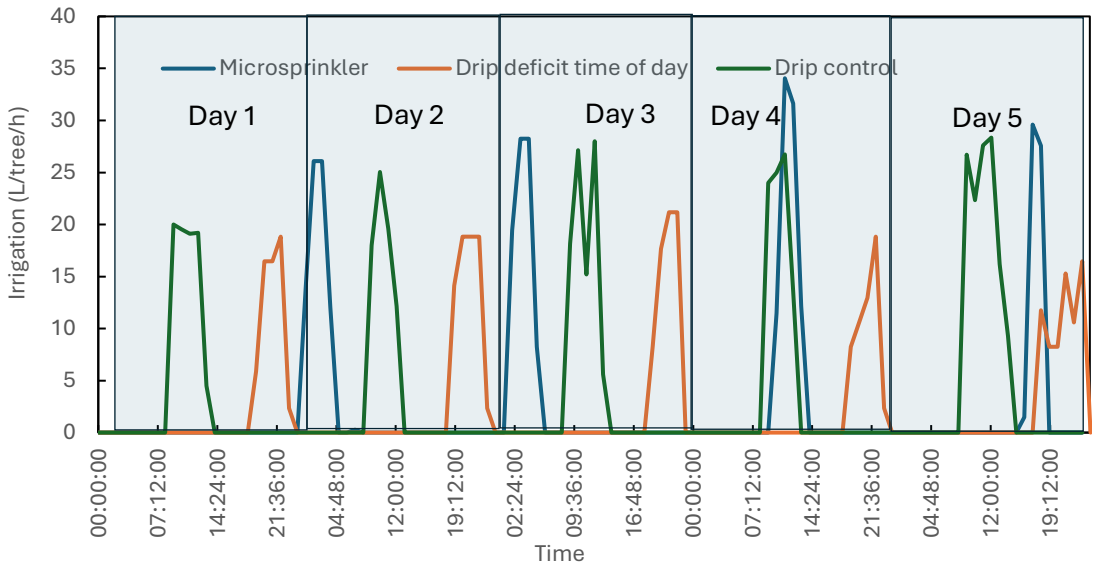


Figure B3. Illustration of the irrigation applied to the various treatments over a five-day period during the peak irrigation period from 15 to 19 December 2025

B2. SUMMARY OF KEY FINDINGS

The typical irrigation levels in the various treatments, over the course of the 2025-2026 growing season, are shown in Figure B4. These data are for the period 01 October 2025 to 02 February 2026. As expected, the micro sprinkler control (MC – current farmer's practice) used the most water, approximately 7460 m^3/ha. Next, was the Drip Control (DC) treatment that used 6 530 m^3/ha. The Micro-sprinkler Deficit (MD), Drip Deficit (DD), and Drip Deficit Late (DDT) irrigation all used less irrigation than the controls. The impact on the average soil water content in the rootzone is shown in Figure B5. The MC treatment received high irrigation levels early in the season, which maintained the high soil water content, compared to the drip treatments. Irrigation in all the treatments was reduced from around 20 December 2025 to about 12 January 2026, which is likely a reflection of the limited water availability at the farm.

Irrigation was ramped up again from mid-January onwards, for the micro-control. Higher irrigation levels were required for the drip treatments to maintain high soil water levels, in order to avoid the decline that is apparent in Figure B5.

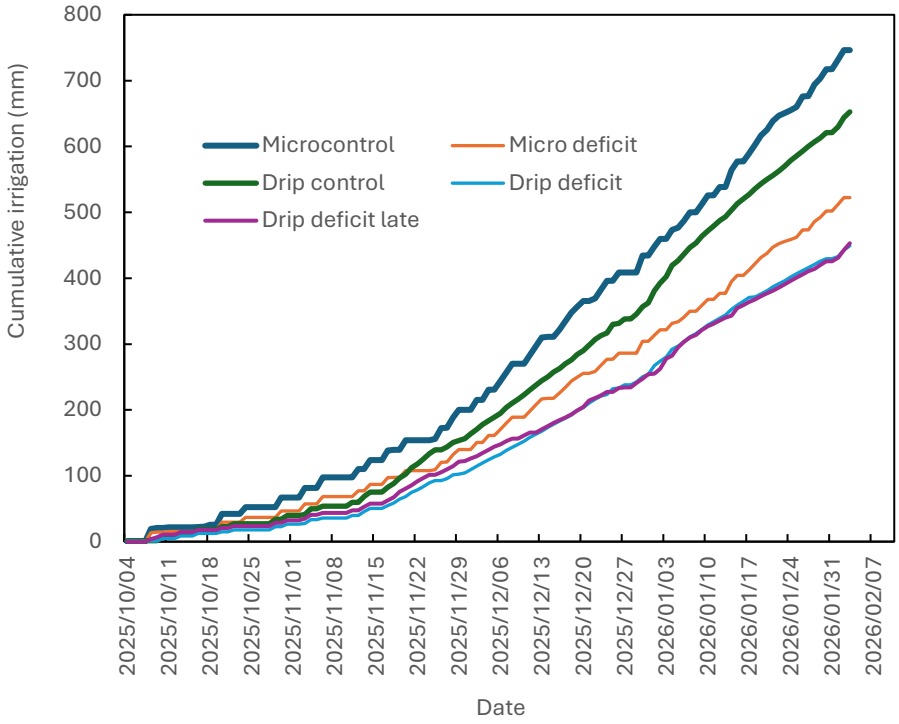


Figure B4. Cumulative irrigation per treatment during the 2025-2026 growing season

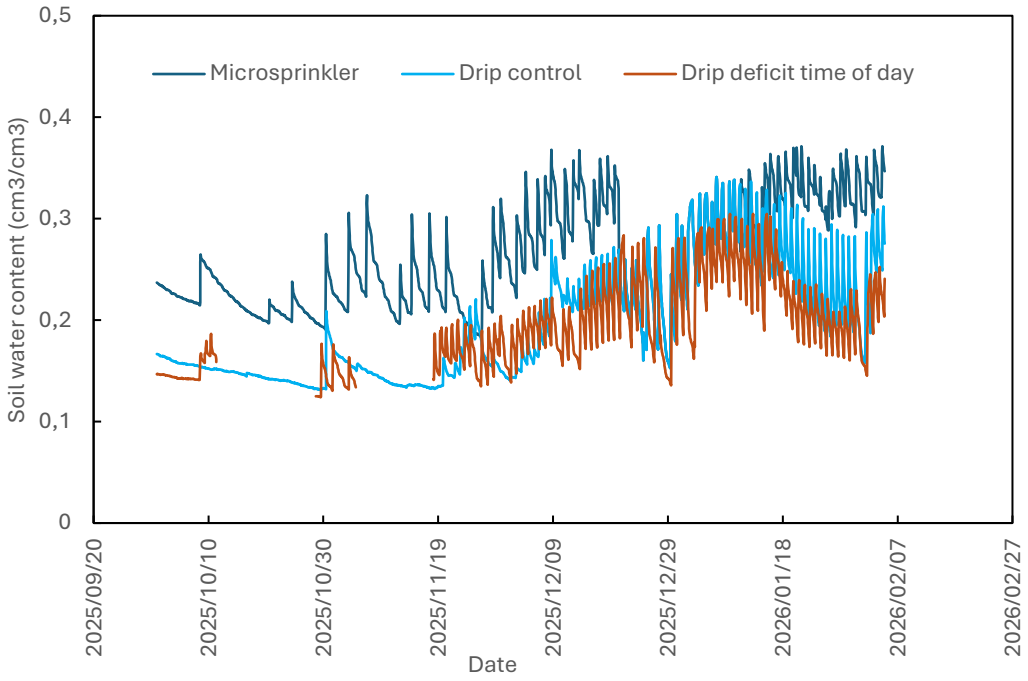


Figure B5. Soil water content averaged in the 20 to 60 cm depth for the micro sprinkler, drip control and the drip deficit applied late afternoon (drip deficit time of day)

The impact of the irrigation regimes on the midday stem water potentials is shown in Figure B7. The pre-dawn leaf water potential gives an indication of the average soil water status in the rootzone of the trees. However, due to the progressive decreases in the soil water potential, as the trees exhausted the available soil water, especially the drip irrigated trees, it became necessary to give the trees at least one deep irrigation per week, in order to replenish the soil profile. This additional irrigation did not substantially increase the overall irrigation levels for the drip irrigated trees, as shown in Figure B4. The midday stem water potential data shows that all treatments were under severe stress early in the season, which is consistent with the soil water content graph in Figure B5. Some literature defines the mild water stress for pears as corresponding with the midday stem water potential of around –1.3 MPa and severe stress of around –1.8 MPa (Blanco et al., 2025). Figures A5 and A6 highlight the dire situation with respect to the water availability at the farm. Adequate irrigation was applied at certain times, but not at other times.

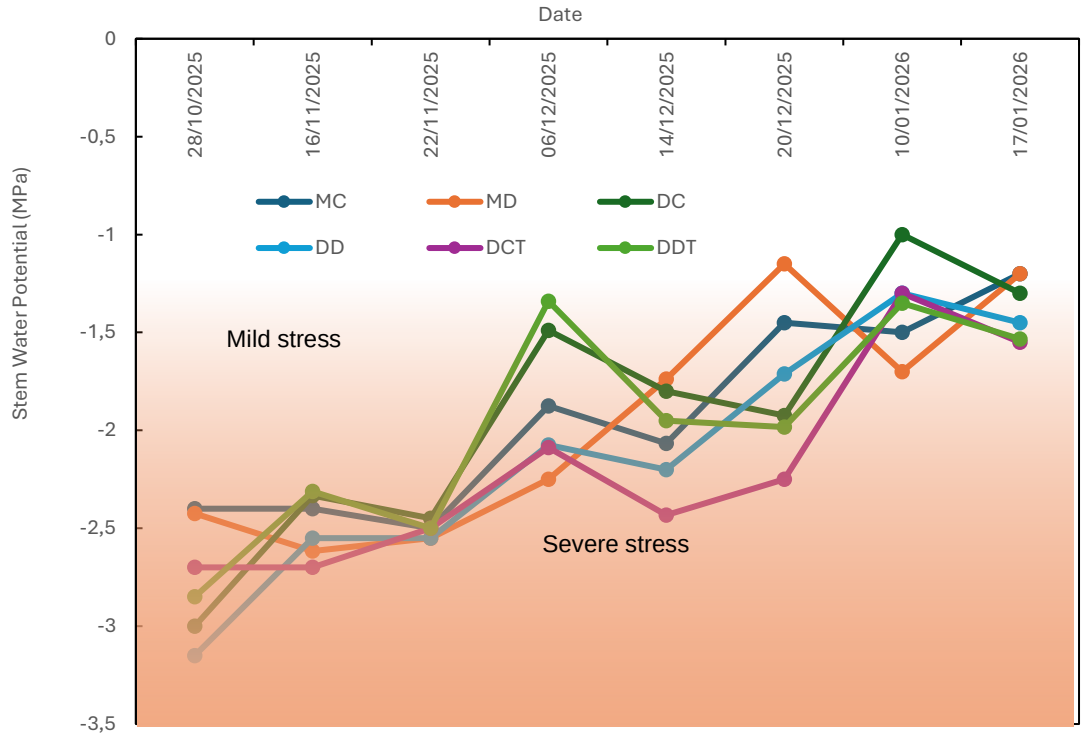


Figure B6. Mid-day stem water potential measurements taken in the various treatments over the 2025-2026 growing season

The average yield in each treatment is summarised in Table B1 for the 2025-2026 season. Data from earlier seasons are not reported, as the irrigation treatments had not been

implemented satisfactorily. These data show that the micro-sprinkler irrigated trees, which received the largest amount of irrigation, also produced the highest yield (MC ~ 89 t/ha). These were followed by the deficit micro-sprinkler treatment (MD ~ 81 t/ha). The drip control late irrigation (DCT) and the drip deficit early morning (DD) had the joint third-highest yield, at 68 t/ha. The early morning Drip Control (DC) had the lowest yield, for unclear reasons. Treatments that received less irrigation had the highest irrigation water productivity (see Table B1). The current grower's practice had the third-lowest water productivity, due to the high irrigation levels, but the micro-sprinkler deficit resulted in a higher water productivity.

Table B1. Summary of the seasonal total irrigation, yield and irrigation water productivity

Treatment	Yield	Average fruit number	Irrigation	Irrig_WP
	(t/ha)		(m^3/ha)	(kg/m^3)
MC	89	344	7463	11.9
MD	81	350	5597	14.5
DC	51	212	6526	7.8
DD	68	297	4493	15.1
DDT	63	278	4531	13.9
DCT	68	267	6526	10.4

Statistical analyses are ongoing to establish whether late irrigations made a significant difference in the performance of the trees. These will be reported in the completed desertation.

B3. CONCLUSIONS

The statistical analyses of the data that have been presented here are still ongoing. Therefore, it is not possible to conclude whether late irrigation is indeed beneficial or not. What seems to be emerging is that the current grower's practice produces the highest yield, but a lower water productivity, when comparing the irrigation amounts. Detailed discussions will be presented in the PhD dissertation, which is due by end of 2026.

APPENDIX C

VASCULAR FLOW DYNAMICS AND THEIR RELATIONSHIP TO FRUIT GROWTH IN P. TRIUMPH AND 'FORELLE' PEAR CULTIVARS

MSc thesis: Mr Johan Pienaar

C0. INTRODUCTION

The fruit is the most important economic product in orchards. In precision farming, it is ideal to monitor fruit growth as an indicator for yield accumulation, as well as the use of important resources, such as water. Electronic dendrometers are increasingly being used in precision irrigation scheduling, with sensors being installed on different plant organs. This study evaluated the growth dynamics of fruit from two pear cultivars that are widely planted in South Africa, namely the 'Packham's Triumph' and 'Forelle'. The aim was to identify and quantify the key drivers of fruit growth and to establish the feasibility of using the fruit as a precise indicator of the tree water status. The fruit growth and vascular flow rates were determined on a mass basis at different stages throughout the 2023/2024 growing season, as well as on a daily and seasonal time scale. A preliminary study in this project explored the possibility of using the fruit as an indicator of water stress in pears, but it yielded unexpected results, as shown in Figure C1, and as published by Dzikiti et al. (2024).

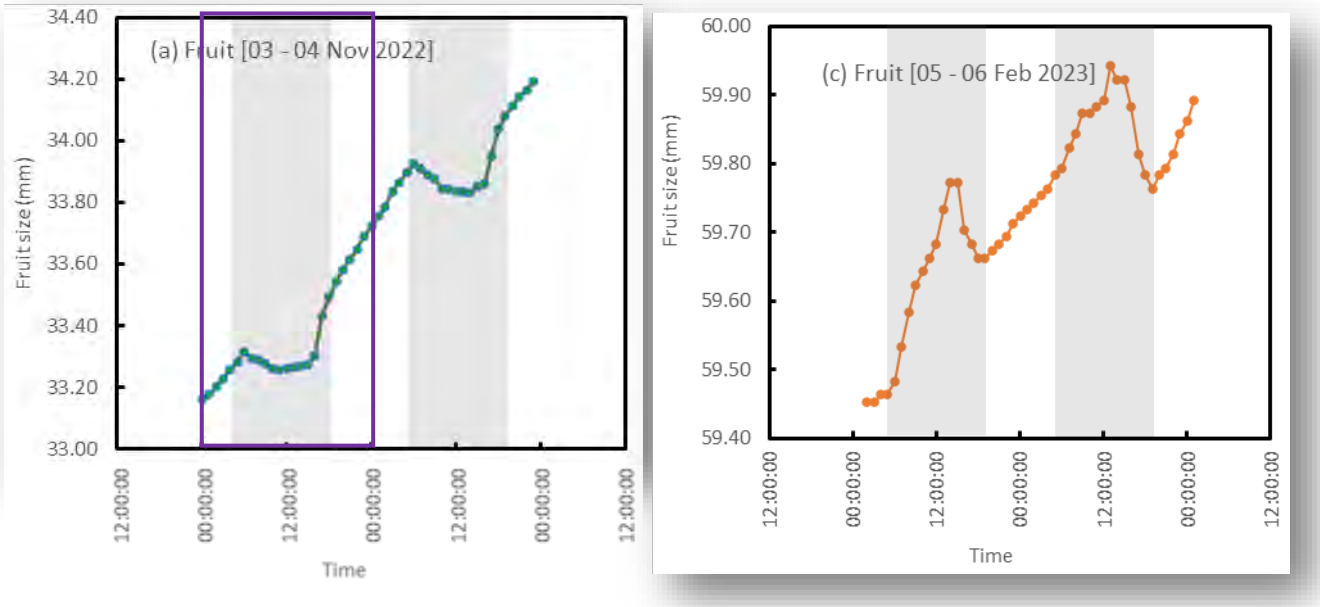


Figure C1. Hourly fruit size dynamics for a Forelle fruit (a) early and (b) late in the growing season. The shaded regions represent the day time, and clear regions the night time (after Dzikiti et al., 2024)

Early in the season (November-early December), the daily dynamics in the pear fruit size behaved like that of the stem or other tree organs (Figure C1a). The fruit size shrinks at sunrise, as water loss from the tree via transpiration exceeds the root water uptake, which is explained in Figure B1. The widely-used indicators of plant size changes, as measured by using dendrometers, include the maximum daily shrinkage and the daily growth rate. The increasing soil water deficit leads to an increased reliance on internally-stored water, which leads to the greater shrinkage of the plant, and the converse is often true. It also widely known that increasing the soil water deficit causes a reduced growth rate i.e. the smaller difference between the peak growth reached between successive days in Figure C1a.

It was surprising to observe that, late in the season (end-December till harvest), the fruit size for pears expanded (rather than shrinking) during the daytime, as shown in Figure C1b. The effect of this is that if we plot a maximum daily shrinkage profile for the fruit over the course of the entire season, the picture shown in Figure C2 emerges for the two cultivars.

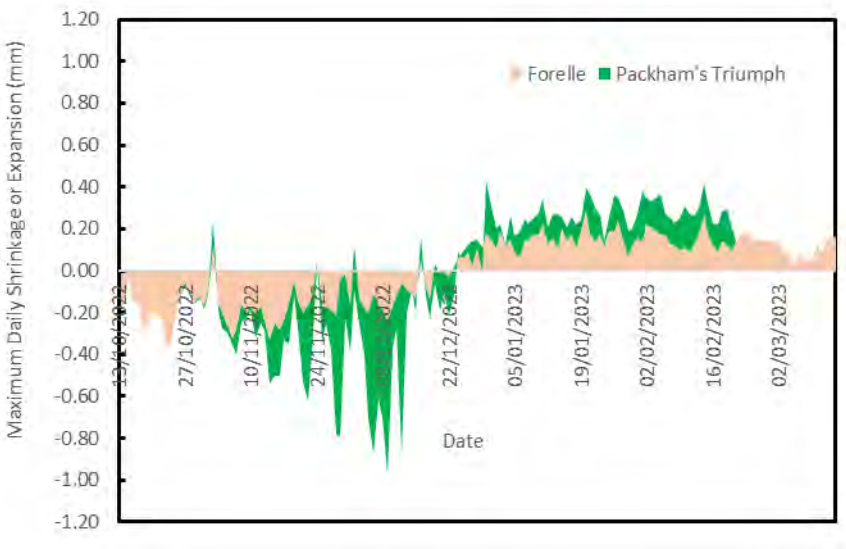


Figure C2. Maximum daily shrinkage profile for Forelle and P. Triumph fruit over the course of a full growing season (after Dzikiti et al ., 2024)

This Figure suggests that the fruit size changes early in the season are consistent with the stem or branch sizes that are measured continuously, by using dendrometers (Steppe et al., 2006; Dzikiti et al., 2007; Fernandez et al., 2017). However, in the second half of the growing season, the fruit size swells during the daytime, and this requires a different interpretation and different thresholds for detecting water stress. For instance, in Figure C3(a), it is apparent that the maximum daily shrinkage of the fruit was strongly correlated with the soil water content early in the season (October to November/December) (see the green dots). As the soil water content depleted, the maximum daily fruit shrinkage increased, as expected. However, a different relationship between the maximum fruit diameter changes with soil water content emerged (see orange dots). A higher soil water content caused a larger maximum expansion of the fruit, with a clearly positive correlation between these two variables (Figure C3a). The maximum daily shrinkage of the stem was expected (Figure C3b). The higher scatter in the stem maximum daily shrinkage data, compared to the fruit early in the season, suggests that the fruit is, in fact, a more sensitive indicator of water stress than the branch (or stem), early in the season

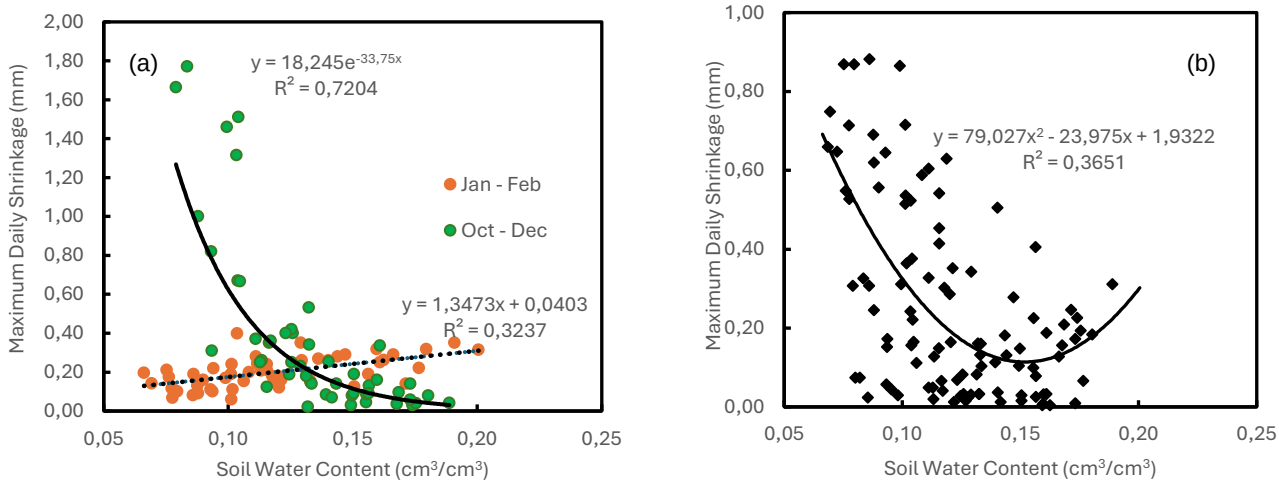


Figure C3. Correlation between the maximum daily (a) fruit shrinkage early (green dots) and swelling late (orange dots) in the season and (b) with branch diameter shrinkage for the same pear tree with the soil water content in the rootzone

For convenience, it is preferable to use a drought stress indicator that will be interpreted in the same way throughout the growing season, when using dendrometers as indicators of the irrigation need. These data suggest that the fruit is not an ideal organ for monitoring and making irrigation decisions throughout the season, as the interpretations of the signal have to change, as the driving forces for the fruit growth change.

How about using the daily fruit growth instead, as an indicator of plant stress? As shown in Figure C4, the daily fruit growth had a reasonable correlation with the soil water content early in the season (green dots). However, there was no correlation between these variables late in the season, which reinforces the idea that the fruit is an inconsistent indicator of water stress, at least in pears. The goal of this MSc study was therefore to attempt to explain the likely reasons of these observed trends.

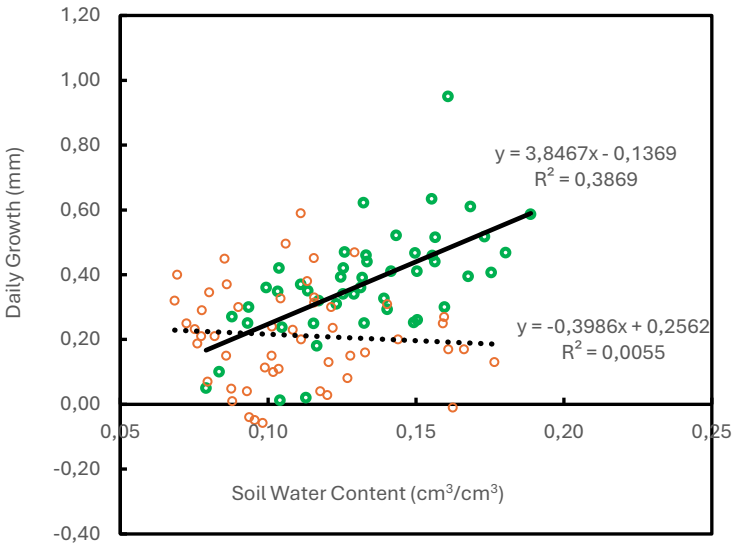


Figure C4. Correlation between the daily growth and soil water content for a Forelle pear fruit in the early (green dots) and late (orange dots) season

C1. MATERIALS AND METHODS

C1.1 MONITORING FRUIT GROWTH

The vascular and transpiration flows were determined from fruits at least ten trees away from the closest orchard edge, and on the east-facing side of the canopy. In each subsequent trial/campaign, a neighbouring tree row was selected for fruit measurements. Custom-made electronic dendrometers (see Pienaar, 2026) in Figure C5 were distributed across five trees, with one or two uninstrumented trees spaced in-between. The fruits were randomly selected.



Figure C5. Custom-made dendrometer for measuring the fruit size, which was converted to fruit mass by using mass-volume relationships for the pear fruit

Three dendrometers were allocated per tree in all trials, except the second, where the number was six sensors in each of the five marked trees. In the second trial, all 30 sensors were deployed in one orchard at a time, while in the other trials, the sensors were divided between the two study orchards, which allowed for simultaneous measurements. The trial was repeated five times in the Forelle orchard during the period 01/11/2023-17/02/2024, but only four times in the early maturing Packham's Triumph orchard from 01/11/2023-20/01/2024, where harvesting took place earlier. Each trial included at least six full days of continuous fruit growth measurements, where the growth data were automatically recorded every 15 minutes by one CR1000 data logger per orchard. The initial fruit cheek diameters (mm) of the selected pears were measured with callipers, before they were instrumented during each trial set-up.

C1.2 QUANTIFYING THE FRUIT VASCULAR FLOWS – THE SUBTRACTION METHOD

The instantaneous xylem, phloem and transpiration flow rates throughout a given day can be calculated for a particular fruit by comparing its instantaneous growth rate values at regular intervals between the days in which the fruit was subjected to different treatment conditions. This so-called subtraction method is based on the assumptions that: 1) the fruit growth in a short time interval is the result of the algebraic sum of the phloem (P), xylem (X) and transpiration (T) components; 2) the xylem flow is not affected by girdling; and 3) transpiration is not affected by detachment (Morandi et al., 2014a) (see Figure C6).

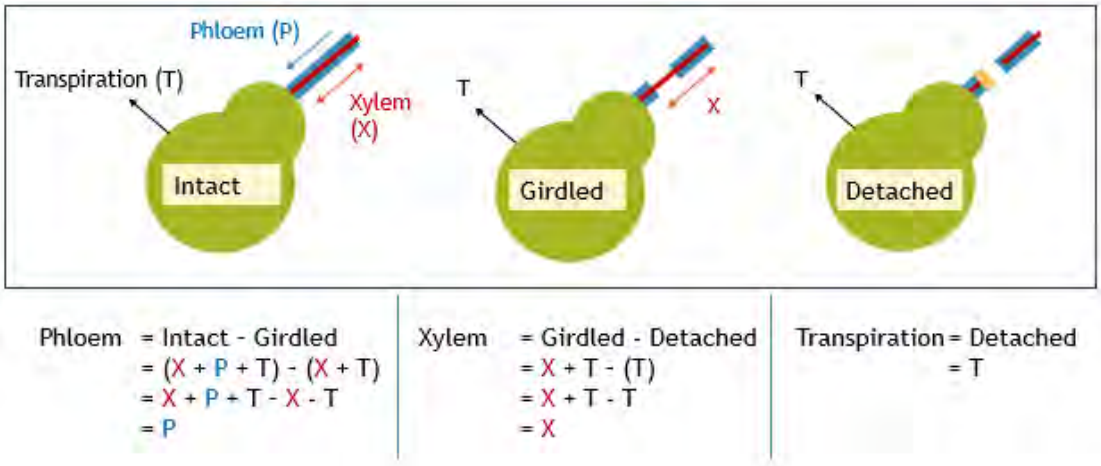


Figure C6. Schematic representation of the subtraction method of quantifying fruit vascular flows

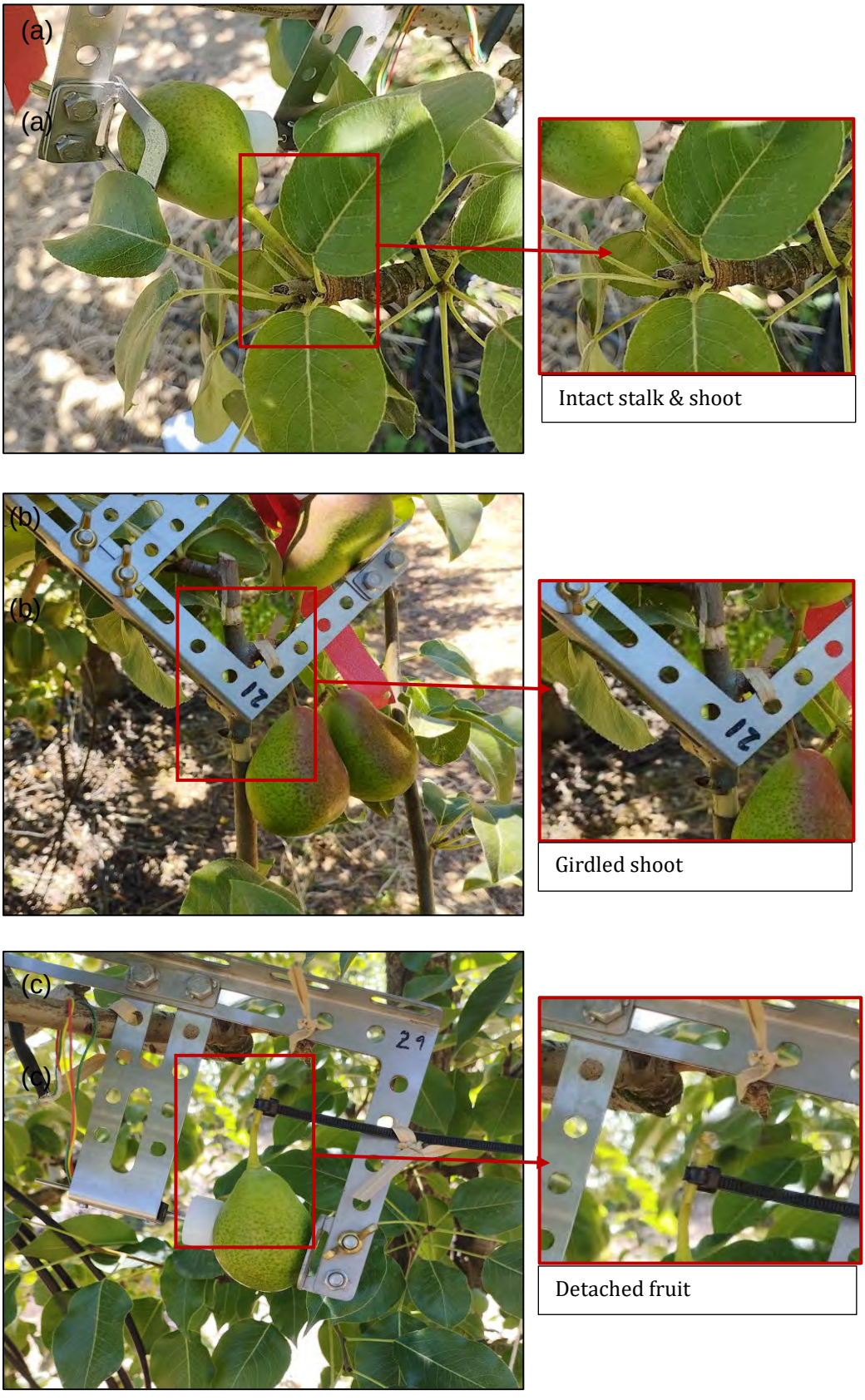


Figure C7. Visual representation of the three treatment conditions of the subtraction method, a) intact, b) girdled and c) detached

The daily growth (change in diameter) of instrumented fruits was continuously monitored over each trial period. The fruits were subjected to the following three subsequent treatment conditions, as shown in Figure C7:

1) intact (I_t) – no treatment was applied;
2) girdled (G_t) – the shoots were girdled, as needed, on one or two sides of the peduncle; and
3) detached (D_t) – the fruit were picked, their peduncles sealed with glue, and then hung close to their original positions in the canopy.

Each treatment condition lasted at least two full days. This allowed the growth rates obtained during each treatment condition to be averaged over the two days, for each fruit. Supporting data, such as the leaf photosynthesis and transpiration, the leaf, xylem and fruit water potentials, the soil moisture content and the weather conditions were collected, as described in Chapters Four and Five. Full details of the measurements are presented in Pienaar (2026).

C2. KEY FINDINGS

The typical results of the fruit vascular flow patterns for the two cultivars during different stages in the growing season are summarised in Figure C8 for Forelle and Figure C9 for P. Triumph. The sign convention used in these graphs is that negative values depict the losses of water/assimilates from the fruit, while the positive fluxes represent the gains. It is clear that transpiration losses, for both cultivars, were quite high early in the season when the fruit were young. Accordingly, the fruit size decreased at sunrise (see the blue line), which represents the shrinkage early in the season, due to the negative transpiration and xylem flows (i.e. water leaving the fruit). The gain in fruit size later in the day was related both to the increasing xylem inflows into the fruit and the decreasing transpiration losses. Phloem inflows into the fruit were positive and reached a peak in the early morning, early in the season, which is likely a result of both the photosynthesis and stomatal conductance being high in the morning (see Chapter Four). By mid-season for the Forelle (Figure C8 corresponding to 120 DAFB), 1), the magnitude of the transpiration flux had decreased, and the xylem inflows were predominantly positive through much of the day, but the phloem inflows were the dominant driver of fruit growth.

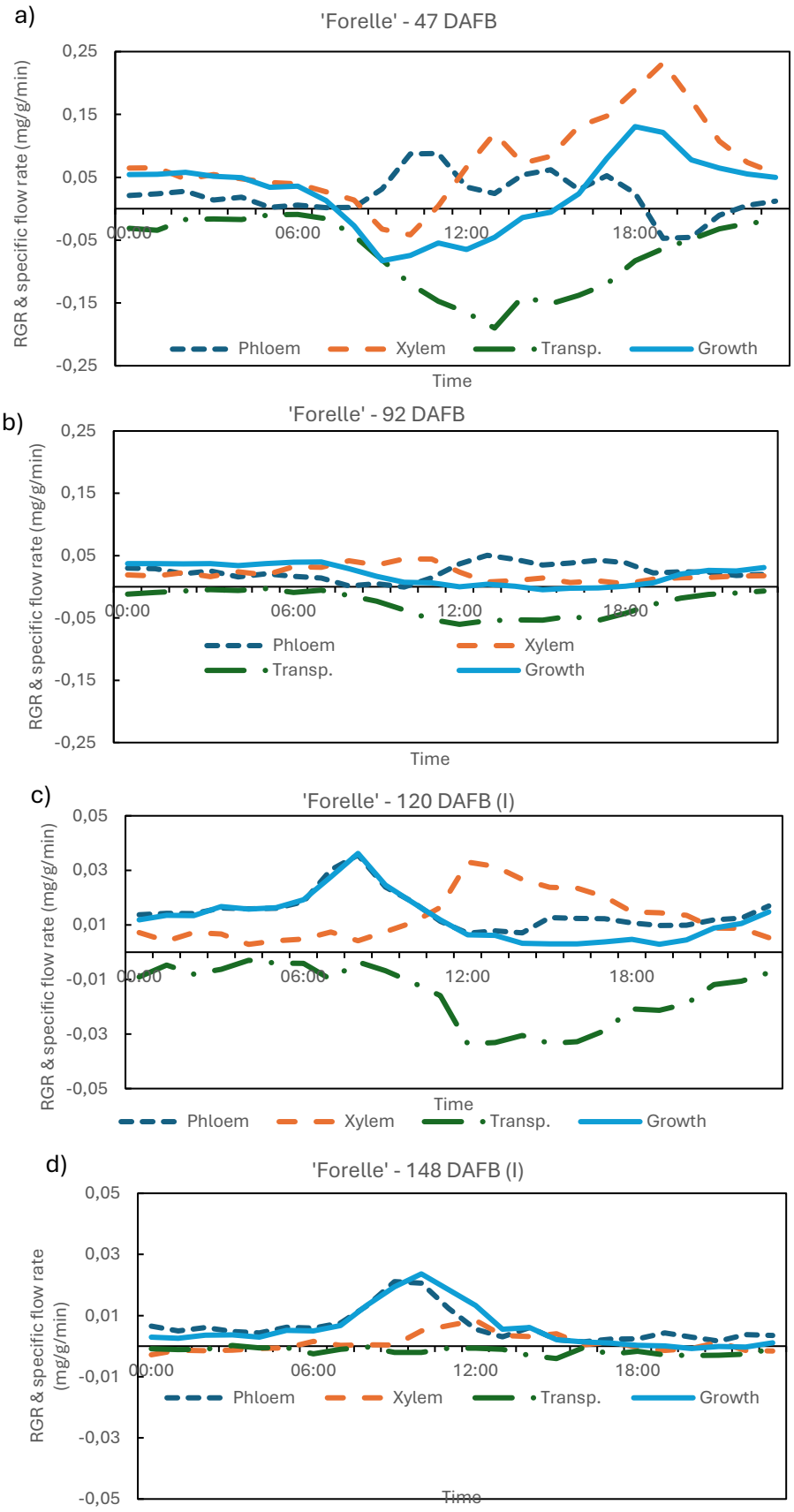


Figure C8. The diurnal patterns of relative growth rate (RGR) and specific phloem-, xylem- and transpiration flow rates (mg/g/min) for 'Forelle' fruit at a) 47 days after full bloom (DAFB), b) 92 DAFB, c) 120 DAFB, and d) 148 DAFB. The flow- and growth rates were calculated using approach I of the subtraction method

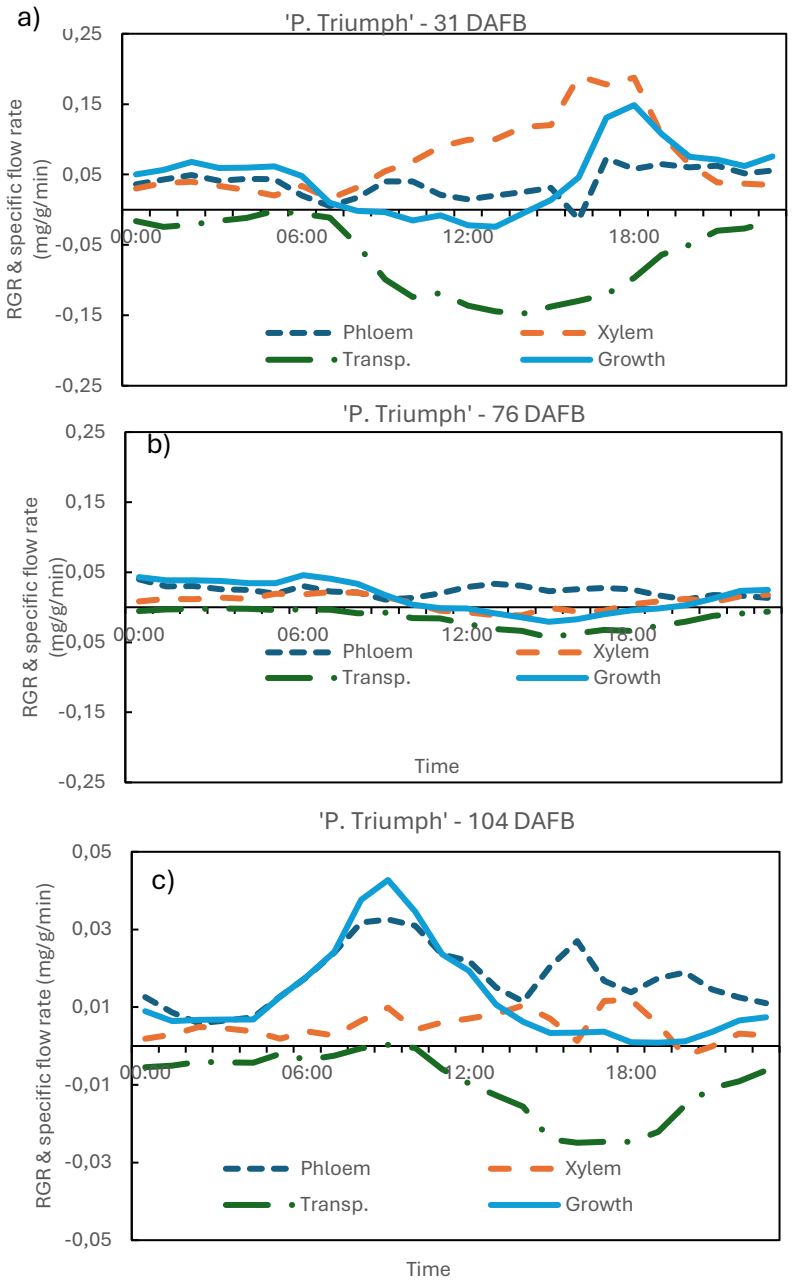


Figure C9. Diurnal patterns of the Relative Growth Rate (RGR) and specific phloem-, xylem- and transpiration flow rates (mg/g/min) for 'P. Triumph' fruit at a) 31 Days After Full Bloom (DAFB), b) 76 DAFB, and c) 104 DAFB. The flow- and growth rates were calculated by using Approach I of the subtraction method

The same trend applied to the early-maturing P. Triumph, as observed on 104 DAFB (Figure C10c). It is important to note that the peel transpiration of the Forelle dropped to zero at harvest (Figure C9d), while P. Triumph had, an albeit low, but non-zero peel transpiration (Figure C9c). The mid-season stages (DAFB 92 for Forelle and 76 for P. Triumph) were transition periods that switched from the daytime shrinking to daytime swelling phases, as reported in

Figure C2. The fruit growth rate at various stages during the season, as well as the contribution of the different fluxes, are shown in Figure C10. Early in the season, the xylem flows contributed the most to the daily gains in fruit mass. However, this diminished as the season progressed, with the phloem inflows becoming dominant from mid-December until harvest, for both cultivars. The relative contributions of the individual fluxes are shown in Figure C11.

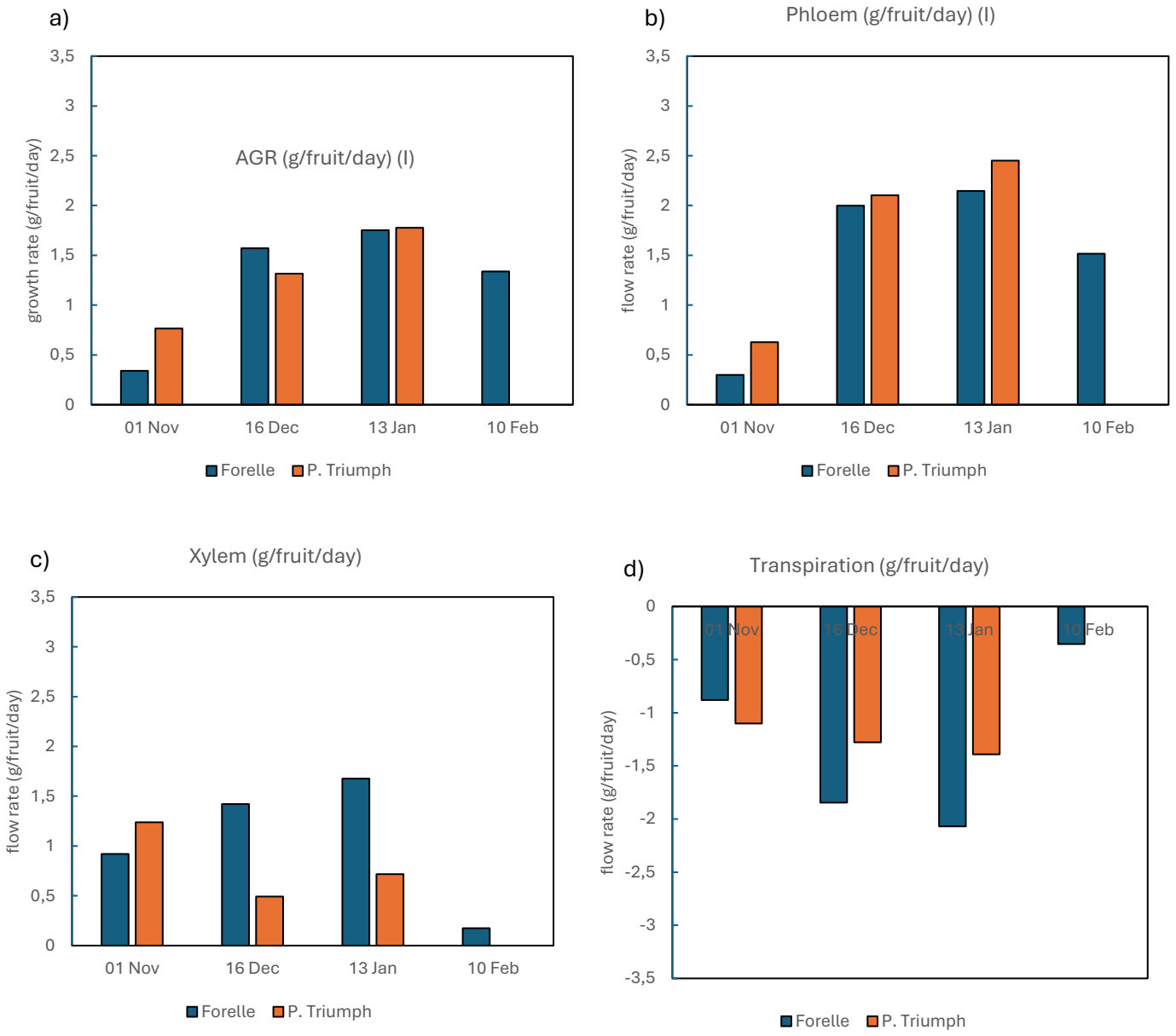


Figure C10. Mean daily a) absolute growth rate (AGR), and whole fruit b) phloem-, c) xylem-, and d) transpiration flow rates (g/fruit/day) for 'Forelle' and 'P. Triumph' fruit at different stages in the 2023/2024 growing season. The flow- and growth rates were calculated using approach I of the subtraction method

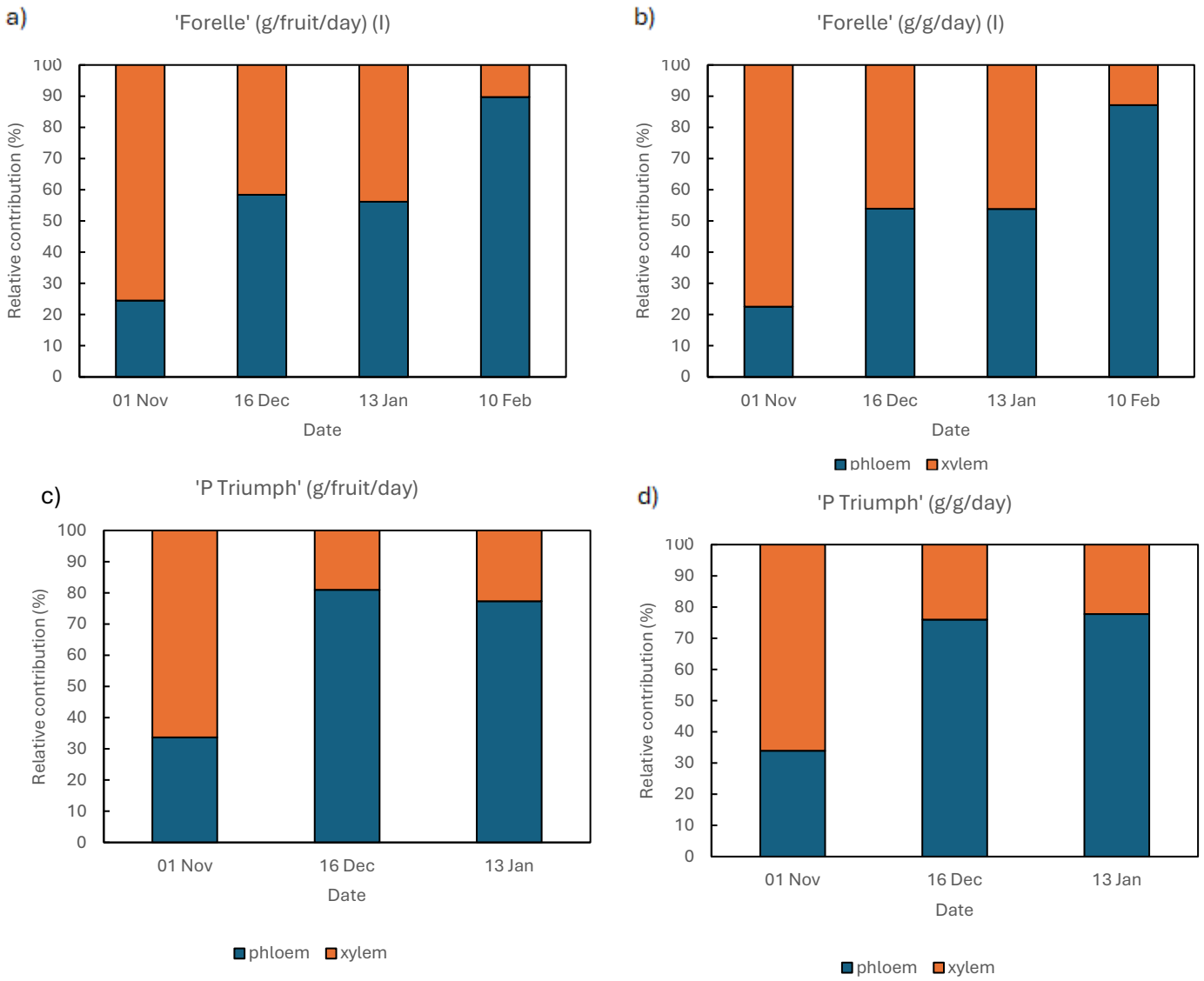


Figure C11. Relative contribution of the average daily phloem and -xylem inflows to the daily mass inflow for 'Forelle' on a) whole fruit- b) specific basis, and for 'P Triumph' on a c) whole fruit- and d) specific basis. The relative contributions were calculated at different times in the 2023/2024 growing season using Approach I of the subtraction method

C3. CONCLUSIONS

Precision irrigation in orchards is increasingly being based on the detection of stress from the plants themselves. Dendrometers are widely used for this purpose, although no studies have reported using these sensors on the fruit. In this study we show that dendrometers potentially provide precise information on the tree water status when installed on pear fruit, but only during the initial stages of fruit growth. When the fruit become mature, the fruit size is

dominated by phloem inflows, which cause the swelling of the fruit during the daytime. This swelling is not strongly related to the soil water status, as the link between the two variables is indirectly happening via photosynthesis. We have designed a detailed study that explained the apparent limitations of the dendrometers installed on pear fruit for precision irrigation management.